AD-A071 485 PENNSYLVANIA STATE UNIV UNIVERSITY PARK APPLIED RESE--ETC F/G 20/11
HANDBOOK OF VIBRATION AND NOISE CONTROL.(U)
APR 79 J C SNOWDON N00024-79-C-6043
UNCLASSIFIED ARL/PSU/TM-79-75 NL

1 OF 3
AD A071485

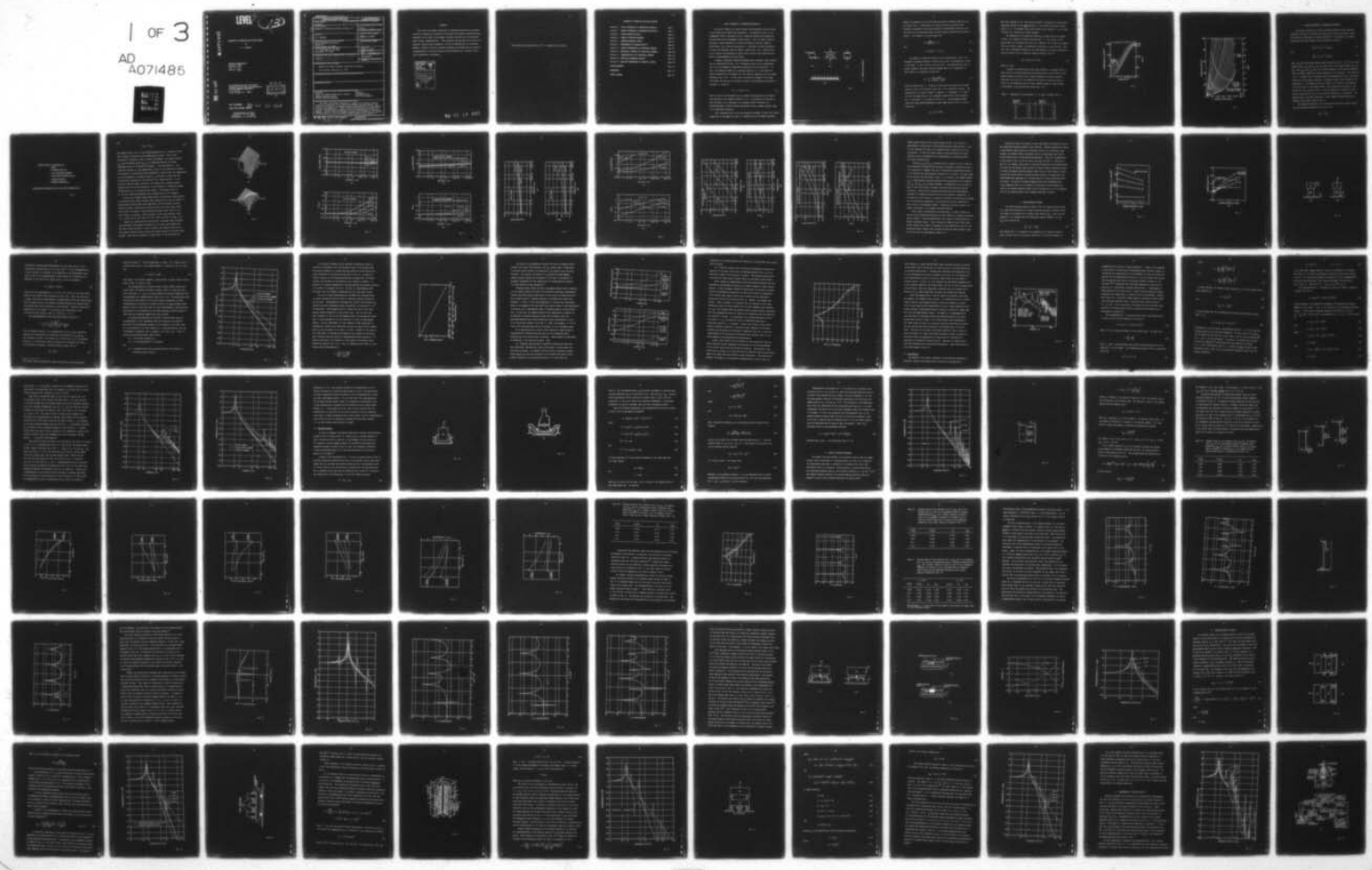

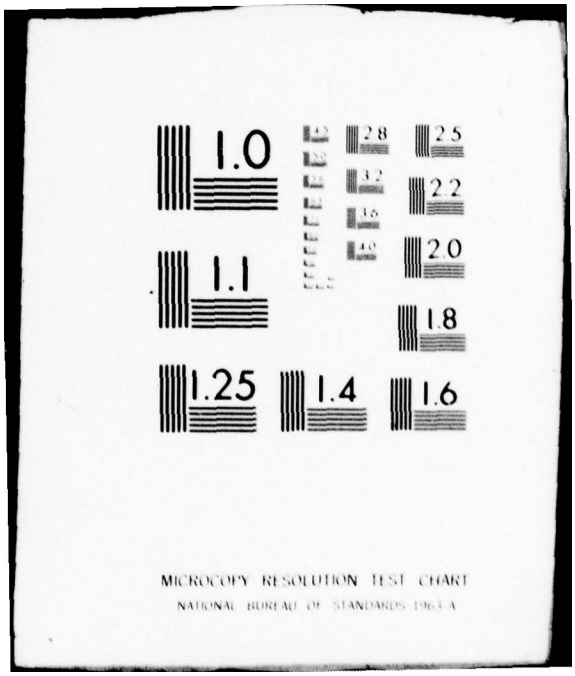
1.0
1.1
1.25
1.4
1.6
2.8
3.2
3.6
4.0
2.5
2.2
2.0
1.8
MICROCOPY RESOLUTION TEST CHART
NATIONAL BUREAU OF STANDARDS 1963-A

LEVEL II

13

AD A071485

DDC FILE COPY

HANDBOOK OF VIBRATION AND NOISE CONTROL

by

J. C. Snowdon

Technical Memorandum
File No. 79-75
April 27, 1979
Copy No. 56

The Pennsylvania State University
Institute for Science and Engineering
APPLIED RESEARCH LABORATORY
P. O. Box 30
State College, PA 16801

NAVY DEPARTMENT

NAVAL SEA SYSTEMS COMMAND

UNCLASSIFIED

SECURITY CLASSIFICATION OF THIS PAGE (When Data Entered)

REPORT DOCUMENTATION PAGE		READ INSTRUCTIONS BEFORE COMPLETING FORM
1. REPORT NUMBER TM 79-75	2. GOVT ACCESSION NO.	3. RECIPIENT'S CATALOG NUMBER
4. TITLE (and Subtitle) Handbook of Vibration and Noise Control (U)		5. TYPE OF REPORT & PERIOD COVERED Final rept.
		6. PERFORMING ORG. REPORT NUMBER
7. AUTHOR(s) J. C. Snowdon		8. CONTRACT OR GRANT NUMBER(s) N00024-79-C-6043
9. PERFORMING ORGANIZATION NAME AND ADDRESS Applied Research Laboratory PO Box 30 State College, PA 16801		10. PROGRAM ELEMENT, PROJECT, TASK AREA & WORK UNIT NUMBERS 27 Apr 79
11. CONTROLLING OFFICE NAME AND ADDRESS U. S. Department of the Navy Washington, DC 20360		12. REPORT DATE April 27, 1979
		13. NUMBER OF PAGES 205 (22) 204p
14. MONITORING AGENCY NAME & ADDRESS(if different from Controlling Office) ARL/PSU/TM-79-75		15. SECURITY CLASS. (of this report) UNCLASSIFIED
		15a. DECLASSIFICATION/DOWNGRADING SCHEDULE

16. DISTRIBUTION STATEMENT (of this Report)

Approved for public release; distribution unlimited.

As per letter dated June 11, 1979.

17. DISTRIBUTION STATEMENT (of the abstract entered in Block 20, if different from Report)

18. SUPPLEMENTARY NOTES

19. KEY WORDS (Continue on reverse side if necessary and identify by block number)

Handbook.
Static and dynamic properties of rubbers.
Compound mounting system.
Dynamic Vibration Absorber.
Impedance.
Transmissibility.
Four-Pole Parameters.

20. ABSTRACT (Continue on reverse side if necessary and identify by block number)

The static and dynamic properties of rubbers are reviewed initially, followed by discussion of the simple and compound mounting systems. Reference is also made to the dynamic vibration absorber and to the measurement of mount transmissibility. Three sections then describe the natural frequencies, the mechanical impedances, and the transmissibility of structural members. Finally, four-pole parameter analyses are reviewed and the relative transmissibility of various mounting systems supported by a variety of

DD FORM 1 JAN 73 1473 EDITION OF 1 NOV 65 IS OBSOLETE

UNCLASSIFIED

SECURITY CLASSIFICATION OF THIS PAGE (When Data Entered)

391 007

ABSTRACT

The static and dynamic properties of rubberlike materials are reviewed initially, followed by discussion of the simple and compound mounting systems. Reference is also made to the dynamic vibration absorber and to the measurement of mount transmissibility. Three sections then describe the natural frequencies, the mechanical impedances, and the transmissibility of structural members. Finally, four-pole parameter analyses are reviewed and the relative transmissibility of various mounting systems supported by a variety of non-rigid foundations is discussed.

This handbook was sponsored by the U. S. Department of the Navy.

HANDBOOK OF VIBRATION AND NOISE CONTROL

1. STATIC PROPERTIES OF RUBBERLIKE MATERIALS

The strain induced in a purely elastic linear material is proportional to the stress that produces the deformation. As explained in Ref. 1, two fundamental types of deformation that a rubberlike material may experience are described by two independent elastic moduli. Thus, the shear modulus G describes a shear deformation for which the material does not change in volume [Fig. 1(a)], and the bulk modulus B describes a volume deformation for which the material does not change in shape [Fig. 1(b)]. Rubbers that do not contain fine particles of carbon black (filler) have shear and bulk moduli of approximately 100 and 10^5 psi.

A sample of material sandwiched between plane, parallel, rigid surfaces in the configuration of Fig. 1(c) is frequently said to be in compression, but it is not homogeneous compression governed by the bulk modulus B. In fact, the mechanical behavior is governed primarily by B only when the lateral dimensions of the sample are very large in comparison with the sample thickness [Fig. 1(d)]. In this event, the material changes in both shape and volume, and the ratio of stress to strain in the material is governed by a modulus M given by

$$M = B + (4G/3) \approx B \quad . \tag{1}$$

This is to say, the resilience that is normally associated with the rubberlike material is not apparent because $B \gg G$. If resilience is required in this situation, it is necessary to use spaced strips of material or a perforated sheet,[2] thereby leaving the material free to expand laterally when it is compressed vertically.

Also considered must be the other geometric extreme, in which the lateral dimensions of the sample are small in comparison with the sample thickness;

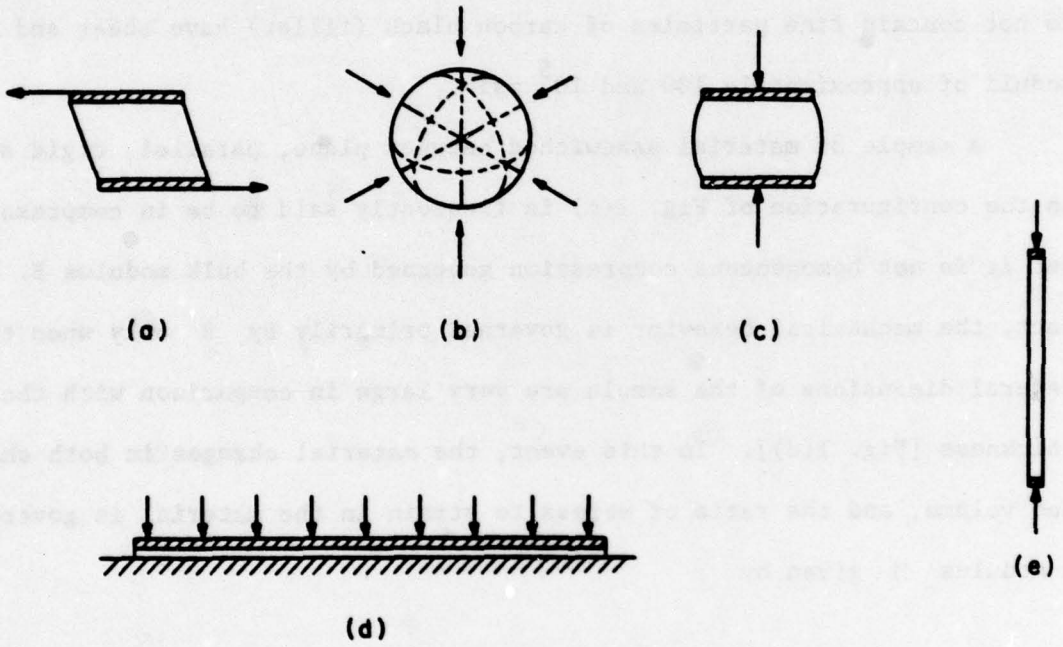

Fig. 1

namely, the sample is a rod or bar and the stress is applied along its axis as in Fig. 1(e). In this event, the ratio of stress to strain in the material is governed by the Young's modulus E (approximately 300 psi), and the ratio of the resulting lateral to axial strain is described by Poisson's ratio ν. For rubbers, it is well known that

$$E = \frac{9BG}{(3B + G)} \approx 3G \tag{2}$$

and

$$\nu = [(E/2G) - 1] \approx 0.5 \quad . \tag{3}$$

An element of rubberlike material in the configuration of Fig. 1(c) possesses an apparent modulus of elasticity E_a that is intermediate in value to the moduli E and M [Figs. 1(d) and 1(e)]. The rubberlike material is usually bonded to the rigid surfaces between which it is compressed, in which case[3] it is possible to state that

$$E_a = \frac{E(1 + \beta S^2)}{[1 + (E/B)(1 + \beta S^2)]} \quad , \tag{4}$$

where the shape factor S is equal to the ratio of the area of one loaded surface to the total force-free area, and β is a numerical constant. The shape factor of a rubber cylinder of diameter D and height ℓ is equal to $D/4\ell$; the shape factor of a rectangular rubber block of side lengths a and b and height ℓ is equal to $ab/\ell(a + b)$. For all samples except those with large lateral dimensions (large shape factors), Eq. (4) can be written as

$$E_a = E(1 + \beta S^2) \quad . \tag{5}$$

Note that, because $E \approx 3G$, the apparent modulus of elasticity is some simple numerical multiple of the shear modulus G. For rubbers unfilled by carbon black, $\beta = 2$. For rubbers filled with carbon black, values of β are listed in Table I as a function of rubber hardness.

The dependence of the apparent modulus E_a on shape factor is plotted in Fig. 2 for rubbers of various hardness (Ref. 3). The curves of this figure have the form predicted by Eq. (4). Equation (5) is valid for samples that are circular, square, or moderately rectangular in cross section. However, for a pronounced rectangular rail-type sample--a so-called compression strip for which $b >> a$--a companion equation pertains; that is

$$E_a = (2/3)\, E\, (2 + \beta S^2) \quad , \tag{6}$$

where $S = a/2\ell$.

A series of stress-strain curves drawn from Ref. 4 is shown in Fig. 3, which refers to various shape factors and deflections of up to 50% (a value seldom reached in practice) for a rubber hardness of 40 Shore Durometer. These data are said not to be limited to one type of rubber but they do relate to room temperature and to rubber samples bonded to rigid surfaces in the manner of an antivibration mount [Fig. 1(c)].

Table 1. Dependence of the parameter β on rubber hardness (Ref. 3).

Hardness IRHD ± 2	β	Hardness IRHD ± 2	β
30	1.86	55	1.28
35	1.78	60	1.14
40	1.70	65	1.08
45	1.60	70	1.06
50	1.46	75	1.04

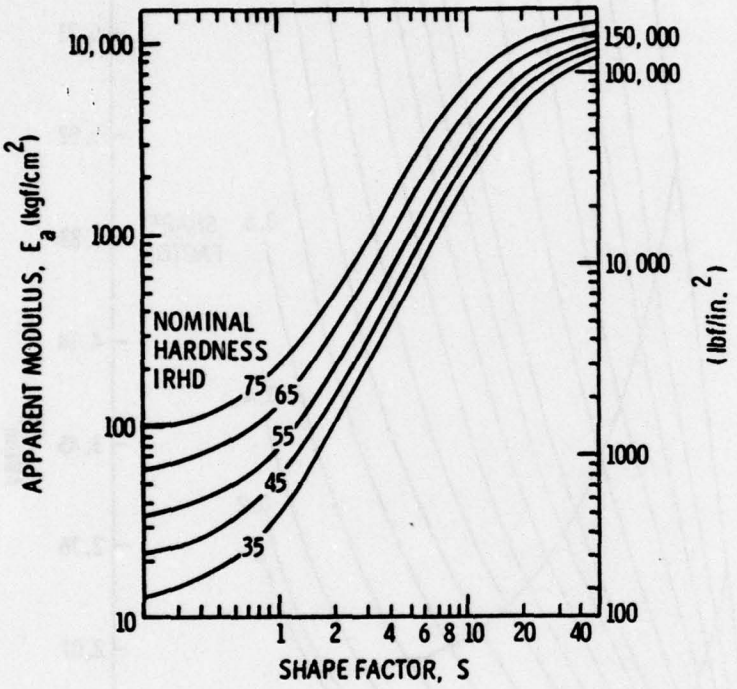
10,000
1000
100
10
APPARENT MODULUS, E_a (kgf/cm^2)
NOMINAL
HARDNESS
IRHD
75
65
55
45
35
1
2
4
6
8
10
20
40
SHAPE FACTOR, S
150,000
100,000
10,000
1000
100
(lbf/in.^{2})

Fig. 2

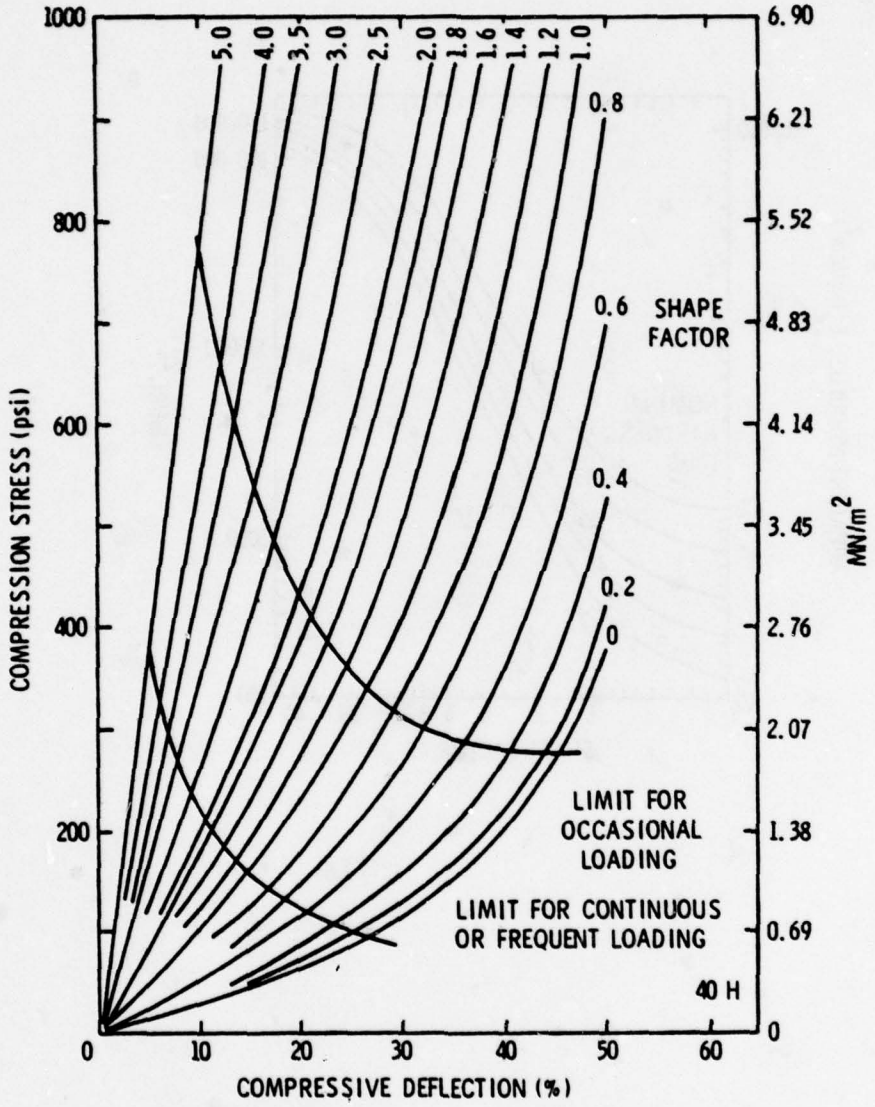
1000
800
600
400
200
0
10
20
30
40
50
60
6.90
6.21
5.52
4.83
4.14
3.45
2.76
2.07
1.38
0.69
0
MN/m²
COMPRESSION STRESS (psi)
COMPRESSIVE DEFLECTION (%)
5.0
4.0
3.5
3.0
2.5
2.0
1.8
1.6
1.4
1.2
1.0
0.8
0.6
0.4
0.2
0
SHAPE FACTOR
LIMIT FOR OCCASIONAL LOADING
LIMIT FOR CONTINUOUS OR FREQUENT LOADING
40 H

Fig. 3

2. DYNAMIC PROPERTIES OF RUBBERLIKE MATERIALS

The dynamic properties of linear rubberlike materials that experience sinusoidal vibration are readily accounted for by writing the elastic moduli that govern the vibration as complex quantities.[1] For example, the Young's modulus and the shear modulus are most generally written as

$$E^*_{\omega,\theta} = E_{\omega,\theta}\,(1 + j\delta_{E\omega,\theta}) \tag{7}$$

and

$$G^*_{\omega,\theta} = G_{\omega,\theta}\,(1 + j\delta_{G\omega,\theta}) \quad . \tag{8}$$

Here, the star superscripts denote complex quantities and $j = \sqrt{-1}$; the so-called dynamic moduli $E_{\omega,\theta}$ and $G_{\omega,\theta}$ are the real parts of the complex moduli $E^*_{\omega,\theta}$ and $G^*_{\omega,\theta}$; and $\delta_{E\omega,\theta}$ and $\delta_{G\omega,\theta}$ are the so-called damping or loss factors associated with the Young's modulus and shear deformations of the material. The subscripts ω and θ indicate that the dynamic moduli and damping factors are, in general, functions of both angular frequency ω (hereafter simply called frequency) and temperature θ. The damping factors are equal to the ratios of the imaginary to the real parts of the complex moduli, and are directly equivalent to the reciprocal of the quality factor Q that is employed in electrical circuit theory to describe the ratio of an inductive reactance to a resistance. The damping factors are also equivalent to other commonly employed measures of damping such as those listed in Fig. 4.

For rubberlike materials, the complex shear and Young's moduli exhibit the same frequency dependence[1]; that is to say,

$$E_{\omega,\theta} = 3G_{\omega,\theta} \tag{9}$$

DAMPING FACTOR δ = LOSS FACTOR η or β

= TAN δ

= 2 (DAMPING RATIO C/C_c)

= $(1/\pi)$ (LOGARITHMIC DECREMENT)

= $(1/2\pi)$ (SPECIFIC DAMPING CAPACITY)

= 1/(QUALITY FACTOR Q)

= (RESONANT BANDWIDTH)/ω_0

(PROVIDED THAT THE DAMPING FACTOR IS LESS THAN APPROXIMATELY 0.3)

Fig. 4

and

$$\delta_{E\omega,\theta} = \delta_{G\omega,\theta} \quad . \tag{10}$$

The dynamic moduli of Eq. (9) are found experimentally to increase in value when frequency increases or when temperature decreases. This is best visualized by reference to Fig. 5, where, for example, the dynamic modulus $G_{\omega,\theta}$ and the damping factor $\delta_{G\omega,\theta}$ of a rubberlike material are shown diagrammatically as a function of frequency ω and temperature θ. The transition frequency ω_t and temperature θ_t refer to the transition of rubberlike materials at sufficiently high frequencies or sufficiently low temperatures to an "inextensible" or glasslike state, $G_{\omega,\theta}$ becoming so large that the characteristic resilience of the material is no longer apparent. At the so-called rubber-to-glass transition, the damping factor passes through a maximum value that lies approximately in the frequency or temperature range through which $G_{\omega,\theta}$ is increasing most rapidly. The damping factors of Eq. (10) are found experimentally not to change greatly with frequency.

Values of the dynamic shear moduli and of the associated damping factor of unfilled natural rubber, natural rubber filled with 50 parts by weight of high-abrasion furnace (HAF) black, SBR rubber (75/25 butadiene styrene), Thiokol RD rubber, plasticized polyvinyl acetate, and butyl rubber filled with 40 parts by weight of medium processing channel (MPC) black per 100 parts rubber, are plotted versus frequency in the audio-frequency range 1 Hz - 10 kHz at 5°C, 20°C, and 35°C (41°F, 68°F, and 95°F) in Figs. 6-11.[1]

Rubbers are reinforced with carbon black to increase their stiffness, tear resistance, and abrasion resistance—to an extent that depends upon the type of black utilized. Furnace, channel, and thermal blacks cover a wide range of particle sizes; furnace and channel blacks are the most finely divided. Note that the presence of carbon black (1) has increased the

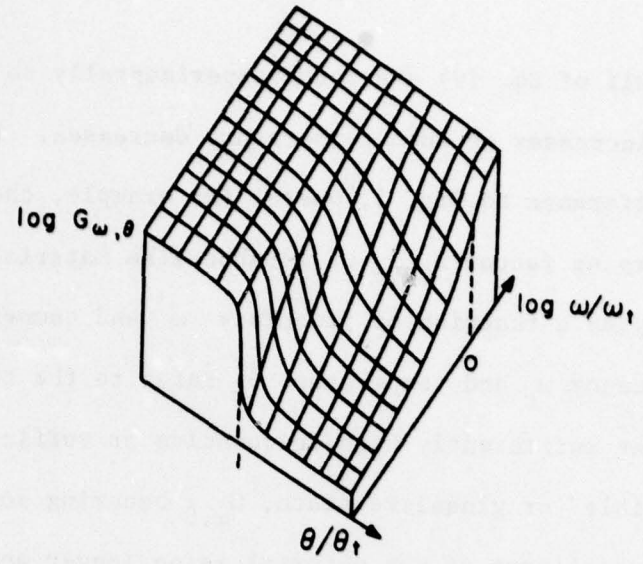
log $G_{\omega,\theta}$
log ω/ω_t
0
1
θ/θ_t

(a)

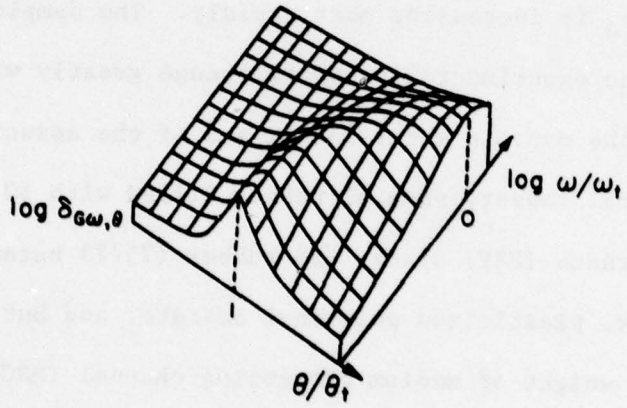
log $\delta_{G\omega,\theta}$
log ω/ω_t
0
1
θ/θ_t

(b)

Fig. 5

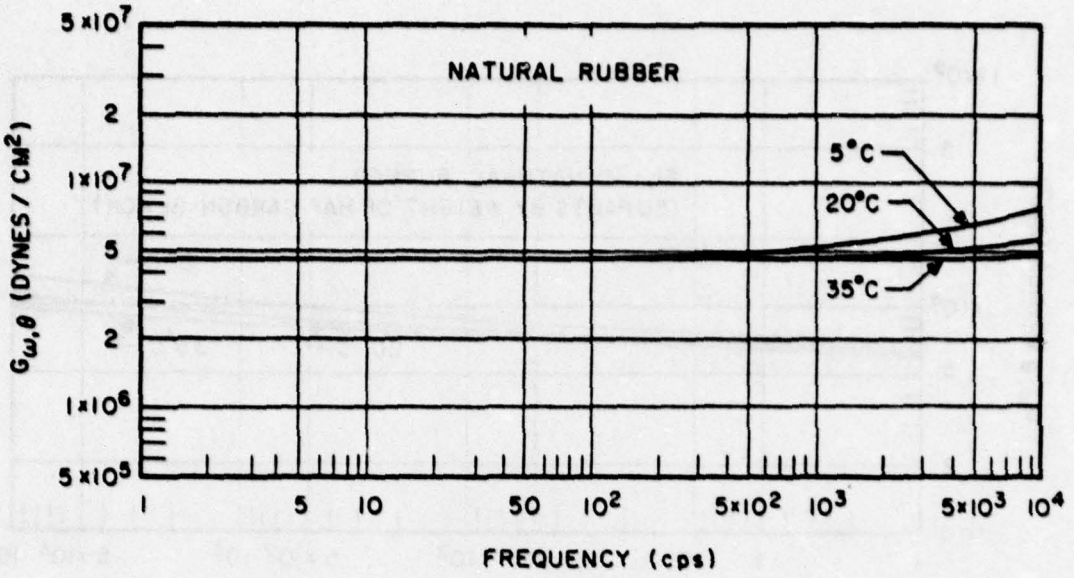
NATURAL RUBBER
5°C
20°C
35°C
$G_{\omega,\theta}$ (DYNES / CM^2)
5x10^7
2
1x10^7
5
2
1x10^6
5x10^5
1
5
10
50
10^2
5x10^2
10^3
5x10^3
10^4
FREQUENCY (cps)

(a)

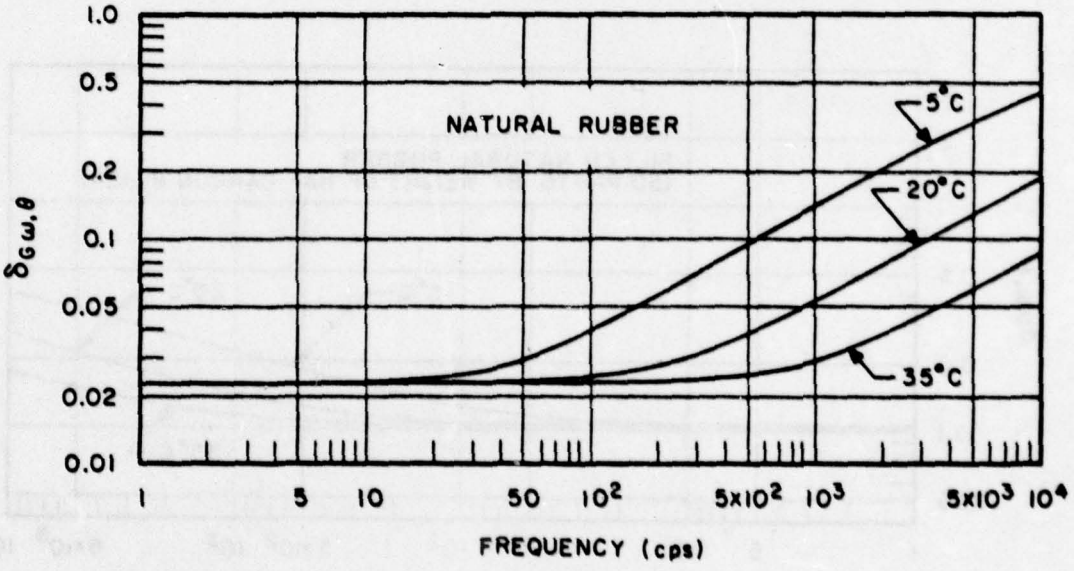
NATURAL RUBBER
5°C
20°C
35°C
$\delta_{G\omega,\theta}$
1.0
0.5
0.2
0.1
0.05
0.02
0.01
1
5
10
50
10^2
5x10^2
10^3
5x10^3
10^4
FREQUENCY (cps)

(b)

Fig. 6

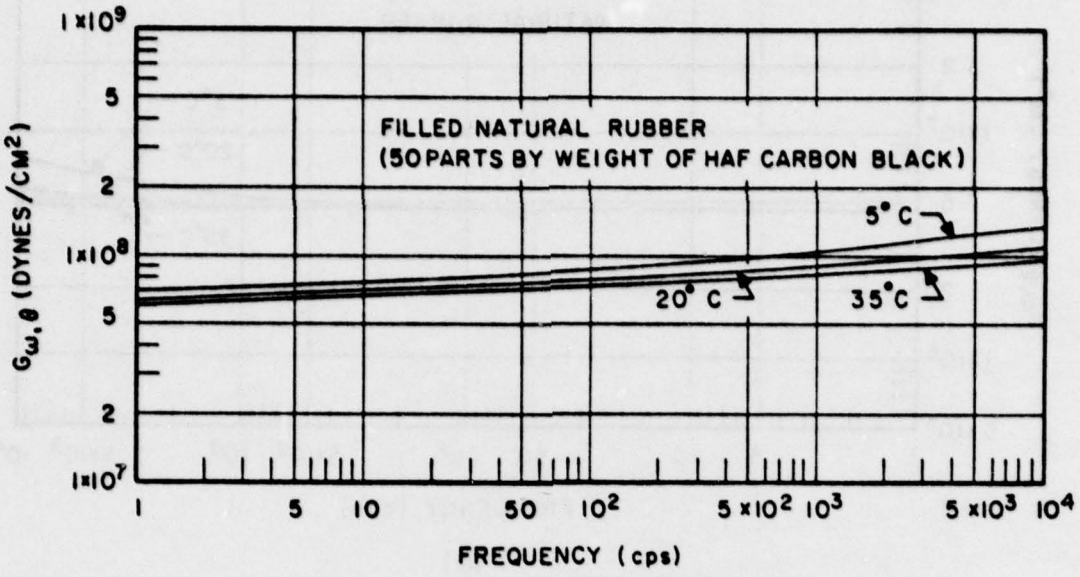
FILLED NATURAL RUBBER
(50 PARTS BY WEIGHT OF HAF CARBON BLACK)
5°C
20°C
35°C
$G_{\omega,\theta}$ (DYNES/CM²)
1×10⁹
5
2
1×10⁸
5
2
1×10⁷
1
5
10
50
10²
5×10²
10³
5×10³
10⁴
FREQUENCY (cps)

(a)

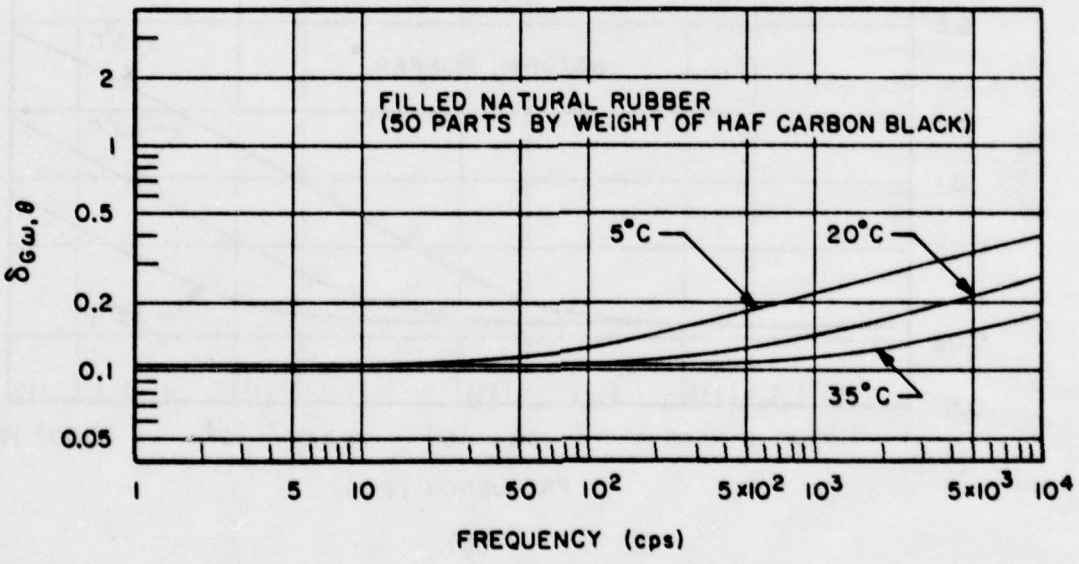
FILLED NATURAL RUBBER
(50 PARTS BY WEIGHT OF HAF CARBON BLACK)
5°C
20°C
35°C
$\delta_{G\omega,\theta}$
2
1
0.5
0.2
0.1
0.05
1
5
10
50
10²
5×10²
10³
5×10³
10⁴
FREQUENCY (cps)

(b)

Fig. 7

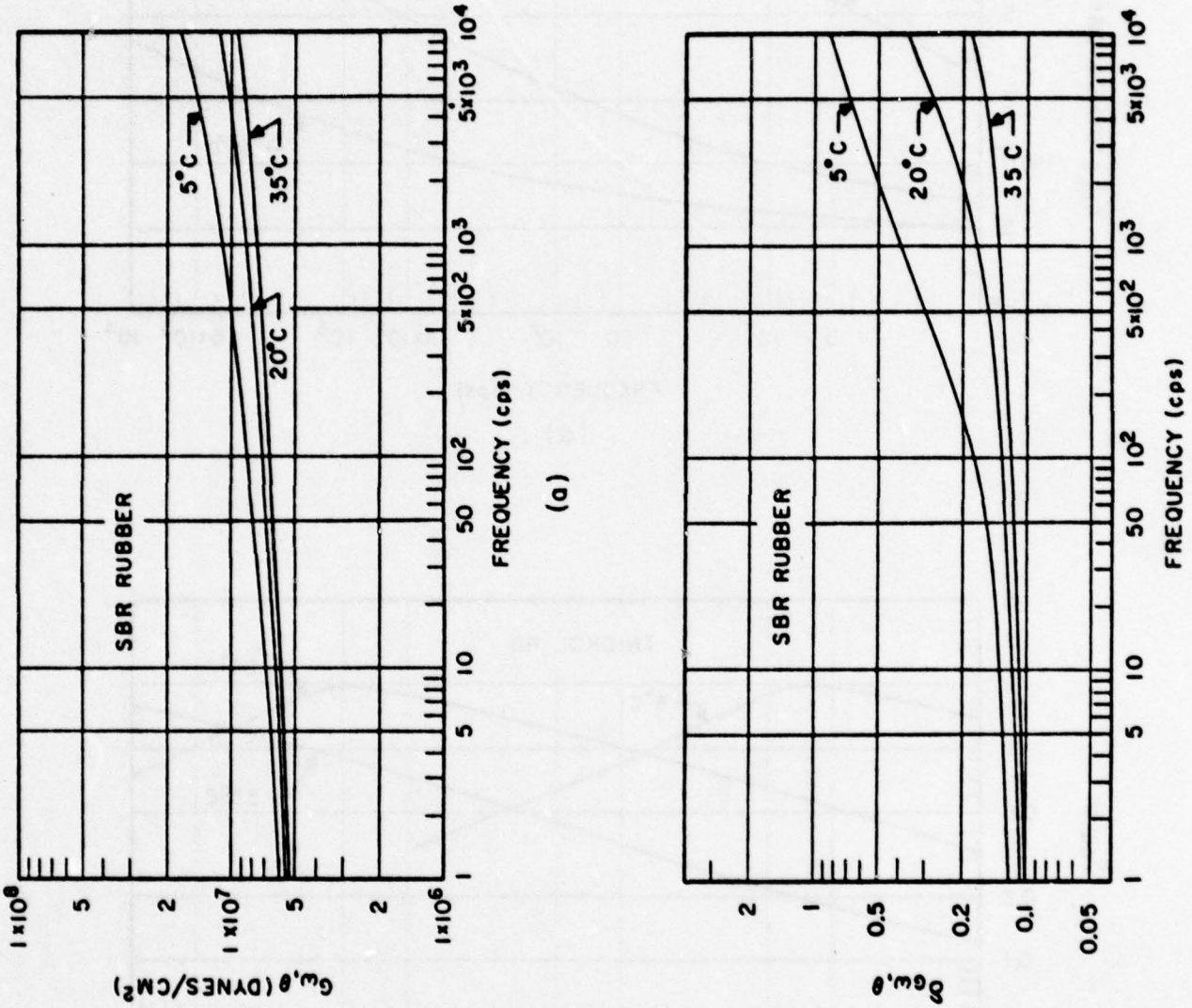
SBR RUBBER
5°C
20°C
35°C
FREQUENCY (cps)
$G_{\omega,\theta}$ (DYNES/CM^2)
(a)
SBR RUBBER
5°C
20°C
35 C
FREQUENCY (cps)
$\delta_{G\omega,\theta}$
(b)

Fig. 8

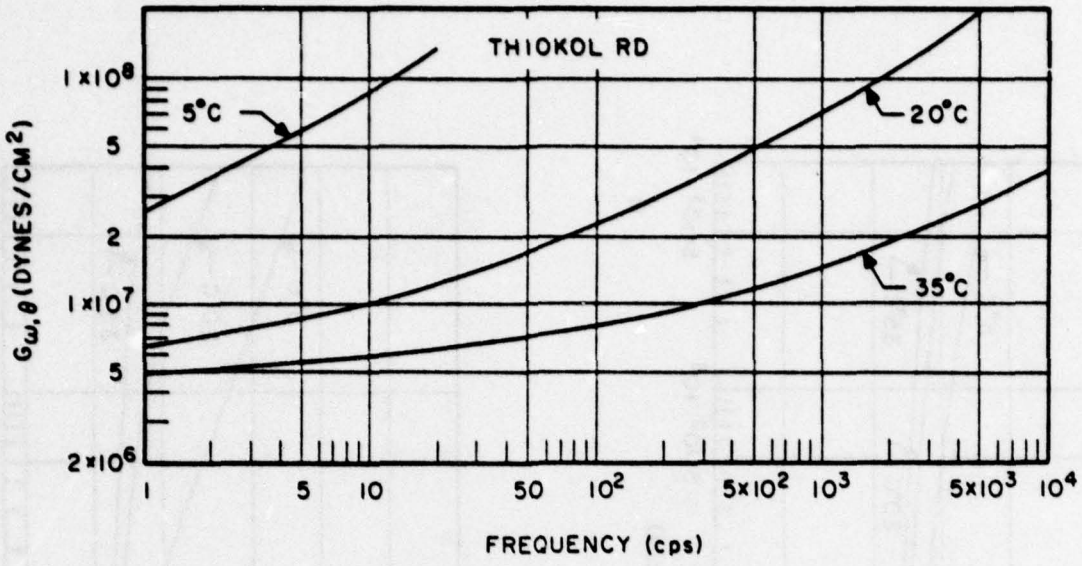
THIOKOL RD
5°C
20°C
35°C
$G_{\omega,\theta}$ (DYNES/CM²)
1x10⁸
5
2
1x10⁷
5
2x10⁶
1
5
10
50
10²
5x10²
10³
5x10³
10⁴
FREQUENCY (cps)

(a)

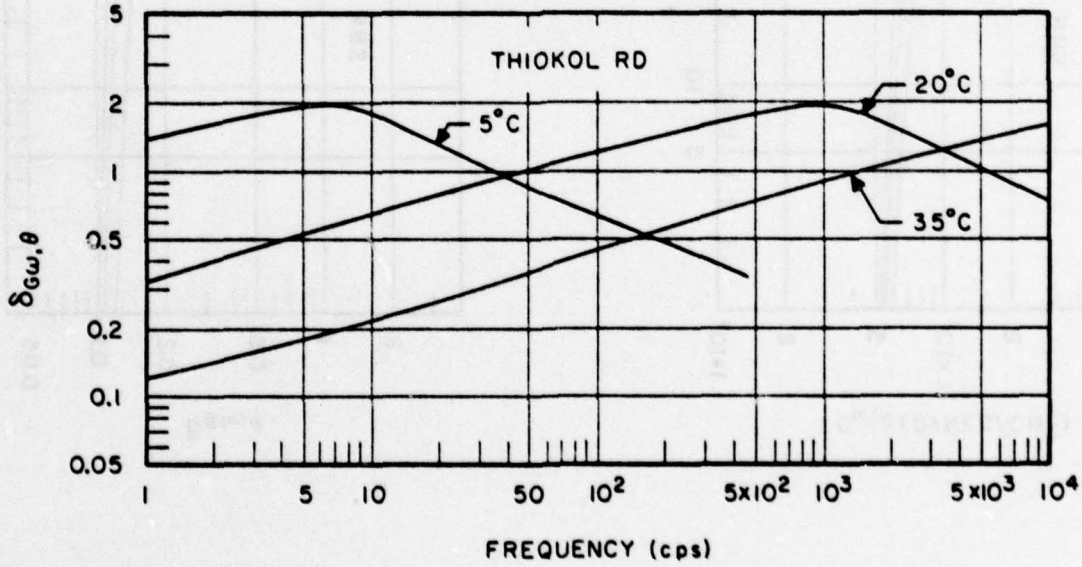
THIOKOL RD
5°C
20°C
35°C
$\delta_{G\omega,\theta}$
5
2
1
0.5
0.2
0.1
0.05
1
5
10
50
10²
5x10²
10³
5x10³
10⁴
FREQUENCY (cps)

(b)

Fig. 9

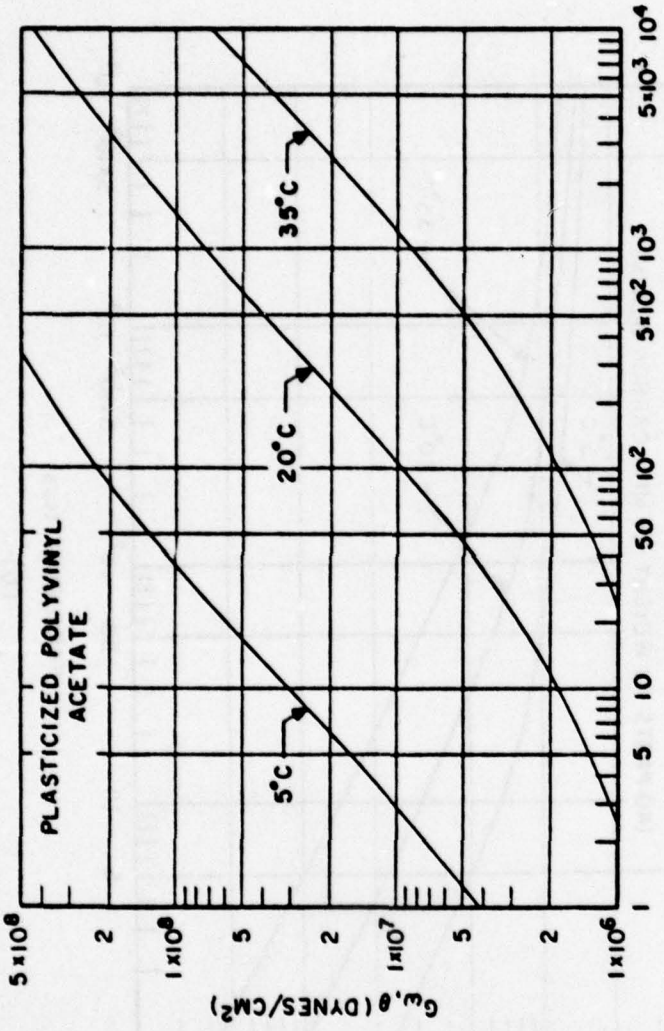
PLASTICIZED POLYVINYL ACETATE
5°C
20°C
35°C
5×10⁸
2
1×10⁸
5
2
1×10⁷
5
2
1×10⁶
1
5
10
50
10²
5×10²
10³
5×10³
10⁴
FREQUENCY (cps)
(a)
PLASTICIZED POLYVINYL ACETATE
5°C
35°C
20°C
10
5
2
1
0.5
0.2
0.1
1
5
10
50
10²
5×10²
10³
5×10³
10⁴
FREQUENCY (cps)
(b)

Fig. 10

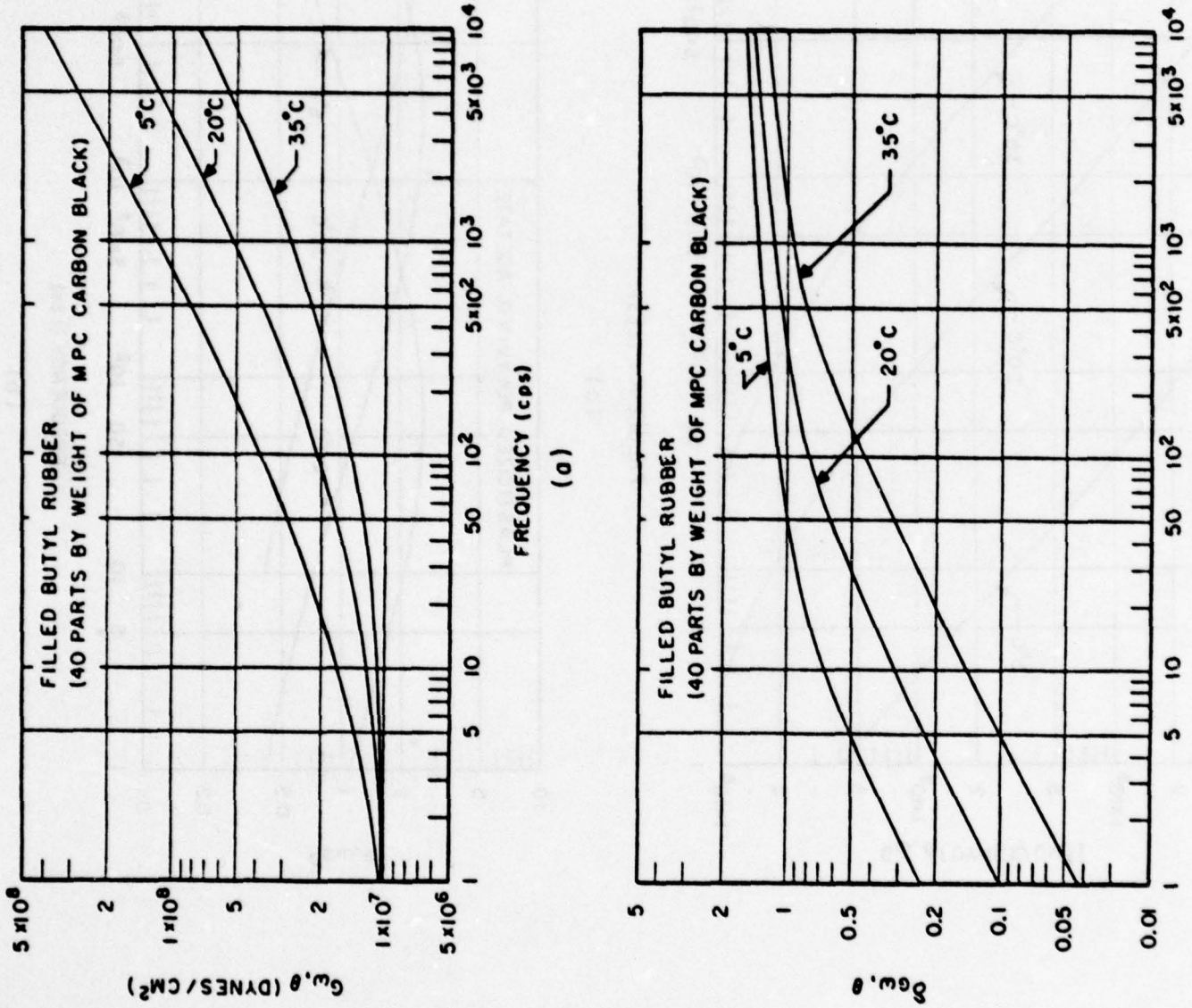
FILLED BUTYL RUBBER
(40 PARTS BY WEIGHT OF MPC CARBON BLACK)
5°C
20°C
35°C
FREQUENCY (cps)
(a)
FILLED BUTYL RUBBER
(40 PARTS BY WEIGHT OF MPC CARBON BLACK)
5°C
20°C
35°C
FREQUENCY (cps)
(b)

Fig. 11

dynamic shear modulus of the natural rubber of Fig. 7 by a factor of approximately 10 above that of the unfilled natural rubber of Fig. 6, and (2) has increased the value of the damping factor, particularly at low frequencies. It should be noted, however, that the addition of carbon black may reduce the damping factor significantly at frequencies above the range considered here.

Although $G_{\omega,\theta}$ and $\delta_{G\omega,\theta}$ increase only by a factor of two or three at room temperature through the four decades in frequency considered in Fig. 7, it is important to remember this fact if satisfactory engineering design is to be achieved when high-frequency vibration is of concern. The same remark can be made for the SBR rubber of Fig. 8. By contrast, the dynamic modulus $G_{\omega,\theta}$ of high-damping rubberlike materials increases greatly with frequency, and $G_{\omega,\theta}$ and $\delta_{G\omega,\theta}$ are strongly dependent on temperature, as the curves of Figs. 9 and 10 for Thiokol RD rubber and plasticized polyvinyl acetate illustrate. Thiokol RD was produced some years ago as an experimental copolymer of butadiene-acrylonitrile and, most probably, chloroprene. It is referred to here because, in analytical studies of antivibration mountings that are described subsequently, its properties have been considered to typify those of high-damping rubbers. Plasticized polyvinyl acetate is a primary constituent of the damping compound Aquaplas.

Butyl rubber is essentially polyisobutylene, in which a small proportion of the isobutylene molecules has been replaced by isoprene (synthetic natural rubber). Like polyisobutylene, butyl rubber is characterized by a diffuse transition region. Thus, although the damping factor takes large values through four decades in frequency at room temperature (Fig. 11), the associated dynamic modulus only increases through the same frequency range by a factor that is approximately equal to 15.

The data of Figs. 6-11 relate to small amplitudes of vibration for which the rubberlike materials exhibit linear behavior. Whereas unfilled and lightly filled rubbers remain linear for increasing strain, up to relatively large strains, the dynamic moduli and damping factors of moderately and heavily filled rubbers show a strong amplitude dependence. This fact is exemplified by the curves of Fig. 12 and 13, which are drawn from Ref. 5. The data of Fig. 12, for example, which refer to exciting frequencies in the range 20-120 Hz, show that the dynamic shear modulus of natural rubber containing 40 parts by volume of medium processing channel (MPC) black per 100 volumes of rubber is more than halved when an alternating shear strain of 3% breaks down the three-dimensional aggregates or so-called matrix of carbon particles within the rubber. The greatly increased damping factor that accompanies this strain amplitude (Fig. 13) is primarily a reflection of the reduction in value of the dynamic modulus--rather than an increase per se in the imaginary part of the complex modulus, which remains essentially constant.

3. SIMPLE MOUNTING SYSTEM

The simple mounting system is shown in Fig. 14, where an item of mass M is supported resiliently by a linear rubberlike material utilized so that its behavior is governed by the complex shear modulus $G^*_{\omega,\theta}$. Here, and subsequently, it is assumed that the temperature remains constant, so that $G^*_{\omega,\theta}$ can be written as

$$G^*_\omega = G_\omega(1 + j\delta_{G\omega}) \quad . \tag{11}$$

The mounted item M is assumed to be supported at its center of gravity, and to vibrate only in the vertical direction; it is excited either by a

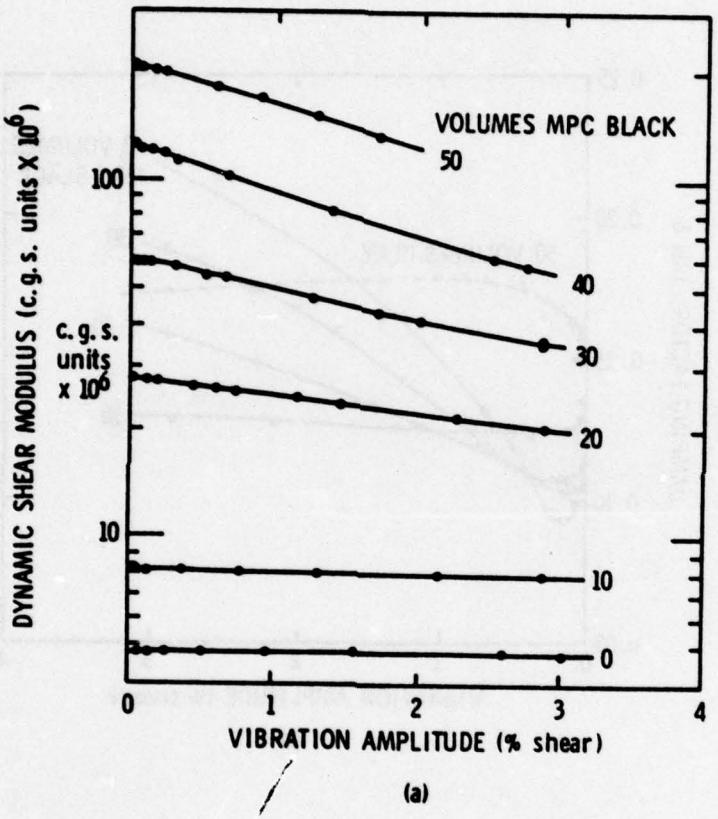
DYNAMIC SHEAR MODULUS (c.g.s. units X 10^6)
c.g.s. units x 10^6
100
10
VOLUMES MPC BLACK
50
40
30
20
10
0
0
1
2
3
4
VIBRATION AMPLITUDE (% shear)
(a)

Fig. 12

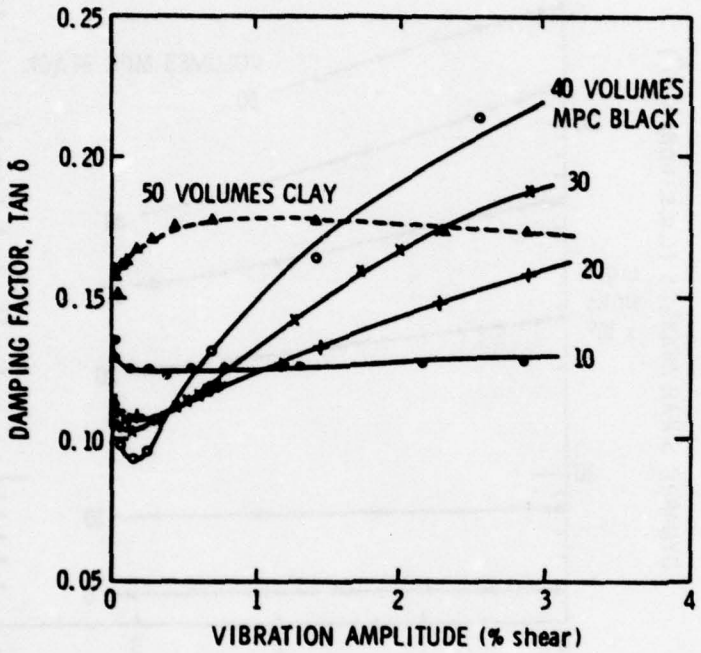
0.25
0.20
0.15
0.10
0.05
0
1
2
3
4
DAMPING FACTOR, TAN δ
VIBRATION AMPLITUDE (% shear)
40 VOLUMES MPC BLACK
30
20
10
50 VOLUMES CLAY
(b)

Fig. 13

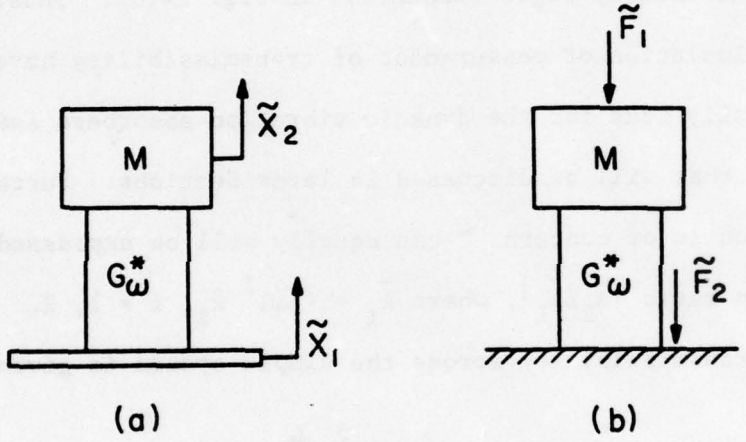

Fig. 14

sinusoidally varying ground displacement $\tilde{x}_1$, as in Fig. 14(a), or by a sinusoidally varying force $\tilde{F}_1$, as in Fig. 14(b).* If the transmissibility T across system (a) is defined as the magnitude of the displacement ratio $|\tilde{x}_2/\tilde{x}_1|$, and if the transmissibility across system (b) is defined as the magnitude of the force ratio $|\tilde{F}_2/\tilde{F}_1|$--then, at any one frequency,

$$T = |\tilde{x}_2/\tilde{x}_1| = |\tilde{F}_2/\tilde{F}_1| \quad , \tag{12}$$

where $\tilde{x}_2$ is the displacement of M in Fig. 14(a) and $\tilde{F}_2$ is the force transmitted to the ideally rigid foundation in Fig. 14(b). Thus, the results of a single calculation or measurement of transmissibility have dual significance. This is equally true for the dynamic vibration absorbers and compound mounting systems that will be discussed in later Sections. Further, because sinusoidal motion is of concern, T can equally well be expressed as the acceleration ratio $|\tilde{A}_2/\tilde{A}_1|$, where $\tilde{A}_i = (j\omega)^2\, \tilde{x}_i$, i = 1, 2.

The transmissibility across the simple system is given[1] by

$$T = \frac{(1 + \delta_{G\omega}^2)^{\frac{1}{2}}}{\{[1 - (\omega/\omega_o)^2 (G_o/G_\omega)]^2 + \delta_{G\omega}^2\}^{\frac{1}{2}}} \quad . \tag{13}$$

From this general equation, the transmissibility of any linear rubberlike material can be calculated, provided that the dependence of G_ω and $\delta_{G\omega}$ upon frequency is known. The quantity G_o is the value of G_ω at the natural frequency ω_o of the system, which is defined as the frequency for which, in the absence of damping, T becomes infinitely large; that is

$$\omega_o^2 = kG_o/M \quad . \tag{14}$$

---

*The tildes, here and henceforth, denote sinusoidally varying quantities.

where the constant k has the dimensions of length. For a rubber mount of cross-sectional area A and length (height) ℓ, reference to Eq. (5) shows that

$$k = 3(A/\ell)(1 + \beta S^2) \quad ; \tag{15}$$

more simply, if the rubber element is used directly in shear, rather than as drawn in Fig. 14, then $k = (A/\ell)$.

The transmissibility of natural rubber, natural rubber filled with carbon black, and Thiokol RD rubber is shown in Fig. 15. Data have been taken from Figs. 6, 7, and 9 for these rubbers and inserted numerically into the expression for transmissibility given by Eq. (13). The natural mounting frequency has been chosen as 5 Hz and the ambient temperature as 20°C. Transmissibility is plotted on a decibel scale as $20 \log_{10} T$ decibels (dB). Negative values of T(dB) mean that the input displacement or force has been attenuated by the introduction of the rubber mounting; positive values of T(dB) mean that undesired magnification has occurred.

An antivibration mounting is required to provide small values of transmissibility at all frequencies that are contained in the Fourier spectrum of the displacement applied to its foundation, as in Fig. 14(a), or in the spectrum of the force applied to, or generated within, the item of equipment or machinery that it supports, as in Fig. 14(b). Thus, an effective antivibration mount should afford

(1) a low natural frequency ω_o,

(2) a low transmissibility at resonance,

and

(3) a transmissibility that decreases rapidly with frequency at frequencies greater than ω_o.

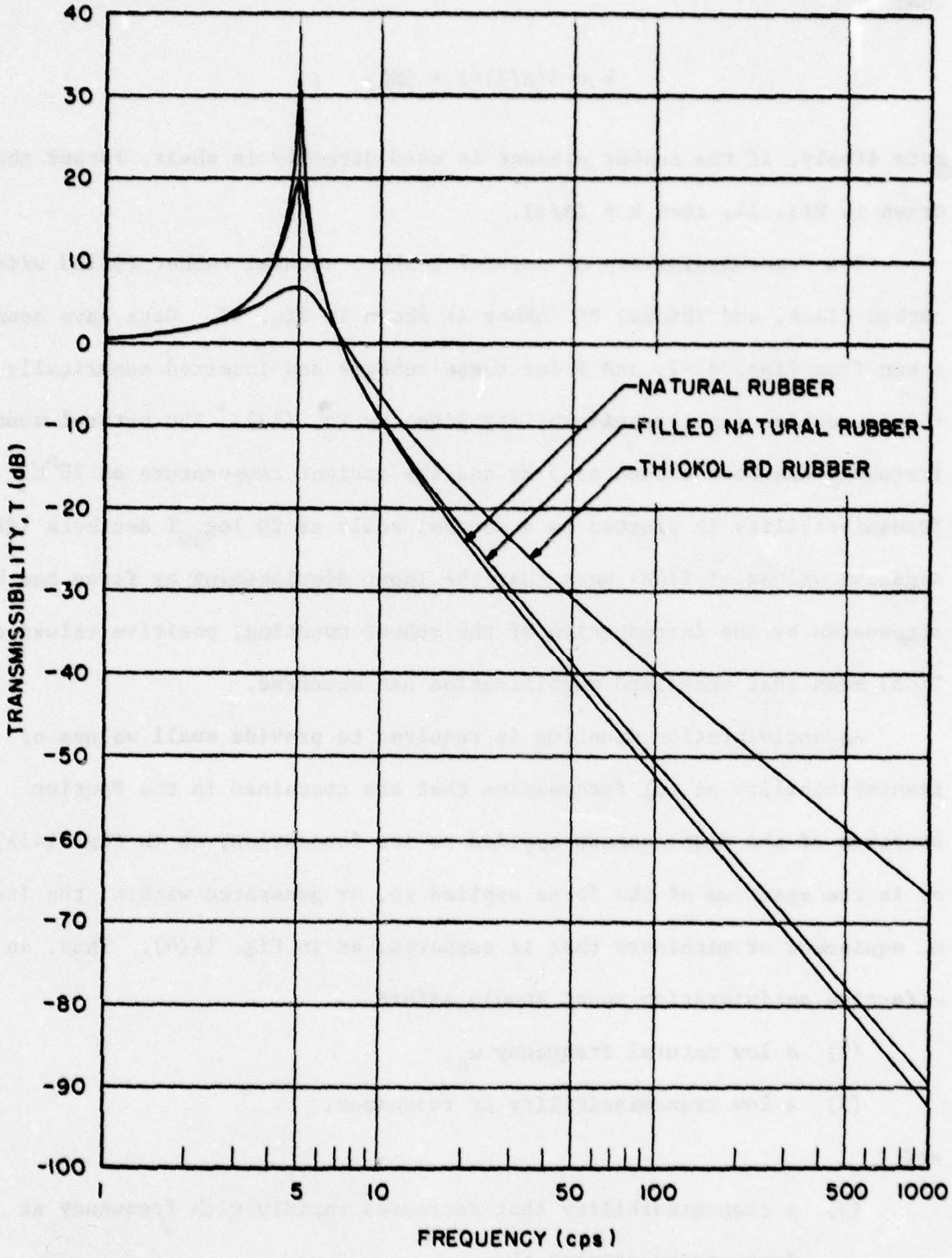
40
30
20
10
0
-10
-20
-30
-40
-50
-60
-70
-80
-90
-100
TRANSMISSIBILITY, T (dB)
1
5
10
50
100
500
1000
FREQUENCY (cps)
NATURAL RUBBER
FILLED NATURAL RUBBER
THIOKOL RD RUBBER

Fig. 15

A low natural frequency can be obtained by employing a mount of suitably low stiffness (or by increasing the mass of the mounted item). The natural frequency of a simple mounting system is plotted versus the static deflection of its antivibration mount in Fig. 16. Because the lateral stability of the mounting system must be maintained, the extent to which the stiffness of the mounting can be reduced is limited. In practice, the natural frequencies of mounting systems are generally selected to be equal to or greater than 5 Hz. The use of a high-damping rubber can ensure that the resonant transmissibility will take small values.

The rate at which transmissibility decreases with frequency above ω_o varies considerably with the type of rubberlike material utilized in the mounting. Transmissibility decreases most rapidly with frequency for natural and other low-damping rubbers--essentially in proportion to $1/\omega^2$ (12 dB/octave). The transmissibility of Thiokol RD and of other high-damping rubbers decreases at a much slower rate. This is one of the major drawbacks to the use of high-damping rubbers in antivibration mountings; a second drawback is the low resistance to creep of high-damping rubbers. The poor performance of these rubbers at high frequencies is predominantly caused by the significant increase in value of their dynamic moduli G_ω with frequency (as in Figs. 9 and 10). Contrary to the supposition often made, the inherent high damping of the rubbers has relatively small influence upon the values of transmissibility above resonance.[1] To explain these facts, it is helpful to refer again to the general transmissibility equation [Eq. (13)]. Thus, at frequencies well above ω_o, this equation may be approximated as

$$T \approx \left(\frac{G_\omega}{G_o}\right) \frac{(1 + \delta_{G\omega}^2)^{1/2}}{(\omega/\omega_o)^2} \quad . \tag{16}$$

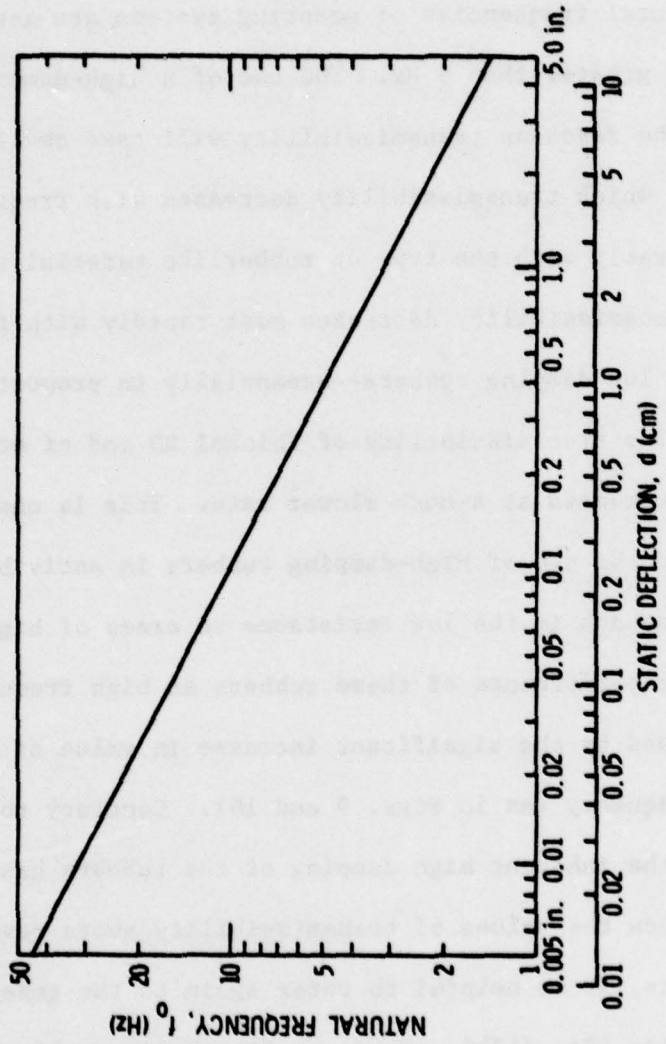
NATURAL FREQUENCY, f_o (Hz)
50
20
10
5
2
1
0.005 in.
0.01
0.02
0.05
0.1
0.2
0.5
1.0
2
5
10
5.0 in.
0.01
0.02
0.05
0.1
0.2
0.5
1.0
2
5
10
STATIC DEFLECTION, d (cm)

Fig. 16

The values of G_ω possessed by natural and other low-damping rubbers increase only slowly with frequency, and $\delta_{G\omega}$ remains small; consequently, T decreases almost directly in proportion to the square of the exciting frequency. By contrast, the values of G_ω possessed by high-damping rubbers increase rapidly with frequency--a fact that, as mentioned, is primarily responsible for the large values of transmissibility observed for these rubbers at high frequencies.[1]

Although natural rubber and other low-damping rubbers such as Neoprene are the rubbers normally utilized in antivibration mountings, high-damping rubbers would have greater application if they could be produced such that their dynamic moduli G_ω remained constant or increased only slowly with frequency. To date, it has proved impossible to satisfy this requirement; however, the suggestion has been made[1] that natural rubber be used mechanically in parallel with a high-damping rubber of suitably smaller cross-sectional area. In this way, the dynamic modulus of the combination of rubbers can be adjusted to increase relatively slowly with frequency, while the associated damping factor takes significant values intermediate to those of the constituent rubbers, as in Fig. 17. Here, the parameter a is the ratio of the cross-sectional area of the high- to the low-damping rubber.

It is appropriate now to mention some reasons why larger values of transmissibility (reduced isolation) may occur at frequencies above resonance than the curves of Fig. 15 predict. These reasons (a) may simply be mechanical or (b) they may be basic. Thus,

(a) Vibration isolation may be impaired by mechanical links that have significant stiffness and, hence, that bypass, to some extent, the antivibration mounts. For example, vibration from a resiliently mounted diesel engine may reach its foundation via an exhaust pipe that is still rigidly connected to a surrounding enclosure, or it may reach the

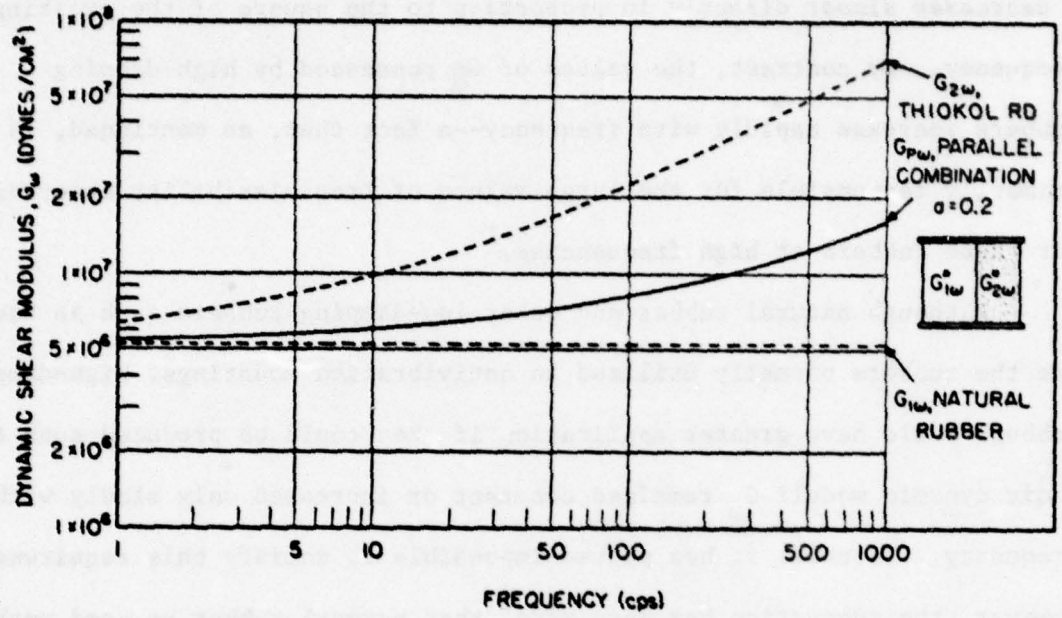
DYNAMIC SHEAR MODULUS, G_{ω} (DYNES/CM^2)
1×10^8
5×10^7
2×10^7
1×10^7
5×10^6
2×10^6
1×10^6
1
5
10
50
100
500
1000
FREQUENCY (cps)
$G_{2\omega}$, THIOKOL RD
$G_{P\omega}$, PARALLEL COMBINATION
a=0.2
$G^*_{1\omega}$
$G^*_{2\omega}$
$G_{1\omega}$, NATURAL RUBBER

(a)

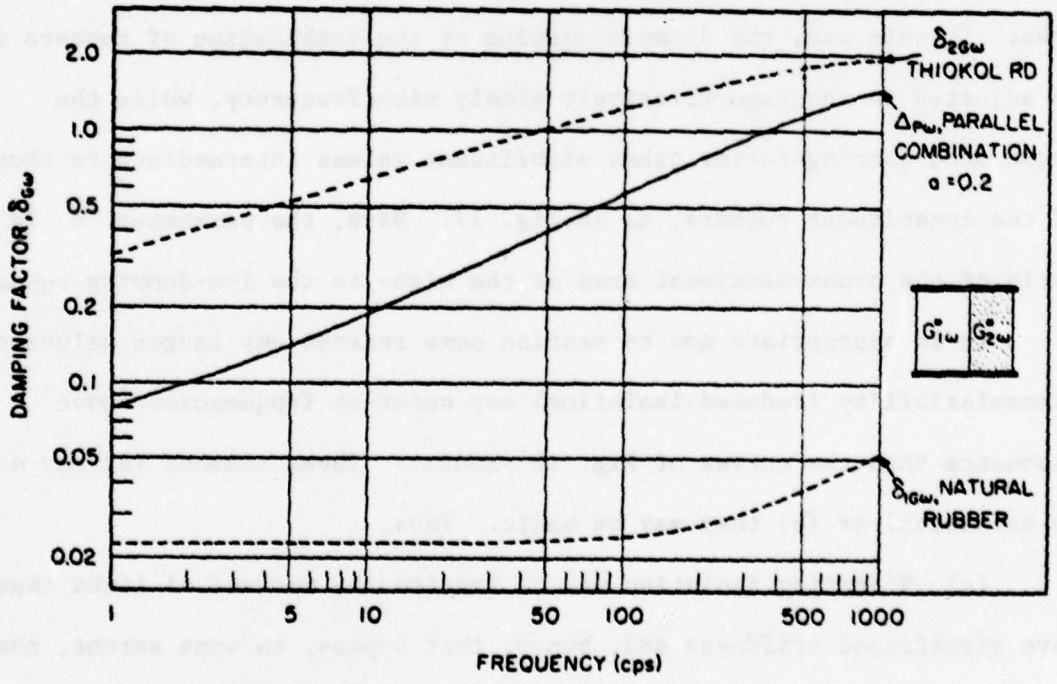
DAMPING FACTOR, $\delta_{G\omega}$
2.0
1.0
0.5
0.2
0.1
0.05
0.02
1
5
10
50
100
500
1000
FREQUENCY (cps)
$\delta_{2G\omega}$ THIOKOL RD
$\Delta_{P\omega}$, PARALLEL COMBINATION
a=0.2
$G^*_{1\omega}$
$G^*_{2\omega}$
$\delta_{1G\omega}$, NATURAL RUBBER

(b)

Fig. 17

foundation via a bearing pedestal that supports a rotating shaft that extends from the engine.

(b) Vibration isolation may be predicted inadequately at higher frequencies for the basic reason that the mounting system of Fig. 14 is too simplified a model of the practical situation. The mounting system can be criticized for three primary reasons, which are outlined in what follows:

First, values of transmissibility have been derived theoretically from knowledge of the mechanical properties of rubbers measured at small dynamic strains. It may be thought, therefore--particularly in the case of rubbers filled with substantial proportions of carbon black--that the performance of the rubbers under greater strains would differ from the performance predicted by curves such as those of Fig. 15. However, two comments may be made. First, although it is possible that the character of the transmissibility curves of filled rubber will be strain dependent near resonance ($\omega \approx \omega_o$), well designed mounting systems normally possess natural frequencies that fall significantly below the spectrum of frequencies that the mountings are required to isolate. In consequence, the exciting frequencies should fall where $\omega >> \omega_o$, and where the strain is relatively small and is decreasing rapidly as ω increases. Second, even should a filled rubber exhibit nonlinear properties at frequencies above resonance, the dynamic stiffness of the rubber would decrease in magnitude (Fig. 12), so that the transmissibility of the mounting system would also decrease; that is, the effectiveness of the mounting would become greater.

Second, "wave effects" may be observed at high frequencies[1] when the mount dimensions become comparable with multiples of the half-wavelengths of the elastic waves traveling through the mounting. Alternatively, wave effects may be thought of as occurring when the elasticity and the distributed mass of the rubber mounting interact at high frequencies. Wave effects are evident, for example, in the measured transmissibility curves of Fig. 18,

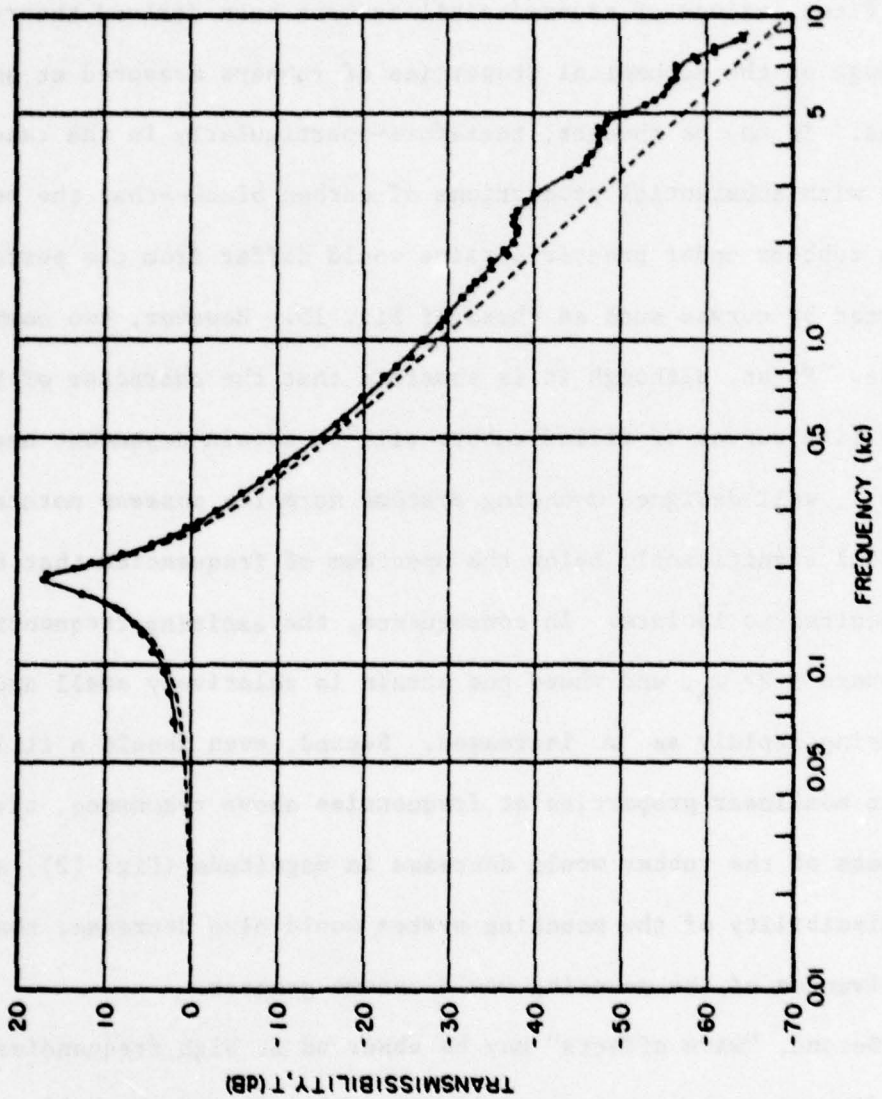
TRANSMISSIBILITY, T (dB)
20
10
0
-10
-20
-30
-40
-50
-60
-70
FREQUENCY (kc)
10
5
1.0
0.5
0.1
0.05
0.01

Fig. 18

which relates to a small natural-rubber mount containing 40 parts by weight of EPC carbon black,[1] and of Fig. 19, which relates to a helical-spring and two natural-rubber mounts.[6] Although many pronounced wave resonances occur in the transmissibility curves of springs, as in Fig. 19, the resonances in the transmissibility curves of practical rubber mounts are not always of primary concern. In fact, (a) the resonances are suppressed reasonably well by the internal damping of the rubber mounts, and (b), as will be demonstrated, even the first of the wave resonances invariably occurs at frequencies in excess of 20 ω_o, where significant isolation has already been achieved.

Third, the mounted item M may not behave as an ideally rigid mass. For example, the flanges or feet on which M is mounted may fail to remain ideally rigid and may resonate because of their poor design, so giving rise to other peaks in the transmissibility curve at high frequencies--even though the bulk of the mounted item may continue to behave as a lumped mass well into the high-frequency region. The peaks in the transmissibility curve may well be troublesome because the internal damping of the metal machine feet will be at least 5 or 10 times smaller than the damping of the rubber mounts in which the previously discussed wave effects occurred. The feet may protrude from the bottom of the mounted item, or from its sides. This will be the case if the usually beneficial step is taken to locate the mounts in a plane that passes through the center of gravity of the mounted item (so minimizing the rocking motion it experiences if subjected to horizontally directed forces). Analyses of a mounted item with self resonances will be described subsequently. Other discussions of the problem appear in Ref. 6-9.

3.1 Wave Effects

The geometry of the rubber components of antivibration mountings is frequently complex, which makes precise theoretical calculations of

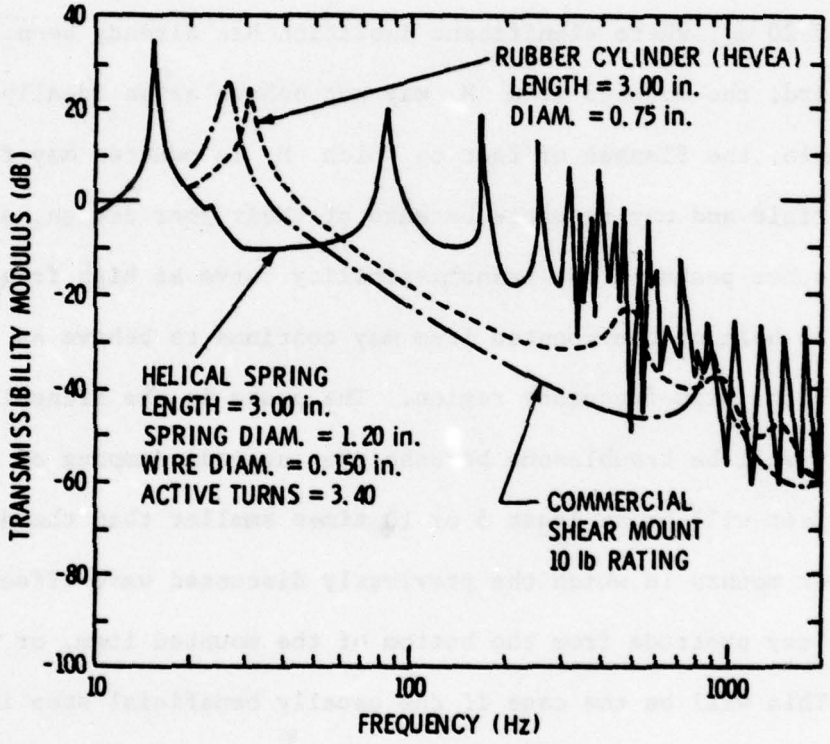
RUBBER CYLINDER (HEVEA)
LENGTH = 3.00 in.
DIAM. = 0.75 in.
HELICAL SPRING
LENGTH = 3.00 in.
SPRING DIAM. = 1.20 in.
WIRE DIAM. = 0.150 in.
ACTIVE TURNS = 3.40
COMMERCIAL
SHEAR MOUNT
10 lb RATING
TRANSMISSIBILITY MODULUS (dB)
FREQUENCY (Hz)
40
20
0
-20
-40
-60
-80
-100
10
100
1000

Fig. 19

transmissibility difficult at high frequencies. A guide to the character of wave effects in antivibration mountings has been obtained, however, by considering the transmissibility of "mountings" that obey the simple wave equation for the longitudinal vibration of a rod of uniform cross section. This approach has been taken by all earlier workers[1] although, on two occasions,[10,11] "mountings" have also been considered to obey the wave equation for a transversely vibrating uniform beam. A disadvantage of these analyses is that they relate to "long" rods and beams with lateral dimensions that remain small in comparison with the wavelength. However, wave effects in a cylindrical rodlike mount of significant lateral dimensions have been analyzed[1] using a "corrected" wave equation given by A. E. H. Love. In the Love theory, the radial motion of the plane cross sections of the mount caused by axial compression and extension is, in some measure, accounted for.

The transmissibility T derived from the simple wave equation for a "long" rod with internal damping can be written[1]

$$T = \left|[\cos n^*\ell - \gamma(n^*\ell)\sin n^*\ell]\right|^{-1} \quad , \tag{17}$$

where n^* is the complex wavenumber of the rodlike mount. The mass ratio

$$\gamma = \frac{M}{M_R} = \frac{M}{\rho A \ell} \quad , \tag{18}$$

where ρ and A are the density and uniform cross-sectional area of the mount and ℓ is its length. The dimensionless product $(n^*\ell)$ is conveniently written as

$$(n^*\ell) = (p + jq) \quad , \tag{19}$$

where

$$p = \frac{n\ell}{D_{E\omega}} \left(\frac{E_o}{E_\omega}\right)^{\frac{1}{2}} \left(\frac{D_{E\omega} + 1}{2}\right)^{\frac{1}{2}} \tag{20}$$

and

$$q = -\frac{n\ell}{D_{E\omega}} \left(\frac{E_o}{E_\omega}\right)^{\frac{1}{2}} \left(\frac{D_{E\omega} - 1}{2}\right)^{\frac{1}{2}} \quad . \tag{21}$$

In these equations, the dynamic Young's modulus $E_\omega = E_o$ at the natural mounting frequency ω_o,

$$n = \omega(\rho/E_o)^{\frac{1}{2}} \quad , \tag{22}$$

and

$$D_{E\omega} = (1 + \delta_{E\omega}^2)^{\frac{1}{2}} \quad . \tag{23}$$

It can be shown that, if the dimensionless quantity $n\ell$ takes the value N_R when $\omega = \omega_o$,

$$n\ell = (\omega/\omega_o)\ N_R \rightarrow (\omega/\omega_o)(\gamma)^{-\frac{1}{2}} \quad . \tag{24}$$

Consequently, as $n\ell$ is varied, corresponding values of ω will be specified because N_R and ω_o will have been designated. In turn, values of E_ω and $\delta_{E\omega}$ will be known for each value of ω (e.g., Figs. 6-11) so that the expressions for p and q can be determined. In practice, it appears that the mass ratio for the majority of mounting systems take values in the range $50 < \gamma < 350$. The smallest value of γ yields the <u>least</u> favorable transmissibility curve. Thus, the wave resonances correspond closely with the natural frequencies

$$\omega_i = i\pi\omega_o \sqrt{\gamma} \quad , \qquad i = 1, 2, 3, \ldots \tag{25}$$

of the mount when clamped rigidly at each end; consequently, the smaller the value of γ, the lower the frequency at which the first wave resonance occurs ($i = 1$) and the more apparent the departure of the transmissibility curve from the predictions of the simple one-degree-of-freedom theory (e.g., Fig. 15). Note that, if $\gamma > 50$, $\omega_1 > \pi\omega_o \sqrt{50} > 20\ \omega_o$.

The transmissibility T determined from the Love theory is identical in form to Eq. (17)[1]:

$$T = \left|[\cos N^*\ell - \gamma(N^*\ell) \sin N^*\ell]\right|^{-1} \quad . \tag{26}$$

In this equation, the dimensionless parameter $N^*\ell$ represents the complex number $(P + jQ)$, where P and Q are functions of the foregoing quantities p and q. In the case of rubberlike materials for which $E_\omega = 3G_\omega$ and $\delta_{E\omega} = \delta_{G\omega}$ [Eqs. (9) and (10)], the expressions for P and Q can be written as

$$P = \tfrac{1}{4}[\mu + (\mu^2 + \chi^2)^{\frac{1}{2}}]^{\frac{1}{2}} \tag{27}$$

and

$$Q = \tfrac{1}{4}[-\mu + (\mu^2 + \chi^2)^{\frac{1}{2}}]^{\frac{1}{2}} \quad , \tag{28}$$

where

$$\mu = [(p^2 - q^2) - \phi^2(p^2 + q^2)^2]/\xi \quad , \tag{29}$$

$$\chi = 2\,pq/\xi \quad , \tag{30}$$

and

$$\xi = [1 - 2\phi^2(p^2 - q^2) + \phi^4(p^2 + q^2)^2] \quad , \tag{31}$$

$$\phi = (r/2\ell) \quad . \tag{32}$$

The quantity r is the radius of gyration of an elementary section of the mount about its longitudinal axis; for example, if the mount has a circular cross-section and has a diameter D, then $r = D/2\sqrt{2}$.

Wave effect calculations based on the "long" rod theory [Eq. (17)] are plotted in Fig. 20 for values of the mass ratio $\gamma = 50$, 100, and 250. It has been assumed that the dynamic Young's modulus and associated damping factor are frequency independent, that $\delta_E = 0.1$, and that the first natural frequency of the system, for which $n\ell = N_R = 0.141$ when $\gamma = 50$--is again $f_o = \omega_o/2\pi = 5$ Hz. The curves of Fig. 20, which may be thought of as describing the transmissibility of natural rubber mounts that are heavily reinforced with carbon black, show how the level to which T is increased by the wave resonances depends upon the value of γ. As mentioned previously, the occurrence of wave resonances becomes of less concern as γ becomes larger; from this point of view, therefore, it is desirable to utilize anti-vibration mounts as near their maximum rated load as possible, thereby making γ a relatively large quantity.

Wave effect calculations based on the Love theory [Eq. (26)] are plotted in Fig. 21 for a representative value of $\gamma = 200$ and for cylindrical mounts having a length-to-diameter ratio $\ell/D = 5$. Values of $E_\omega = 3G_\omega$ and $\delta_{E\omega} = \delta_{G\omega}$ drawn from Figs. 6, 7, and 9 for unfilled natural rubber, natural rubber filled with carbon black, and the high damping rubber Thiokol RD have been inserted numerically into Eqs. (20) and (21) for p, q, and hence into Eqs. (27) and (28) for P and Q. Transmissibility curves calculated from the simple one-degree-of-freedom theory [Eq. (13)] for the same three rubberlike materials are redrawn in Fig. 21 for comparison. Although the transmissibility of the natural-rubber mountings is increased appreciably by the occurrence of wave resonances at high frequencies, the peak values of transmissibility occur at significantly lower levels than would be

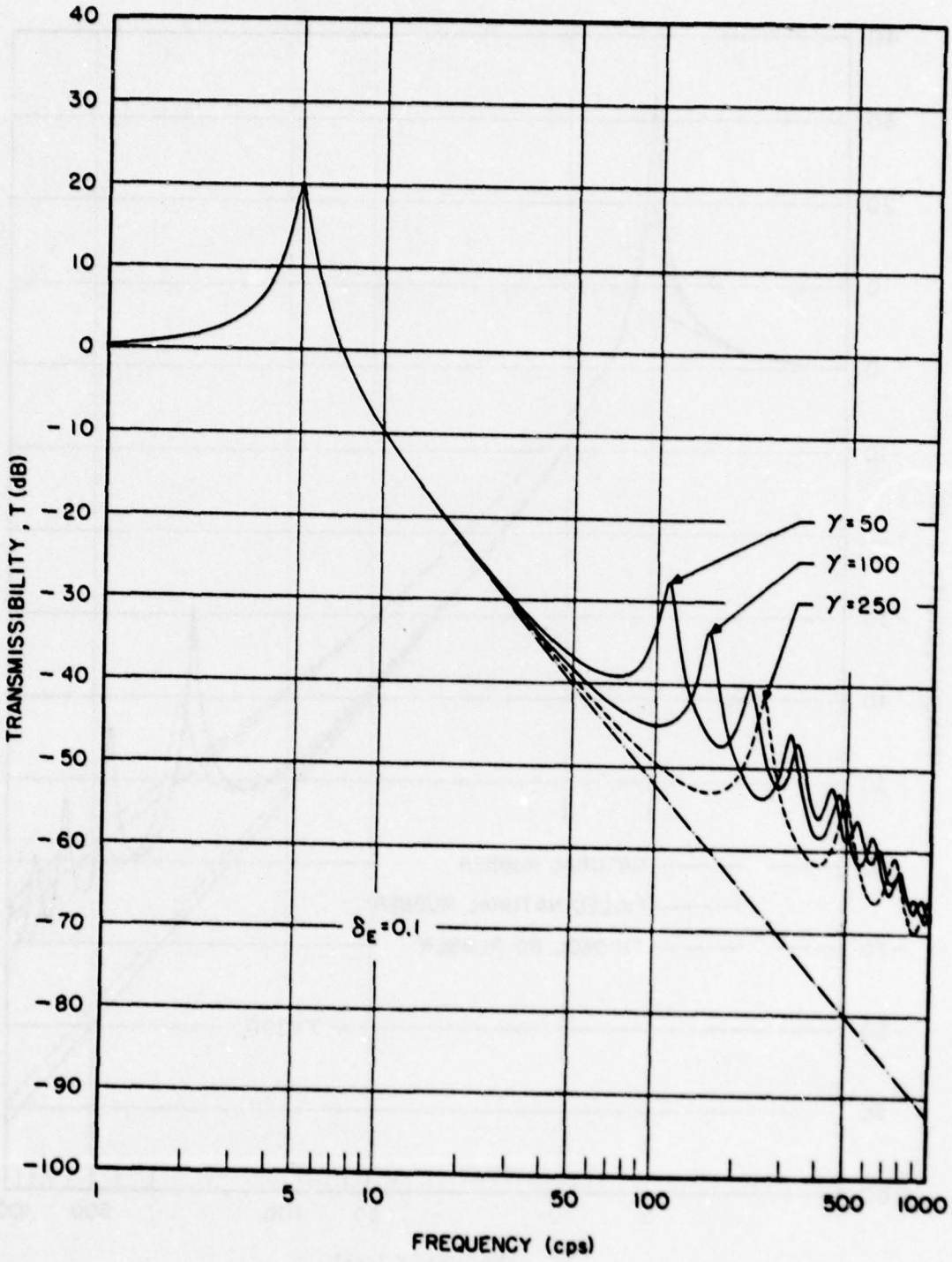
40
30
20
10
0
-10
-20
-30
-40
-50
-60
-70
-80
-90
-100
TRANSMISSIBILITY, T (dB)
1
5
10
50
100
500
1000
FREQUENCY (cps)
γ=50
γ=100
γ=250
δE=0.1

Fig. 20

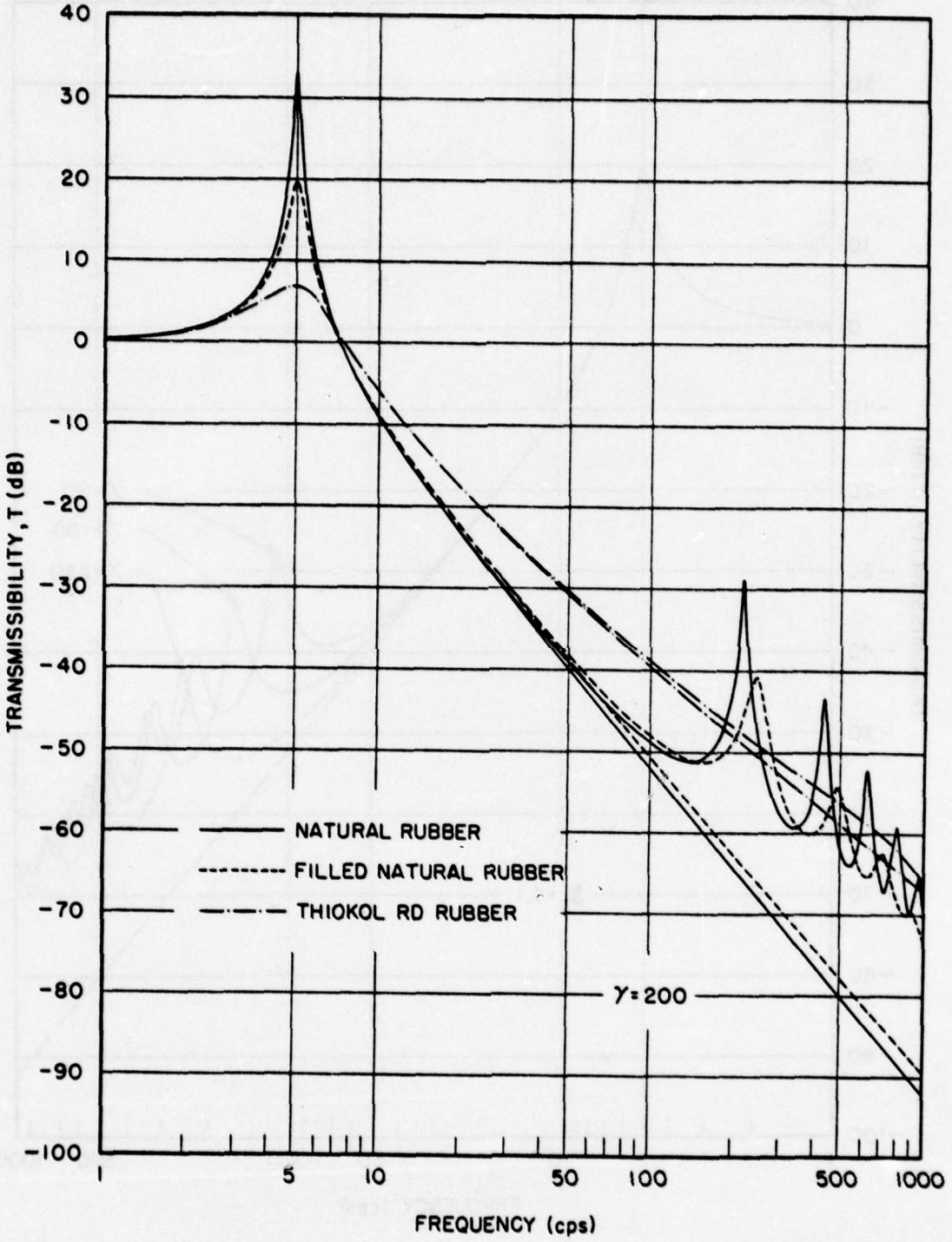
40
30
20
10
0
-10
-20
-30
-40
-50
-60
-70
-80
-90
-100
TRANSMISSIBILITY, T (dB)
1
5
10
50
100
500
1000
FREQUENCY (cps)
NATURAL RUBBER
FILLED NATURAL RUBBER
THIOKOL RD RUBBER
γ = 200

Fig. 21

observed if $\gamma = 50$. Wave effects increase the transmissibility of the Thiokol RD rubber by a relatively small amount; in fact, the simple theory provides a remarkably accurate prediction of the transmissibility of this and other high-damping rubbers. On the other hand, the transmissibility of the heavily filled natural rubber is increased by approximately 20 dB at high frequencies as compared with the prediction of the simple theory. However, if γ were larger and if the ratio ℓ/D were smaller than considered here, as could well be the case in practice, the wave resonances would shift to higher frequencies and to lower levels, and the transmissibility curve would roll off at frequencies following the first wave resonance ($\omega > \omega_1$) more rapidly than observed at present.

3.2 Nonrigid Flanges

An item of equipment or machinery supported by nonrigid (multiresonant) flanges or feet is shown in Fig. 22. This is not a contrived problem; in fact, one does not have to look far to find examples of such situations. For instance, a marine engine attached to a subframe having significant unsupported length is shown in Fig. 23; here, the subframe is fashioned so that the mounting points lie on the same horizontal as the center of gravity of the engine.[12]

A guide to the transmissibility T across the simple system of Fig. 22 has been obtained by visualizing the feet of the mounted item as short shear beams; that is, as beams with length-to-depth ratios of approximately three or less for which it can realistically be assumed that the beam deflection due to bending is much less than the deflection due to shear.[13] The mounts are assumed here, and subsequently, to have the complex stiffness

$$K^* = K(1 + \delta_K) \quad , \tag{33}$$

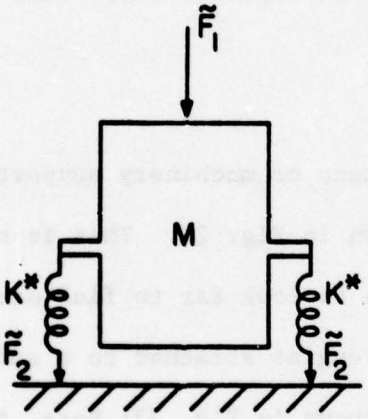

Fig. 22

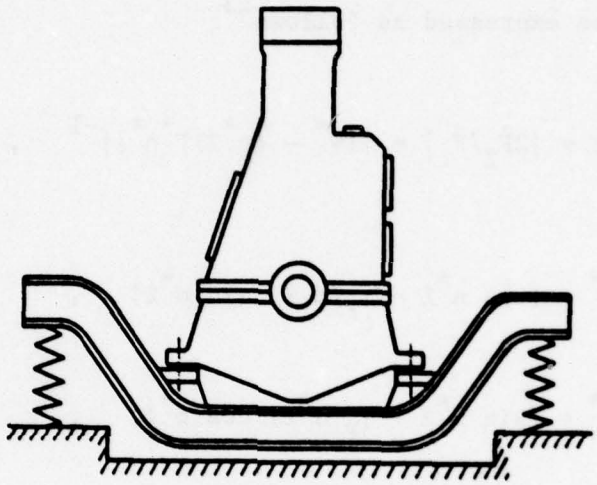

(b)

Fig. 23

where K and the damping factor δ_K are directly analogous to the previously utilized quantities kG_ω [k is specified by Eq. (15)] and $\delta_{E\omega} = \delta_{G\omega}$. Because future discussions will be restricted to small values of $\delta_K \approx 0.05$, the quantities K and δ_K are taken to be frequency independent, a justifiable assumption for natural, neoprene, SBR, and other low-damping rubbers.

With the foregoing assumptions, the transmissibility across the system of Fig. 22 can be expressed as follows[13]:

$$T = |2\tilde{F}_2/\tilde{F}_1| = |[\Psi^* - (n^*\ell)\Gamma^*\eta^*]|^{-1} \quad , \tag{34}$$

where

$$\Psi^* = [\cos n^*\ell - \gamma_F(n^*\ell) \sin n^*\ell] \quad , \tag{35}$$

$$\eta^* = [\sin n^*\ell + \gamma_F(n^*\ell) \cos n^*\ell] \quad , \tag{36}$$

$$n^*\ell = (p + jq) \quad , \tag{37}$$

and

$$\Gamma^* = \Gamma(1 + j\delta_F)/(1 + j\delta_K) \quad . \tag{38}$$

In these equations, n^* is the complex wavenumber of the shear-beam feet, ℓ is their length,

$$\gamma_F = M/2M_F \quad , \tag{39}$$

and

$$\Gamma = K_F/K \quad , \tag{40}$$

where M_F, K_F, and δ_F are the mass, static stiffness, and damping factor of each shear-beam foot. In addition,

$$p = \frac{n\ell}{D_F}\left(\frac{D_F + 1}{2}\right)^{\frac{1}{2}} \tag{41}$$

and

$$q = \frac{-n\ell}{D_F}\left(\frac{D_F - 1}{2}\right)^{\frac{1}{2}} , \tag{42}$$

where

$$D_F = (1 + \delta_F^2)^{\frac{1}{2}} \tag{43}$$

and

$$n\ell = (\omega/\omega_o)\, N_F = \Omega N_F . \tag{44}$$

Here, the natural frequency ω_o of the mounting system is given by the equation

$$\omega_o^2 = \frac{2KK_F}{M(K + K_F)} = \frac{2K}{M}\left(\frac{\Gamma}{1 + \Gamma}\right) , \tag{45}$$

and N_F is the value of $n\ell$ for which the first peak value of T would be observed (when $\omega = \omega_o$) if $\delta_F = \delta_K = 0$. A close guide to this value of N_F can be obtained from the relation

$$N_F \approx [(\gamma_F + 1)\Gamma + \gamma_F]^{-\frac{1}{2}} \tag{46}$$

or, if both γ_F and Γ are large, from

$$N_F \approx (\gamma_F \Gamma)^{-\frac{1}{2}} . \tag{47}$$

Therefore, as the angular frequency ω of the impressed force is varied, corresponding values of $n\ell$ are specified by Eq. (44), and the expressions for p and q, and hence T, may be evaluated.

Representative calculations of T are plotted as a function of the frequency ratio $\Omega = \omega/\omega_o$ in Fig. 24, where the shear-beam feet have 1/40 of the mass of the mounted item ($\gamma_F = M/2M_F = 40$) and stiffnesses 5, 25, and 100 times greater than that of the mounts supporting them from below; the damping factors $\delta_K = 0.05$ and $\delta_F = 0.01$. The resonances of the shear-beam feet, which are responsible for the pronounced peak values of T at high frequencies, are seen to be of the least consequence when the stiffness ratio Γ is largest. In fact, the resonances will advantageously occur at the highest possible frequency when the ratio of the static stiffness to mass of the feet is made as large as possible; that is, in this simple example, when the shear-beam feet are made as short as possible. Their first resonance occurs at the approximate frequency

$$\omega_1 \approx (\pi\omega_o/2)\sqrt{(\gamma_F\Gamma)} = (\pi/2)\sqrt{(K_F/M_F)} \quad , \tag{48}$$

provided that γ_F and Γ are relatively large ($\Gamma > 5$).

4. DYNAMIC VIBRATION ABSORBER

The dynamic vibration absorber is a mechanical device (mass and damped spring), which is attached to a vibrating item, as in Fig. 25, to minimize its displacement amplitude at resonance or to minimize the force transmissibility from it at resonance. When attached to a mass-spring vibrator with negligible damping, mass M_1, and reference frequency $\omega_o = [K_1/(M_1 + M_2)]^{\frac{1}{2}}$, the dynamic vibration absorber with viscous damping (parallel spring and dashpot) is said to have optimum tuning when the tuning ratio[1]

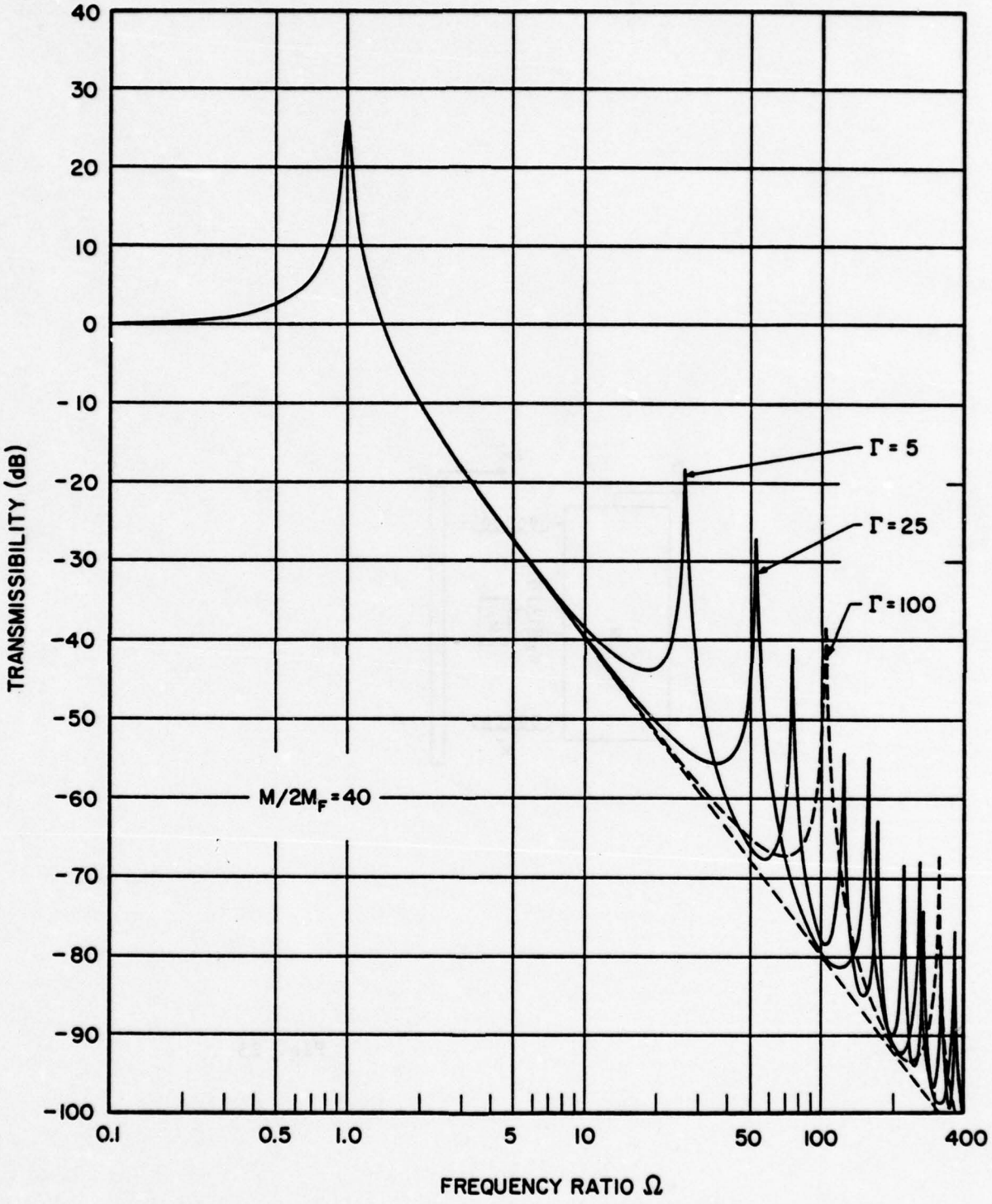
40
30
20
10
0
-10
-20
-30
-40
-50
-60
-70
-80
-90
-100
TRANSMISSIBILITY (dB)
0.1
0.5
1.0
5
10
50
100
400
FREQUENCY RATIO Ω
Γ = 5
Γ = 25
Γ = 100
M/2M_F = 40

Fig. 24

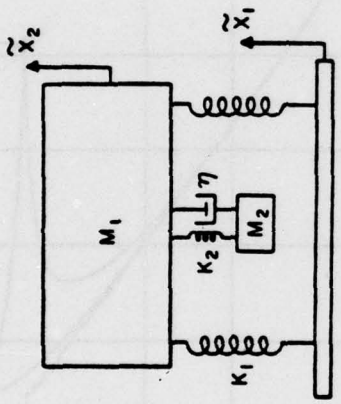

Fig. 25

$$n = \omega_a/\omega_o = \mu^{1/2} = \left(\frac{M_1}{M_1 + M_2}\right)^{1/2} \quad , \tag{49}$$

where $\omega_a = \sqrt{(K_2/M_2)}$ is the resonant frequency to which the absorber should be tuned and M_2 is the absorber mass. The absorber is said to have optimum damping when the damping ratio[1]

$$\delta_R = [(3/8)(1 - \mu)]^{1/2} \quad , \tag{50}$$

where $\delta_R = (\omega_a \eta/2K_2)$; K_2 is the stiffness of the absorber spring, and η is the required coefficient of viscosity of the absorber dashpot. For these values of tuning and damping, the maximum transmissibility becomes

$$T_{max} = \left(\frac{1 + \mu}{1 - \mu}\right)^{1/2} \quad . \tag{51}$$

For example, if $M_2 = M_1/5$, then $\mu = 5/6 = 0.8333$, $\delta_R = 0.25$, and $n = 0.9129$; $T_{max} = 3.317 = 10.4$ dB.

For a dynamic absorber in which the absorber stiffness and damping are provided by a low-damping rubberlike material, the optimum absorber tuning is again given by Eq. (49). The optimum solid-type damping factor is given by the following equation:

$$\delta_G = \left(\frac{1 - \mu}{8\mu}\right)^{1/2} [\Omega_a(2 + \Omega_a^2)^{1/2} + \Omega_b(2 + \Omega_b^2)^{1/2}] \left(\frac{10.5 - \mu}{10}\right) \left(\frac{1 - \Omega_a}{\Omega_b - 1}\right)^{1/2} \quad . \tag{52}$$

In this equation,

$$\Omega_{a,b}^2 = 1 \mp \left(\frac{1 - \mu}{1 + \mu}\right)^{1/2} \quad . \tag{53}$$

For example, if $M_2 = M_1/5$, then $\mu = 0.8333$ again, $n = 0.9129$, and $\delta_G = 0.569$. T_{max} will now be somewhat <u>greater</u> than $3.317 = 10.4$ dB.

Increased effectiveness in suppressing resonant vibration can be achieved through the use of a so-called three-element dynamic absorber, as described in Ref. 14. Conventional dynamic absorbers are also of value in suppressing the resonant vibration of undamped cantilever beams,[1] and in suppressing the vibration of virtually undamped circular plates.[15] In the former case (Fig. 26), optimum tuning and damping parameters are shown graphically in Figs. 27-30; maximum values of transmissibility ($T = |\tilde{F}_1/\tilde{F}_o|$) are plotted in Figs. 31 and 32. (In Figs. 27-30, ω_m is the frequency of the fundamental and second beam resonances to which the absorber is tuned, and $\gamma = M_a/M_b$, where M_a and M_b are the absorber and beam masses, respectively.) In the latter case of circular plates, the optimum tuning and damping parameters can be listed as in Tables II and III.

Table II. Optimum values of the frequency ratio (ω_a/ω_m), the damping ratio δ_R, and the corresponding values of maximum transmissibility T_{max} for a dynamic absorber tuned to the fundamental resonance of frequency ω_m of an undamped circular plate of mass M_P with a clamped boundary (Ref. 15).

M_a/M_P	(ω_a/ω_m)	δ_R	T_{max}
0.025	0.908	0.222	6.304
0.05	0.828	0.306	4.496
0.10	0.698	0.408	3.202
0.25	0.465	0.549	2.086

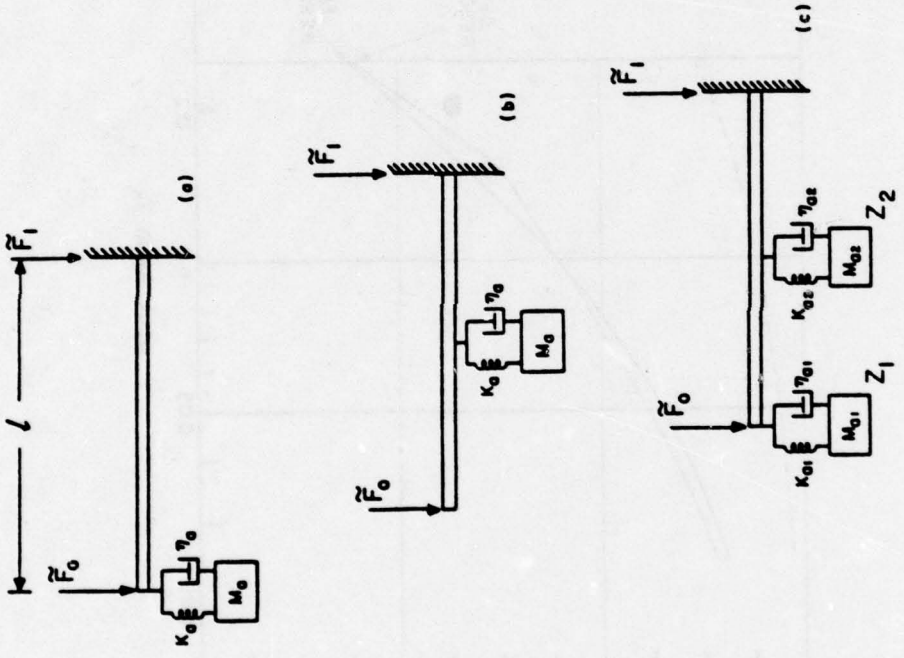
(a)
(b)
(c)
$\tilde{F}_1$
$\tilde{F}_0$
ℓ
η_0
M_0
K_0
η_{01}
M_{01}
K_{01}
η_{02}
M_{02}
K_{02}
Z_1
Z_2

Fig. 26

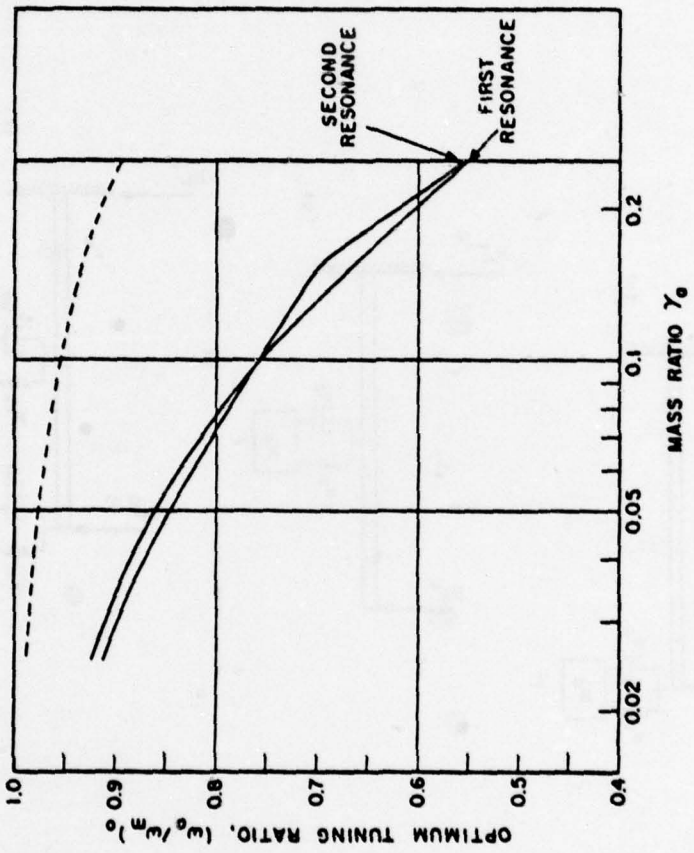
SECOND RESONANCE
FIRST RESONANCE
MASS RATIO γ_e
0.2
0.1
0.05
0.02
OPTIMUM TUNING RATIO, $(\omega_e/\omega_m)_o$
1.0
0.9
0.8
0.7
0.6
0.5
0.4

Fig. 27

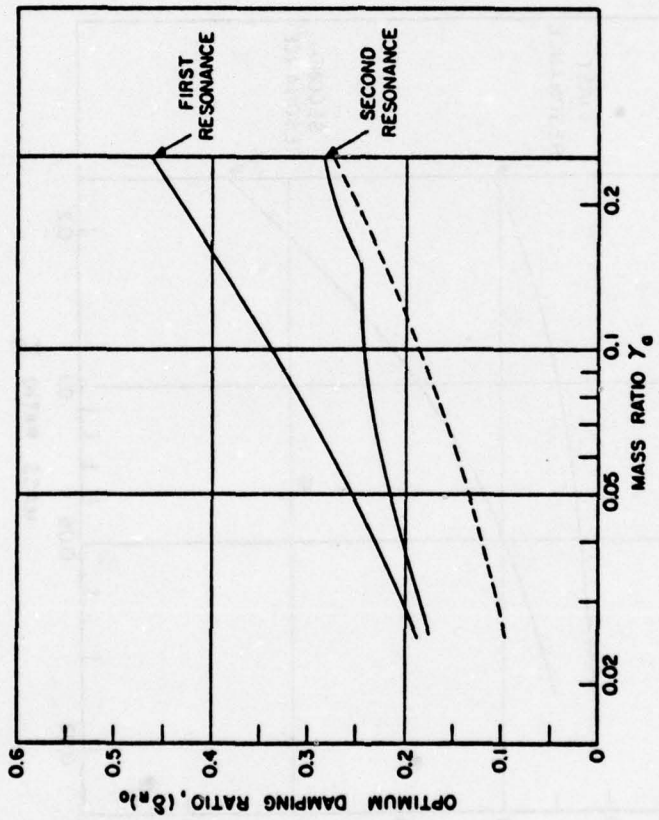
FIRST RESONANCE
SECOND RESONANCE
OPTIMUM DAMPING RATIO, $(\beta_n)_o$
0.6
0.5
0.4
0.3
0.2
0.1
0
0.02
0.05
0.1
0.2
MASS RATIO γ_a

Fig. 28

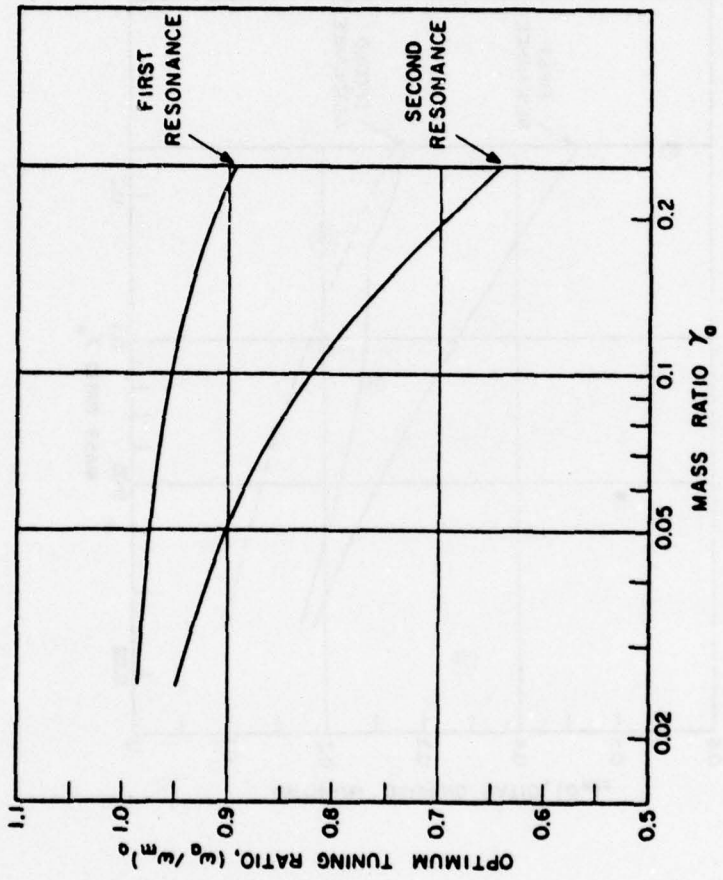
FIRST RESONANCE
SECOND RESONANCE
MASS RATIO γ_o
0.02
0.05
0.1
0.2
OPTIMUM TUNING RATIO, $(\omega_a/\omega_m)_o$
0.5
0.6
0.7
0.8
0.9
1.0
1.1

Fig. 29

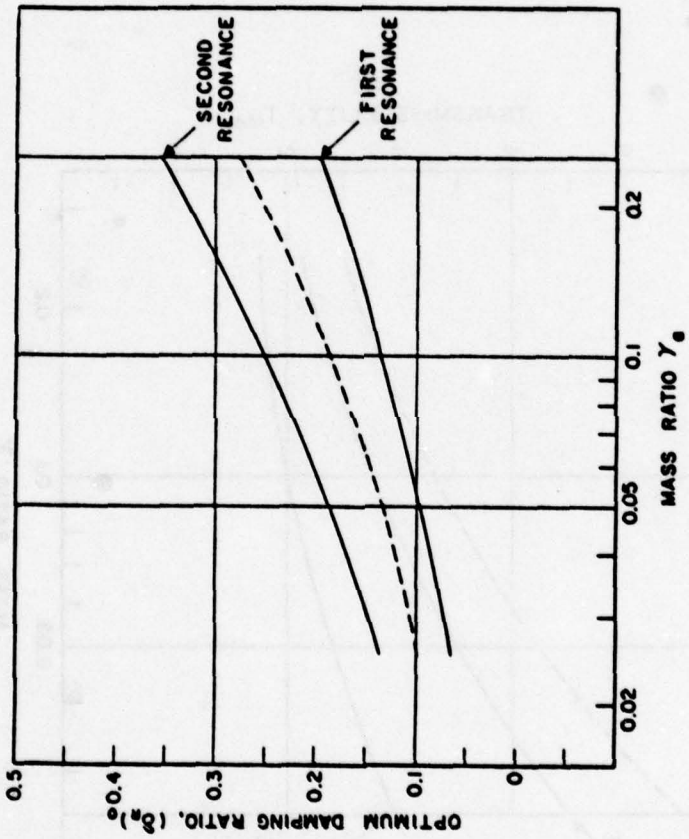
SECOND RESONANCE
FIRST RESONANCE
0.2
0.1
0.05
0.02
MASS RATIO γ_a
0.5
0.4
0.3
0.2
0.1
0
OPTIMUM DAMPING RATIO, $(\beta_a)_o$

Fig. 30

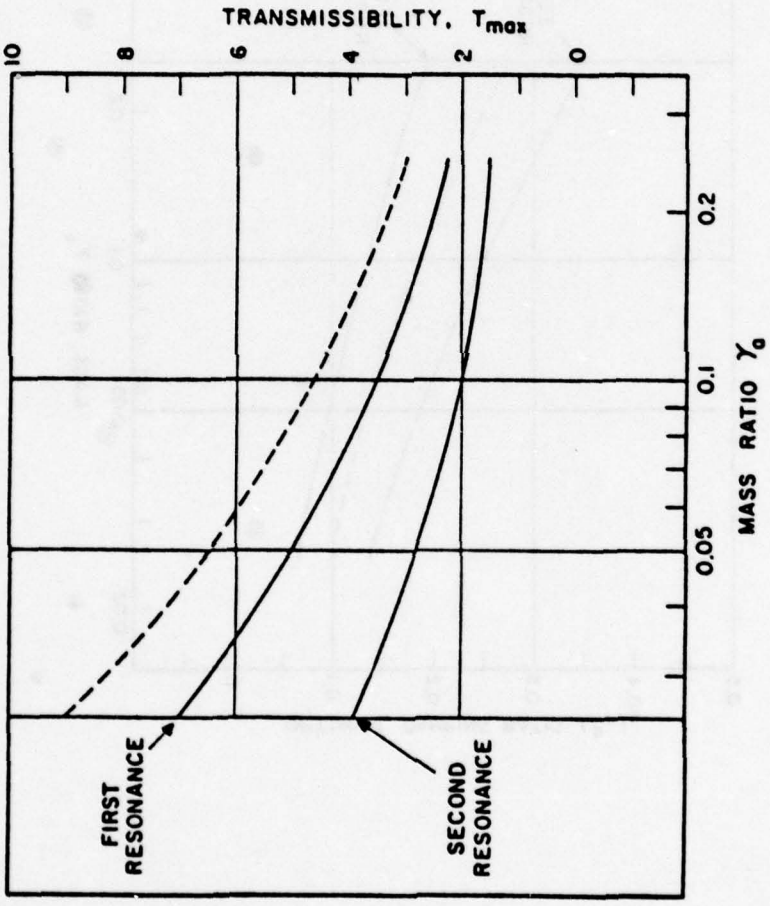
TRANSMISSIBILITY, T_{max}
10
8
6
4
2
0
0.2
0.1
0.05
MASS RATIO γ_0
FIRST RESONANCE
SECOND RESONANCE

Fig. 31

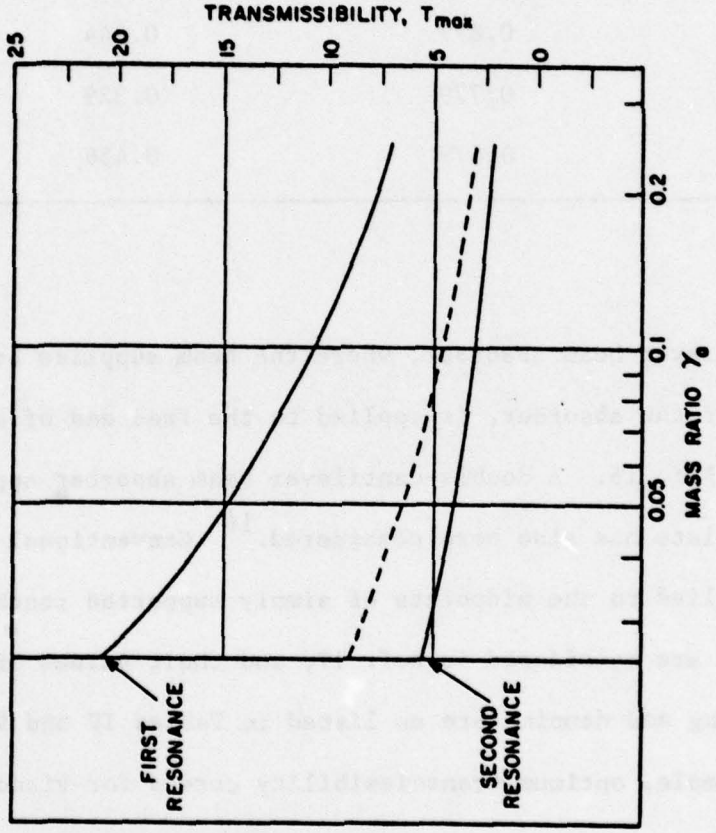
TRANSMISSIBILITY, T_{max}
25
20
15
10
5
0
0.2
0.1
0.05
MASS RATIO γ_e
FIRST RESONANCE
SECOND RESONANCE

Fig. 32

Table III. Optimum values of the frequency ratio (ω_a/ω_m), the damping ratio δ_R, and the corresponding values of maximum transmissibility T_{max} for a dynamic absorber tuned to the fundamental resonance of frequency ω_m of an undamped circular plate of mass M_p with a simply supported boundary (Ref. 15).

M_a/M_p	(ω_a/ω_m)	δ_R	T_{max}
0.025	0.935	0.177	7.227
0.05	0.877	0.244	5.174
0.10	0.779	0.329	3.701
0.25	0.579	0.456	2.407

A cantilever beam absorber, where the beam supplies both the stiffness and damping of the absorber, is applied to the free end of a vertical stanchion in Ref. 16. A double-cantilever beam absorber applied to a rectangular plate has also been considered.[16] Conventional dynamic absorbers applied to the midpoints of simply supported rectangular and square plates are considered in Ref. 17, and their values of optimum absorber tuning and damping are as listed in Tables IV and V.

For example, optimum transmissibility curves for viscously damped dynamic absorbers attached to an undamped primary system are shown in Fig. 33 for absorber masses that are one-tenth, one-fifth, and equally large as the primary mass. The transmissibility to the root of an undamped cantilever beam of length ℓ when driven by a vibratory force at its free end, to which point a dynamic absorber is attached [Fig. 26(a)] is shown in Fig. 34. The absorber has one-fourth of the beam mass. The dashed-line curve shows the transmissibility in the absence of the absorber.

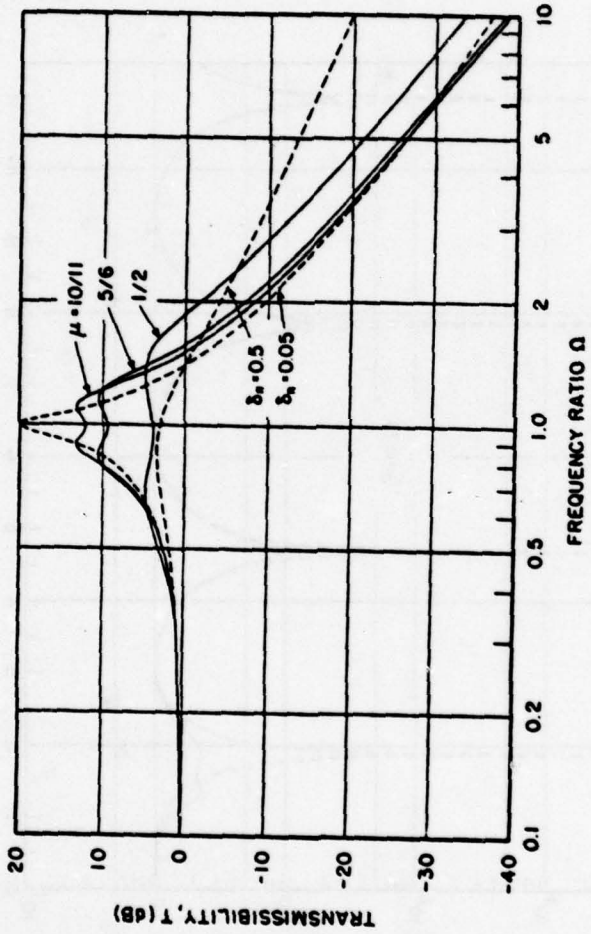
μ=10/11
5/6
1/2
δ=0.5
δ=0.05
FREQUENCY RATIO Ω
TRANSMISSIBILITY, T (dB)
20
10
0
-10
-20
-30
-40
0.1
0.2
0.5
1.0
2
5
10

Fig. 33

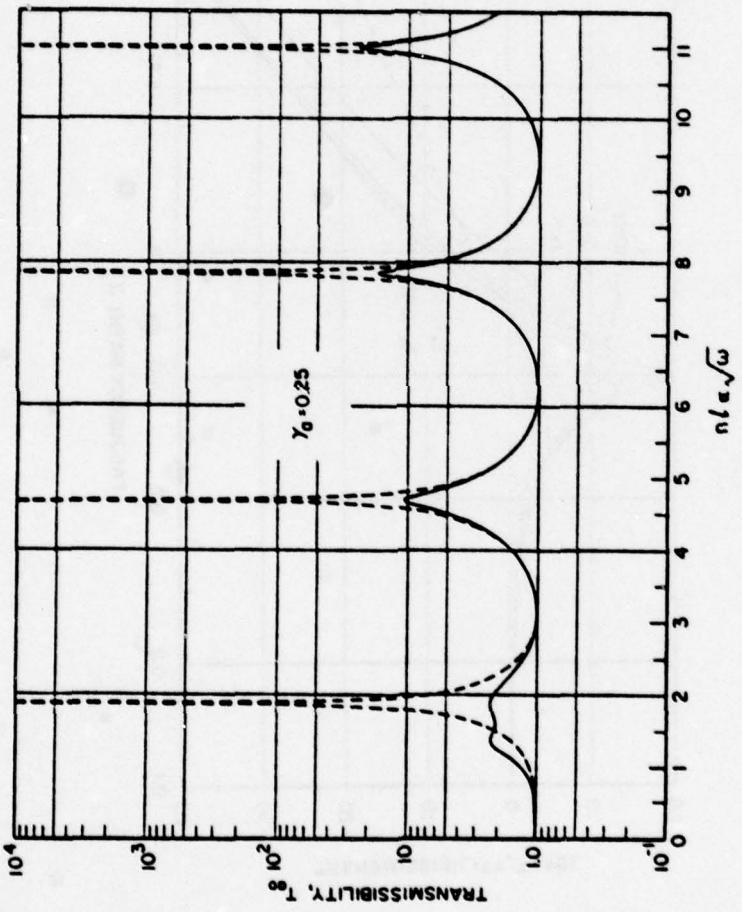
$\gamma_0 = 0.25$
$n l \epsilon \sqrt{\omega}$
TRANSMISSIBILITY, T_{es}
10^{-1}
1.0
10
10^2
10^3
10^4
0
1
2
3
4
5
6
7
8
9
10
11

Fig. 34

Table IV. Optimum values of the frequency ratio (ω_a/ω_m) and of the damping ratio δ_R, and the corresponding values of maximum transmissibility T_{max}, for a dynamic absorber of mass M_a tuned to the fundamental resonance of frequency ω_m of a centrally driven square plate of mass M_P with negligible damping and with simply supported boundaries (Ref. 17).

M_a/M_P	(ω_a/ω_m)	δ_R	T_{max}
0.025	0.928	0.189	6.977
0.05	0.865	0.260	4.990
0.1	0.758	0.350	3.564
0.25	0.547	0.482	2.316

Table V. Optimum values of the frequency ratio (ω_a/ω_m) and of the damping ratio δ_R, and the corresponding values of maximum transmissibility T_{max}, for a dynamic absorber of mass M_a tuned to the fundamental resonance of frequency ω_m of a centrally driven rectangular plate of mass M_P with negligible damping and with simply supported boundaries (Ref. 17).

	$\mu = 1/2$*			$\mu = 1/3$*		
M_a/M_P	(ω_a/ω_m)	δ_R	T_{max}	(ω_a/ω_m)	δ_R	T_{max}
0.025	0.932	0.192	7.010	0.941	0.200	7.125
0.05	0.869	0.268	5.026	0.880	0.292	5.155
0.1	0.760	0.369	3.592	0.763	0.424	3.712
0.25	0.537	0.520	2.322	0.611	0.600	2.994

*The parameter μ is the ratio of the lengths of the shorter to longer sides of the rectangular plates.

The horizontal axis is the dimensionless product of the beam length ℓ and beam wavenumber $n = (\omega^2\rho/r^2E)^{\frac{1}{4}}$, where ρ is the beam density, r is the radius of gyration of its cross section, and E is its Young's modulus of elasticity.

The force transmissibility to the clamped boundary of a virtually undamped circular plate of radius a is shown in Fig. 35. The plate is driven by a central force and carries a central viscously damped dynamic absorber of mass equal to one-tenth of the plate mass (solid-line curve) or to one-quarter of the plate mass (chain-line curve). The dashed-line curve shows the transmissibility in the absence of the absorbers. The horizontal axis is the dimensionless product of the plate radius and wave-number, a quantity that is proportional to the square root of frequency. Again, the force transmissibility to the simply supported boundary of a virtually undamped square plate ($\delta_E = \delta_G = 0.01$) is shown in Fig. 36 for a central driving force and a centrally located viscously damped absorber. For the solid- and chain-line curves, the absorber has one-twentieth and one-quarter of the plate mass, respectively. For the dashed-line curve, the absorbers are absent. The horizontal axis is the dimensionless product of one-half the plate wavenumber and the common plate side--a quantity that is directionaly proportional to the square root of frequency.

The force transmissibility to the root of a virtually undamped stanchion driven by a transverse force at its free end, to which point a cantilever-beam absorber (Fig. 37) is attached is shown in Fig. 38 by the chain-line curve for which the absorber has one-fifth of the stanchion mass. The dashed-line curve shows the transmissibility in the absence of the absorber. The horizontal axis is the product of the stanchion wavenumber and length, a dimensionless quantity that is again directly proportional to the square

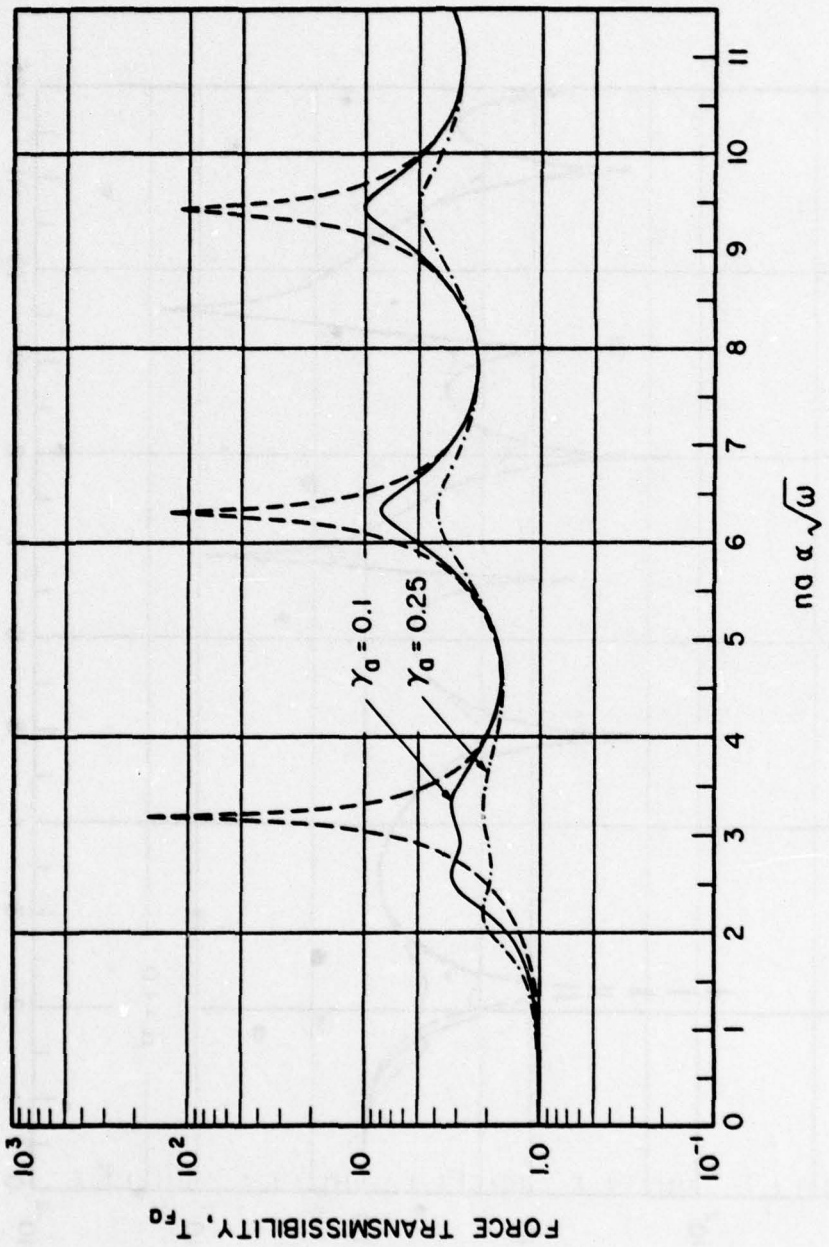
FORCE TRANSMISSIBILITY, T_{Fa}
10^3
10^2
10
1.0
10^{-1}
0
1
2
3
4
5
6
7
8
9
10
11
$\eta a \propto \sqrt{\omega}$
$\gamma_a = 0.1$
$\gamma_a = 0.25$

Fig. 35

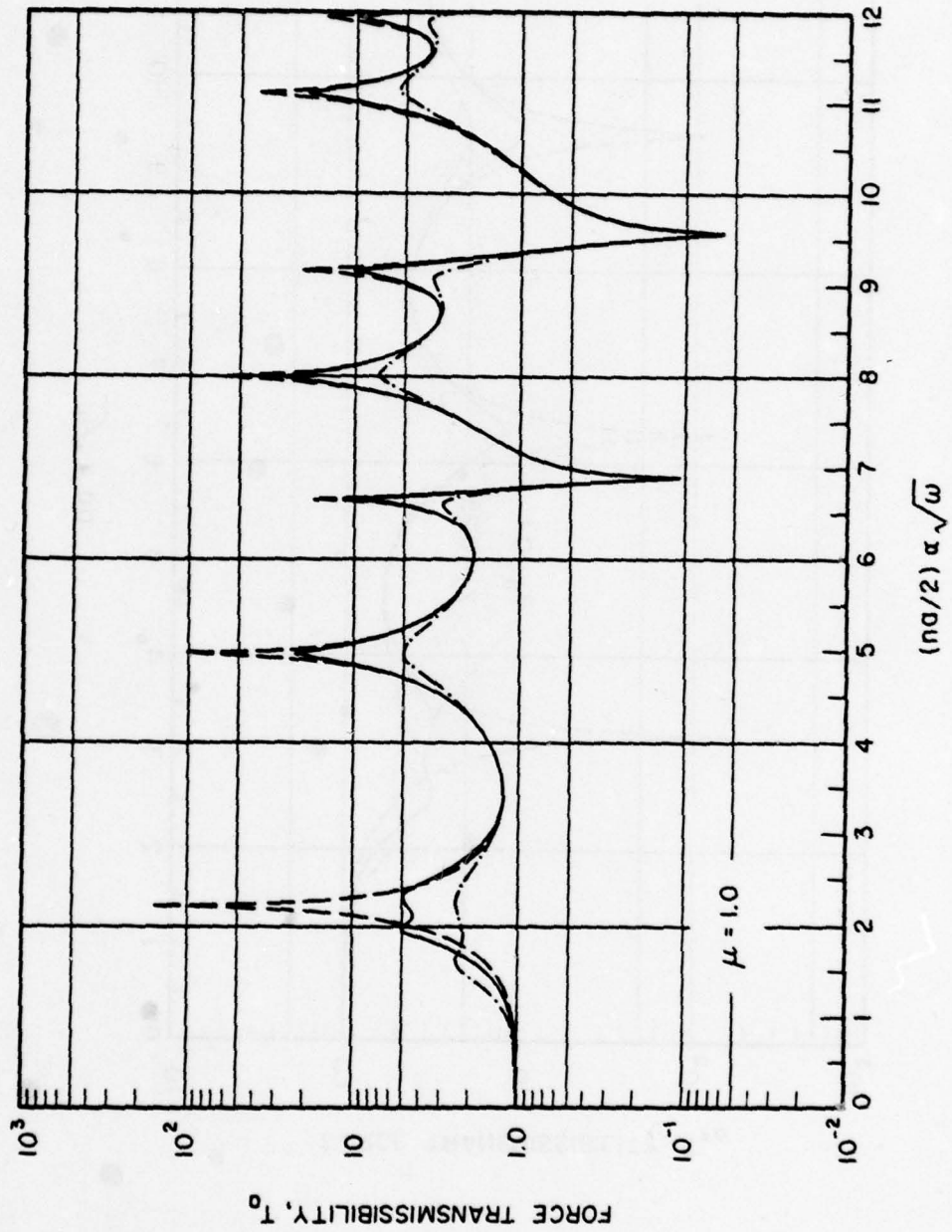
FORCE TRANSMISSIBILITY, T_Q
10^3
10^2
10
1.0
10^{-1}
10^{-2}
0
1
2
3
4
5
6
7
8
9
10
11
12
$\mu = 1.0$
$(n\alpha/2) \propto \sqrt{\omega}$

Fig. 36

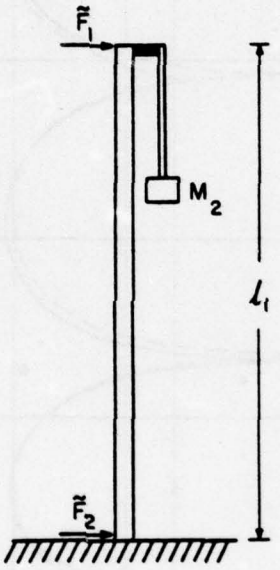

Fig. 37

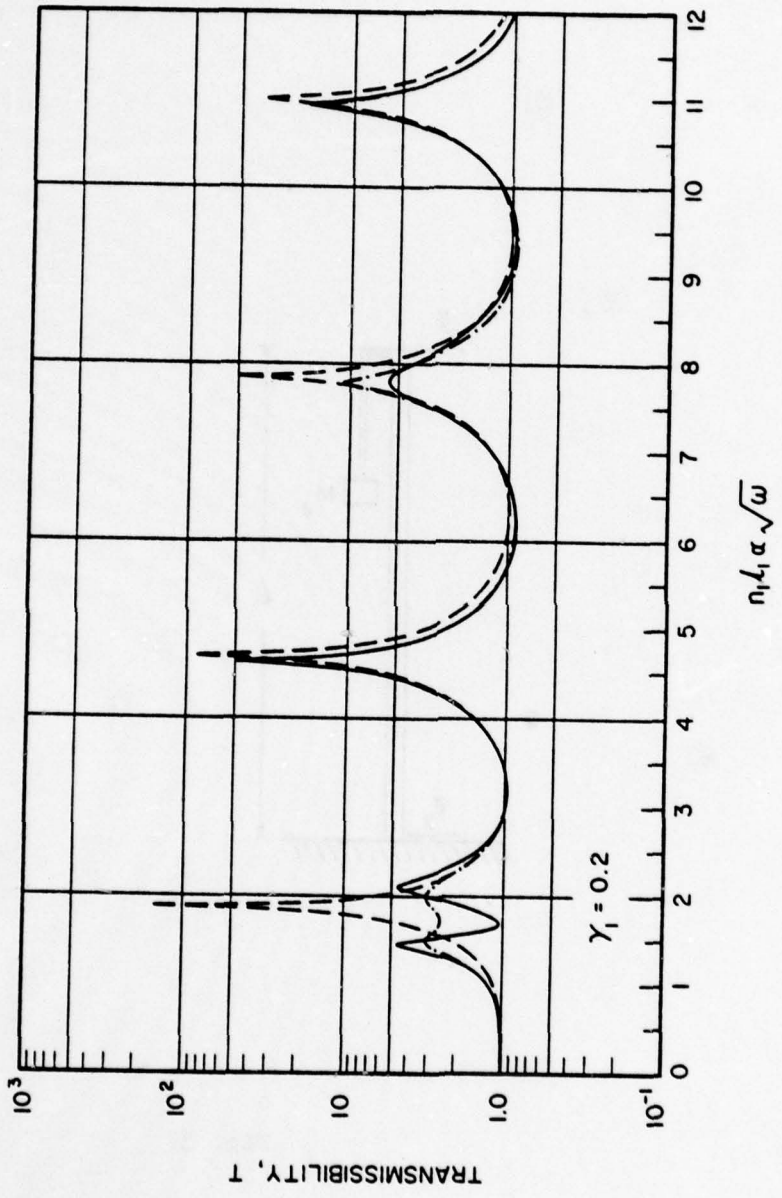
TRANSMISSIBILITY, T
10^3
10^2
10
1.0
10^{-1}
0
1
2
3
4
5
6
7
8
9
10
11
12
$\gamma_1 = 0.2$
$n_1 L_1 \propto \sqrt{\omega}$

Fig. 38

root of frequency. The solid-line curve shows the force transmissibility for quasi-optimum values of absorber tuning and damping.[16]

One other valuable application of the dynamic absorber is in those situations where it is feasible to damp the primary system heavily, in which event the absorber can have negligible damping. In that case, transmissibility is as plotted in Ref. 1, and as plotted and confirmed experimentally in Ref. 19. One figure drawn from Ref. 1 is reproduced here as an example in Fig. 39. The absorber has one-fifth of the mass of the primary system, which has a damping ratio $\delta_R = 0.5$ (half critical damping). The absorber has negligible damping and is tuned in turn to 2/3, 1.0, and 1.5 times the reference frequency of the system (the resonant frequency of the system obtained when the absorber mass is attached rigidly to the primary mass).

Finally, one additional and somewhat novel application of the dynamic absorber arises when the absorber is tuned <u>off</u> resonance to produce a narrow-band region of attenuation at, for example, the frequency of a troublesome machinery discrete. This region of attenuation is usually accompanied by a compensating narrow-band region of amplification at a neighboring frequency that, hopefully, does not coincide with another machinery discrete because these are normally separated widely in frequency. An example is shown in Fig. 40, where a virtually undamped absorber for which $\mu = 5/6$ is tuned consecutively at frequencies 0.2, 0.5, 2.0, and 5.0 times the reference frequency of the undamped primary system. Other examples are given in Figs. 41-43, where (a) a rectangular plate with simply supported boundaries and with an aspect ratio of 3 ($\mu = 1/3$) is centrally driven and loaded by a dynamic absorber, which has one-tenth of the plate mass and is tuned to 0.2 of the fundamental resonant frequency of the plate, and (b) a circular plate of radius a with a clamped boundary

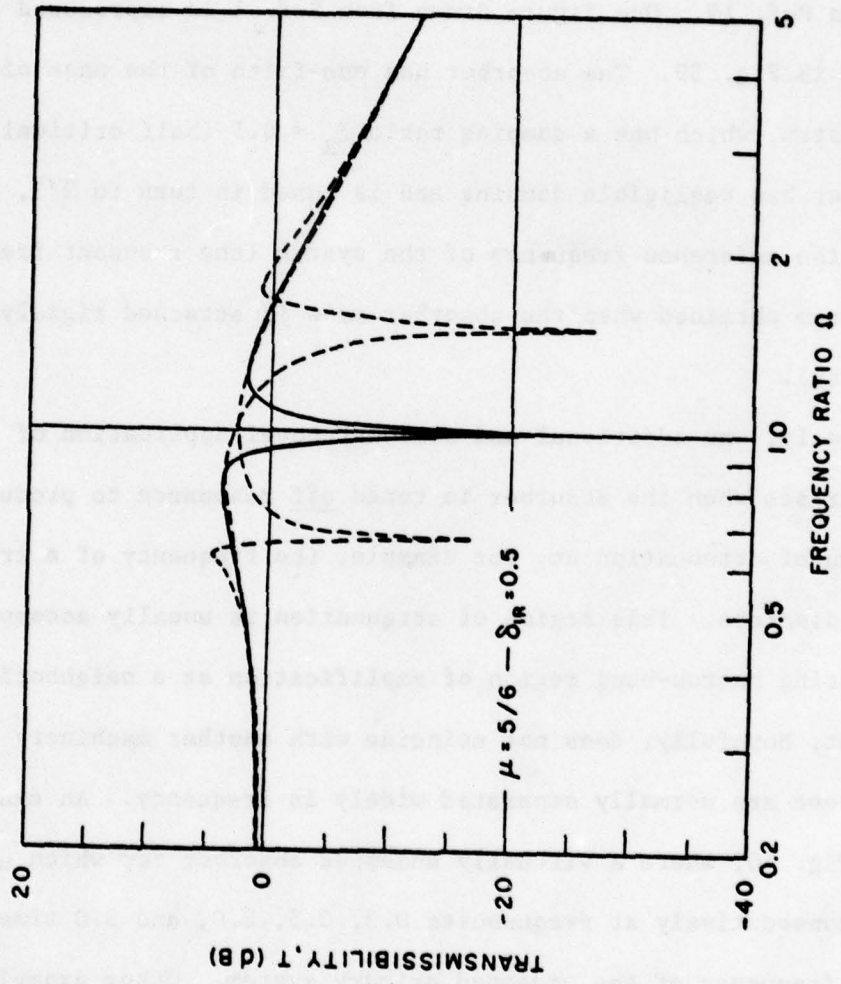
TRANSMISSIBILITY, T (dB)
20
0
-20
-40
0.2
0.5
1.0
2
5
FREQUENCY RATIO Ω
μ = 5/6 — δ_IR = 0.5

Fig. 39

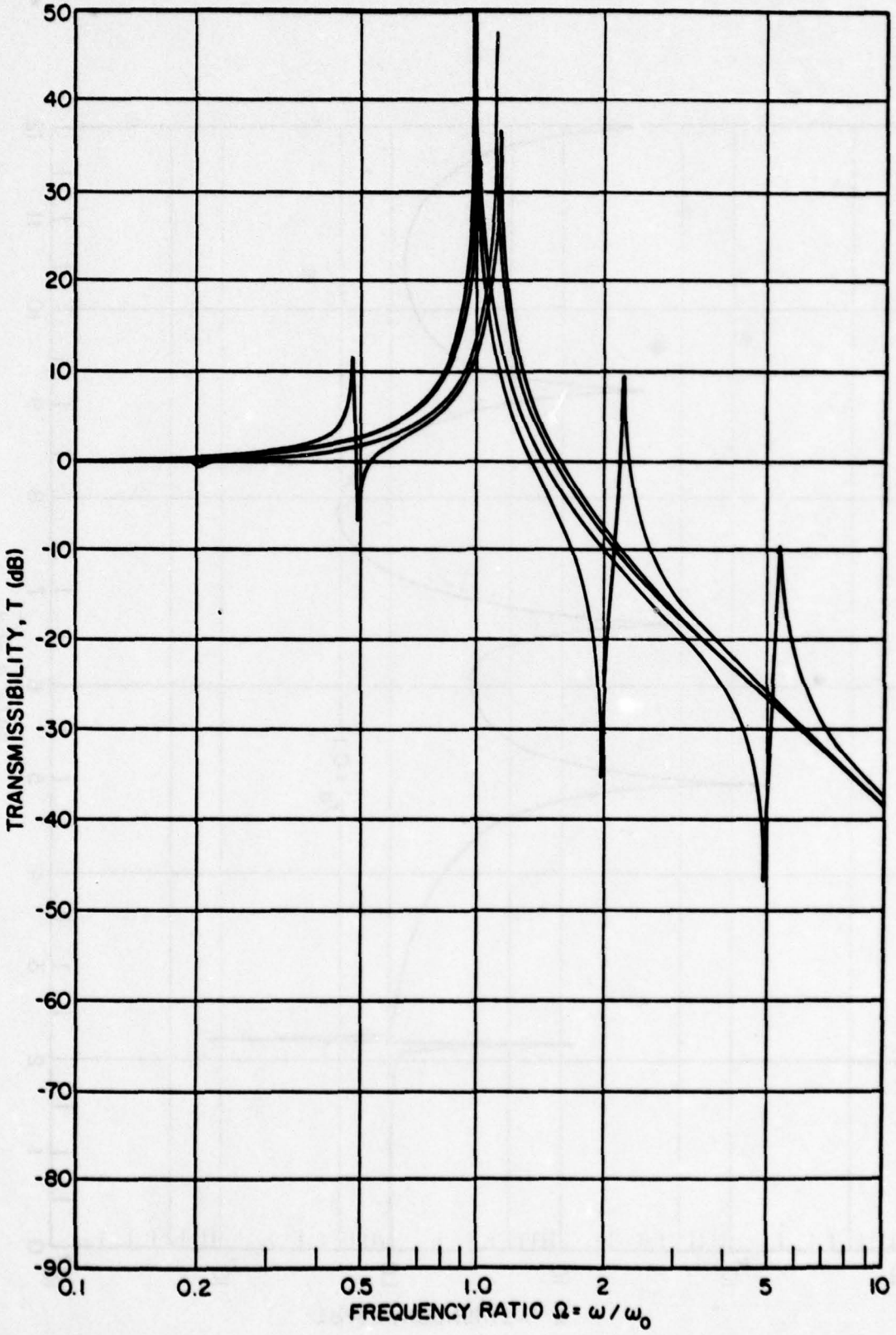
50
40
30
20
10
0
-10
-20
-30
-40
-50
-60
-70
-80
-90
TRANSMISSIBILITY, T (dB)
0.1
0.2
0.5
1.0
2
5
10
FREQUENCY RATIO Ω = ω / ω0

Fig. 40

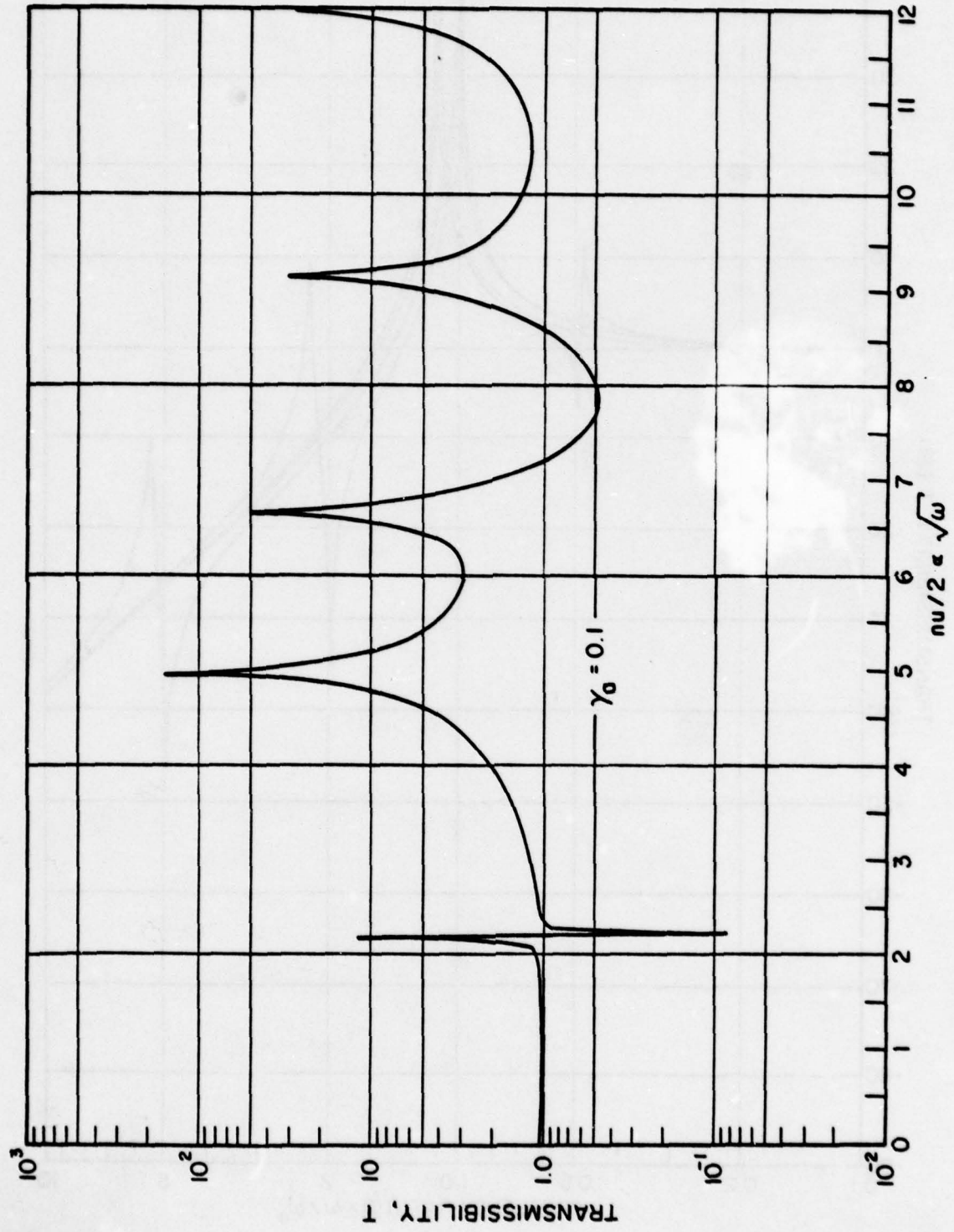
TRANSMISSIBILITY, T
10^3
10^2
10
1.0
10^{-1}
10^{-2}
0
1
2
3
4
5
6
7
8
9
10
11
12
$\eta u/2 \propto \sqrt{\omega}$
$\gamma_0 = 0.1$

Fig. 41

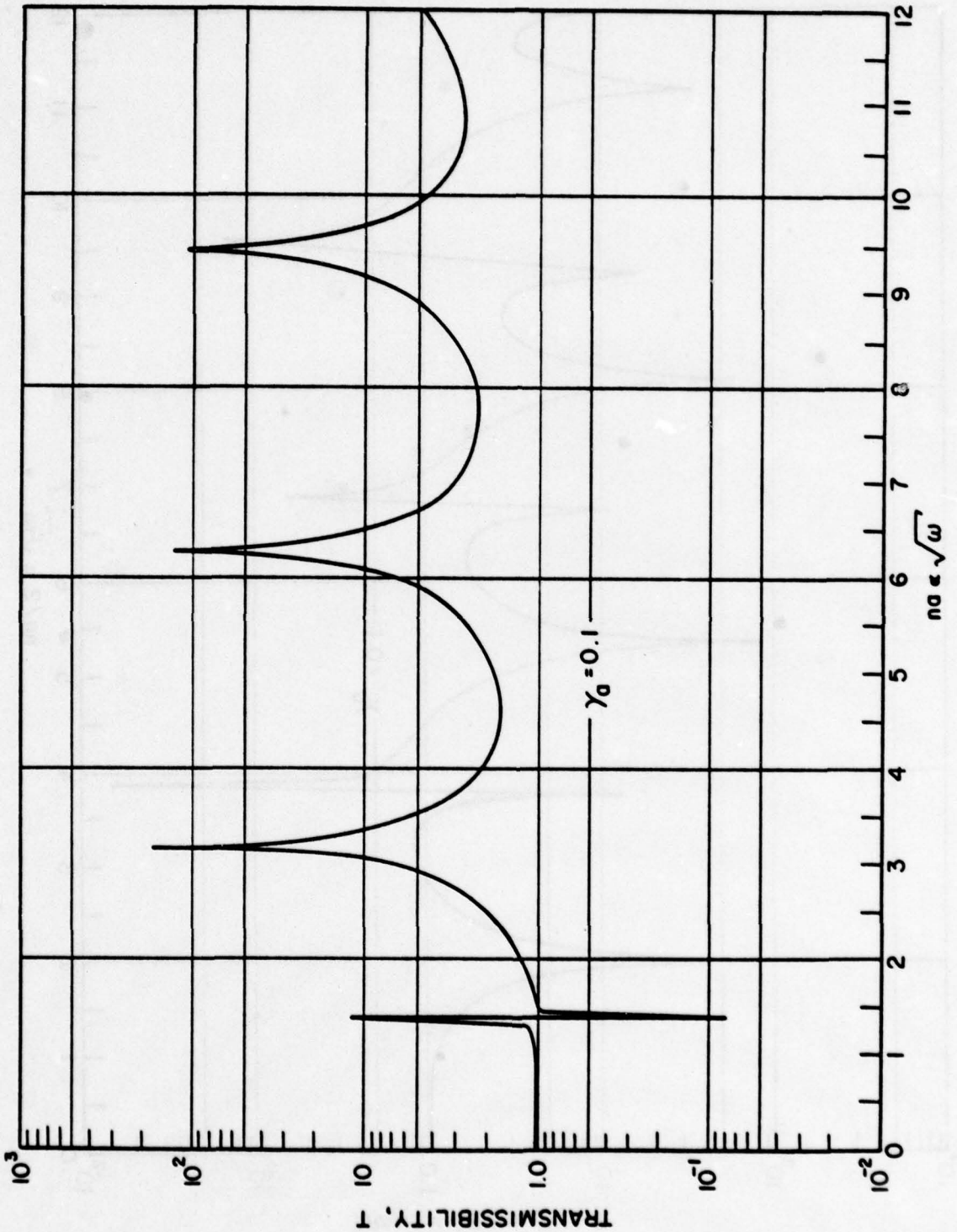
TRANSMISSIBILITY, T
10^3
10^2
10
1.0
10^{-1}
10^{-2}
0
1
2
3
4
5
6
7
8
9
10
11
12
$\gamma_0 = 0.1$
$\eta a \propto \sqrt{\omega}$

Fig. 42

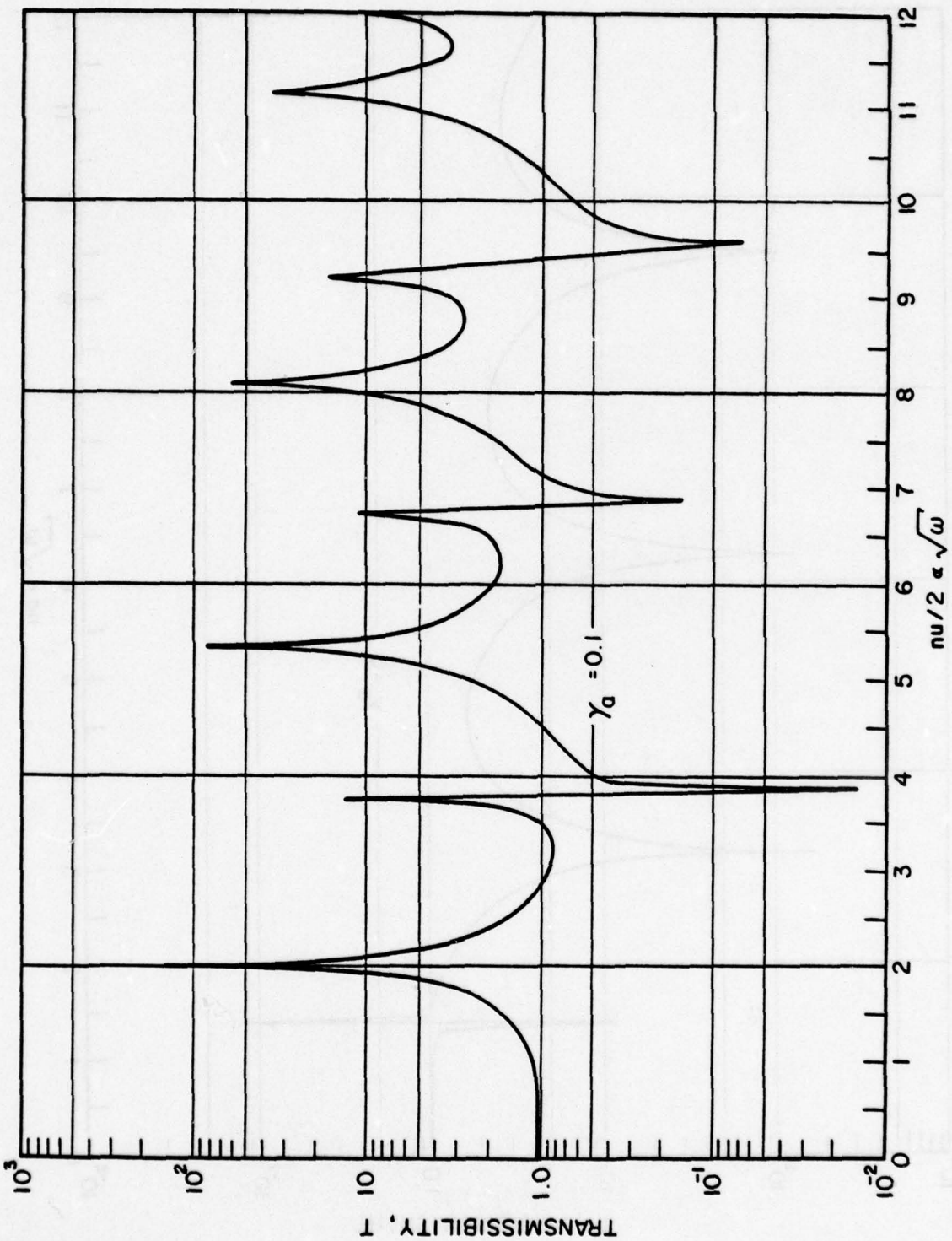
TRANSMISSIBILITY, T
10^3
10^2
10
1.0
10^{-1}
10^{-2}
0
1
2
3
4
5
6
7
8
9
10
11
12
$\gamma_a = 0.1$
$\pi u/2 \propto \sqrt{\omega}$

Fig. 43

that is centrally driven and loaded by a dynamic absorber having one-tenth of the plate mass and tuned to 0.2 times the fundamental resonant frequency of the plate, and (c) a square plate with simply supported boundaries that is centrally driven and loaded by a dynamic absorber also having one tenth of the plate mass and tuned to three times the fundamental resonant frequency of the plate. The parameter u is the length of the longer plate sides.

Also mentioned must be the platelike dynamic absorber (Figs. 44 and 45),[20] which comprises a damped circular plate that is attached centrally to the vibrating primary system and which is loaded around its circumference by a rigid annular mass that has the same radius as the plate, which supplies both the stiffness and damping of the absorber. The plate could either be coated with damping compound or be built up from several steel/viscoelastic laminations. Such laminates can be produced with the relatively large damping factors needed in many absorber applications. The optimum tuning of the absorber is taken to be identical with that specified by Eq. 49, and curves showing this optimum tuning and the accompanying damping factor, for which equal peak heights are obtained in the transmissibility curve, are plotted in Fig. 46. The resultant transmissibility across the system of Fig. 44 with the absorber of Fig. 45(a) is shown in Fig. 47 for which the absorber mass ratio μ = 50/51, 10/11, and 2/3 (M_2/M_1 = 0.02, 0.1, and 0.5). The absorber may equally well be applied to suppress the resonant vibration of circular plates (bulkheads)[20] and rectangular plates (panels)[20] for which the optimum tuning and damping criteria will differ slightly from those of Fig. 46.[20] Also considered in Ref. 20 is an annular-plate absorber, which is somewhat easier to tune than the circular-plate absorber [Fig. 45(b)]. The absorbers share the advantagesof mechanical simplicity and planar geometry, which makes them particularly well suited for flush-mounted application on bulkheads and panels--and, for example, beneath the floors and seats of the passenger and crew compartments of flight vehicles.

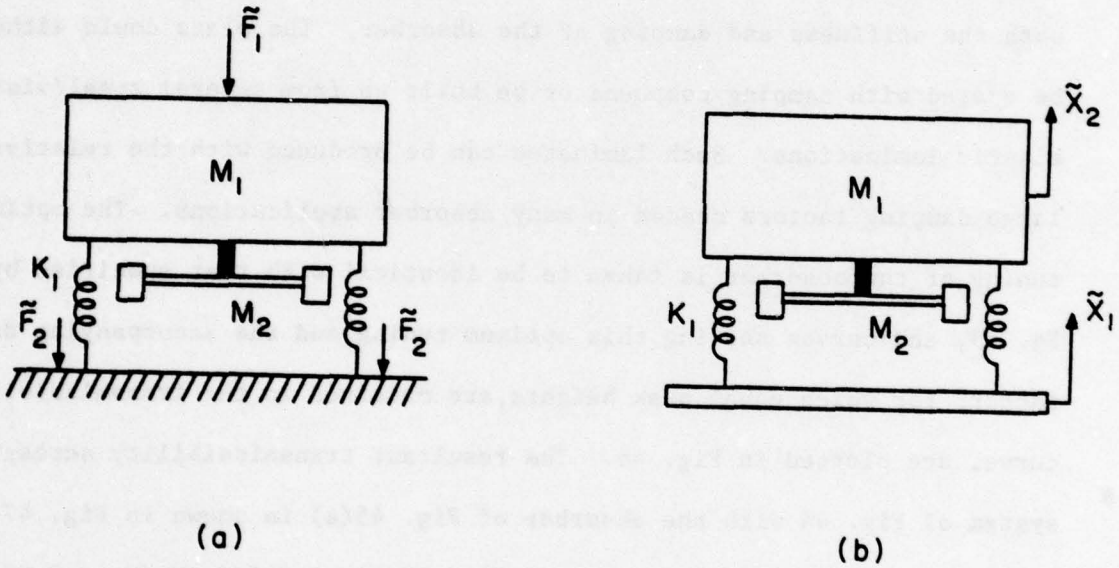

Fig. 44

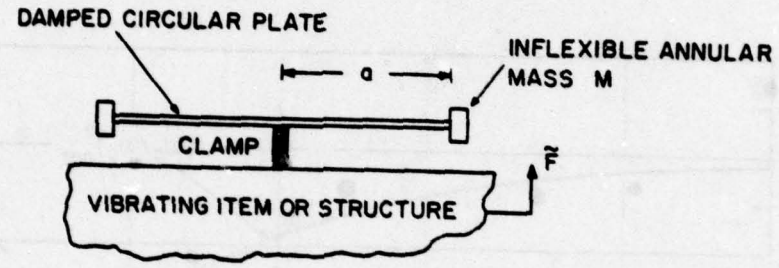
DAMPED CIRCULAR PLATE
a
INFLEXIBLE ANNULAR MASS M
CLAMP
F̃
VIBRATING ITEM OR STRUCTURE

(a)

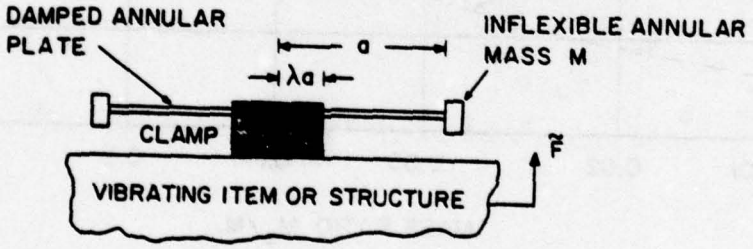
DAMPED ANNULAR PLATE
a
λa
INFLEXIBLE ANNULAR MASS M
CLAMP
F̃
VIBRATING ITEM OR STRUCTURE

(b)

Fig. 45

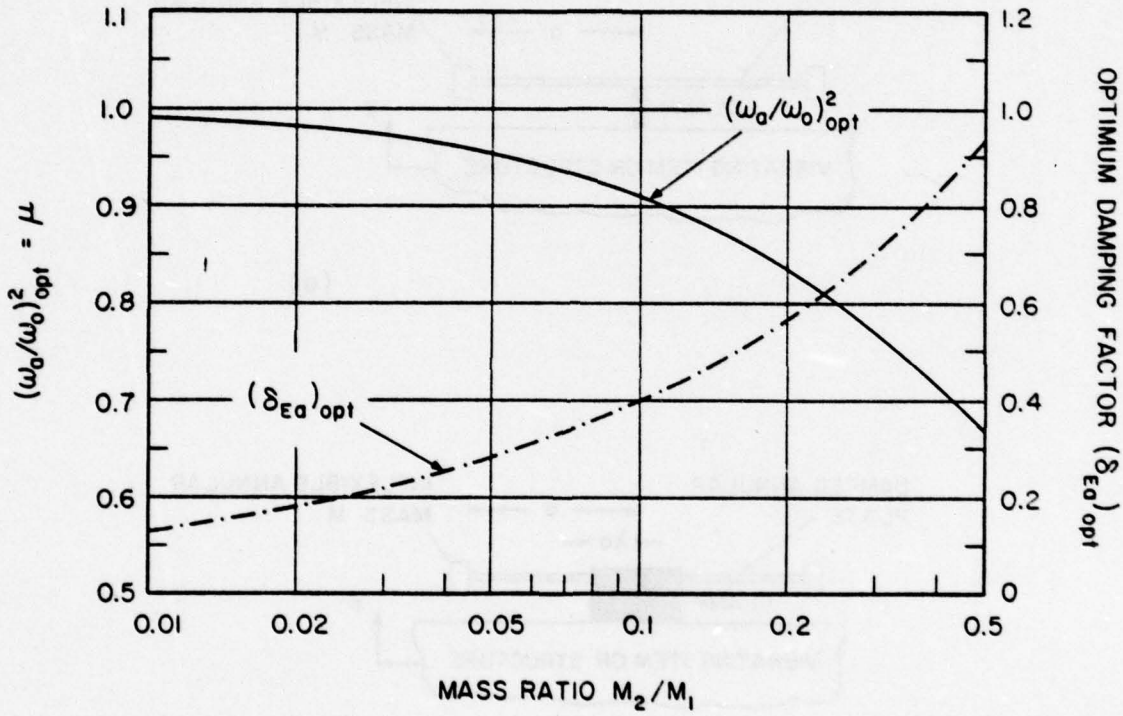
1.1
1.0
0.9
0.8
0.7
0.6
0.5
1.2
1.0
0.8
0.6
0.4
0.2
0
0.01
0.02
0.05
0.1
0.2
0.5
$(\omega_a/\omega_o)^2_{opt}$
$(\delta_{Ea})_{opt}$
$(\omega_a/\omega_o)^2_{opt} = \mu$
OPTIMUM DAMPING FACTOR $(\delta_{Ea})_{opt}$
MASS RATIO M_2/M_1

Fig. 46

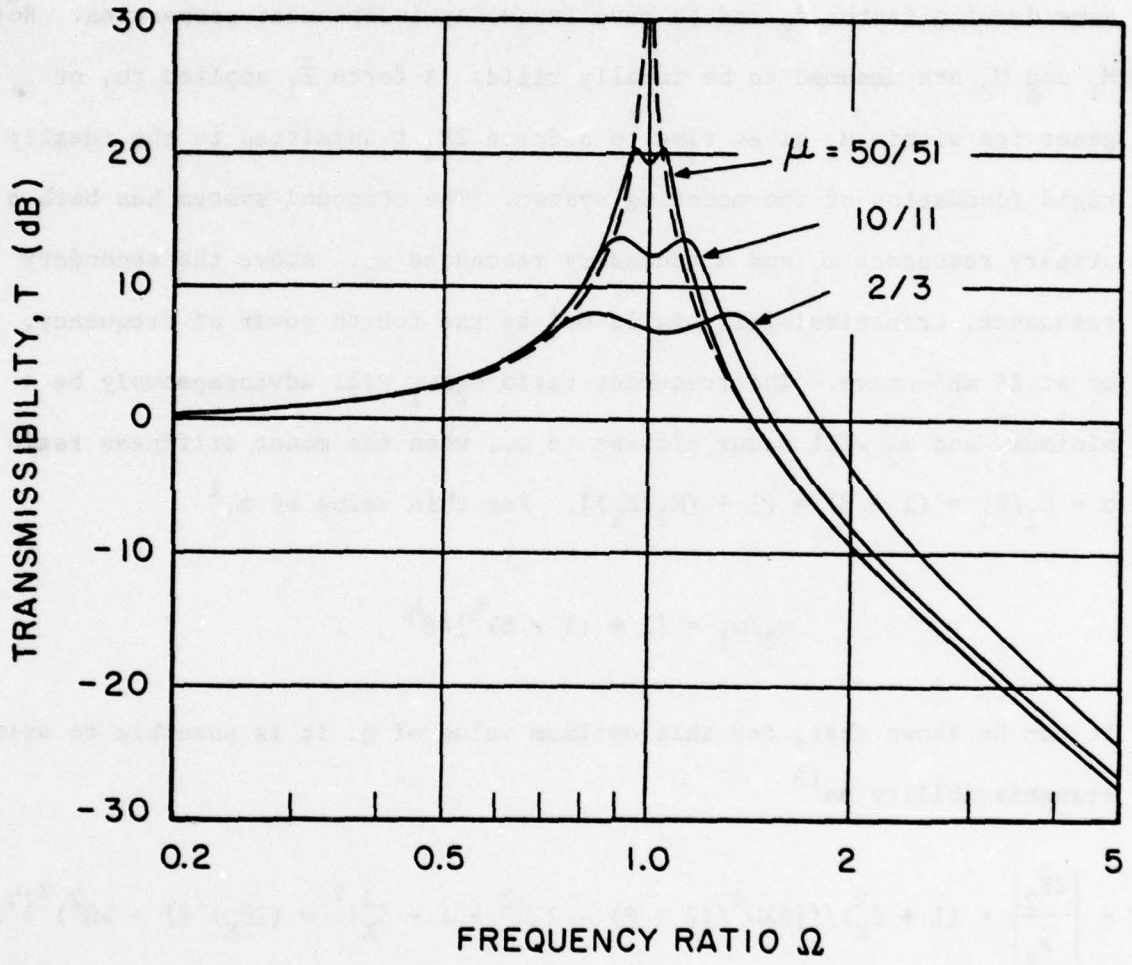
30
20
10
0
-10
-20
-30
TRANSMISSIBILITY, T (dB)
μ = 50/51
10/11
2/3
0.2
0.5
1.0
2
5
FREQUENCY RATIO Ω

Fig. 47

5. COMPOUND MOUNTING SYSTEM

The compound system is a two-stage mounting in which the resilient support for the primary mass M_1 is divided into two by an intermediate or secondary mass M_2, as in Fig. 48(a).[1,13] The upper and lower mount stiffness are K_1 and K_2, respectively. The mounts will be assumed to share the same damping factor δ_K and to have frequency-independent properties. Both M_1 and M_2 are assumed to be ideally rigid. A force $\tilde{F}_1$ applied to, or generated within M_1 gives rise to a force $2\tilde{F}_2$ transmitted to the ideally rigid foundation of the mounting system. The compound system has both a primary resonance ω_1 and a secondary resonance ω_2. Above the secondary resonance, transmissibility falls off as the fourth power of frequency, or at 24 dB/octave. The frequency ratio ω_2/ω_1 will advantageously be a minimum, and ω_2 will occur closest to ω_1, when the mount stiffness ratio $\alpha = K_2/K_1 = (1 + \beta) = [1 + (M_2/M_1)]$. For this value of α,[1]

$$\omega_2/\omega_1 = [1 + (1 + \beta)^{1/2}]/\beta^{1/2} \quad . \tag{54}$$

It can be shown that, for this optimum value of α, it is possible to write transmissibility as[13]

$$T = \left|\frac{2\tilde{F}_2}{\tilde{F}_1}\right| = (1 + \delta_K^2)/\{[\beta\lambda\Omega^4/(2 + \beta) - 2\lambda\Omega^2 + 1 - \delta_K^2]^2 + (2\delta_K)^2(1 - \lambda\Omega^2)^2\}^{1/2}, \tag{55}$$

where

$$\lambda = \left(\frac{1 + \beta}{2 + \beta}\right) \tag{56}$$

and

$$\Omega = \omega/\omega_o \quad , \tag{57}$$

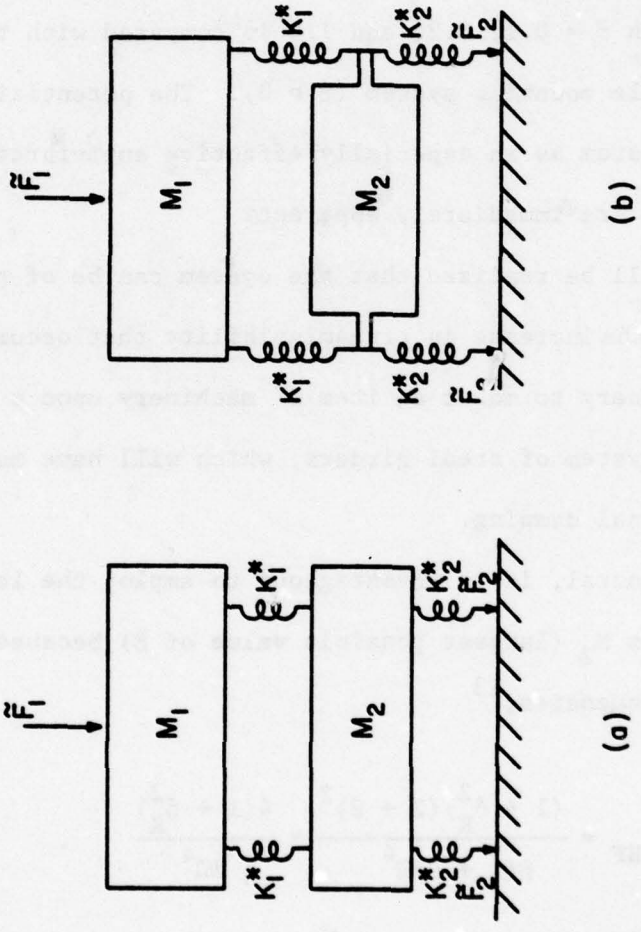

Fig. 48

where ω_o is the reference frequency of the compound system:

$$\omega_o^2 = \frac{2K_1K_2}{(K_1 + K_2)M_1} \quad , \tag{58}$$

which is the natural frequency of the simple system obtained when $M_2 = 0$.

The transmissibility of a compound system that utilizes natural-rubber mounts is shown in Fig. 49, where the transmissibility of three compound systems with $\beta = 0.1$, 0.2, and 1.0 is compared with the transmissibility of the simple mounting system ($\beta = 0$). The potential advantages of the compound system as an especially effective antivibration mounting at high frequencies are immediately apparent.

It will be realized that the system can be of particular value in mitigating the increase in transmissibility that occurs, for example, when it is necessary to mount an item of machinery upon a nonrigid foundation such as a system of steel girders, which will have many resonances and very small internal damping.

In general, it is advantageous to employ the largest possible intermediate mass M_2 (largest possible value of β) because it can be shown that, at high frequencies,[13]

$$T_{HF} = \frac{(1 + \delta_K^2)(2 + \beta)^2}{\beta(1 + \beta)\Omega^4} \approx \frac{4(1 + \delta_K^2)}{\beta\Omega^4} \quad . \qquad (\beta \leq 0.5) \tag{59}$$

A large-scale application of the system is considered in Ref. 21, which describes the compound mounting of 17,000 lb and 80,000 lb diesel generators on one extensive intermediate mass. An adaption of the arrangement employed is shown in Fig. 50. Two, much smaller, applications of the compound system are described in Refs. 9 and 22, in both of which the system has effectively been compacted into an "off-the-shelf" antivibration mount. The design of

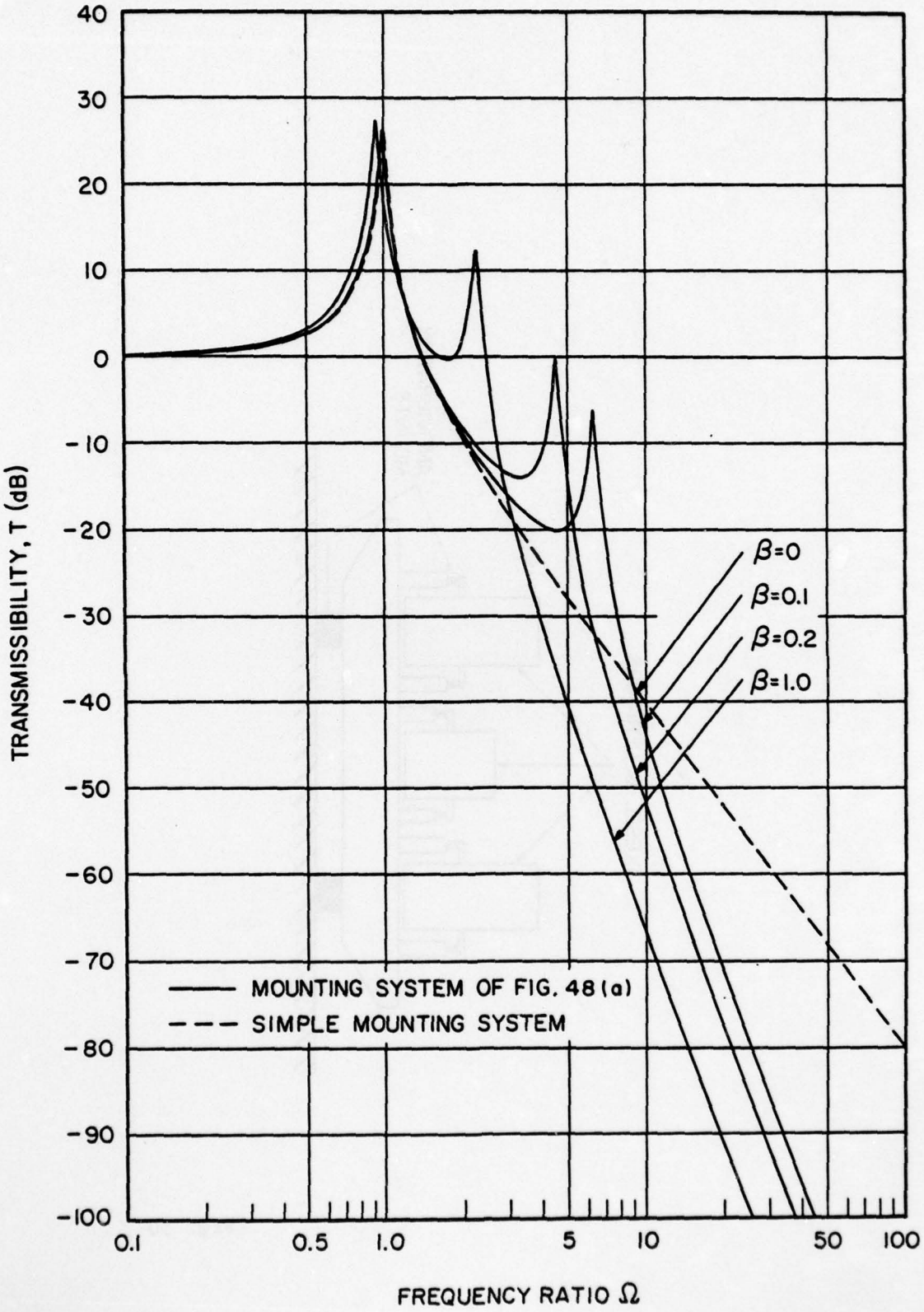
40
30
20
10
0
-10
-20
-30
-40
-50
-60
-70
-80
-90
-100
TRANSMISSIBILITY, T (dB)
0.1
0.5
1.0
5
10
50
100
FREQUENCY RATIO Ω
β=0
β=0.1
β=0.2
β=1.0
MOUNTING SYSTEM OF FIG. 48(a)
SIMPLE MOUNTING SYSTEM

Fig. 49

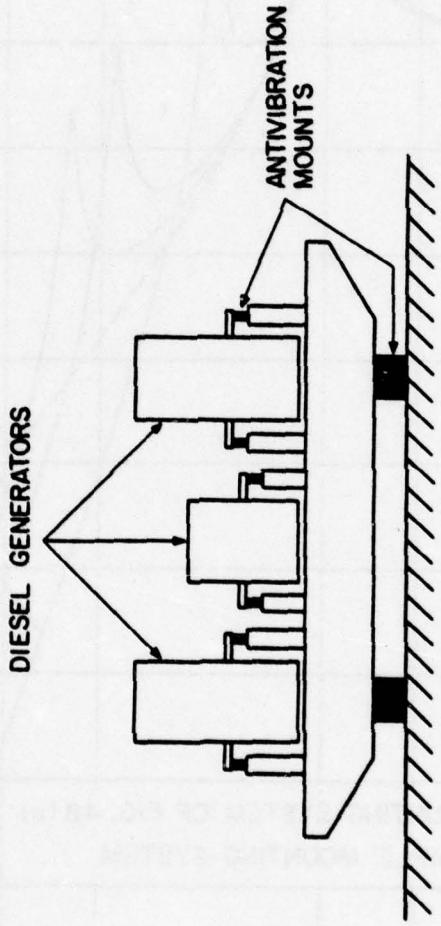

Fig. 50

one mount[22] is shown in Fig. 51, where the secondary mass comprises two cylindrical lumped masses 10, a spacer yoke 12, and the resilient elements comprise 16.

Other references to the compound system are listed in Ref. 1; analyses of the three-dimensional vibration response of the system appear in Refs. 23 and 24.

If the compound system is to provide small values of transmissibility as predicted, it is <u>vital</u> that the intermediate mass M_2 remains masslike. If it does not, the performance of the system will be seriously <u>impaired</u> at high frequencies. This situation is described in Fig. 48(b), where the flanges from which M_2 is supported behave as springs at some high frequencies because of their poor design. To provide a quantitative illustration of the increase in transmissibility that can be expected in this case, the compound system of Fig. 48(b) has been analyzed by modeling the nonrigid (multiresonant) flanges as short shear beams. The force transmissibility across the system then becomes[13]

$$T = \left|\frac{2\tilde{F}_2}{\tilde{F}_1}\right| = (1 + \delta_K^2)/\{[\Omega^2(\lambda\zeta_R - 1) + (1 - \zeta_R + \delta_K\zeta_I)]^2 + [\lambda\zeta_I\Omega^2 - \delta_K\zeta_R - \zeta_I + \delta_K]^2\}^{\frac{1}{2}} \quad , \tag{60}$$

where λ (Eq. 56) and δ_K have the same significance as before, and ζ_R and ζ_I are the real and imaginary parts of a quantity ζ^* that is defined as follows:

$$\zeta^* = (\eta^*/\Psi^*)(n^*\ell)\Gamma^* \quad , \tag{61}$$

where Ψ^* and η^* are given by Eqs. (35) and (36); Γ^* is given by Eq. (38), and

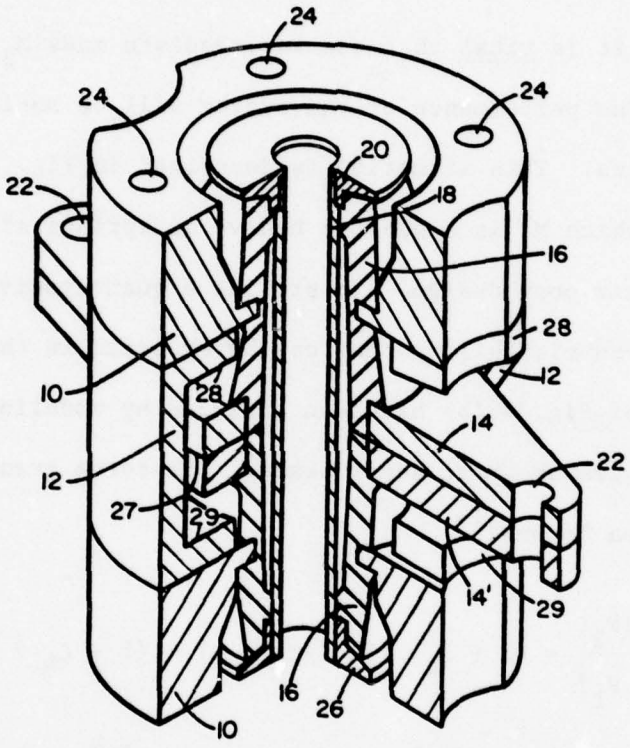

Fig. 51

$$(n^{*}\ell) = (p + jq) \quad , \tag{62}$$

where p and q are again given by Eqs. (41) and (42). In these equations, n^{*} is the complex wavenumber of the shear beam flanges (feet), ℓ is their length, and the quantity Γ in Eq. (38) is again given by

$$\Gamma = K_F/K_2 \quad , \tag{63}$$

where K_F is the static stiffness of each foot.

The results of one calculation of transmissibility made from Eq. (60) are plotted in Fig. 52 as the chain-line curve for which $\gamma_F = M_2/2M_F = 40$, $\Gamma = 5$, $\delta_F = 0.01$, and $\beta = 0.2$, $\delta_K = 0.05$. Pronounced peaks now appear in the transmissibility curve--to degrade the performance of the compound system at high frequencies where the shear-beam flanges resonate, their ends having large motion and their roots, which are attached to the mass M_2, having relatively small motion. In addition, pronounced minima occur in the transmissibility curve at the antiresonant frequencies of the flanges for which the flange ends have little motion and their roots, together with M_2, have relatively large motion; in fact, at these frequencies, M_2 and the flanges are analogous in their behavior to the mass and stiffness of a dynamic vibration absorber. The solid-line curve in Fig. 52 shows the transmissibility across the system with $\beta = 0.2$ when the intermediate mass M_2 is ideally rigid.

Another valuable application of the dynamic absorber is in reducing the transmissibility of the compound system at its secondary resonant frequency. This situation is illustrated in Fig. 53,[18] where the absorber is attached to the intermediate mass, for which it is possible to write

$$T = \left|\frac{2\tilde{F}_2}{\tilde{F}_1}\right| = \frac{(1 + \delta_K^2)\ [(n^2\phi^2 - \Omega^2)^2 + (2n\phi\delta_R\Omega)^2]^{\frac{1}{2}}}{(R_D^2 + I_D^2)^{\frac{1}{2}}} \quad , \tag{64}$$

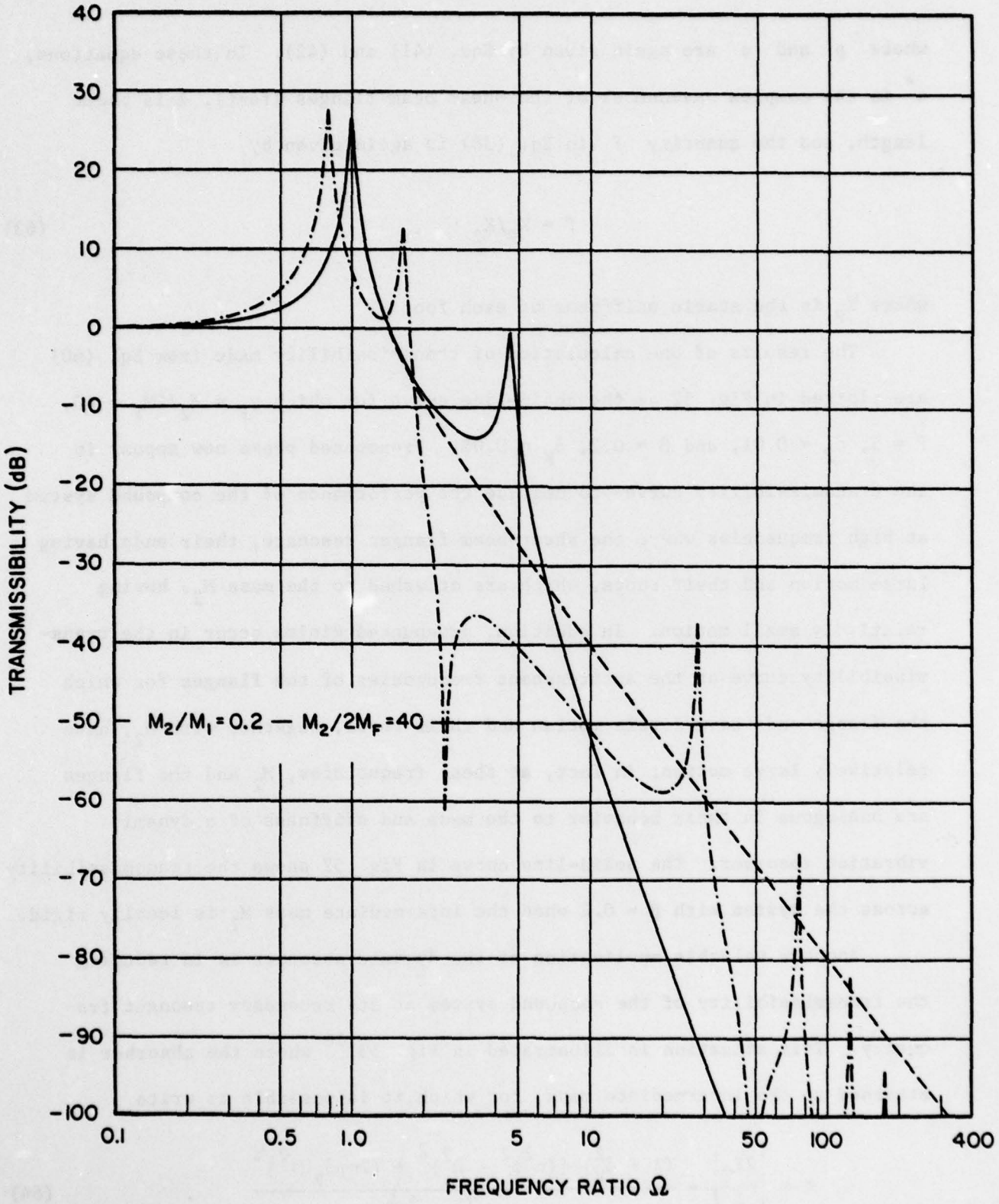
40
30
20
10
0
-10
-20
-30
-40
-50
-60
-70
-80
-90
-100
TRANSMISSIBILITY (dB)
$M_2/M_1 = 0.2$ — $M_2/2M_F = 40$
0.1
0.5
1.0
5
10
50
100
400
FREQUENCY RATIO Ω

Fig. 52

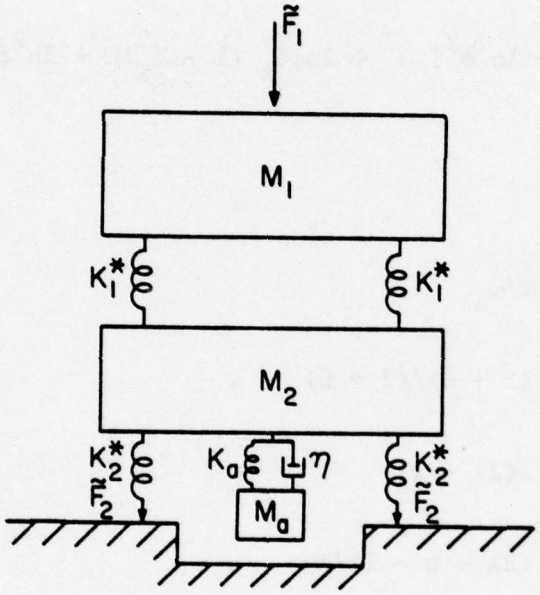

Fig. 53

where

$$R_D = \{-\Lambda\Omega^6 + \lambda[2 + (2\lambda - 1)(n^2\phi^2/\mu)]\Omega^4 + 2\lambda n\phi\delta_R\delta_K\Omega^3 T$$

$$-[(1 - \delta_K^2) + \lambda^2 n^2\phi^2 T]\Omega^2 - 4n\phi\delta_R\delta_K\Omega + n^2\phi^2(1 - \delta_K^2)\} \quad (65)$$

and

$$I_D = \{2\Lambda(n\phi\delta_R/\mu)\Omega^5 + 2\phi\delta_K\Omega^4 - 2\lambda n\phi\delta_R T\Omega^3$$

$$-\delta_K\,(2 + \lambda n^2\phi^2 T)\Omega^2 + 2n\phi\delta_R\,(1 - \delta_K^2)\Omega + 2n^2\phi^2\delta_K\} \quad . \quad (66)$$

In these equations,

$$\Omega = \omega/\omega_o \quad , \quad (67)$$

$$\lambda = (1 + \beta)/(2 + \beta) \quad , \quad (68)$$

$$\Lambda = \lambda(2\lambda - 1) \quad , \quad (69)$$

$$T = (2\lambda + \mu - 1)/\lambda\mu \quad , \quad (70)$$

$$\phi = \omega_2/\omega_o = \{[(1 + \beta) + (1 + \beta)^{1/2}]/\lambda\beta\}^{1/2} \quad , \quad (71)$$

and

$$\mu = M_2/(M_2 + M_a) \quad , \quad (72)$$

where M_a is the absorber mass, and the absorber tuning ratio

$$n = \omega_a/\omega_2 \quad , \quad (73)$$

where

$$\omega_a = (K_a/M_a)^{1/2} \quad . \quad (74)$$

Finally, the absorber damping ratio

$$\delta_R = \omega_a \eta / 2K_a \quad . \tag{75}$$

The optimum absorber damping is taken to be that specified by Eq. (50). By analogy to Eq. (49), the optimum tuning ratio is written as

$$n_{opt} = \omega_a / \omega_2 = (\varepsilon\mu)^{\frac{1}{2}} \quad , \tag{76}$$

where an appropriate value of ε has been established for each value of μ utilized. For example, if $\mu = 5/6$ ($M_a = M_2/5$) or $\mu = 25/26$ ($M_a = M_2/25$), then $\varepsilon = 0.76$ or 0.90, respectively.[18] For these values of ε, the secondary peak in the transmissibility curve is suppressed effectively in a smoothly continuous manner. It is a considerable advantage that, for any given value of μ, the same value of ε remains relevant throughout the range of β values considered here.

The three solid-line curves of Fig. 54 show the results of representative transmissibility calculations made from Eq. (64) for the same values of β that were considered previously, and for values of $\mu = 5/6$, $\delta_K = 0.05$, $\delta_R = 0.25$, and $\varepsilon = 0.76$. An additional chain-line curve shows the results of calculations made for the compound system possessing the largest secondary mass, and for values of $\mu = 25/26$, $\delta_K = 0.05$, $\delta_R = 0.12$, and $\varepsilon = 0.90$. Note that the transmissibility at the secondary resonance of the compound systems has always been suppressed effectively as compared with the peak values of transmissibility evident in Fig. 49. If the mount damping factors were smaller than the ones considered in Fig. 49, as they would be if the mounts were steel springs, then these peak values would be increased correspondingly--whereas the secondary peak heights in Fig. 54 would remain essentially unchanged.

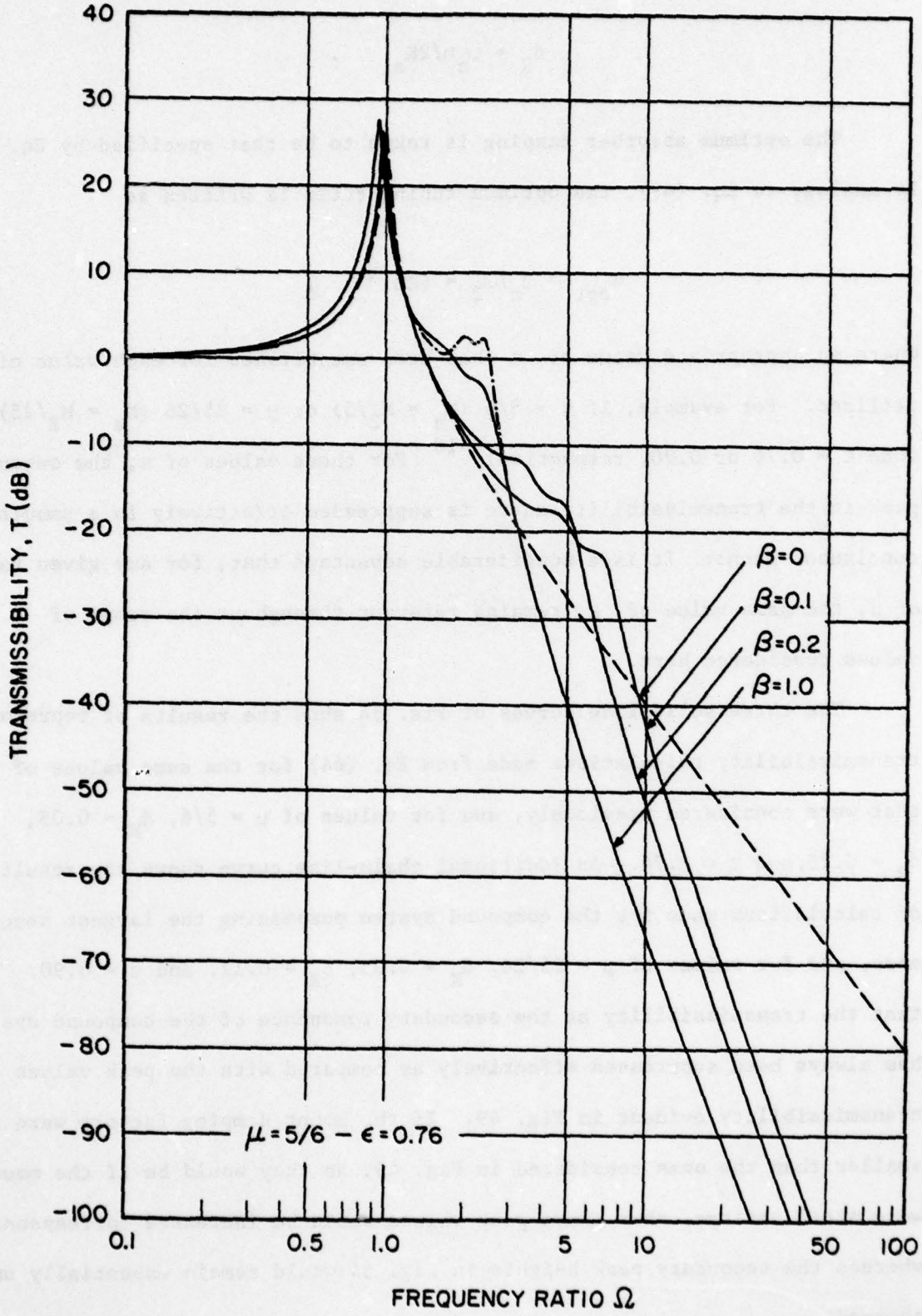
40
30
20
10
0
-10
-20
-30
-40
-50
-60
-70
-80
-90
-100
TRANSMISSIBILITY, T (dB)
β=0
β=0.1
β=0.2
β=1.0
μ=5/6 − ϵ=0.76
0.1
0.5
1.0
5
10
50
100
FREQUENCY RATIO Ω

Fig. 54

As a final example, the great effectiveness of the compound system is illustrated in Fig. 55, where the compound system is supported by a simply supported rectangular plate with an aspect ratio $\mu = 1/2$, and a fundamental natural frequency ω_1. The plate has relatively small internal damping ($\delta_E = \delta_G = 0.01$), the primary mass has four times the plate mass, and the fundamental natural frequency of the primary system is $\omega_1/4$. The mounts are located symmetrically about the plate center at distances of 1/3 the lengths of the plate sides from each plate corner. The mount damping factors $\delta_K = 0.05$. The mass ratio $\beta = 1.0$, 0.2, 0.1, and 0 (simple mounting system shown by the dashed-line curve).

6. MEASUREMENT OF TRANSMISSIBILITY

Reported throughout the literature are transmissibility measurements that have been obtained in one of two ways based on the simple sketches of Fig. 14. No other methods of transmissibility measurement are known to have been used previously or described elsewhere in the literature. Almost exclusively, apparatus has been built to simulate the simple mounting system of Fig. 14(a), the foundation and mounted item of which vibrate with the amplitudes $\tilde{x}_1$ and $\tilde{x}_2$. Transmissibility has been recorded as the readily measurable ratio of the companion accelerations; that is, $T = |(j\omega)^2\tilde{x}_2/(j\omega)^2\tilde{x}_1| = |\tilde{x}_2/\tilde{x}_1|$. The design of a representative experiment to establish T in this way, and a block diagram of the associated electronics, are reproduced from Ref. 25 as Fig. 56. Only three early German workers chose to build apparatus to record transmissibility as the force ratio $T = |\tilde{F}_2/\tilde{F}_1|$, thus simulating the simple mounting system of Fig. 14(b).

An early experiment to determine the transmissibility of the compound system is described in Ref. 26. It is remarkable that this reference, apparently overlooked in the many years since its publication in 1931, should have introduced

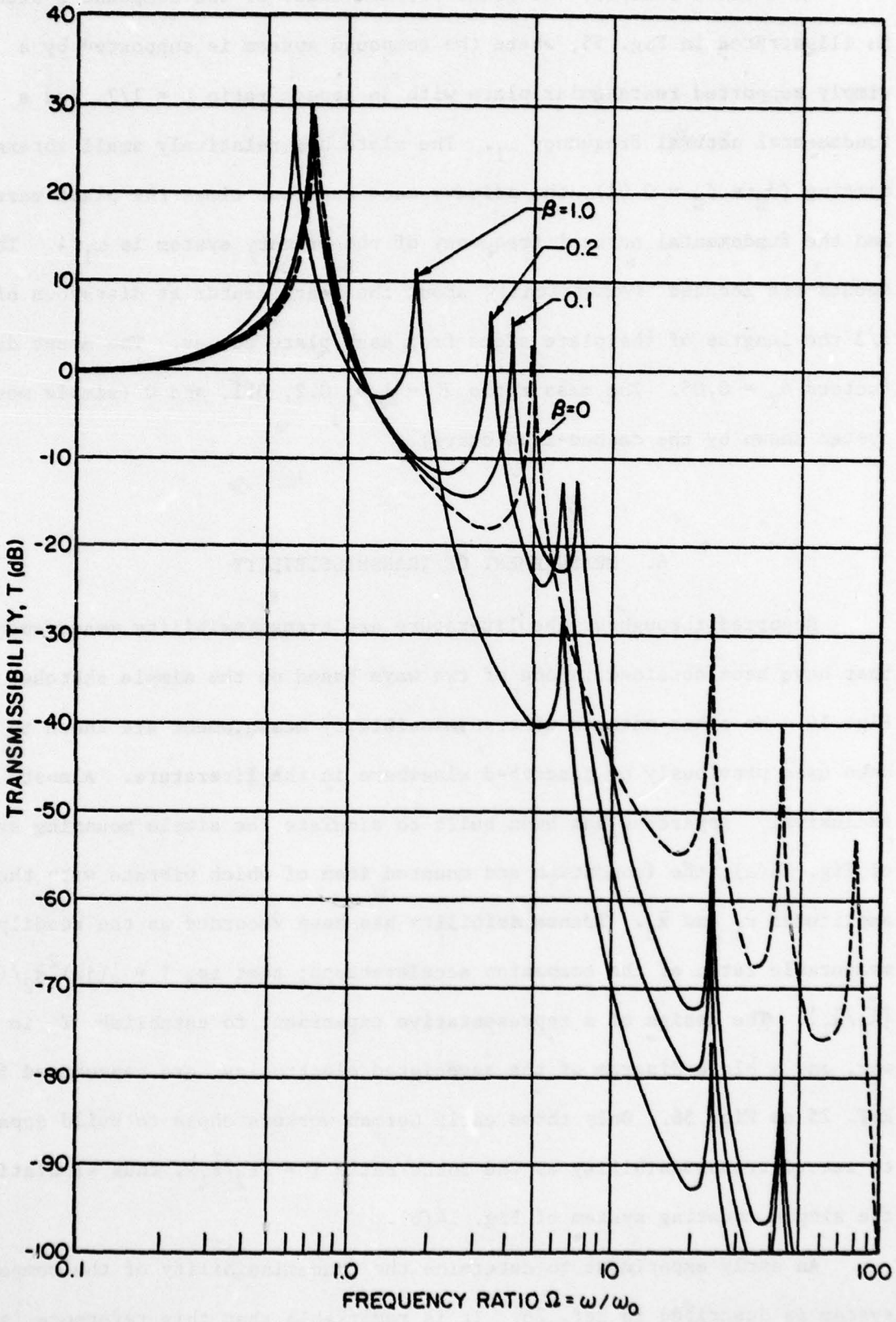
40
30
20
10
0
-10
-20
-30
-40
-50
-60
-70
-80
-90
-100
TRANSMISSIBILITY, T (dB)
β=1.0
0.2
0.1
β=0
0.1
1.0
10
100
FREQUENCY RATIO Ω = ω/ω0

Fig. 55

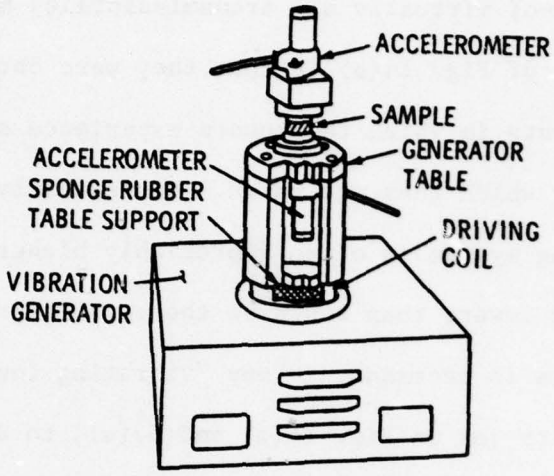
ACCELEROMETER
SAMPLE
GENERATOR TABLE
ACCELEROMETER SPONGE RUBBER TABLE SUPPORT
DRIVING COIL
VIBRATION GENERATOR

(a)

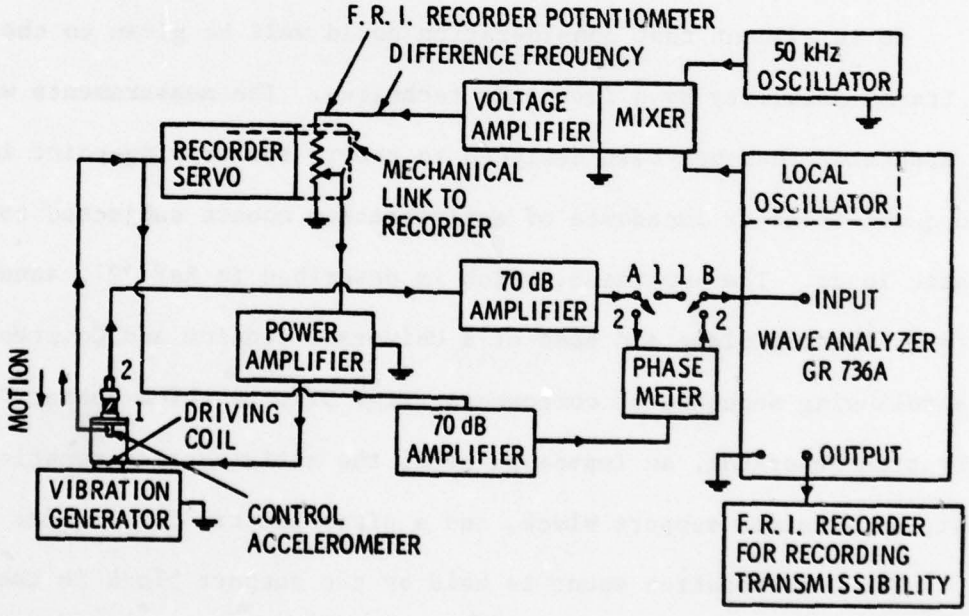
F. R. I. RECORDER POTENTIOMETER
DIFFERENCE FREQUENCY
50 kHz OSCILLATOR
VOLTAGE AMPLIFIER
MIXER
RECORDER SERVO
MECHANICAL LINK TO RECORDER
LOCAL OSCILLATOR
70 dB AMPLIFIER
A 1 1 B
INPUT
2
2
POWER AMPLIFIER
WAVE ANALYZER GR 736A
PHASE METER
MOTION
2
1
DRIVING COIL
70 dB AMPLIFIER
OUTPUT
VIBRATION GENERATOR
CONTROL ACCELEROMETER
F. R. I. RECORDER FOR RECORDING TRANSMISSIBILITY

(b)

Fig. 56

AD-A071 485 PENNSYLVANIA STATE UNIV UNIVERSITY PARK APPLIED RESE--ETC F/G 20/11
HANDBOOK OF VIBRATION AND NOISE CONTROL.(U)
APR 79 J C SNOWDON N00024-79-C-6043
UNCLASSIFIED ARL/PSU/TM-79-75 NL

2 OF 3
AD A071485

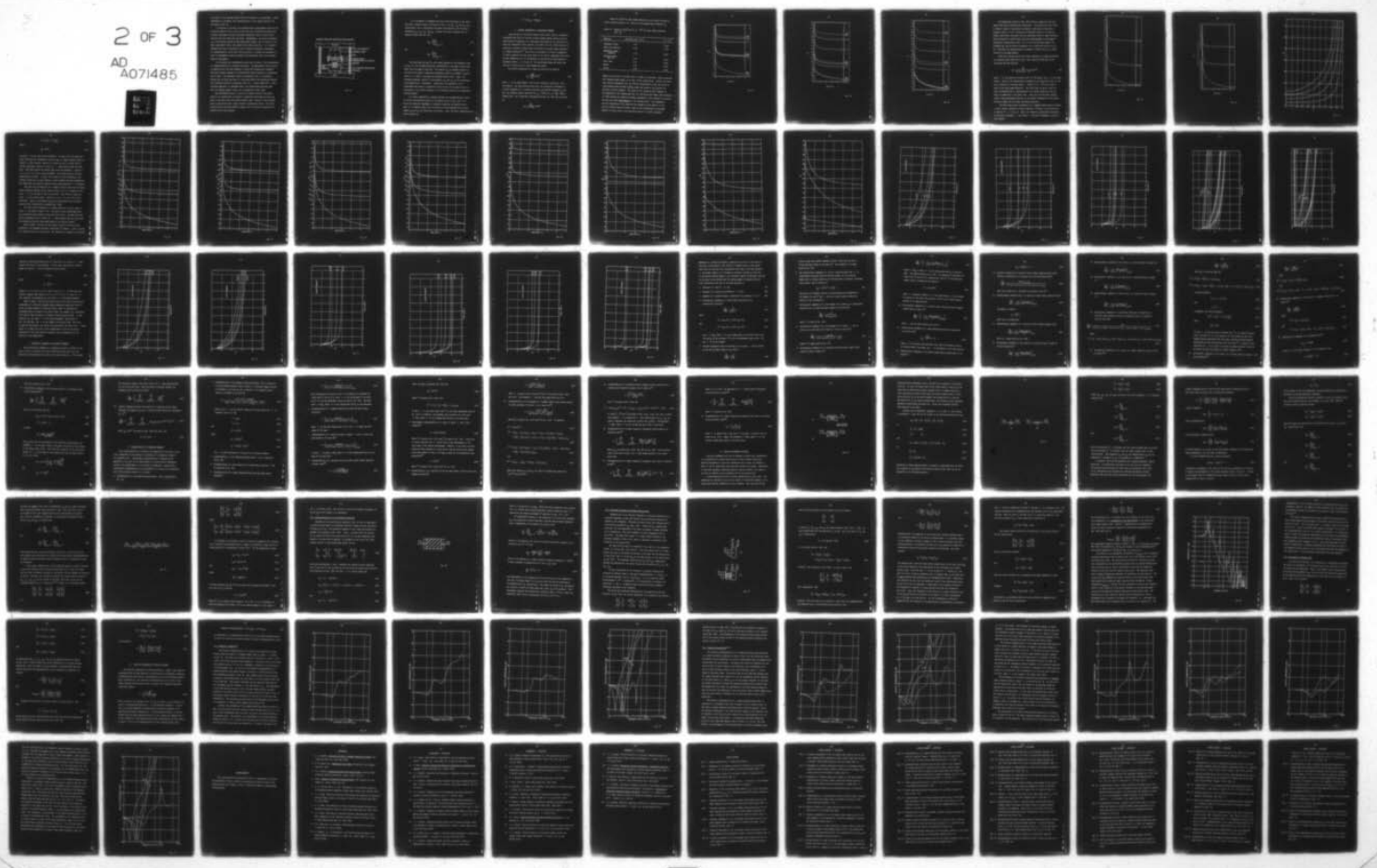

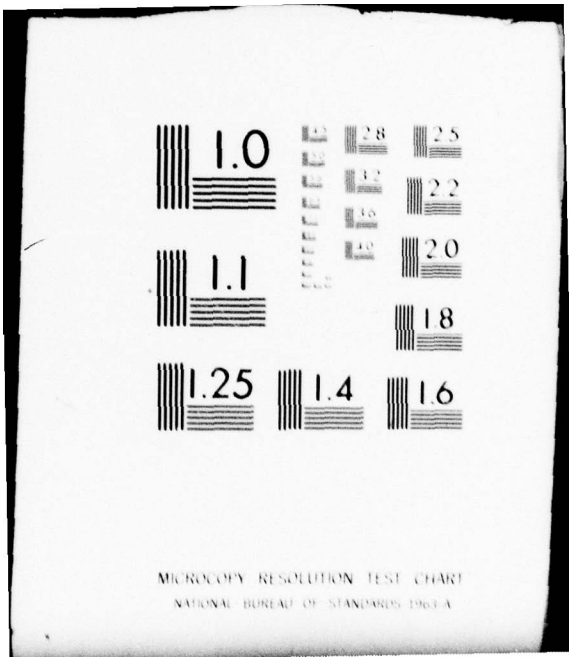
1.0
1.1
1.25
1.4
1.6
2.8
3.2
3.6
4.0
2.5
2.2
2.0
1.8
MICROCOPY RESOLUTION TEST CHART
NATIONAL BUREAU OF STANDARDS 1963-A

the theory of the compound system and have confirmed it by experiment. Recent experiments to determine the transmissibility of the dynamic absorber are described in Ref. 19.

A criticism of virtually all transmissibility measurements based on the reciprocal method of Fig. 14(a) is that they were obtained from small-scale or model experiments in which the mounts experience smaller static loads than the ones for which they are rated. Consequently, the natural frequency ω_o of the mounting system is often appreciably higher, and the strain in the mount appreciably lower, than would be the case in practice. It is readily apparent that care is necessary in any "vibrating foundation" measurement of transmissibility [as in Fig. 14(a) and 56(a)] to design the foundation so that its fundamental resonant frequency lies adequately above the frequency range of measurement.

It is evident that consideration could well be given to the determination of transmissibility by a four-pole technique. The measurements would utilize an apparatus that has been designed to record the driving-point impedance and quasi-transfer impedance of antivibration mounts subjected to significant static loads. The apparatus, which is described in Ref. 27, sandwiches between the top plate and base of a Universal Tension and Compression Machine the following sequence of components (Fig. 57): a thick rubber pad, a small vibration generator, an impedance head, the antivibration mounting under test, an aluminum support block, and a piezoelectric force gage.

The antivibration mount is held by the support block in the manner likely to be encountered "in service," preferably contacting the lower end plate of the mount over the largest possible area. Mounts of other designs would be mated with other support blocks of appropriate shape. The blocks should have the greatest possible rigidity and could well be machined from alumina rather than aluminum.

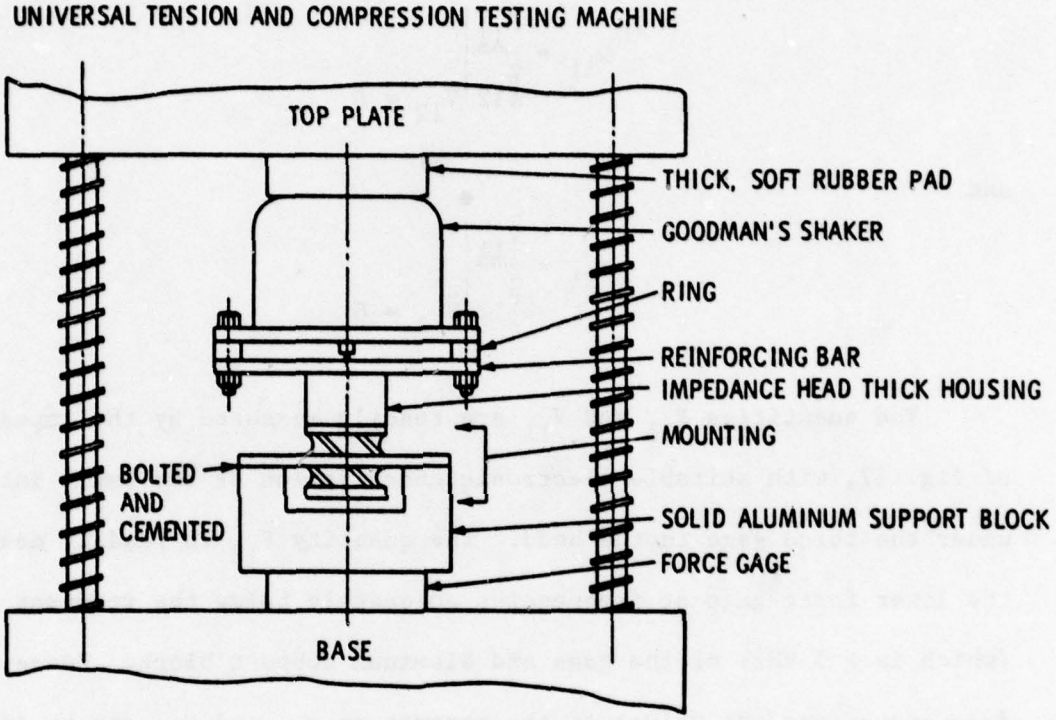
UNIVERSAL TENSION AND COMPRESSION TESTING MACHINE
TOP PLATE
THICK, SOFT RUBBER PAD
GOODMAN'S SHAKER
RING
REINFORCING BAR
IMPEDANCE HEAD THICK HOUSING
MOUNTING
BOLTED
AND
CEMENTED
SOLID ALUMINUM SUPPORT BLOCK
FORCE GAGE
BASE

Fig. 57

It is convenient to designate the forces and velocities at the input and output terminal pairs of the mount in Fig. 57 as $\tilde{F}_{11}$, $\tilde{V}_{11}$ and $\tilde{F}_{12}$, $\tilde{V}_{12}$, respectively, and to characterize the mount performance by the four-pole parameters α_{11}, α_{12}, α_{21}, and α_{22}. Because the output terminal pair is rigidly blocked (See Sec. 10),

$$\alpha_{11} = \left.\frac{\tilde{F}_{11}}{\tilde{F}_{12}}\right|_{\tilde{V}_{12} = 0} \tag{77}$$

and

$$\alpha_{21} = \left.\frac{\tilde{V}_{11}}{\tilde{F}_{12}}\right|_{\tilde{V}_{12} = 0} . \tag{78}$$

The quantities $\tilde{F}_{11}$ and $\tilde{V}_{11}$ are readily measured by the impedance head of Fig. 57, with suitable electronic concellation of the small integral mass under the force gage in the head. The quantity $\tilde{F}_{12}$ is readily measured by the lower force gage at frequencies adequately below the resonant frequency (which is > 5 kHz) of the gage and aluminum support block. Hence, the frequency-dependent values of the parameters α_{11} and α_{21} can be established by straightforward measurement. Importantly, the parameters can be established when there is significant static strain in the mount--which is introduced, to the extent required, by the Universal Tension and Compression Testing Machine.

If a basic comparison is required between the transmissibility curves of various antivibration mounts in the simple system of Fig. 14(b), for which the foundation impedance is extremely large and the mounted item of mass M is ideally rigid, then it suffices to have knowledge of the parameters α_{11} and α_{21} for each mount of interest. Thus, the force transmissibility can be written as

$$T = |1/(\alpha_{11} + j\omega M\alpha_{21})| \quad . \tag{79}$$

7. NATURAL FREQUENCIES OF STRUCTURAL MEMBERS

Loads carried by structural members reduce their natural frequencies. Considered here first is the way in which loading masses reduce the first three natural frequencies of a cantilever beam loaded at its free end by a mass with negligible rotary inertia, and reduce the first three natural frequencies of centrally loaded beams and plates with either simply supported or clamped boundaries.[28] The plates are assumed to be thin in comparison to their diameters, and the beams either to be long in comparison with their lateral dimensions or to be rectangular in section and to have length-to-thickness ratios ψ of 10 and 20. The mass-loaded beams and plates are excited to vibrate only in their symmetrical modes.

The natural frequencies of a beam are given by the equation

$$f_R = \frac{r_g N_R^2}{2\pi L^2} (E/\rho)^{1/2} \quad , \tag{80}$$

where L is the beam length, E its Young's modulus of elasticity, and ρ its density. For beam cross sections that are rectangular (thickness d), circular (diameter D), or annular (internal and external diameters D_1 and D_2), the relevant radii of gyration are $r_g = d/\sqrt{12}$, $D/4$, or $\sqrt{(D_1^2 + D_2^2)}/4$, respectively. For a beam with rectangular section, Eq. (80) may be written as

$$f_R = \frac{N_R^2}{21.77\psi L} (E/\rho)^{1/2} \quad . \tag{81}$$

Values of $(E/\rho)^{1/2}$ for some common materials are as listed in Table VI, which is drawn from Ref. 29. Values of the dimensionless parameter N_R

Table VI. Values of $(E/\rho)^{1/2}$ and of $(1 - \nu^2)^{1/2}$ for some common materials (Ref. 29).

Material	$(E/\rho)^{1/2}$(in./sec x 10^{-5})	$(1 - \nu^2)^{1/2}$
Aluminum, rolled	1.97	0.935
Brass (70 Cu/30 Zn)	1.35	0.927
Magnesium, drawn, annealed	1.94	0.952
Stainless steel, No. 347	1.97	0.954
Iron, cast	1.76	0.963
Nickel	1.93	0.942
Lucite	0.724	0.917

depend on the value of the mass ratio $\gamma = M/M_b$ for cantilever, simply supported, and clamped-clamped beams, as in Figs. 58-60, respectively. Because the beams have natural frequencies that are directly proportional to N_R^2, the curves of these figures show how mass loading causes the values of the natural frequencies to shift downward. The extent of the frequency shift depends on the magnitude of the loading mass but, for the second and higher beam resonances, it cannot exceed the original frequency separation of the resonance of interest and the next lower antiresonance of the unloaded beam.[1] The fundamental natural frequencies of the beams are not bounded in this manner; in fact, they are shifted downward without limit as the loading mass is increased because, in every case, no antiresonance exists at a lower frequency.[1]

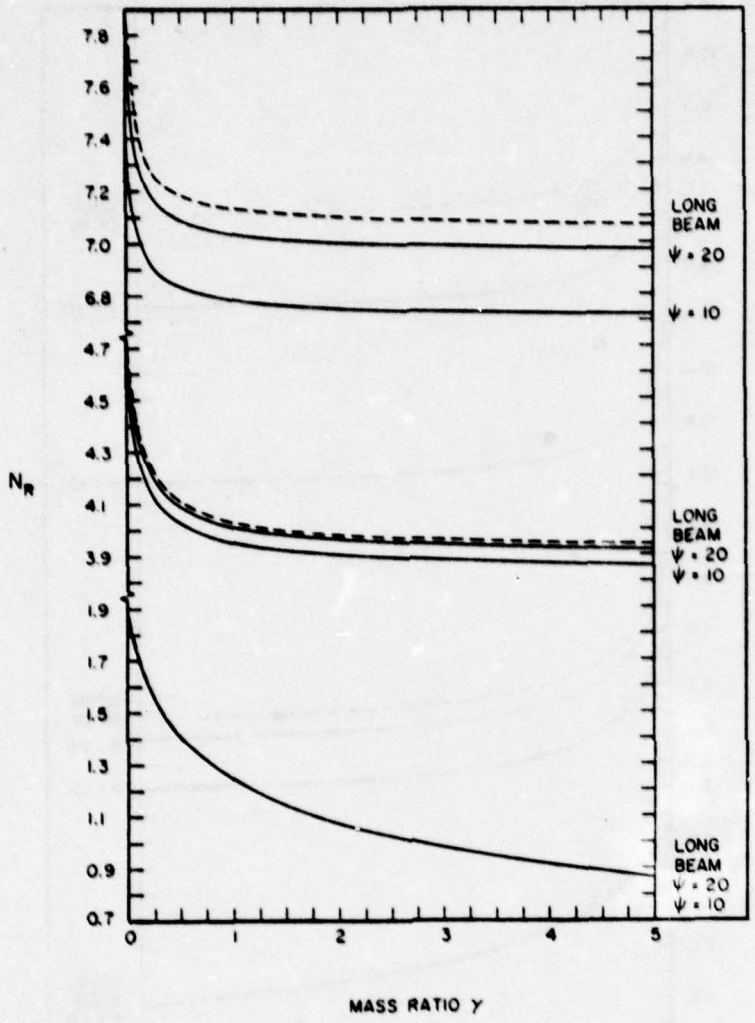
7.8
7.6
7.4
7.2
7.0
6.8
4.7
4.5
4.3
4.1
3.9
1.9
1.7
1.5
1.3
1.1
0.9
0.7
N_R
0
1
2
3
4
5
MASS RATIO γ
LONG BEAM ψ = 20
ψ = 10
LONG BEAM ψ = 20 ψ = 10
LONG BEAM ψ = 20 ψ = 10

Fig. 58

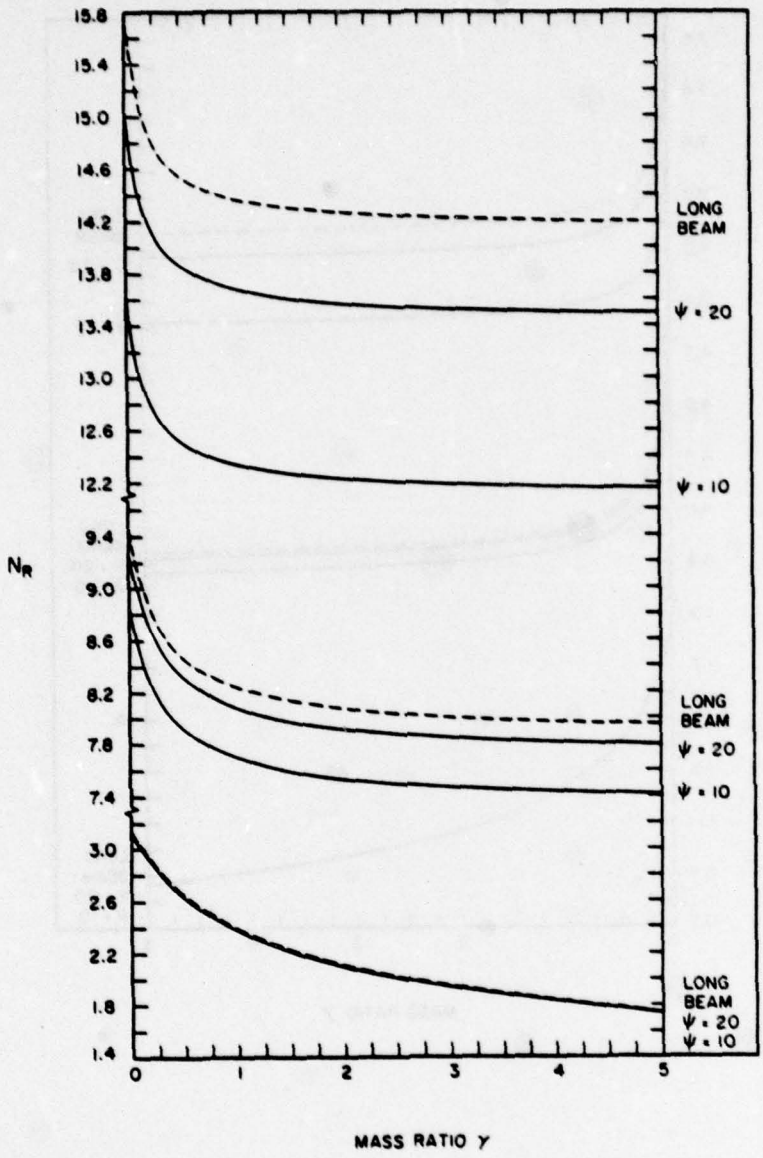
15.8
15.4
15.0
14.6
14.2
13.8
13.4
13.0
12.6
12.2
9.4
9.0
8.6
8.2
7.8
7.4
3.0
2.6
2.2
1.8
1.4
N_R
0
1
2
3
4
5
MASS RATIO γ
LONG BEAM
ψ = 20
ψ = 10
LONG BEAM
ψ = 20
ψ = 10
LONG BEAM
ψ = 20
ψ = 10

Fig. 59

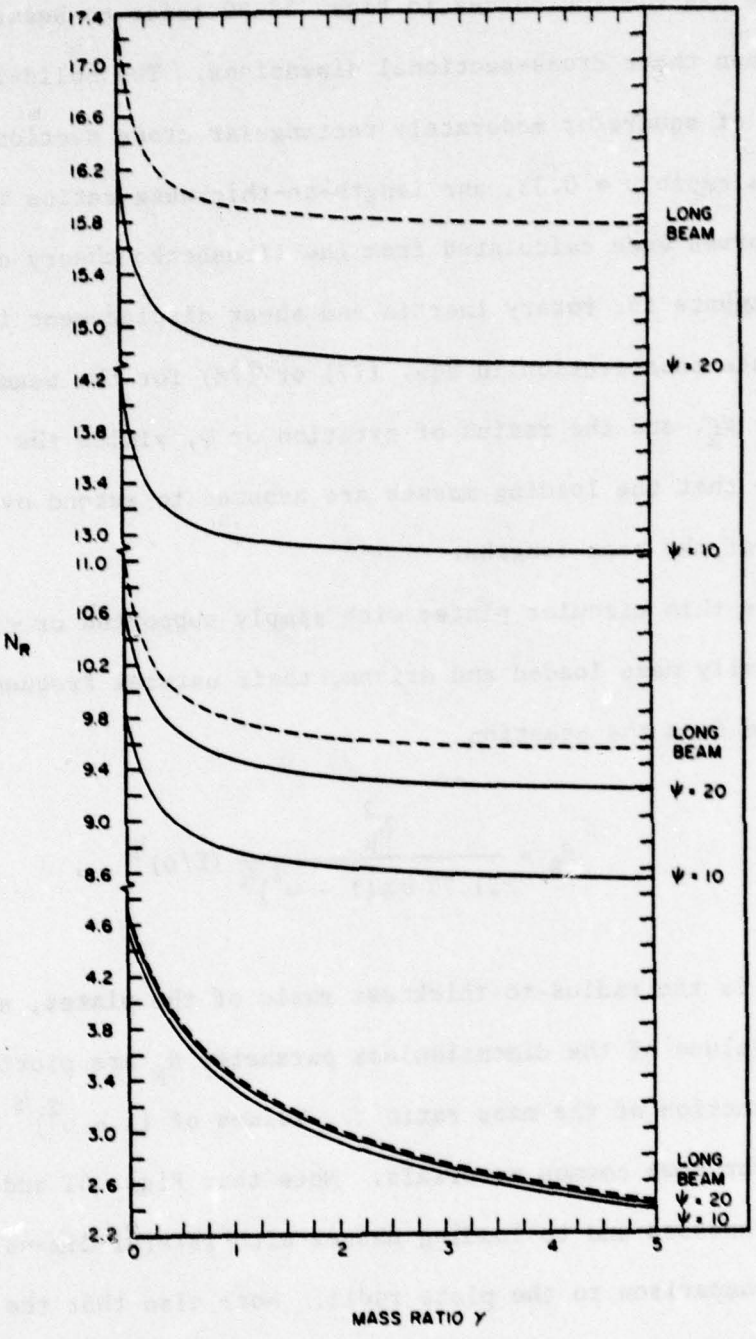
17.4
17.0
16.6
16.2
15.8
15.4
15.0
14.2
13.8
13.4
13.0
11.0
10.6
10.2
9.8
9.4
9.0
8.6
4.6
4.2
3.8
3.4
3.0
2.6
2.2
N_R
LONG BEAM
ψ = 20
ψ = 10
LONG BEAM
ψ = 20
ψ = 10
LONG BEAM
ψ = 20
ψ = 10
0
1
2
3
4
5
MASS RATIO γ

Fig. 60

The dashed-line curves in Figs. 58-60 refer to beams that are much longer than their cross-sectional dimensions. The solid-line curves refer to beams of square or moderately rectangular cross section that have a Poisson's ratio $\nu = 0.33$, and length-to-thickness ratios $\psi = 10$ and 20. (These curves were calculated from the Timoshenko theory of beam vibration, which accounts for rotary inertia and shear displacement in the beams.[1]) Appropriate substitution in Eqs. (77) or (78) for the beam length, the parameter N_R, and the radius of gyration or ψ, yields the value of f_R in Hz. Note that the loading masses are assumed to extend over only a small fraction of the beam lengths.

When thin circular plates with simply supported or clamped boundaries are centrally mass loaded and driven, their natural frequencies can be calculated from the equation

$$f_R = \frac{N_R^2}{21.77\,\theta\, a(1 - \nu^2)^{\frac{1}{2}}} (E/\rho)^{\frac{1}{2}} \quad , \tag{82}$$

where θ is the radius-to-thickness ratio of the plates, and a is the plate radius. Values of the dimensionless parameter N_R are plotted in Figs. 61 and 62 as a function of the mass ratio γ. Values of $(1 - \nu^2)^{\frac{1}{2}}$ are listed in Table VI for some common materials. Note that Figs. 61 and 62 relate to plate thicknesses and to loading masses with lateral dimensions that are small in comparison to the plate radii. Note also that the mass loading causes a more pronounced reduction in the natural frequencies of the plates than was evident for the beams considered previously.

The first four natural frequencies of a clamped annular plate of radius a with a central concentric circular aperture of radius μa are plotted as a function of μ in Fig. 63. Here, the ordinate N_R represents the product of the plate wavenumber n and radius a. The plate wavenumber is given by the equation

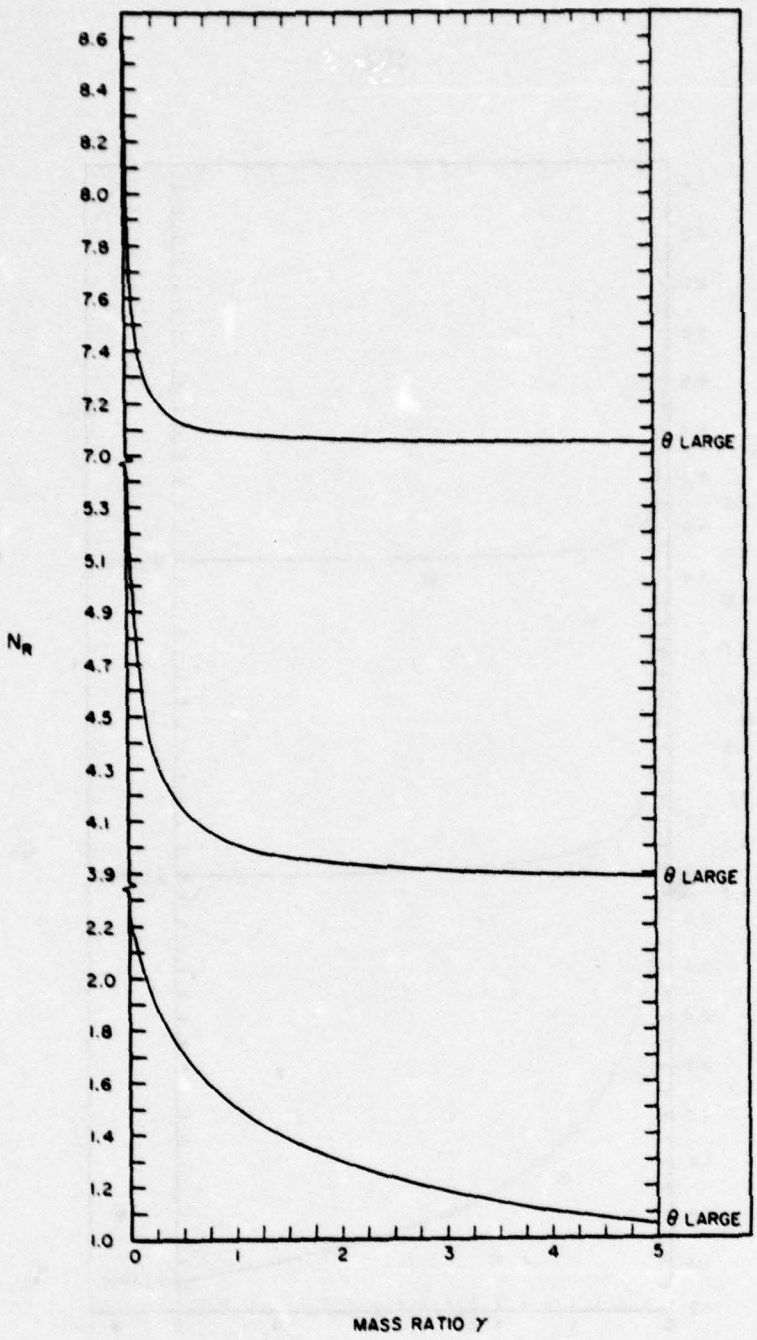
8.6
8.4
8.2
8.0
7.8
7.6
7.4
7.2
7.0
5.3
5.1
4.9
4.7
4.5
4.3
4.1
3.9
2.2
2.0
1.8
1.6
1.4
1.2
1.0
N_R
θ LARGE
θ LARGE
θ LARGE
0
1
2
3
4
5
MASS RATIO γ

Fig. 61

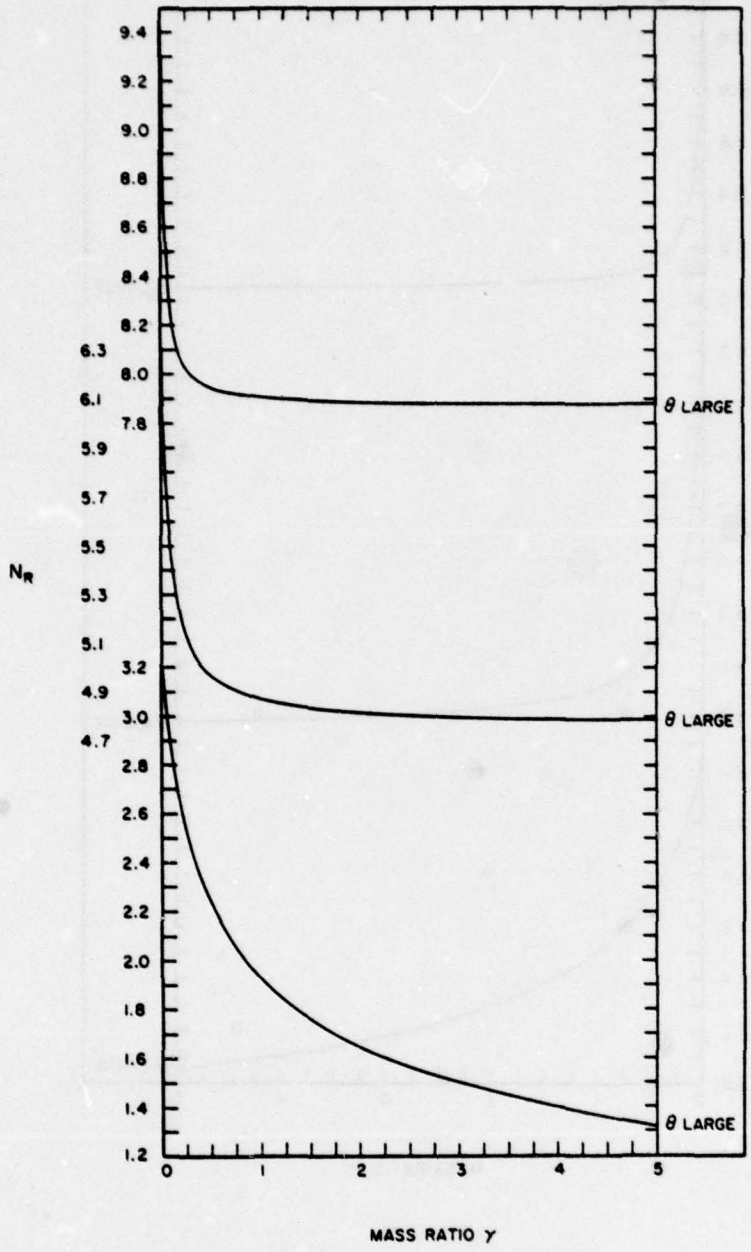
9.4
9.2
9.0
8.8
8.6
8.4
8.2
6.3
8.0
6.1
7.8
5.9
5.7
5.5
5.3
5.1
3.2
4.9
3.0
4.7
2.8
2.6
2.4
2.2
2.0
1.8
1.6
1.4
1.2
N_R
θ LARGE
θ LARGE
θ LARGE
0
1
2
3
4
5
MASS RATIO γ

Fig. 62

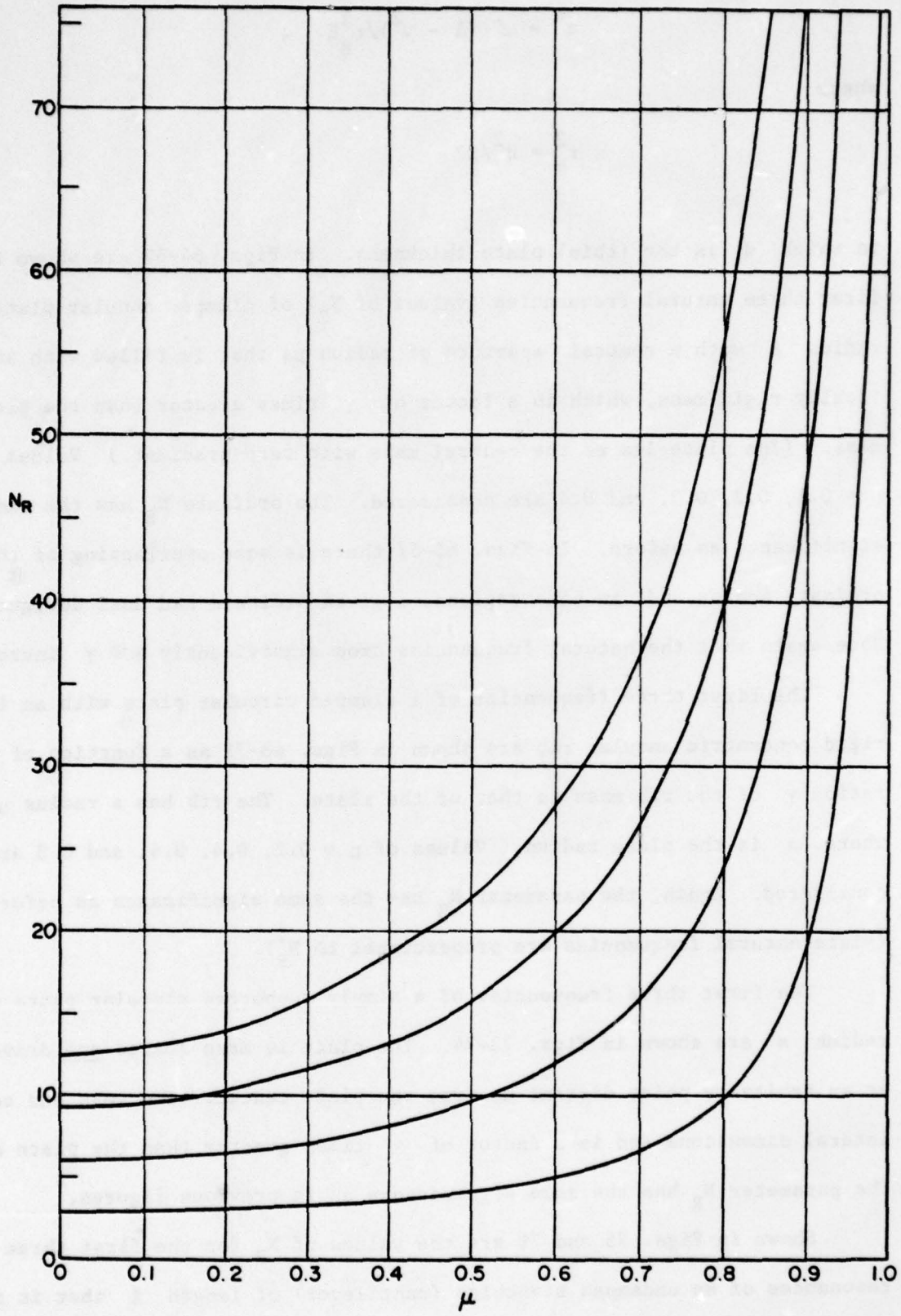

Fig. 63

$$n^4 = \omega^2\rho(1 - \nu^2)/r_g^2E \quad , \tag{83}$$

where

$$r_g^2 = d^2/12 \tag{84}$$

in which d is the (thin) plate thickness. In Figs. 64-67 are shown the first three natural frequencies (values of N_R) of clamped annular plates of radius a with a central aperture of radius μa that is filled with an ideally rigid mass, which is a factor of γ times greater than the plate mass. (The plate leaves the central mass with zero gradient.) Values of $\mu = 0.1$, 0.2, 0.3, and 0.4 are considered. The ordinate N_R has the same significance as before. In Figs. 65-67 there is some overlapping of the ordinate scales and, in some regions, a given ordinate had dual designation. Note again that the natural frequencies drop significantly as γ increases.

The first three frequencies of a clamped circular plate with an ideally rigid concentric annular rib are shown in Figs. 68-71 as a function of the ratio γ of the rib mass to that of the plate. The rib has a radius μa, where a is the plate radius. Values of $\mu = 0.2$, 0.4, 0.6, and 0.8 are considered. Again, the parameter N_R has the same significance as before (plate natural frequencies are proportional to N_R^2).

The first three frequencies of a simply supported circular plate of radius a are shown in Figs. 72-74. The plate is mass loaded and driven at an arbitrary point distant μa from the plate center. The mass has small lateral dimensions and is a factor of γ times greater than the plate mass. The parameter N_R has the same significance as in previous figures.

Shown in Figs. 75 and 76 are the values of N_R for the first three resonances of an undamped stanchion (cantilever) of length ℓ that is driven by a vibratory force at its free end. The stanchion is loaded at an arbitrary

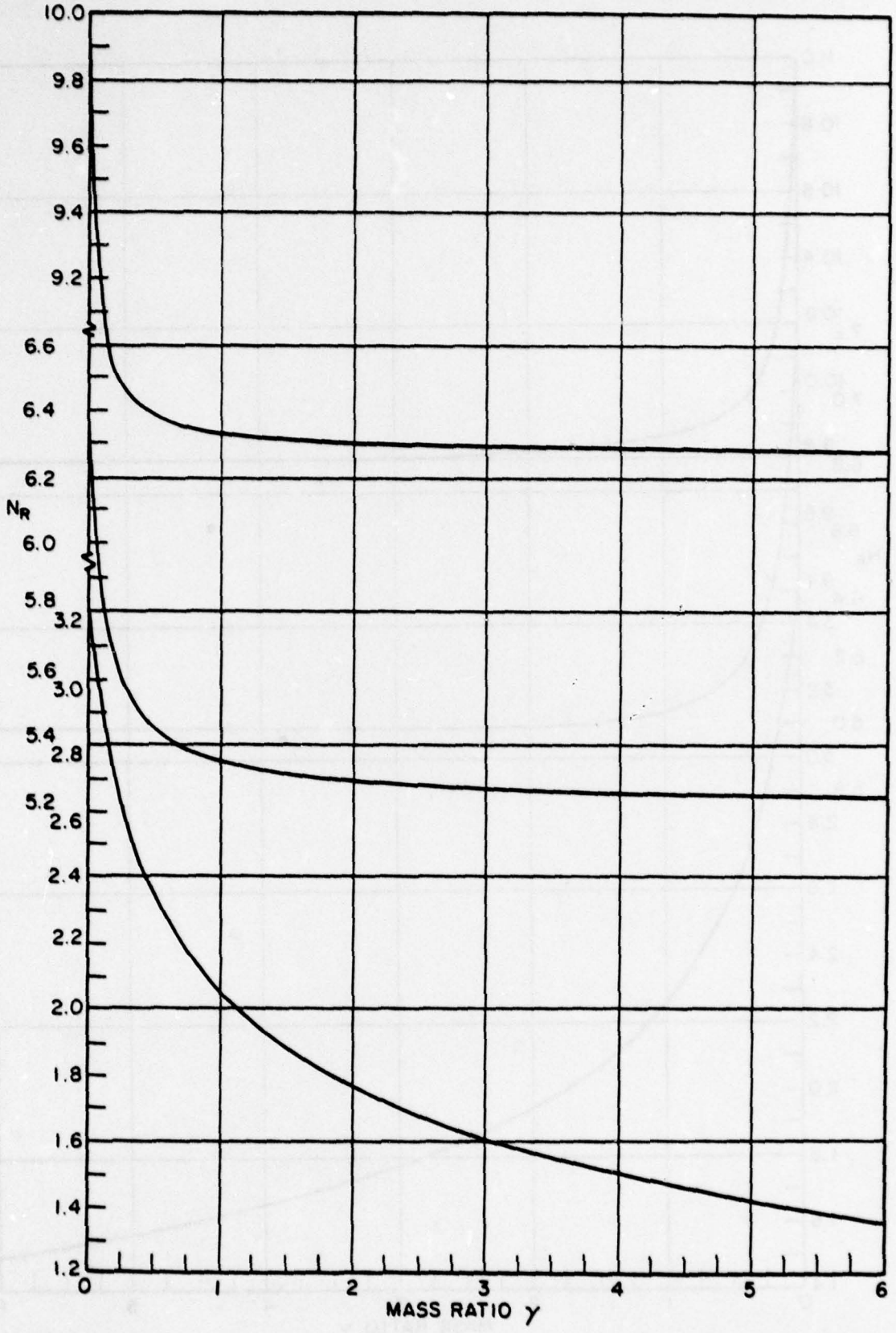
10.0
9.8
9.6
9.4
9.2
6.6
6.4
6.2
N_R
6.0
5.8
3.2
5.6
3.0
5.4
2.8
5.2
2.6
2.4
2.2
2.0
1.8
1.6
1.4
1.2
0
1
2
3
4
5
6
MASS RATIO γ

Fig. 64

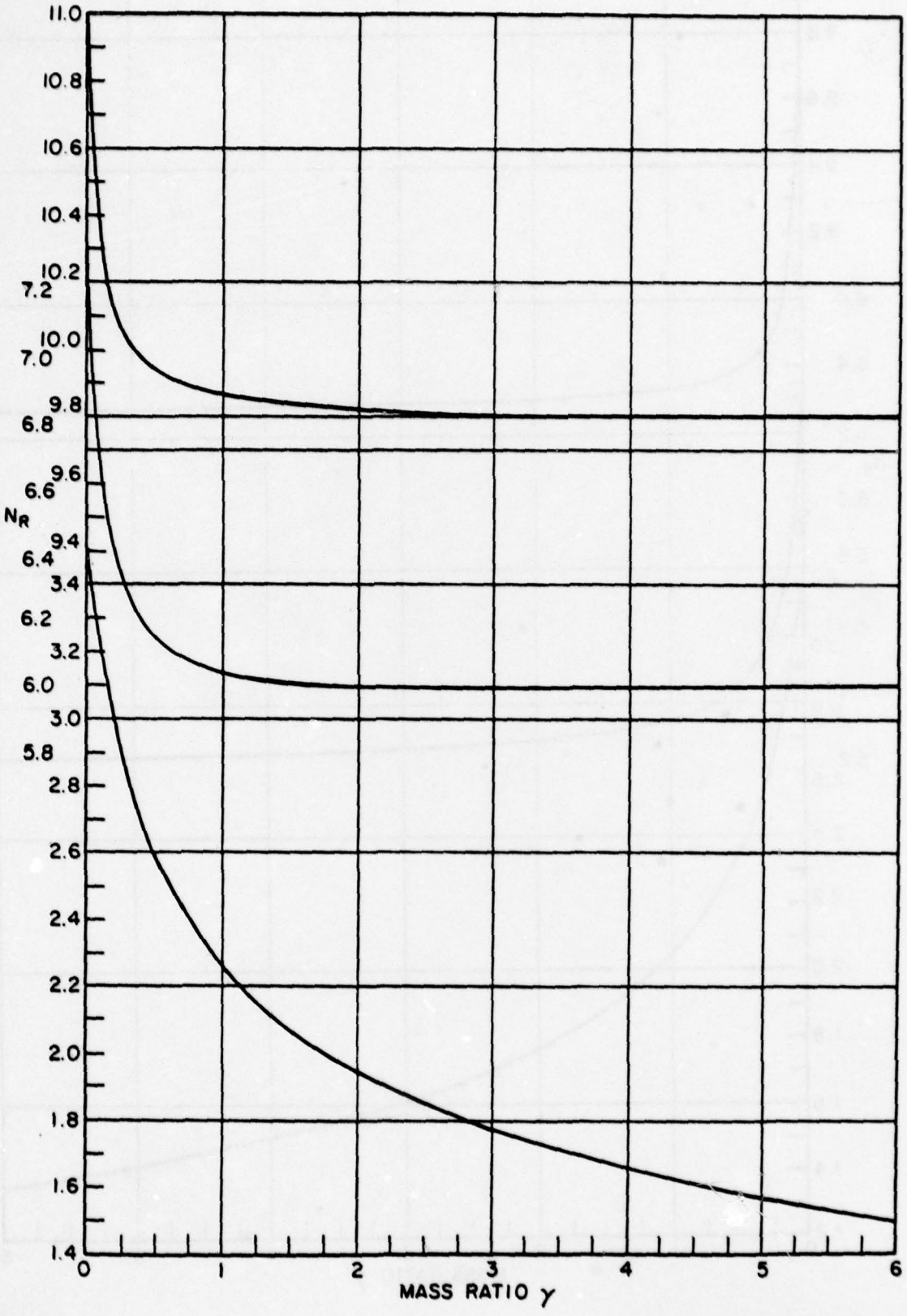
11.0
10.8
10.6
10.4
10.2
7.2
10.0
7.0
9.8
6.8
9.6
6.6
N_R
9.4
6.4
3.4
6.2
3.2
6.0
3.0
5.8
2.8
2.6
2.4
2.2
2.0
1.8
1.6
1.4
0
1
2
3
4
5
6
MASS RATIO γ

Fig. 65

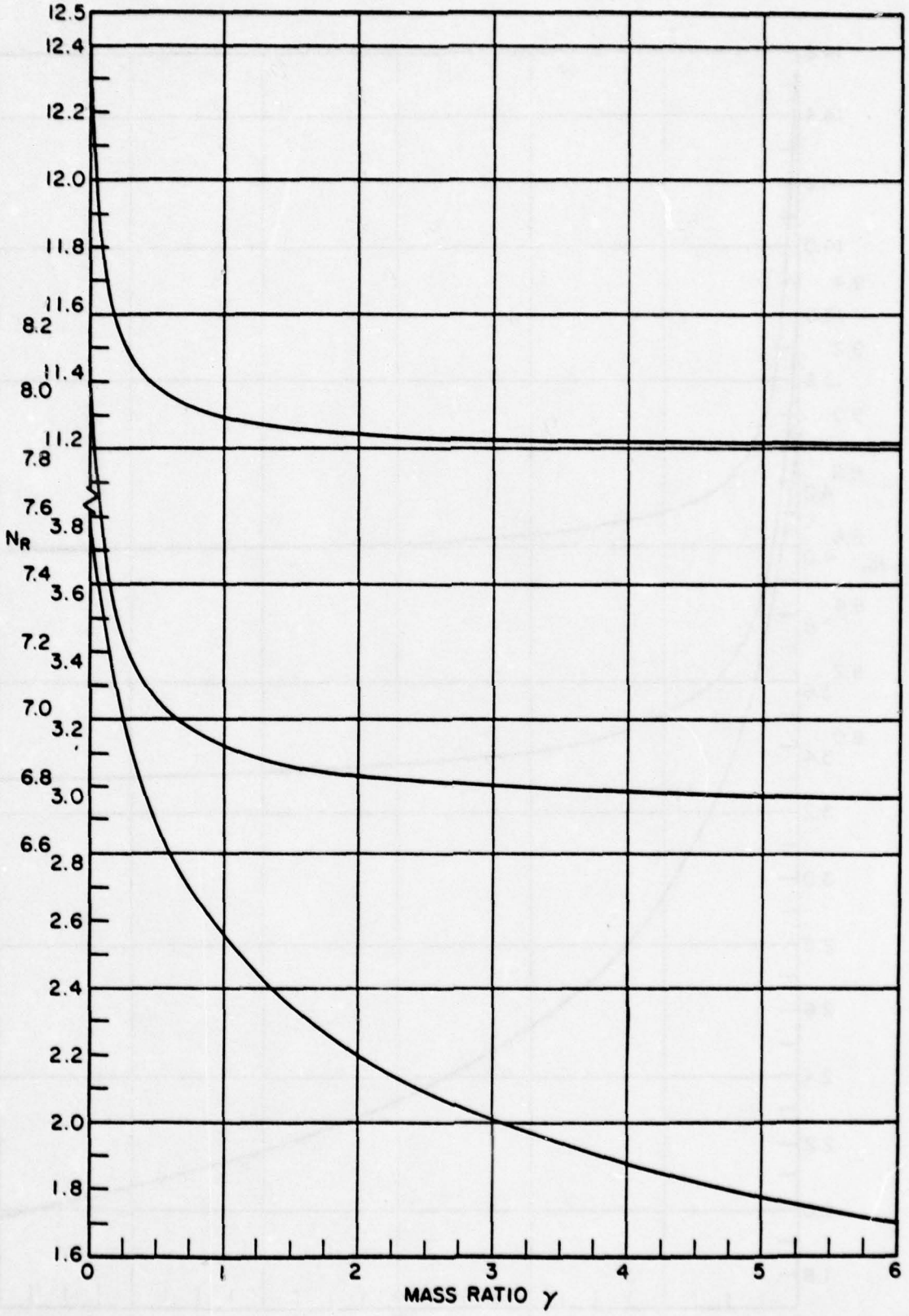
12.5
12.4
12.2
12.0
11.8
11.6
8.2
11.4
8.0
11.2
7.8
7.6
3.8
N_R
7.4
3.6
7.2
3.4
7.0
3.2
6.8
3.0
6.6
2.8
2.6
2.4
2.2
2.0
1.8
1.6
0
1
2
3
4
5
6
MASS RATIO γ

Fig. 66

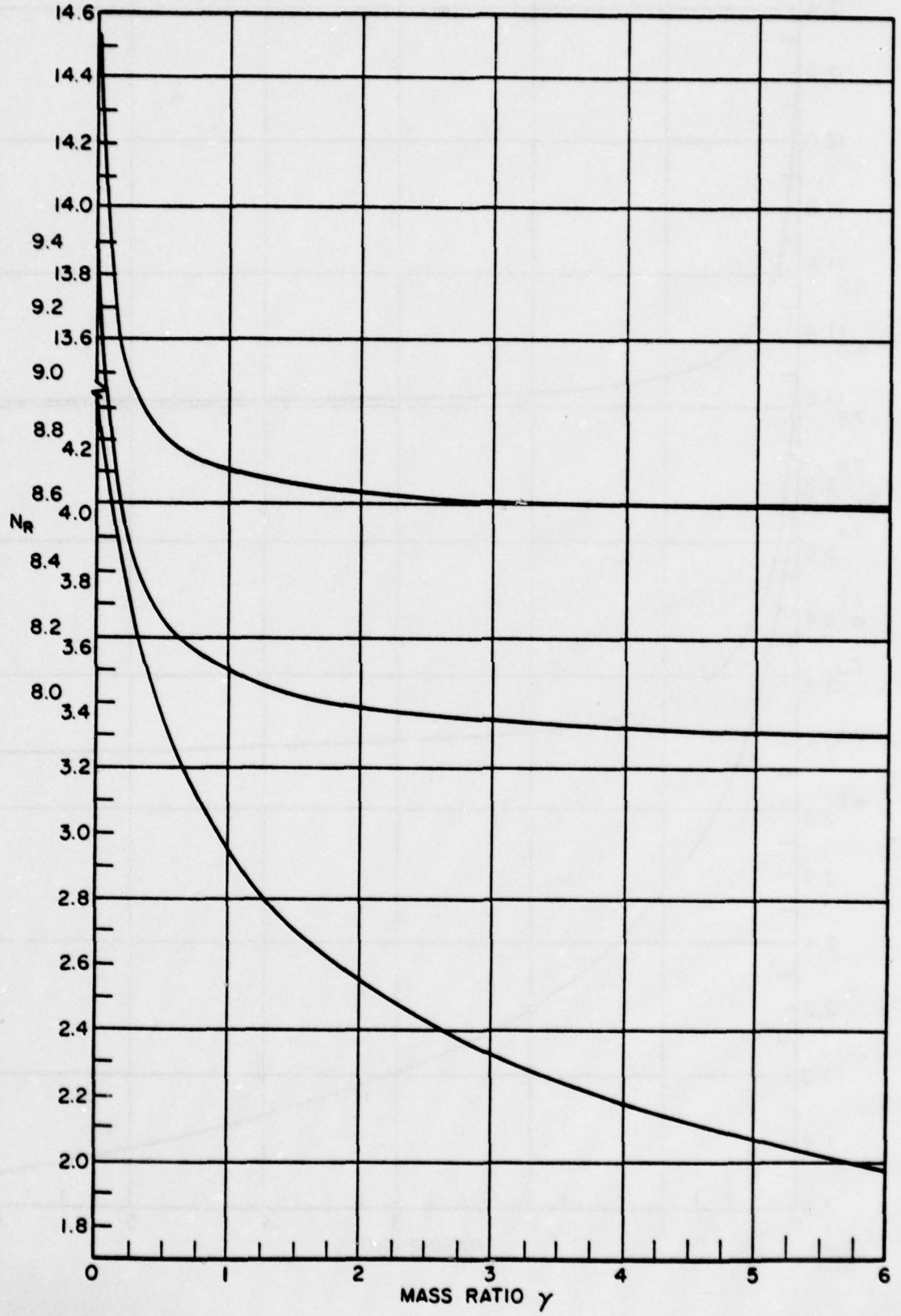
14.6
14.4
14.2
14.0
9.4
13.8
9.2
13.6
9.0
8.8
4.2
8.6
4.0
N_R
8.4
3.8
8.2
3.6
8.0
3.4
3.2
3.0
2.8
2.6
2.4
2.2
2.0
1.8
0
1
2
3
4
5
6
MASS RATIO γ

Fig. 67

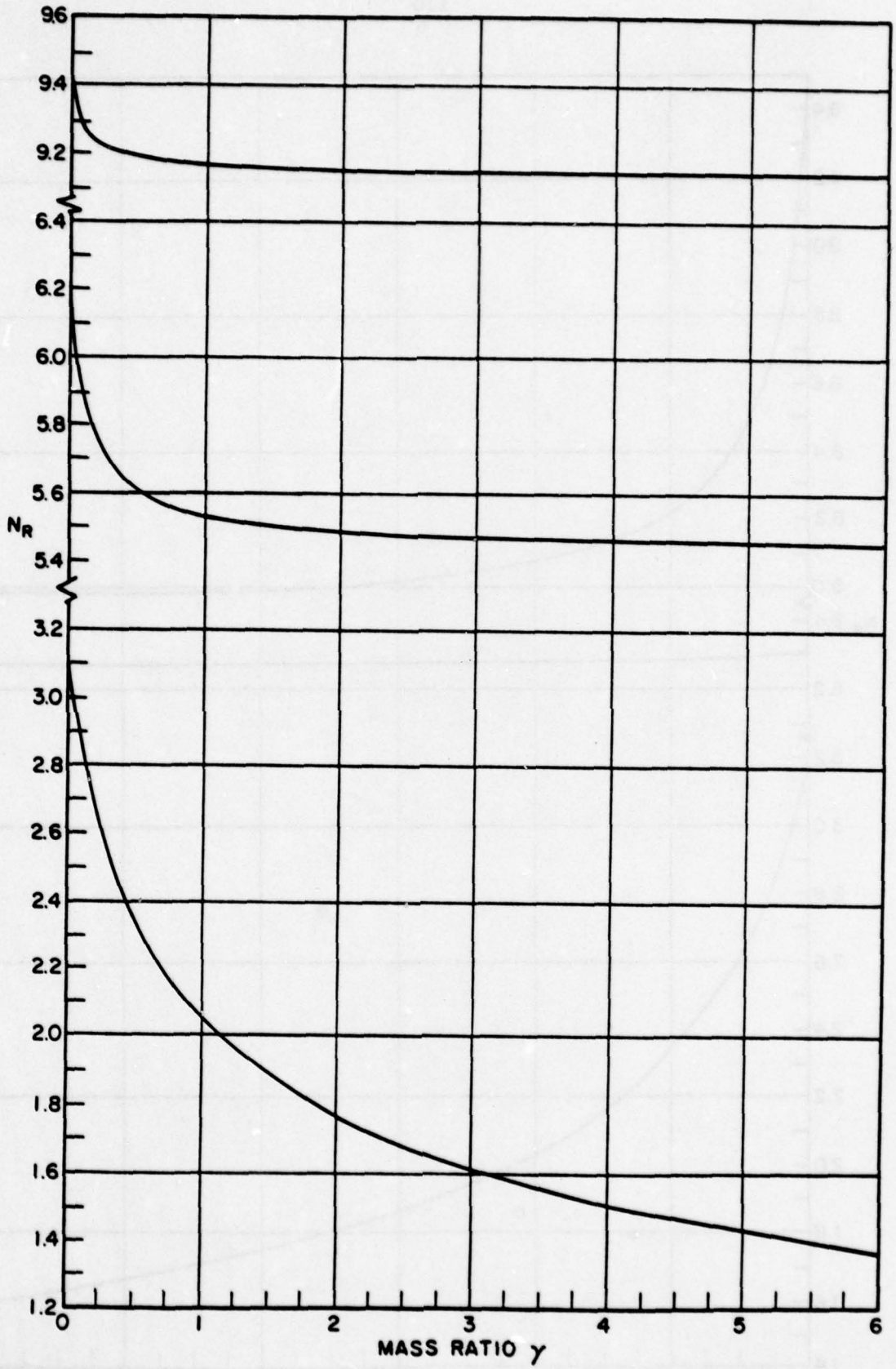
9.6
9.4
9.2
6.4
6.2
6.0
5.8
5.6
N_R
5.4
3.2
3.0
2.8
2.6
2.4
2.2
2.0
1.8
1.6
1.4
1.2
0
1
2
3
4
5
6
MASS RATIO γ

Fig. 68

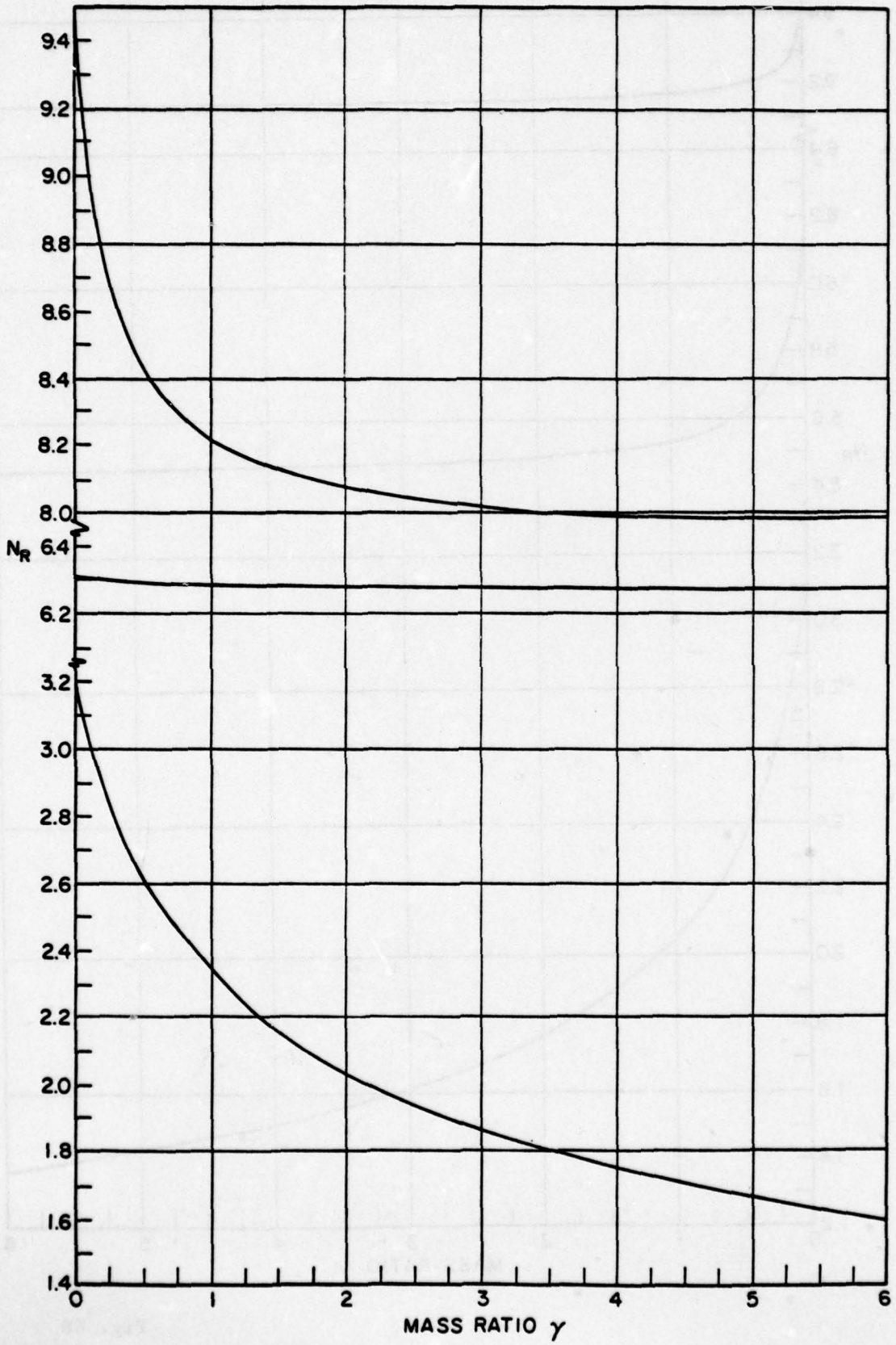
9.4
9.2
9.0
8.8
8.6
8.4
8.2
8.0
N_R 6.4
6.2
3.2
3.0
2.8
2.6
2.4
2.2
2.0
1.8
1.6
1.4
0
1
2
3
4
5
6
MASS RATIO γ

Fig. 69

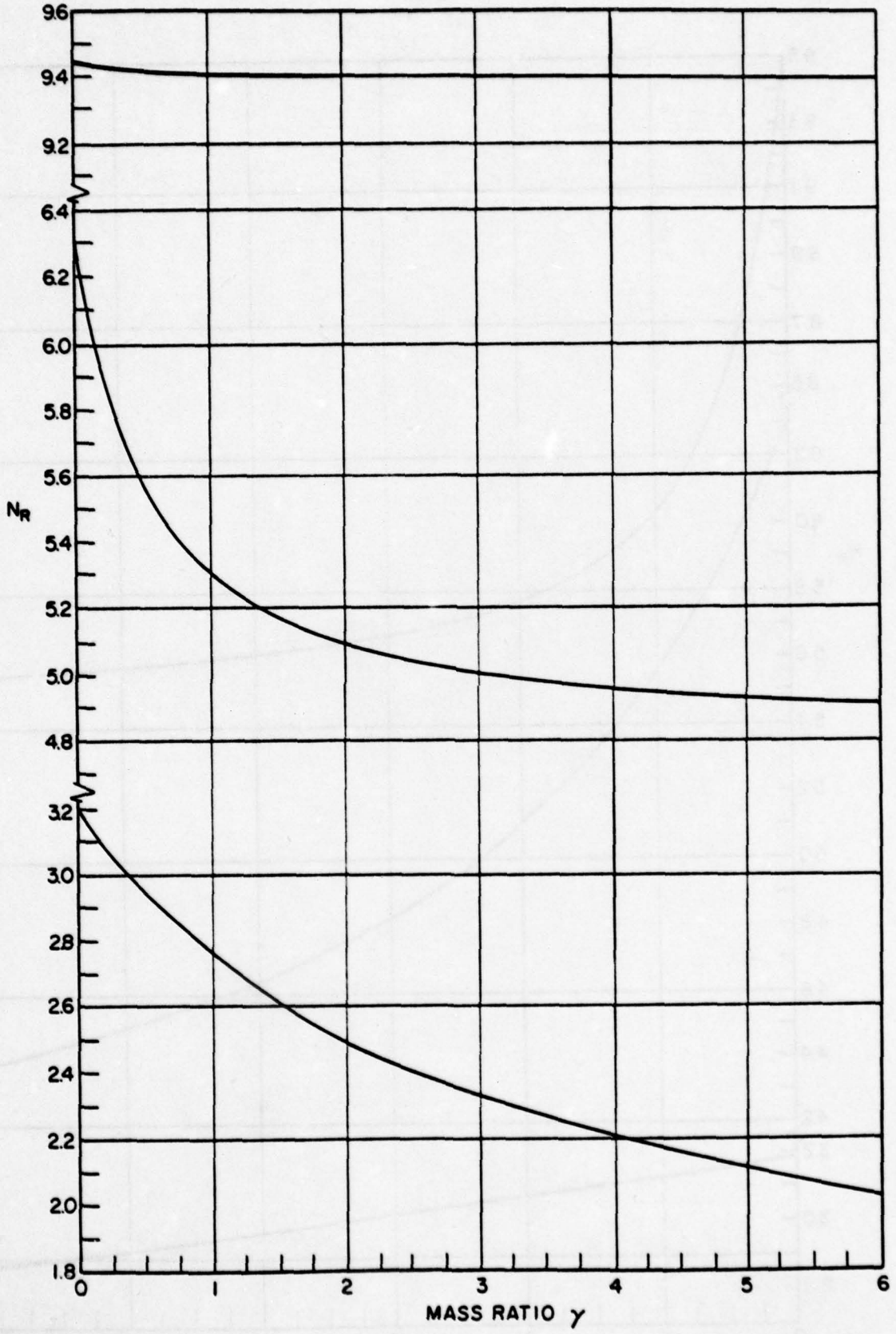
9.6
9.4
9.2
6.4
6.2
6.0
5.8
5.6
N_R
5.4
5.2
5.0
4.8
3.2
3.0
2.8
2.6
2.4
2.2
2.0
1.8
0
1
2
3
4
5
6
MASS RATIO γ

Fig. 70

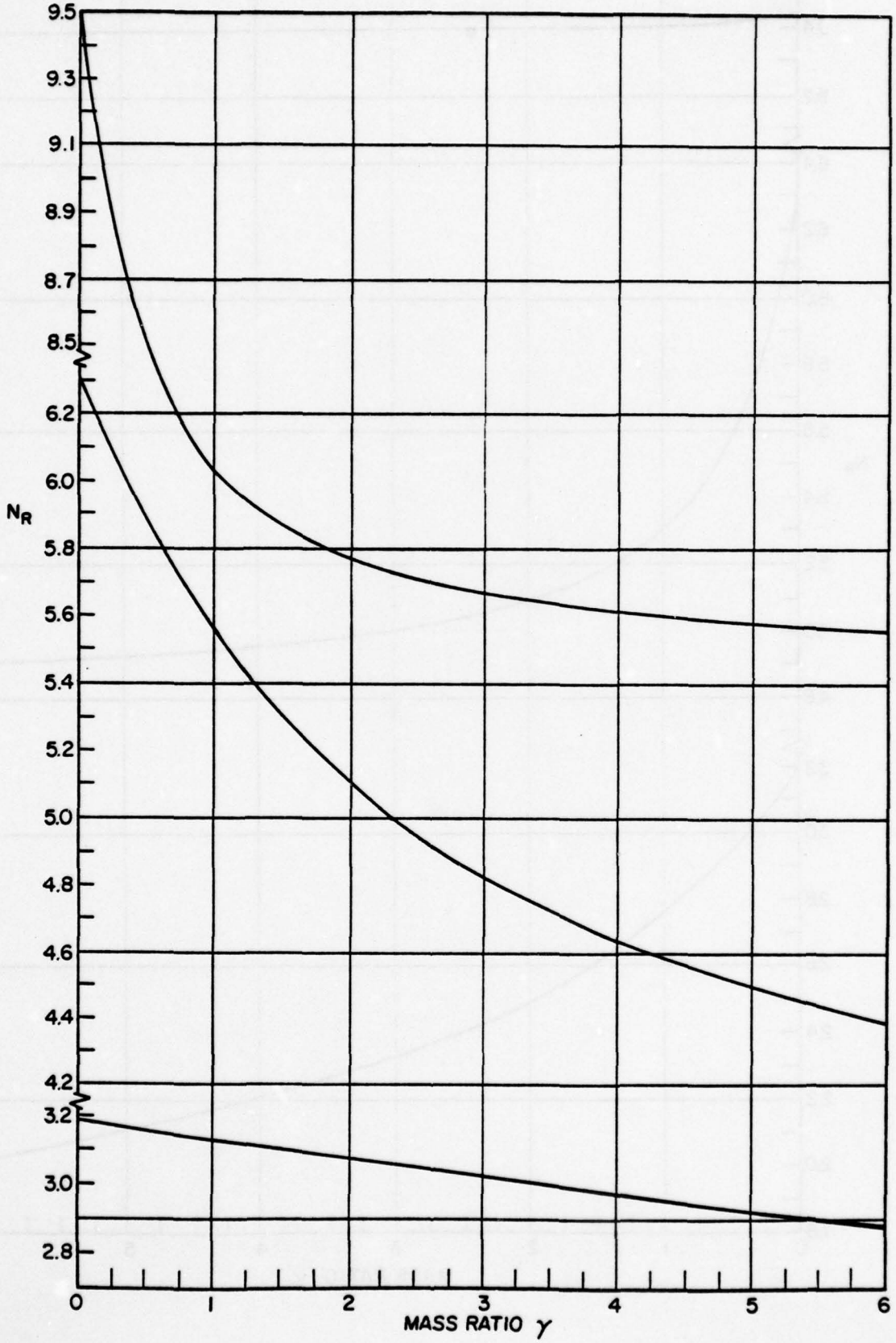
9.5
9.3
9.1
8.9
8.7
8.5
6.2
6.0
5.8
5.6
5.4
5.2
5.0
4.8
4.6
4.4
4.2
3.2
3.0
2.8
N_R
0
1
2
3
4
5
6
MASS RATIO γ

Fig. 71

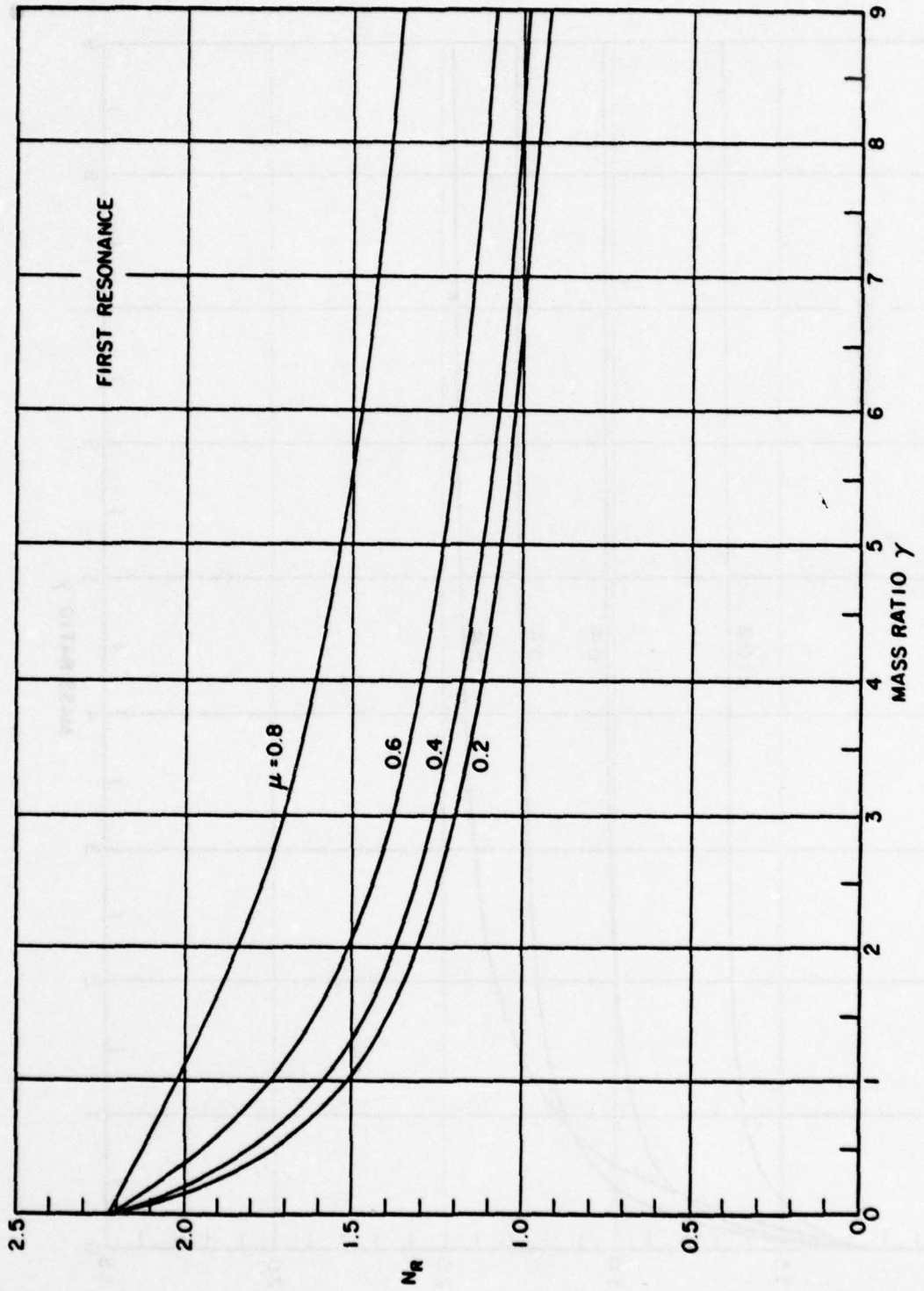
FIRST RESONANCE
μ=0.8
0.6
0.4
0.2
N_R
MASS RATIO γ
0
0.5
1.0
1.5
2.0
2.5
1
2
3
4
5
6
7
8
9

Fig. 72

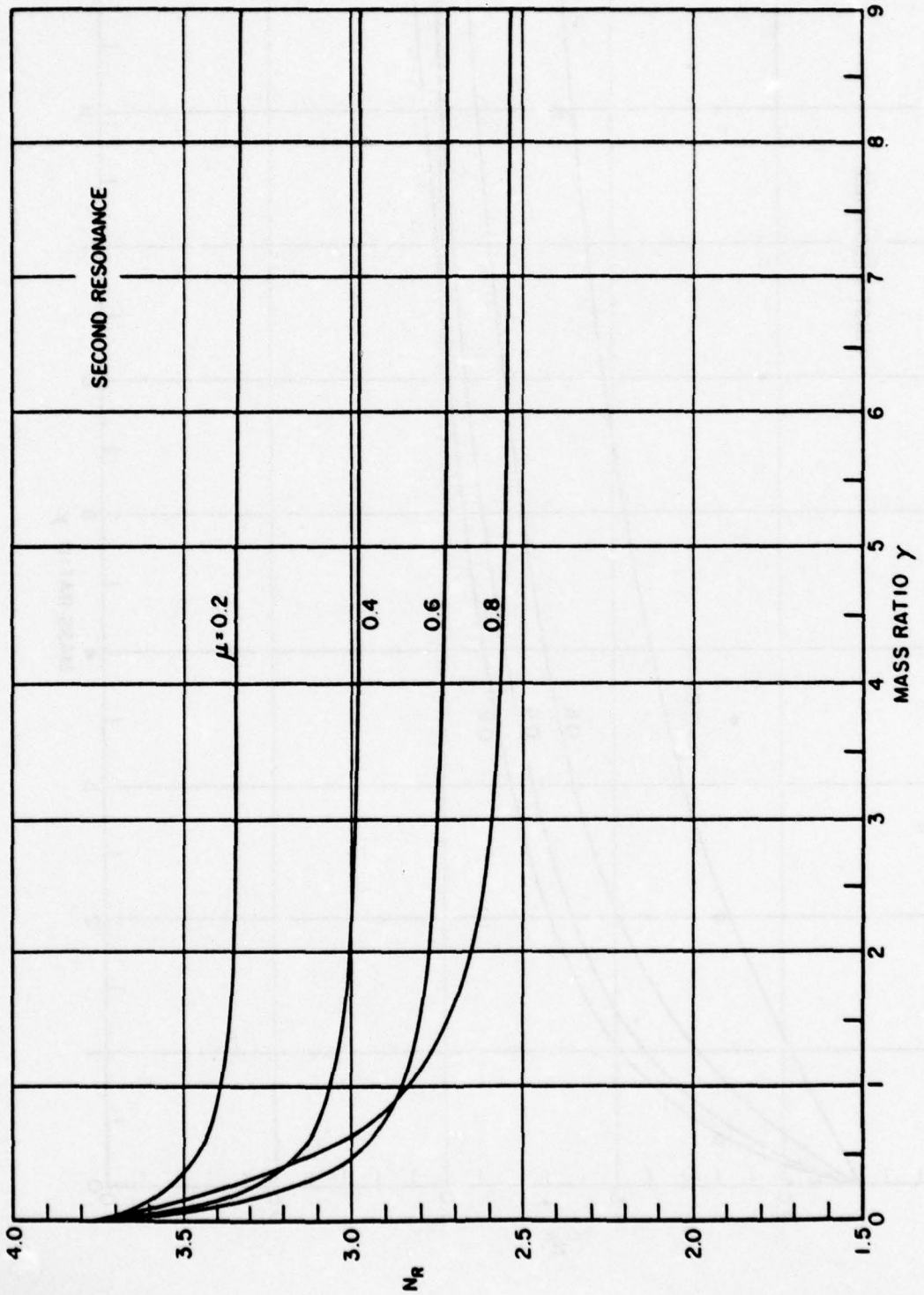
SECOND RESONANCE
μ=0.2
0.4
0.6
0.8
4.0
3.5
3.0
2.5
2.0
1.5
N_R
0
1
2
3
4
5
6
7
8
9
MASS RATIO γ

Fig. 73

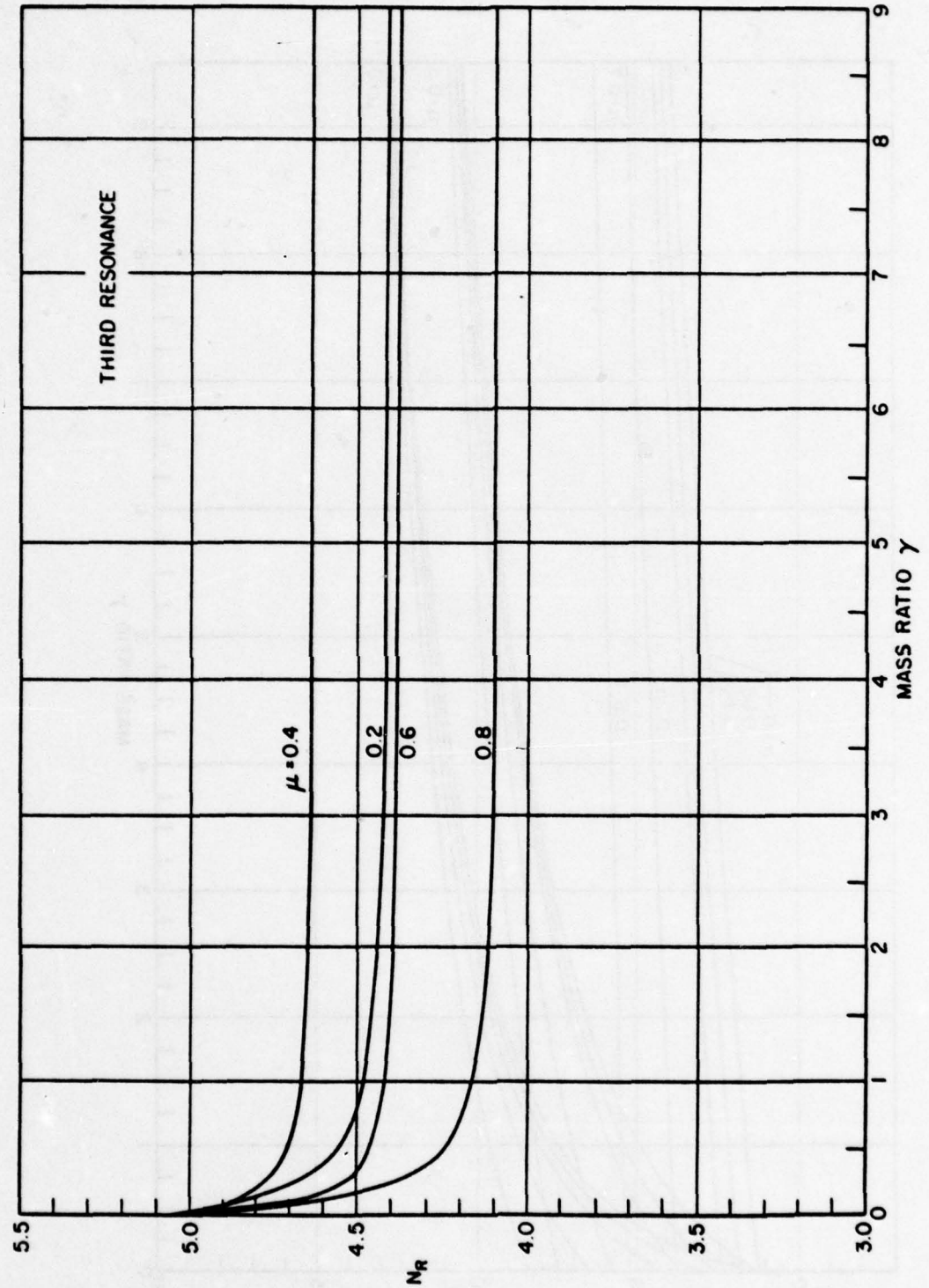
THIRD RESONANCE
μ=0.4
0.2
0.6
0.8
N_R
MASS RATIO γ
5.5
5.0
4.5
4.0
3.5
3.0
0
1
2
3
4
5
6
7
8
9

Fig. 74

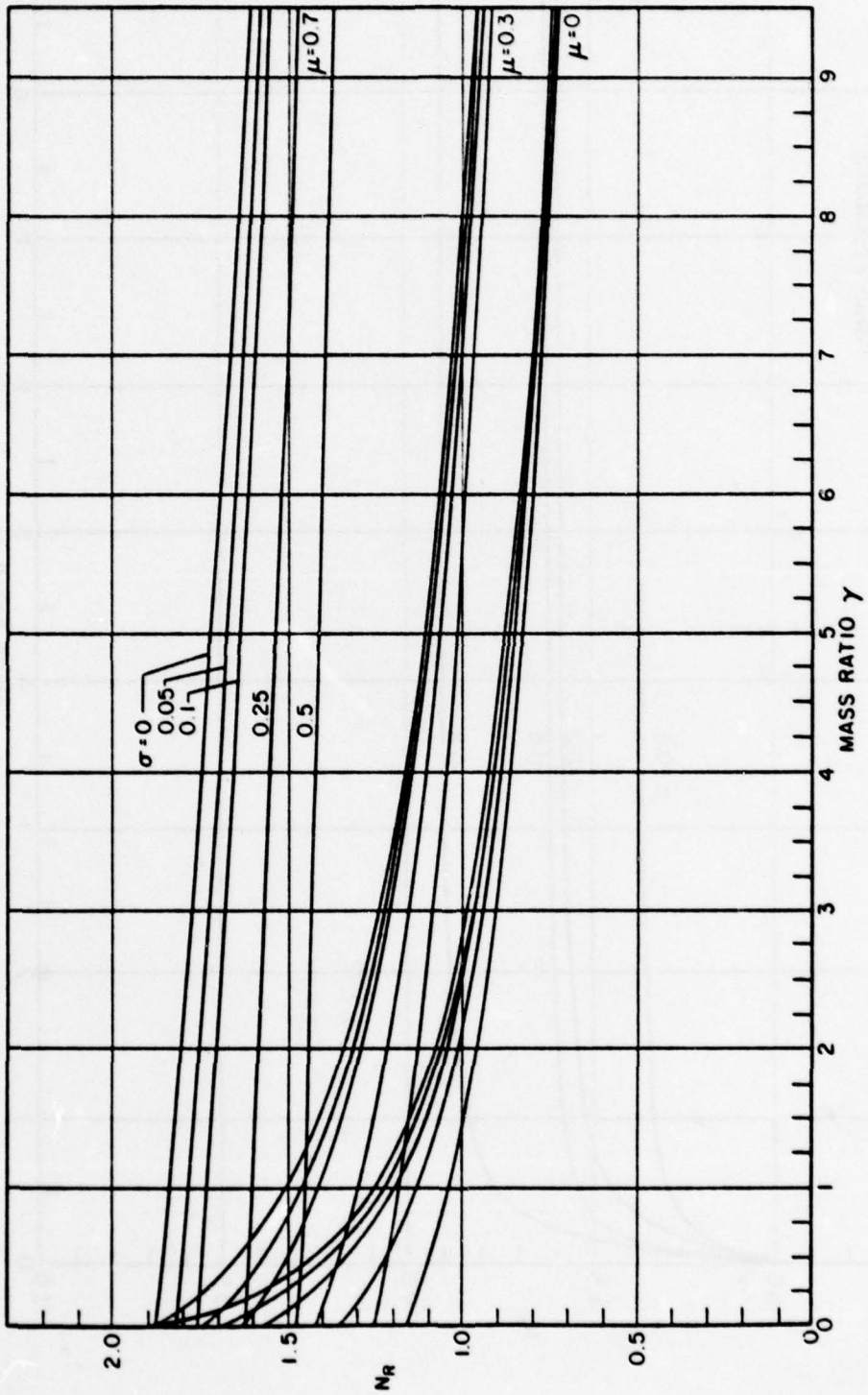
μ=0.7
μ=0.3
μ=0
σ=0
0.05
0.1
0.25
0.5
2.0
1.5
1.0
0.5
0
N_R
0
1
2
3
4
5
6
7
8
9
MASS RATIO γ

Fig. 75

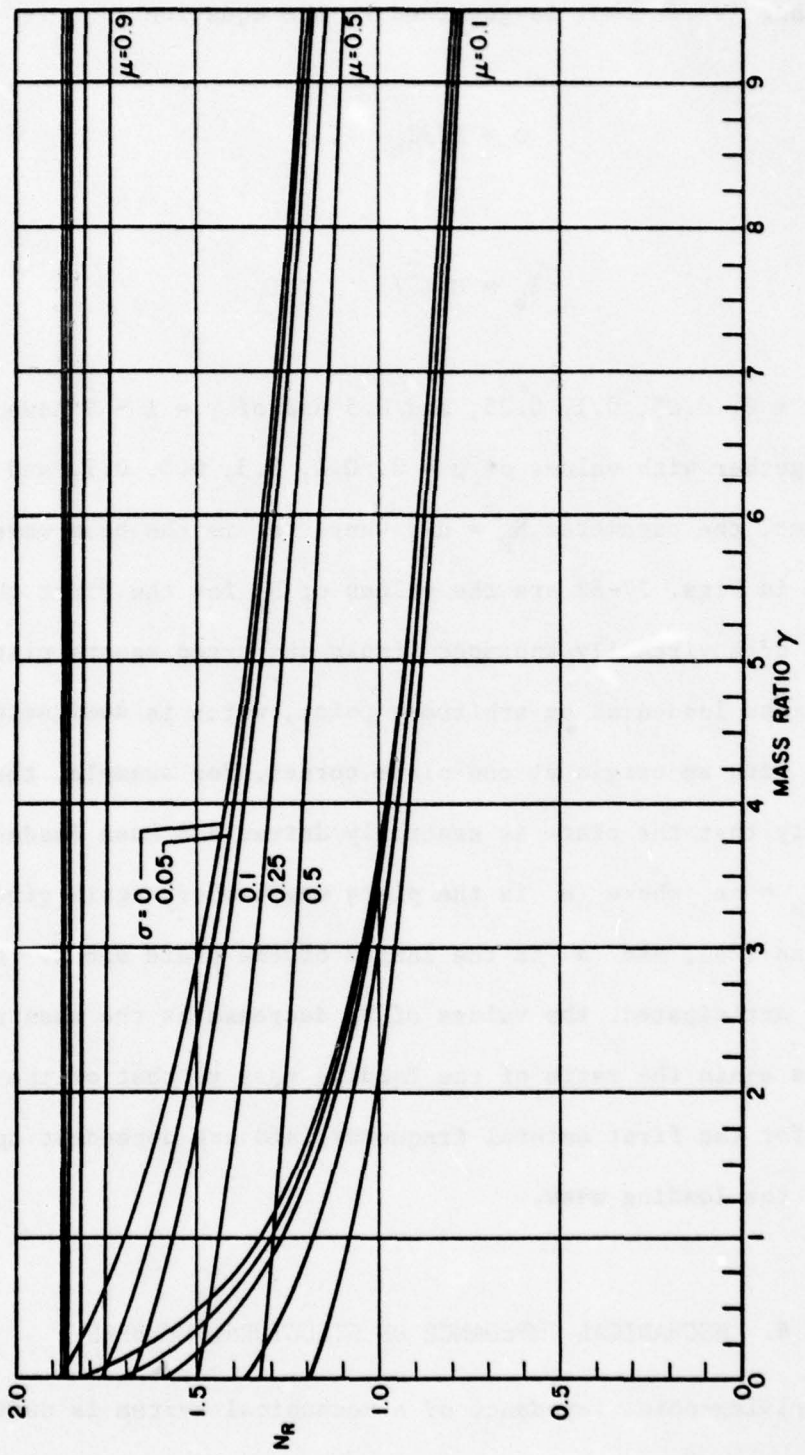
μ=0.9
μ=0.5
μ=0.1
σ=0
0.05
0.1
0.25
0.5
2.0
1.5
1.0
0.5
0
N_R
0
1
2
3
4
5
6
7
8
9
MASS RATIO γ

Fig. 76

distance $\mu\ell$ from the driving point by a mass that is a factor of γ times greater than that of the stanchion. In this case, the mass has a finite moment of inertia I that is governed by the equation

$$\sigma = I/3I_b \quad , \tag{85}$$

where

$$I_b = M_b \ell^2/3 \quad . \tag{86}$$

Values of $\sigma = 0$, 0.05, 0.1, 0.25, and 0.5 and of $\gamma = 1 - 9$ have been considered, together with values of $\mu = 0$, 0.1, 0.3, 0.5, 0.7, and 0.9. In this instance, the parameter $N_R = n\ell$, where n is the beam wavenumber.

Shown in Figs. 77-82 are the values of N_R for the first three natural frequencies of a virtually undamped simply supported square plate that is driven and mass loaded at an arbitrary point, which is designated by coordinates with an origin at one plate corner, for example, the coordinates $(\frac{1}{2},\frac{1}{2})$ specify that the plate is centrally driven and mass loaded. In this instance, $N_R = na$, where n is the plate wavenumber, again given by Eqs. (83) and (84), and a is the length of the plate sides. Note that, as might be anticipated, the values of N_R decrease as the mass ratio γ grows larger (γ is again the ratio of the loading mass to that of the plate), especially for the first natural frequency, and are dependent upon the location of the loading mass.

8. MECHANICAL IMPEDANCE OF STRUCTURAL MEMBERS

The driving-point impedance of a mechanical system is defined as the ratio of force to velocity at a point within the system when force and velocity vary sinusoidally with time at the same frequency ω. The transfer

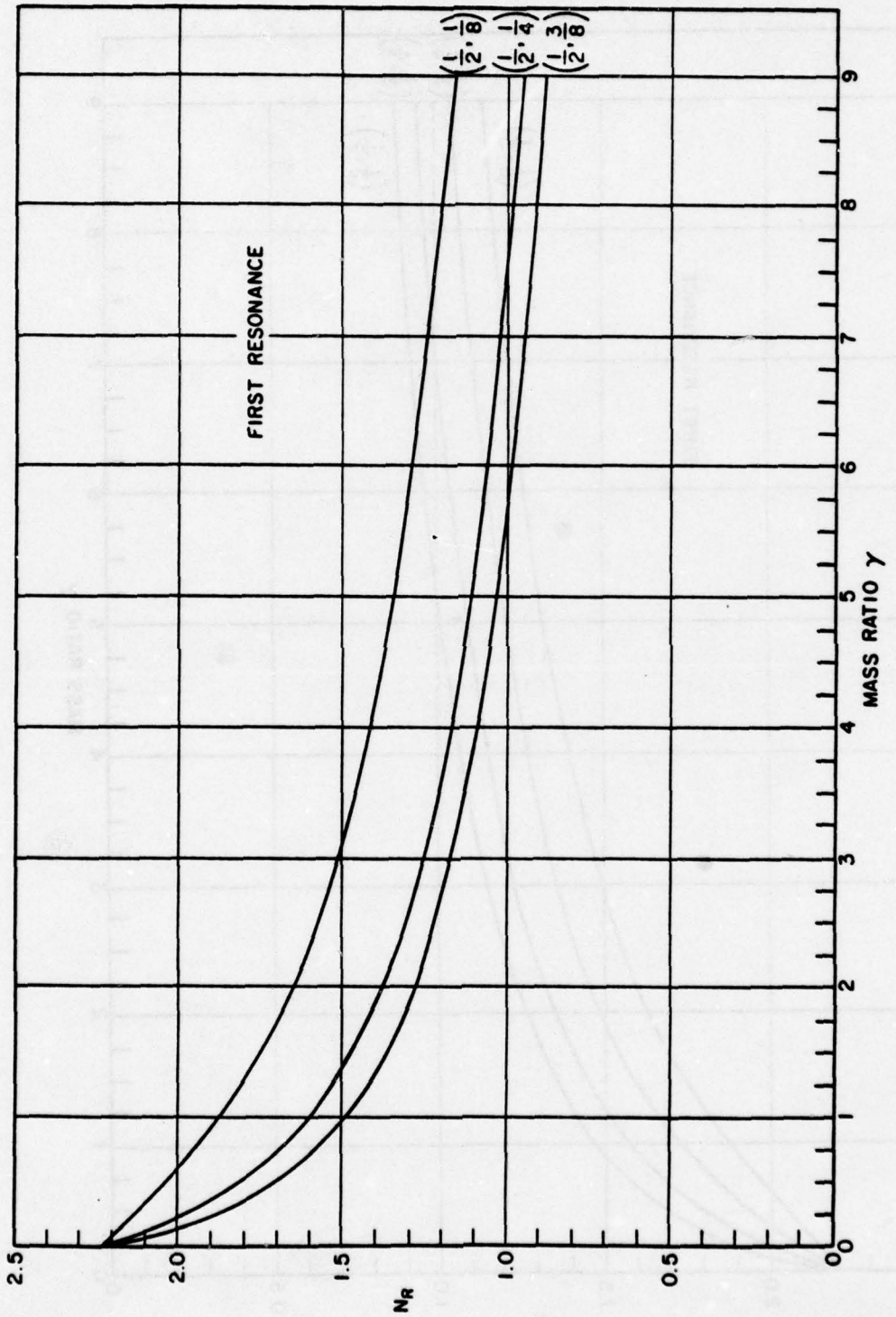
FIRST RESONANCE
$(-\frac{1}{2}, \frac{1}{8})$
$(-\frac{1}{2}, \frac{1}{4})$
$(-\frac{1}{2}, \frac{3}{8})$
N_R
2.5
2.0
1.5
1.0
0.5
0
0
1
2
3
4
5
6
7
8
9
MASS RATIO γ

Fig. 77

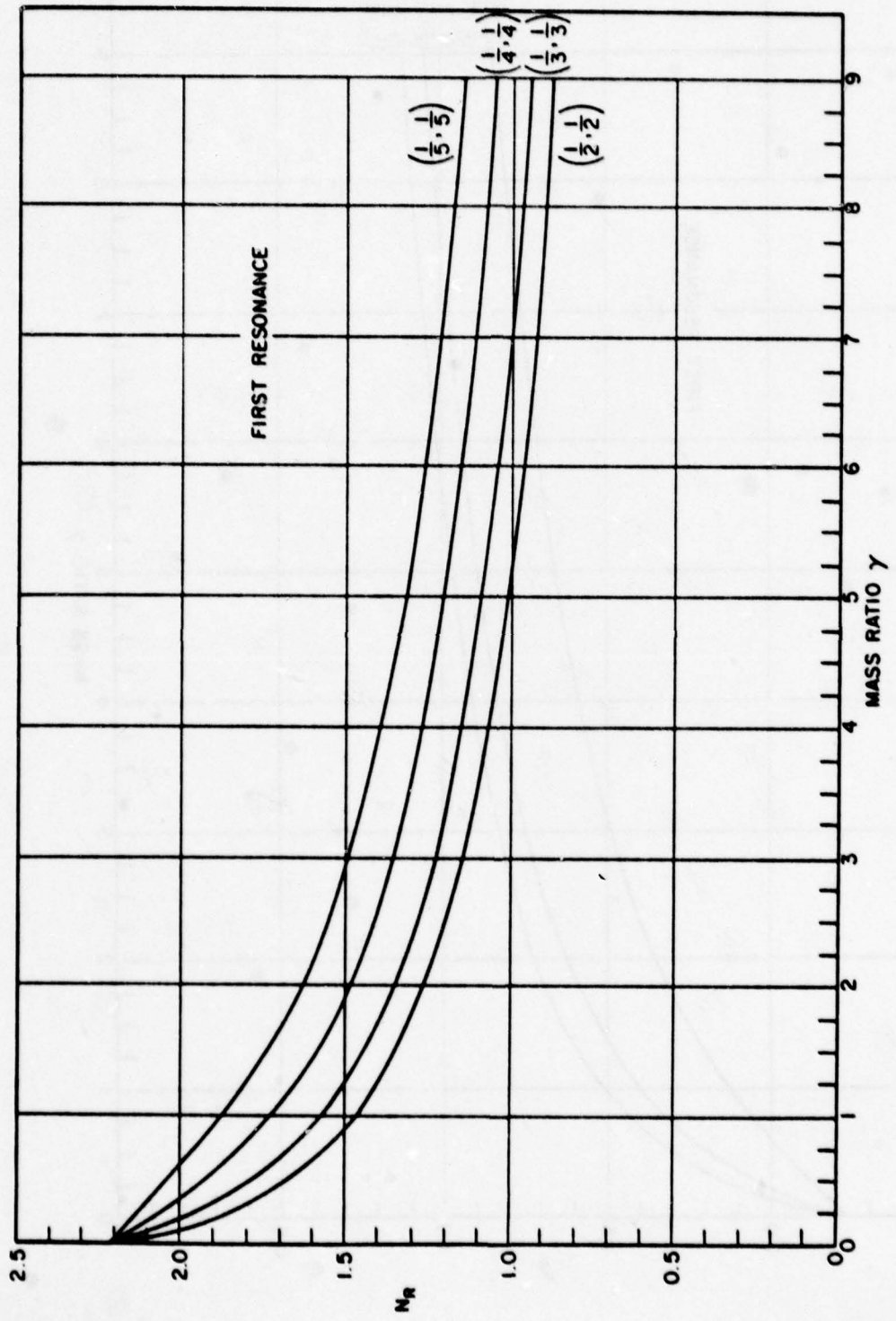
FIRST RESONANCE
$\left(\frac{1}{5},\frac{1}{5}\right)$
$\left(\frac{1}{4},\frac{1}{4}\right)$
$\left(\frac{1}{3},\frac{1}{3}\right)$
$\left(\frac{1}{2},\frac{1}{2}\right)$
N_R
2.5
2.0
1.5
1.0
0.5
0
0
1
2
3
4
5
6
7
8
9
MASS RATIO γ

Fig. 78

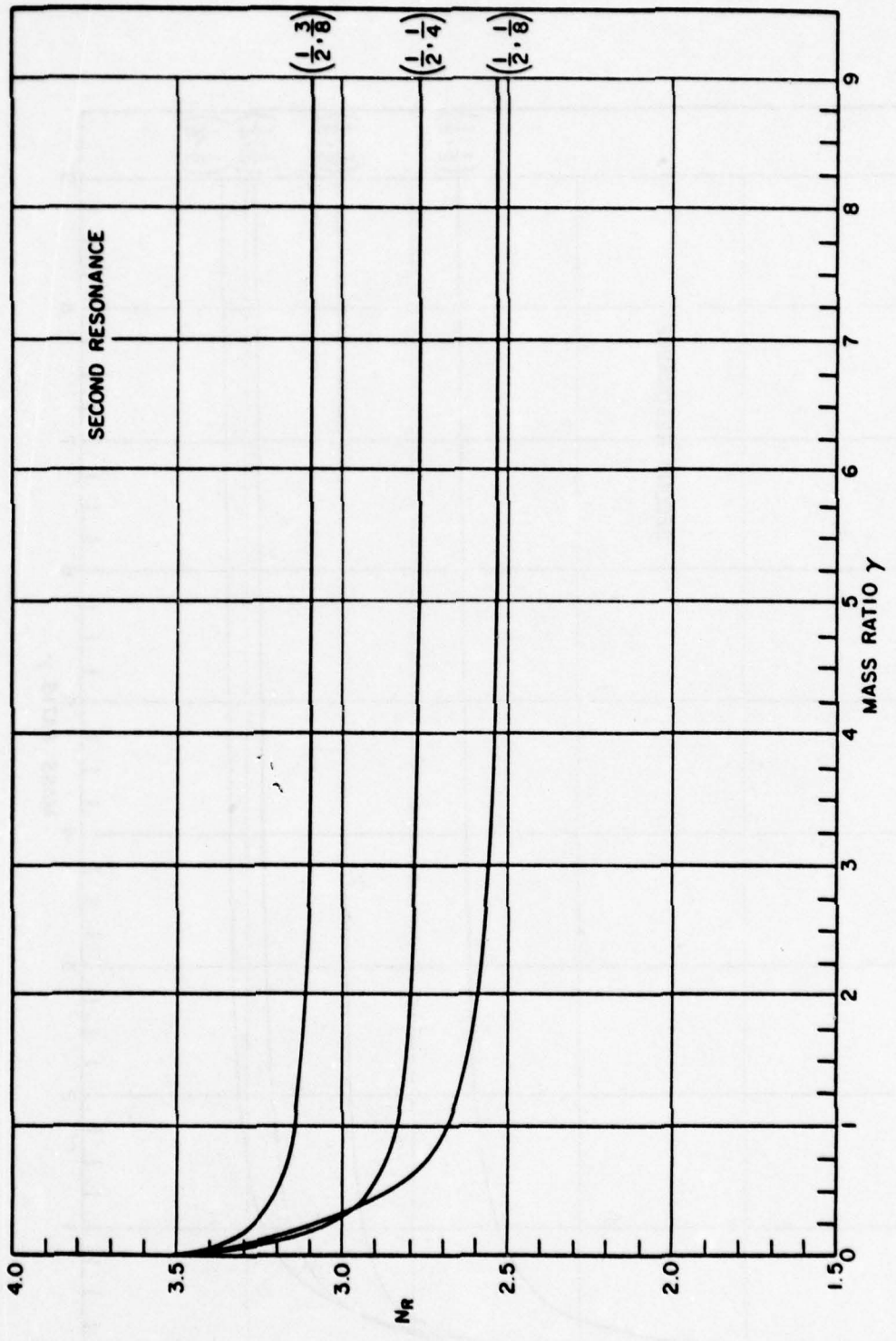
SECOND RESONANCE
$\left(\frac{1}{2},\frac{3}{8}\right)$
$\left(\frac{1}{2},\frac{1}{4}\right)$
$\left(\frac{1}{2},\frac{1}{8}\right)$
4.0
3.5
3.0
2.5
2.0
1.5
N_R
0
1
2
3
4
5
6
7
8
9
MASS RATIO γ

Fig. 79

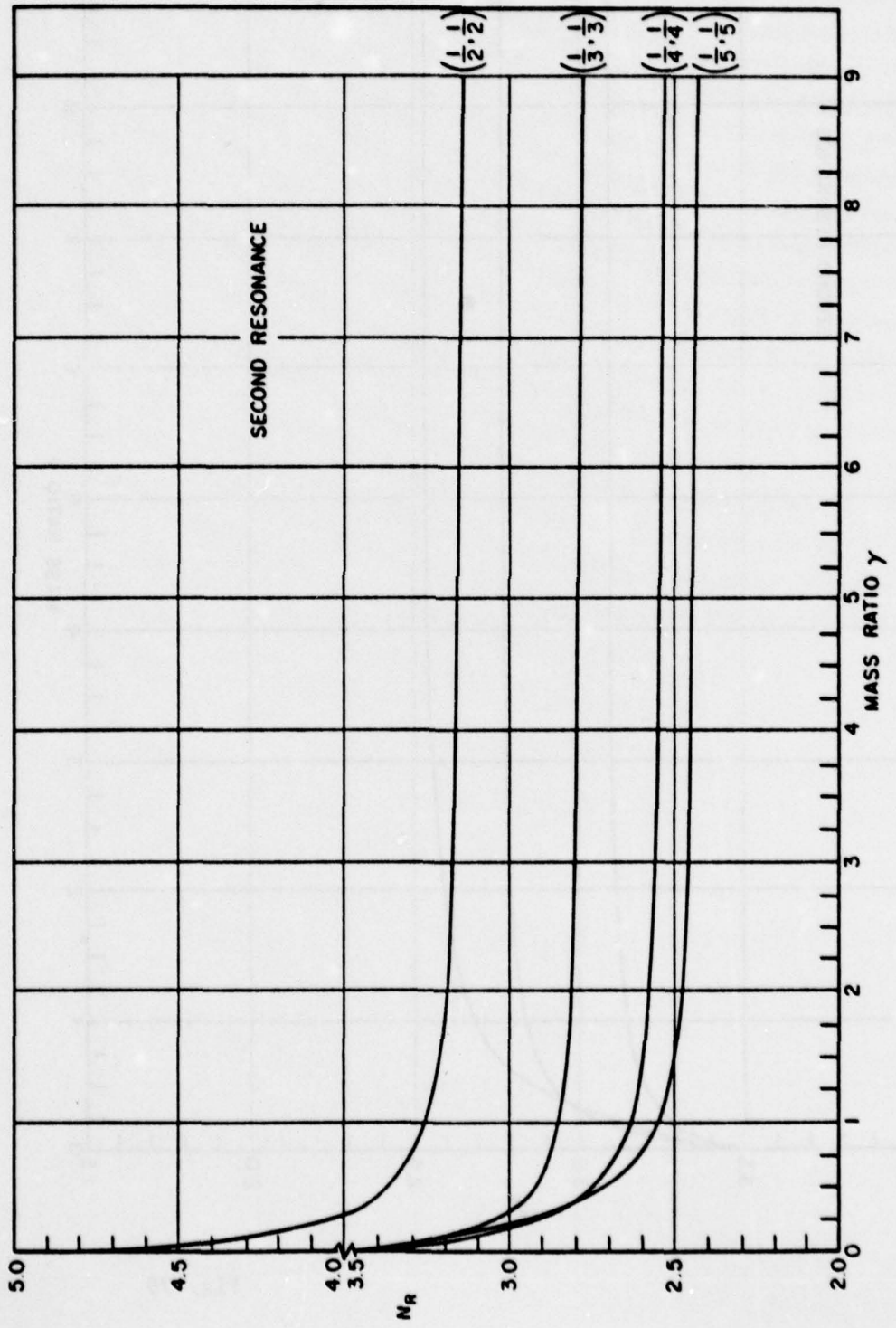
SECOND RESONANCE
$\left(\frac{1}{2},\frac{1}{2}\right)$
$\left(\frac{1}{3},\frac{1}{3}\right)$
$\left(\frac{1}{4},\frac{1}{4}\right)$
$\left(\frac{1}{5},\frac{1}{5}\right)$
N_R
5.0
4.5
4.0
3.5
3.0
2.5
2.0
0
1
2
3
4
5
6
7
8
9
MASS RATIO γ

Fig. 80

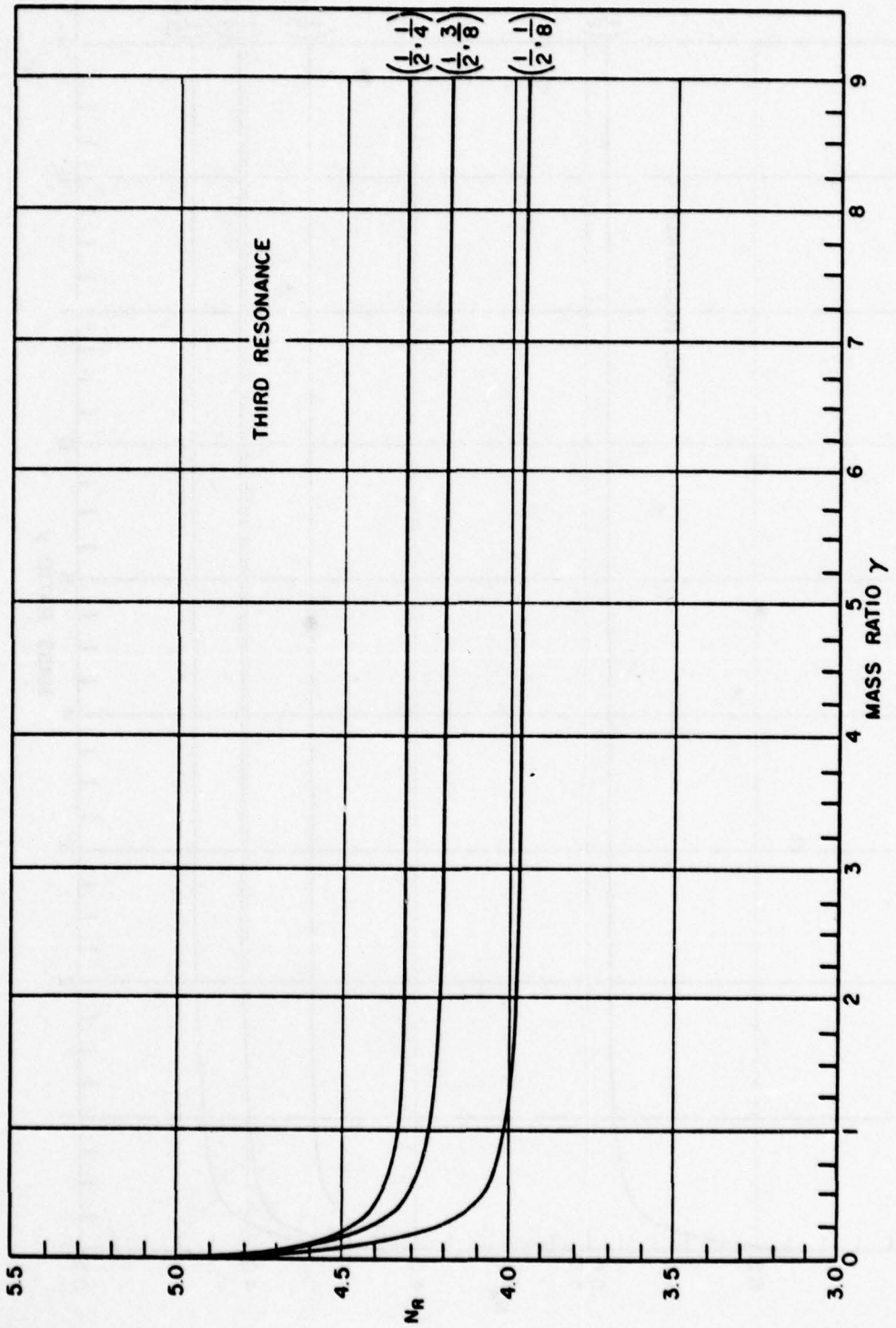
THIRD RESONANCE
$(\frac{1}{2},\frac{1}{4})$
$(\frac{1}{2},\frac{3}{8})$
$(\frac{1}{2},\frac{1}{8})$
N_R
5.5
5.0
4.5
4.0
3.5
3.0
0
1
2
3
4
5
6
7
8
9
MASS RATIO γ

Fig. 81

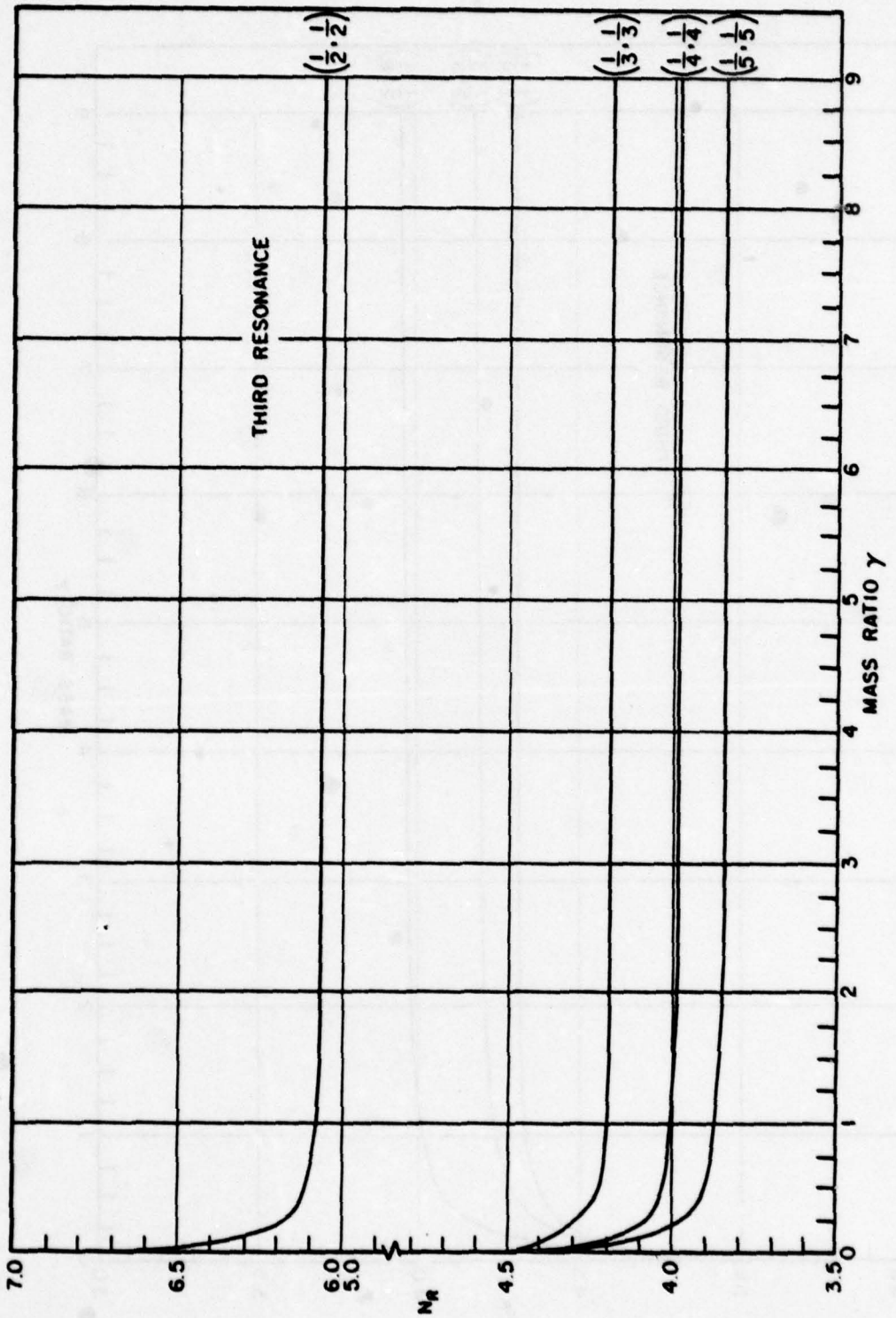
THIRD RESONANCE
$(\frac{1}{2},\frac{1}{2})$
$(\frac{1}{3},\frac{1}{3})$
$(\frac{1}{4},\frac{1}{4})$
$(\frac{1}{5},\frac{1}{5})$
N_R
7.0
6.5
6.0
5.0
4.5
4.0
3.5
0
1
2
3
4
5
6
7
8
9
MASS RATIO γ

Fig. 82

impedance of a mechanical system is defined as the ratio of the force at one point in the system to the velocity at another point in the system when force and velocity vary sinusoidally with time at the same frequency ω. The moment impedance of a mechanical system is defined as the ratio of the applied bending moment to the resultant angular (rotational) velocity at one point in the system when the bending moment and angular velocity vary sinusoidally with time at the same frequency ω.

1. Impedance of a mass M: $Z = j\omega M$ (87)

2. Impedance of a spring of stiffness K: $Z = K/j\omega$ (88)

3. Impedance of a dashpot having a coefficient of viscosity η: $Z = \eta$ (89)

4. Driving-point impedance of a mass-loaded free-free rod in longitudinal vibration[1]:

$$\frac{Z_m}{j\omega M_R} = \frac{\theta^*}{(n^*\ell)\eta^*} \quad , \tag{90}$$

where

$$\eta^* = [\cos n^*\ell - \gamma(n^*\ell) \sin n^*\ell] \tag{91}$$

and

$$\theta^* = [\sin n^*\ell + \gamma(n^*\ell) \cos n^*\ell] \quad ; \tag{92}$$

here, $\gamma = M/M_R$, where M is the loading mass at the driven end of the rod and M_R is the rod mass; n^* is the rod wavenumber given by Eq. (22), and ℓ is the rod length.

5. Transfer impedance across a free-free rod of length ℓ that is driven at one end and mass loaded at the other[1]:

$$\frac{TZ_m}{j\omega M_R} = \frac{\theta^*}{(n^*\ell)} \quad , \tag{93}$$

which is also the transfer impedance across a free-free rod that is driven and mass loaded at the same end. The parameter θ^* is again given by Eq. (92).

6. The characteristic impedance of a rod of cross-sectional area A in longitudinal vibration that has infinite length, or is so heavily damped that no energy returns to the driving point to produce a standing-wave pattern, can be written as[1]:

$$Z_{ch} = A(E^*\rho)^{\frac{1}{2}} = (A\rho)C_L^* \quad , \tag{94}$$

where C_L^* is the complex velocity of longitudinal wave propagation in the damped rod, and E^* and ρ are the complex Young's modulus and density of the rod material.

7. Driving-point impedance of a free-clamped rod of mass M_R in longitudinal vibration that is driven and mass loaded at the same end[1]:

$$\frac{Z_m}{j\omega M_R} = \frac{-\eta^*}{(n^*\ell)\sin n^*\ell} \quad , \tag{95}$$

where η^* is given by Eq. (91).

8. Driving-point impedance of a free-clamped rod of length ℓ that is driven at an arbitrary point distant $\mu\ell$ from its free end[1]:

$$\frac{Z_\mu}{j\omega M_R} = \frac{-\cos n^*\ell}{(n^*\ell)\cos \mu n^*\ell \sin (1-\mu)n^*\ell} \quad , \tag{96}$$

where n^* is again given by Eq. (22).

9. Driving-point impedance of a centrally driven and mass loaded simply supported beam of length $2a$[1]:

$$\frac{Z_m}{j\omega M_b} = \left[\gamma + \frac{2}{(n^*a)}\left(\frac{\text{ch.c.}}{\text{sh.c.}-\text{ch.s.}}\right)_{(n^*a)}\right] \quad , \tag{97}$$

where $\gamma = M/M_b$ in which M is the loading mass and M_b is the beam mass. Such abbreviations as ch. and c. are employed to represent the terms cosh n^*a and cos n^*a, respectively, where n^* is the beam wavenumber, which is defined by the equation

$$n^* = (\omega^2\rho/r^2E^*)^{\frac{1}{4}} \quad , \tag{98}$$

where ω is angular frequency, ρ is the beam density, r is the radius of gyration of the beam cross section, and E^* is the complex Young's modulus of the beam material.

10. Driving-point impedance of a centrally mass loaded and driven clamped-clamped beam of length $2a$[1]:

$$\frac{Z_m}{j\omega M_b} = \left[\gamma + \frac{1}{(n^*a)}\left(\frac{\text{sh.c.}+\text{ch.s.}}{\text{ch.c.}-1}\right)_{(n^*a)}\right] \quad , \tag{99}$$

where γ has the same significance as in 9.

11. Characteristic impedance of a semi-infinite beam driven transversely at its free end[1]:

$$Z_{ch} = \frac{\rho A C_B^*}{2}(1 + j) \quad , \tag{100}$$

where A is the beam cross-sectional area, C_B^* is the complex velocity of bending waves on the beam, and ρ is the density of the beam material.

12. Characteristic impedance of an infinite beam driven transversely at its midpoint[1]:

$$Z_{ch} = 2\rho A C_B^* (1 + j) \quad . \tag{101}$$

13. Transfer impedance of a centrally driven simply supported beam, where velocity is monitored at a distance of μa from the beam center[1]:

$$\frac{TZ_\mu}{j\omega M_b} = \frac{2(\text{ch.c.})_{(n^*a)}}{n^*a\,[\text{sh.c.ch}\mu\text{.}-\text{ch.s.c}\mu\text{.}-\text{ch.c.}(\text{sh}\mu\text{.}-\text{s}\mu\text{.})]_{(n^*a)}} \quad , \tag{102}$$

where such terms as chμ. represent the quantity cosh $\mu n^* a$.

14. Bending moment impedance BZ_o of a centrally driven simply supported beam[1]:

$$\frac{BZ_o}{j\omega I_b} = \frac{6}{(n^*a)^3}\left(\frac{\text{sh.}-\text{s.}}{\text{sh.c.}-\text{ch.s.}}\right)_{(n^*a)} \quad . \tag{103}$$

The moment of inertia

$$I_b = M_b a^2/3 \quad , \tag{104}$$

where M_b is the beam mass.

15. Bending-moment impedance of a centrally driven clamped-clamped beam[1]:

$$\frac{BZ_o}{j\omega I_b} = \frac{3}{(n^*a)^3}\left(\frac{\text{sh.c.}-\text{ch.s.}}{1-\text{ch.c.}}\right)_{(n^*a)} \quad , \tag{105}$$

where I_b is again given by Eq. (104).

16. Driving-point impedance at the center of a free-free beam of length 2a driven transversely[1]:

$$\frac{Z_o}{j\omega M_b} = \frac{1}{(n^*a)}\left(\frac{\text{sh.c.}+\text{ch.s.}}{\text{ch.c.}+1}\right)_{(n^*a)} \quad . \tag{106}$$

17. Bending-moment impedance at the center of a free-free beam of length $2a$[1]:

$$\frac{BZ_o}{j\omega I_b} = \frac{3}{(n^*a)^3}\left(\frac{\text{ch.s.}-\text{sh.c.}}{\text{ch.c.}+1}\right)_{(n^*a)} . \tag{107}$$

18. Driving-point impedance at the free end of a cantilever beam of length ℓ[1]:

$$\frac{Z_o}{j\omega M_b} = \frac{1}{(n^*\ell)}\left(\frac{\text{ch.c.}+1}{\text{sh.c.}-\text{ch.s.}}\right)_{(n^*\ell)} . \tag{108}$$

19. Bending-moment impedance at the free end of a cantilever beam of length ℓ[1]:

$$\frac{BZ_o}{j\omega I_b} = \frac{-3}{(n^*\ell)^3}\left(\frac{\text{ch.c.}+1}{\text{sh.c.}+\text{ch.s.}}\right)_{(n^*\ell)} . \tag{109}$$

20. Driving-point impedance of a cantilever beam that is excited at an arbitrary point distant μa from its clamped end and at a distance a from its free end[1]:

$$\frac{Z_\mu}{j\omega M_b} = \frac{2\Psi^*}{(n^*a)(1+\mu)[(\text{sh.c.}-\text{ch.s.})(\text{ch.c.}-1)_\mu + (\text{ch.c.}+1)(\text{sh.c.}-\text{ch.s.})_\mu]_{(n^*a)}} , \tag{110}$$

where

$$\Psi^* = [1 - (\text{sh.s.})(\text{sh.s.})_\mu + (\text{sh.c.})(\text{sh.c.})_\mu - (\text{ch.s.})(\text{ch.s.})_\mu + (\text{ch.c.})(\text{ch.c.})_\mu]_{(n^*a)} . \tag{110}$$

21. Driving-point impedance at the center of a simply supported circular plate of radius a[30]:

$$\frac{Z_o}{j\omega M_p} = \frac{8\Xi^*}{\pi(n^*a)^2\Psi^*} \quad , \tag{112}$$

where M_p is the plate mass and

$$\Xi^* = [-2J_oI_o + \phi_a^*(J_oI_1 + I_oJ_1)]_{(n^*a)} \quad , \tag{113}$$

$$\Psi^* = \{2(Y_oI_o + \Lambda J_oK_o) + \phi_a^*[(J_o - I_o)(Y_1 + \Lambda K_1) - (J_o + I_1)(Y_o + \Lambda K_o)]\}_{(n^*a)}. \tag{114}$$

In these equations,

$$\phi_a^* = (1 - \nu^*)/(n^*a) \tag{115}$$

and

$$\Lambda = 2/\pi \quad ; \tag{116}$$

in addition, the plate wavenumber

$$(n^*)^4 = \omega^2\rho[1 - (\nu^*)^2]/r_g^2E^* \quad , \tag{117}$$

where

$$r_g^2 = d^2/12 \tag{118}$$

in which d is the thin plate thickness and ν^* is the complex Poisson's ratio, and where ν^* is a real quantity for those materials that have damping factors associated with the Young's modulus and shear-modulus deformations of the plate material that are equal.[30] In addition, such quantities as J_o and I_1 refer to ordinary and modified Bessel functions of orders zero and one having the complex argument (n^*a).

22. Driving-point impedance at the center of a circular plate of radius a with free boundaries[30]:

$$\frac{Z_o}{j\omega M_P} = \frac{8\theta^*}{\pi(n^*a)^2\phi^*} \quad , \tag{119}$$

where

$$\theta^* = [-(J_oI_1 + J_1I_o) + 2\phi_a^* J_1I_1](n^*a) \tag{120}$$

and

$$\phi^* = \{[(J_o + I_o)(Y_1 - \Lambda K_1) - (J_1 - I_1)(Y_o - \Lambda K_o)] + 2\phi_a^*(\Lambda J_1K_1 - Y_1I_1)\}(n^*a) \quad . \tag{121}$$

23. Driving-point impedance at the center of a clamped circular plate of radius a[31]:

$$\frac{Z_o}{j\omega M_P} = \frac{4\Lambda T^*}{(n^*a)^2\Gamma^*} \quad , \tag{122}$$

where

$$T^* = (J_oI_1 + J_1I_o)(n^*a) \tag{123}$$

and

$$\Gamma^* = [(J_o - I_o)(Y_1 + \Lambda K_1) - (J_1 + I_1)(Y_o + \Lambda K_o)](n^*a) \quad . \tag{124}$$

24. Characteristic impedance of an undamped plate[30]:

$$Z_{ch} = 8\sqrt{(Dd\rho)} \quad , \tag{125}$$

where d is the plate thickness, ρ is its density, and

$$D = dEr_g^2/(1 - \nu^2) \quad , \tag{126}$$

where r_g^2 is given by Eq. (118).

25. Driving-point impedance at an arbitrary point on a rectangular plate driven transversely[32]:

$$\frac{Z_o}{j\omega M_p} = \left[\frac{1}{4} \sum_{k=1,3,5,\ldots}^{\infty} \sum_{m=1,3,5\ldots}^{\infty} \frac{4\varphi_{k,m}^2}{\lambda^*} \right]^{-1} , \tag{127}$$

where M_p is the plate mass and

$$\varphi_{k,m} = \sin k\pi \, (h_x/a) \sin m\pi \, (h_y/b) , \tag{128}$$

$$\lambda^* = [(\beta^*)^4 - 1] , \tag{129}$$

in which

$$\beta^* = \frac{\pi[k^2 + (m/\mu)^2]^{\frac{1}{2}}}{(p + jq)} \tag{130}$$

and h_x and h_y are the coordinates of the arbitrary driving point; the parameter μ is the aspect ratio of the plate (the ratio of the shorter to the longer plate sides). The term (n^*a), where n^* is the plate wavenumber and a is the length of the longer plate side has been written as $(p + jq)$, where

$$p,q = \pm (na) \left[\frac{1}{2\sqrt{D_E}} \pm \frac{(1 + D_E)^{\frac{1}{2}}}{2\sqrt{2}\, D_E} \right]^{\frac{1}{2}} \tag{131}$$

and

$$D_E = (1 + \delta_E^2)^{\frac{1}{2}} . \tag{132}$$

The coordinate origin is one plate corner, the x axis being parallel to the longer plate side. When the plate is centrally driven, the impedance can be written as follows:

$$\frac{Z_o}{j\omega M_p} = \left[- \sum_{k=1,3,5,\ldots}^{\infty} \sum_{m=1,3,5,\ldots}^{\infty} \left(\frac{4}{\lambda^*} \right) \right]^{-1} \tag{133}$$

26. Transfer impedance between the midpoint of a centrally driven simply supported rectangular plate and an arbitrary point having the coordinates h_x, h_y [32]:

$$\frac{TZ_o}{j\omega M_p} = \{ - \sum_{k=1,3,5,\ldots}^{\infty} \sum_{m=1,3,5,\ldots}^{\infty} [4\varphi_{k,m}(h_x,h_y)(-1)^{(\theta-1)}]/\lambda^* \}^{-1} \quad , \tag{134}$$

where $\varphi_{k,m}$ and λ^* are given by Eqs. (128) and (129), and

$$\theta = (k + m)/2 \quad . \tag{135}$$

9. TRANSMISSIBILITY OF STRUCTURAL MEMBERS

Force transmissibility is defined as the magnitude of the ratio of the force transmitted to the boundary or boundaries of a mechanical system to the impressed force. Displacement transmissibility is defined as the magnitude of the ratio of the displacement of a point within a mechanical system to the displacement of its boundary or boundaries. Equally well, displacement transmissibility can be expressed as a velocity or acceleration ratio when sinusoidal motion is of concern.

1. Transmissibility of the simple mounting system: This is specified by Eq. (13).

2. Transmissibility of the dynamic vibration absorber; this is specified by the following equation, which relates to a viscously damped absorber of stiffness K_2 and mass M_2 that is applied to an undamped primary system of stiffness K_1 and mass M_1:

$$T^2 = \frac{(-\Omega^2 + n^2)^2 + (2n\Omega\delta_R)^2}{\{[\mu\Omega^4 - \Omega^2(1 + n^2) + n^2]^2 + (2n\Omega\delta_R)^2(1 - \Omega^2)^2\}} \quad , \tag{136}$$

where δ_R and n are the absorber damping and tuning ratios and Ω is a frequency ratio such that

$$n = \omega_a/\omega_o \quad , \tag{137}$$

$$\Omega = \omega/\omega_o \quad , \tag{138}$$

and

$$\delta_R = \omega_a\eta/2K_2 \quad , \tag{139}$$

where

$$\omega_a = (K_2/M_2)^{1/2} \quad , \tag{140}$$

$$\omega_o = [K_1/(M_1 + M_2)]^{1/2} \quad , \tag{141}$$

and η is the coefficient of viscosity of the absorber dashpot.

3. Transmissibility of the compound mounting system: this is specified by Eq. (55).

4. Transmissibility of a mass-loaded rod in longitudinal vibration: this is specified by Eq. (17).

5. Transmissibility of a simply supported beam driven and mass loaded centrally[1]:

$$T = \left| \frac{(\text{ch.}+\text{c.})}{2\ \text{ch.c.} + \gamma(n^*a)(\text{sh.c.}-\text{ch.s.})} \right|_{(n^*a)} , \tag{142}$$

where abbreviations such as ch. and c. are employed to represent the terms cosh n^*a and cos n^*a, where a is the half-length of the beam and n^* is the beam wavenumber, which is given by Eq. (98). The parameter $\gamma = M/M_b$, where M is the loading mass and M_b is the beam mass.

6. Transmissibility of a clamped-clamped beam driven and mass loaded centrally[1]:

$$T = \left| \frac{(\text{sh.}+\text{s.})}{(\text{sh.c.}+\text{ch.s.}) + \gamma(n^*a)(\text{ch.c.}-1)} \right|_{(n^*a)} , \tag{143}$$

where γ has the same significance as in 5 and a is again the half length of the beam.

7. Transmissibility of a cantilever beam of length ℓ that is driven and mass loaded at its free end[1]:

$$T = \left| \frac{(\text{ch.}+\text{c.})}{2[\gamma(n^*\ell)(\text{sh.c.}-\text{ch.s.}) + (\text{ch.c.}+1)]} \right|_{(n^*\ell)} , \tag{144}$$

in which γ is again $= M/M_b$, where M is the loading mass and M_b is the mass of the cantilever.

8. Transmissibility of a centrally driven and mass loaded simply supported circular plate[30]:

$$T = T_o \left| \frac{(Z_o/j\omega M_p)}{\gamma + (Z_o/j\omega M_p)} \right| , \tag{145}$$

where $(Z_o/j\omega M_p)$ is given by Eq. (112) and

$$T_o = |\Omega^*/\Xi^*| \quad , \tag{146}$$

where Ξ^* is given by Eq. (113), and

$$\Omega^* = [-(J_o + I_o) + \phi_a^*(J_1 + I_1)]_{(n^*a)} \tag{147}$$

in which a is the plate radius and n^* is the plate wavenumber given by Eq. (117); in addition, the parameter ϕ_a^* is given by Eq. (115) and $\gamma = M/M_p$, where M is the loading mass and M_p is the plate mass.

9. Displacement transmissibility of a plate of radius a with a free boundary[30]:

$$T = |4\Omega^*/\pi(n^*a)\Phi^*| \quad , \tag{148}$$

where Ω^* is given by Eq. (147) and Φ^* is given by Eq. (121). This plate is driven centrally and T is the ratio of the displacement of the plate edge to the central displacement. However, if the plate is driven around its free boundary by a ring force, then the ratio of the central plate displacement to that of its edge is given by an alternative transmissibility[30]

$$T = |\Omega^*/\Xi^*| \quad , \tag{149}$$

where Ξ^* is given by Eq. (113) and Ω^* by Eq. (147).

10. Transmissibility of a centrally driven and mass-loaded circular plate with clamped boundaries[31]:

$$T = \left| \frac{4\Lambda(J_1 + I_1)}{4\Lambda T^* + \gamma(n^*a)^2 \Gamma^*} \right| \quad , \tag{150}$$

where Λ is given by Eq. (116) and T^* and Γ^* are given by Eqs. (123) and (124). The parameter γ has the same significance as in 8.

11. Transmissibility to the boundary of a clamped annular plate driven around its inner perimeter of radius a by a ring force[31]:

$$T = \left| \frac{2(\lambda\Omega^* + \phi_a^*\Pi^*)}{\lambda(n^*a)[\lambda(\psi^* + \theta^*) + 2\phi_a^*\eta^*]} \right| \quad , \tag{151}$$

where ϕ_a^* is given by Eq. (115) and Ω^* by Eq. (147). In addition,

$$\psi^* = 2\Lambda/\lambda(n^*a)^2 \quad , \tag{152}$$

$$\theta^* = [(Y_oI_1 + I_oY_1)(J_1K_o - K_1J_o)_\lambda + (J_1K_o - K_1J_o)(Y_oI_1 + Y_1I_o)_\lambda + (Y_oK_1 - K_oY_1)(J_oI_1 + J_1I_o)_\lambda + (J_oI_1 + J_1I_o)(Y_oK_1 - Y_1K_o)_\lambda]_{(n^*a)} \quad , \tag{153}$$

$$\eta^* = [(Y_oI_1 + Y_1I_o)(J_1K_1)_\lambda - (J_oI_1 + J_1I_o)(Y_1K_1)_\lambda - (Y_oK_1 - Y_1K_o)(J_1I_1)_\lambda - (J_1K_o - J_oK_1)(Y_1I_1)_\lambda]_{(n^*a)} \quad , \tag{154}$$

and

$$\Pi^* = [(Y_1J_{1\lambda} - J_1Y_{1\lambda}) + \Lambda(I_1K_{1\lambda} - K_1I_{1\lambda})]_{(n^*a)} \quad , \tag{155}$$

where such terms as $J_{1\lambda}$ and $K_{1\lambda}$ are used to represent the quantities $J_1(\lambda n^*a)$ and $K_1(\lambda n^*a)$.

12. Transmissibility of a centrally driven clamped circular plate with an ideally rigid concentric annular rib of radius μa[31]:

$$T = \left| \frac{4\Pi^* (J_{1\mu} + I_{1\mu})}{(n^* a)\varphi^*} \right| , \tag{156}$$

where Π^* is given by Eq. (155) and

$$\varphi^* = \{4\mu(J_{1\mu}I_{1\mu})(\theta^* - \psi^*) + (J_{o\mu}I_{1\mu} + J_{1\mu}I_{o\mu})[4\mu\eta^* + \gamma(n^* a)(\theta^* - \psi^*)]\} , \tag{157}$$

in which ψ^*, θ^* and η^* are given by Eqs. (152), (153), and (154) in which the parameter λ is replaced by μ. Such abbreviations as $J_{1\mu}$, $I_{1\mu}$ are used to represent the quantities $J_1(\mu n^* a)$ and $I_1(\mu n^* a)$. The parameter $\gamma = M/M_p$, where M is the rib mass and M_p is that of the plate.

13. Transmissibility of a simply supported rectangular plate driven at an arbitrary point[32]:

$$T = \left| \sum_{k=1,3,5,\ldots}^{\infty} \sum_{m=1,3,5,\ldots}^{\infty} \frac{16\varphi_{k,m}}{\pi^2 km} \left[\frac{(\beta^*)^4}{(\beta^*)^4 - 1} \right] \right| , \tag{158}$$

where $\varphi_{k,m}$ is given by Eq. (128), and (β^*) by Eq. (130). The coordinate orgin is one plate corner, the x axis being parallel to the longer plate side.

14. Transmissibility of a simply supported rectangular plate that is centrally driven[32]:

$$T = \left| \sum_{k=1,3,5,\ldots}^{\infty} \sum_{m=1,3,5,\ldots}^{\infty} \frac{16}{\pi^2 km} \left[\frac{(\beta^*)^4}{(\beta^*)^4 - 1} \right] (-1)^{(\theta - 1)} \right| , \tag{159}$$

where $\theta = (k + m)/2$. An expression for T having faster convergence can be written as follows[32]:

$$T = \left| \left[1 + \sum_{k=1,3,5,\ldots}^{\infty} \sum_{m=1,3,5,\ldots}^{\infty} \frac{16(-1)^{(\theta-1)}}{\pi^2 km\lambda^*} \right] \right| , \qquad (160)$$

where λ^* is given by Eq. (129).

15. Transmissibility of a simply supported rectangular plate that is centrally driven and mass loaded[32]:

$$T_m = T \left| \frac{\psi^*}{(\gamma + \psi^*)} \right| , \qquad (161)$$

where T is given by Eq. (160) and $\psi^* = (Z_o/j\omega M_p)$, a quantity that is given by Eq. (133). Again, the parameter $\gamma = M/M_p$, where M is the central loading mass and M_p is the plate mass.

10. FOUR-POLE PARAMETER ANALYSES

Four-pole parameters will now be referred to widely and, consequently, it is appropriate to review briefly some of their relevant properties. Detailed discussions of four-pole parameters can be found, for example in Refs. 15 and 33, where many other pertinent articles are listed. Application of four-pole parameter techniques enables a general account to be taken of the lack of rigidity in the foundation and in the mounted item.

A linear mechanical system is shown schematically in Fig. 83(a). The system may be comprised of one or more lumped or distributed elements, or be constructed from any combination of such elements. The input side of the

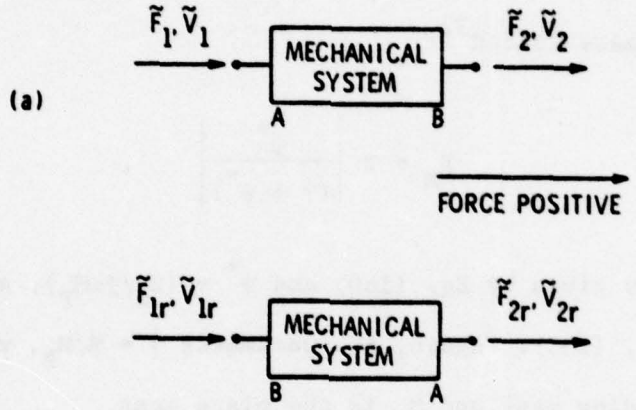
$\tilde{F}_1, \tilde{V}_1$
MECHANICAL SYSTEM
$\tilde{F}_2, \tilde{V}_2$
A
B
(a)
FORCE POSITIVE
$\tilde{F}_{1r}, \tilde{V}_{1r}$
MECHANICAL SYSTEM
$\tilde{F}_{2r}, \tilde{V}_{2r}$
B
A
(b)

Fig. 83

system vibrates sinusoidally with a velocity $\tilde{V}_1$ in response to an applied force $\tilde{F}_1$. In turn, the output side of the system exerts a force $\tilde{F}_2$ on the input side of some further system, sharing with it a common velocity $\tilde{V}_2$. Thus, the system is said to have input and output terminal pairs, a force $\tilde{F}_1$ and velocity $\tilde{V}_1$ at the input terminal pair giving rise to a force $\tilde{F}_2$ and velocity $\tilde{V}_2$ at the output terminal pair, the reaction of any subsequent mechanical system being accounted for. Forces are considered positive when directed to the right.

Consider now the mechanical impedance Z of a mass M and a spring of stiffness K (Fig. 84) in the context of the foregoing discussion; thus,

$$Z_M = j\omega M = (\tilde{F}_1 - \tilde{F}_2)/\tilde{V}_1 = (\tilde{F}_1 - \tilde{F}_2)/\tilde{V}_2 \tag{162}$$

or

$$\tilde{F}_1 = \tilde{F}_2 + j\omega M\tilde{V}_2 \quad , \tag{163}$$

$$\tilde{V}_1 = \tilde{V}_2 \quad , \tag{164}$$

and

$$Z_K = (K/j\omega) = \tilde{F}_1/(\tilde{V}_1 - \tilde{V}_2) = \tilde{F}_2/(\tilde{V}_1 - \tilde{V}_2) \tag{165}$$

or

$$\tilde{F}_1 = \tilde{F}_2 \quad , \tag{166}$$

$$\tilde{V}_1 = \tilde{F}_2(j\omega/K) + \tilde{V}_2 \quad . \tag{167}$$

Inspection of these equations makes it possible to understand that the vibration response of the general four-terminal system of Fig. 83(a) can be represented by the following equations:

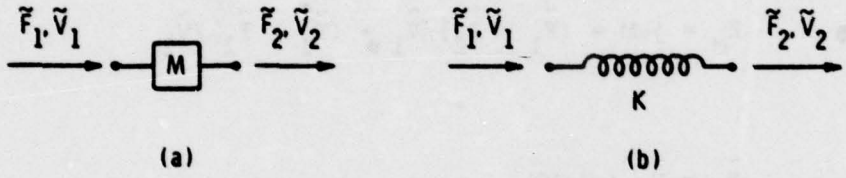
$\tilde{F}_1, \tilde{V}_1$
M
$\tilde{F}_2, \tilde{V}_2$
(a)
$\tilde{F}_1, \tilde{V}_1$
K
$\tilde{F}_2, \tilde{V}_2$
(b)

Fig. 84

$$\tilde{F}_1 = \alpha_{11}\tilde{F}_2 + \alpha_{12}\tilde{V}_2 \tag{168}$$

$$\tilde{V}_1 = \alpha_{21}\tilde{F}_2 + \alpha_{22}\tilde{V}_2 \quad , \tag{169}$$

where α_{11}, α_{22}, α_{21}, and α_{22} are known as four-pole parameters. It is directly apparent that

$$\alpha_{11} = \left.\frac{\tilde{F}_1}{\tilde{F}_2}\right|_{\tilde{V}_2 = 0} \quad , \tag{170}$$

$$\alpha_{12} = \left.\frac{\tilde{F}_1}{\tilde{V}_2}\right|_{\tilde{F}_2 = 0} \quad , \tag{171}$$

$$\alpha_{21} = \left.\frac{\tilde{V}_1}{\tilde{F}_2}\right|_{\tilde{V}_2 = 0} \quad , \tag{172}$$

and

$$\alpha_{22} = \left.\frac{\tilde{V}_1}{\tilde{V}_2}\right|_{\tilde{F}_2 = 0} \quad , \tag{173}$$

where the subscript $\tilde{V}_2 = 0$ indicates that the output terminal pair is blocked and the subscript $\tilde{F}_2 = 0$ indicates that the output terminal pair is free (unrestrained). The parameters α_{11} and α_{22} are dimensionless; α_{12} has the dimensions of impedance and α_{21} the dimensions of $(\text{impedance})^{-1}$.

In general, the four-pole parameters are frequency-dependent complex quantities. Of considerable advantage is the fact that the parameters characterize only the system for which they are determined; their value is not influenced by the preceding and subsequent mechanical systems. Equations (168) and (169) enable expressions for the driving-point and

transfer impedance and for the force and displacement transmissibilities to be written down concisely; thus, driving-point impedance,

$$Z_1 = \frac{\tilde{F}_1}{\tilde{V}_1} = \left(\frac{\alpha_{11}\tilde{F}_2 + \alpha_{12}\tilde{V}_2}{\alpha_{21}\tilde{F}_2 + \alpha_{22}\tilde{V}_2}\right) = \left(\frac{\alpha_{11}Z_T + \alpha_{12}}{\alpha_{21}Z_T + \alpha_{22}}\right) \quad ; \tag{174}$$

transfer impedance

$$TZ_{12} = \frac{\tilde{F}_1}{\tilde{V}_2} = (\alpha_{11}Z_T + \alpha_{12}) \quad ; \tag{175}$$

force transmissibility

$$T_{F12} = \left|\frac{\tilde{F}_2}{\tilde{F}_1}\right| = \left|\frac{Z_T}{(\alpha_{12} + \alpha_{11}Z_T)}\right| \quad ; \tag{176}$$

and displacement transmissibility

$$T_{D12} = \left|\frac{\tilde{V}_2}{\tilde{V}_1}\right| = \left|\frac{1}{(\alpha_{22} + \alpha_{21}Z_T)}\right| \quad . \tag{177}$$

In these equations, $Z_T = \tilde{F}_2/\tilde{V}_2$ is the driving-point impedance of the mechanical system subsequent to the one under consideration.

It can be demonstrated that, without exception,

$$(\alpha_{11}\alpha_{22} - \alpha_{12}\alpha_{21}) = 1 \quad ; \tag{178}$$

consequently, knowledge of only three of the four-pole parameters is sufficient to specify the performance of the system completely (Refs. 15 and 33). Further, in the special case of a symmetrical system (when it does not matter which terminal pair is input or output),

$$\alpha_{11} = \alpha_{22} \tag{179}$$

and knowledge of only two independent four-pole parameters is sufficient to determine the system performance completely.

Should the mechanical system be reversed, so that the original output and input terminal pairs are interchanged, as in Fig. 83(b), then the relevant four-pole equations become

$$\tilde{F}_{1r} = \alpha_{22}\tilde{F}_{2r} + \alpha_{12}\tilde{V}_{2r} \quad , \tag{180}$$

$$\tilde{V}_{1r} = \alpha_{21}\tilde{F}_{2r} + \alpha_{11}\tilde{V}_{2r} \quad , \tag{181}$$

where the input and output forces and velocities are now $\tilde{F}_{1r}$, $\tilde{V}_{1r}$ and $\tilde{F}_{2r}$, $\tilde{V}_{2r}$, respectively, and

$$\alpha_{11} = \left.\frac{\tilde{V}_{1r}}{\tilde{V}_{2r}}\right|_{\tilde{F}_{2r} = 0} \quad , \tag{182}$$

$$\alpha_{12} = \left.\frac{\tilde{F}_{1r}}{\tilde{V}_{2r}}\right|_{\tilde{F}_{2r} = 0} \quad , \tag{183}$$

$$\alpha_{21} = \left.\frac{\tilde{V}_{1r}}{\tilde{F}_{2r}}\right|_{\tilde{V}_{2r} = 0} \quad , \tag{184}$$

and

$$\alpha_{22} = \left.\frac{\tilde{F}_{1r}}{\tilde{F}_{2r}}\right|_{\tilde{V}_{2r} = 0} \quad . \tag{185}$$

Although the values of the four-pole parameters α_{11} and α_{22} remain unchanged, their definitions differ here from those of Eqs. (169) and (172); in fact, the parameters have dual significance and can be determined in alternate ways, which is sometimes an advantage. By comparing the companion definitions of α_{11} and α_{22}, it follows that

$$\frac{1}{\alpha_{11}} = \frac{\tilde{F}_2}{\tilde{F}_1}\bigg|_{\tilde{V}_2 = 0} = \frac{\tilde{V}_{2r}}{\tilde{V}_{1r}}\bigg|_{\tilde{F}_{2r} = 0} \tag{186}$$

and

$$\frac{1}{\alpha_{22}} = \frac{\tilde{V}_2}{\tilde{V}_1}\bigg|_{\tilde{F}_2 = 0} = \frac{\tilde{F}_{2r}}{\tilde{F}_{1r}}\bigg|_{\tilde{V}_{2r} = 0} . \tag{187}$$

These equations show, as noted previously (Section 2), that the force and displacement (and, therefore, the velocity and acceleration) transmissibilities in opposite directions between the two terminal pairs of a mechanical system are identical.

If the output terminal pair of one mechanical system is rigidly connected to the input terminal pair of another system (Fig. 85), so that the output from the first is exactly the input to the second, the two systems are connected in series. Moreover, for n systems in series, the output force and velocity $\tilde{F}_{(n+1)}$, $\tilde{V}_{(n+1)}$ can be related to the input force and velocity by the continued product of n 2 x 2 matrices.[15,33] Simply, for a two-stage system,

$$\begin{bmatrix} \tilde{F}_1 \\ \tilde{V}_1 \end{bmatrix} = \begin{bmatrix} \alpha'_{11} & \alpha'_{12} \\ \alpha'_{21} & \alpha'_{22} \end{bmatrix} \begin{bmatrix} \alpha''_{11} & \alpha''_{12} \\ \alpha''_{21} & \alpha''_{22} \end{bmatrix} \begin{bmatrix} \tilde{F}_3 \\ \tilde{V}_3 \end{bmatrix} \tag{188}$$

or

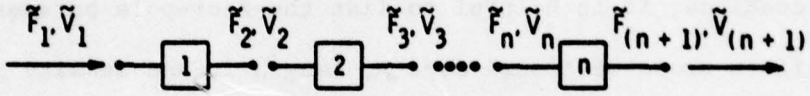
$\tilde{F}_1, \tilde{V}_1$
$\tilde{F}_2, \tilde{V}_2$
$\tilde{F}_3, \tilde{V}_3$
$\tilde{F}_n, \tilde{V}_n$
$\tilde{F}_{(n+1)}, \tilde{V}_{(n+1)}$
1
2
n

Fig. 85

$$\begin{bmatrix} \tilde{F}_1 \\ \tilde{V}_1 \end{bmatrix} = \begin{bmatrix} \upsilon_{11} & \upsilon_{12} \\ \upsilon_{21} & \upsilon_{22} \end{bmatrix} \begin{bmatrix} \tilde{F}_3 \\ \tilde{V}_3 \end{bmatrix} \quad , \tag{189}$$

where

$$\begin{bmatrix} \upsilon_{11} & \upsilon_{12} \\ \upsilon_{21} & \upsilon_{21} \end{bmatrix} = \begin{bmatrix} (\alpha'_{11}\alpha''_{11} + \alpha'_{12}\alpha''_{21}) & (\alpha'_{11}\alpha''_{12} + \alpha'_{12}\alpha''_{22}) \\ (\alpha'_{21}\alpha''_{11} + \alpha'_{22}\alpha''_{21}) & (\alpha'_{21}\alpha''_{12} + \alpha'_{22}\alpha''_{22}) \end{bmatrix} \quad . \tag{190}$$

To conclude, it is helpful to list the four-pole parameters for a slender rod of uniform cross-sectional area A, length ℓ, and density ρ when the rod is driven axially by a sinusoidally varying force. For this symmetrical system,

$$\alpha_{11} = \alpha_{22} = \cos n^* \ell \quad , \tag{191}$$

$$\alpha_{12} = \mu_R^* \sin n^* \ell \quad , \tag{192}$$

and

$$\alpha_{21} = - \sin n^* \ell / \mu_R^* \quad , \tag{193}$$

where

$$\mu_R^* = (j\omega M_R / n^* \ell) \quad . \tag{194}$$

In these equations, M_R and n^* are the mass and the complex wavenumber of the rod; that is, $M_R = \rho A \ell$ and

$$n^* = (\omega^2 \rho / E^*)^{\frac{1}{2}} \quad , \tag{195}$$

where E^* is the complex Young's modulus. As in Sec. 3, it is convenient to write the dimensionless product $n^* \ell$ as the complex number $(p + jq)$, where p

and q are given by Eqs. (20) and (21) in which the frequency dependence of E_ω and $\delta_{E\omega}$ is now assumed to be negligible.

10.1 Characterization of an Antivibration Mounting

Consider now the antivibration mounting of Fig. 86 that is comprised of a uniform rodlike sample of rubberlike "material" bonded to metal end plates of masses M_1 and M_2. The mechanical behavior of the rubberlike material is assumed to be governed by Eqs. (191) - (194). An input force and velocity $\tilde{F}_1$, $\tilde{V}_1$ produce an output force and velocity $\tilde{F}_2$, $\tilde{V}_2$ at some termination subsequent to the end plate of mass M_2. An equation of the form of Eq. (188) remains relevant to this three-stage system, but now

$$\begin{bmatrix} \upsilon_{11} & \upsilon_{12} \\ \upsilon_{21} & \upsilon_{22} \end{bmatrix} = \begin{bmatrix} 1 & j\omega M_1 \\ 0 & 1 \end{bmatrix} \begin{bmatrix} c. & \mu_R^* s. \\ (\mu_R^*)^{-1} s. & c. \end{bmatrix} \begin{bmatrix} 1 & j\omega M_2 \\ 0 & 1 \end{bmatrix} , \tag{196}$$

where the abbreviations s. and c. represent the complex circular functions $\sin n^*\ell$ and $\cos n^*\ell$, and the matrices for the masses M_1 and M_2 follow directly from inspection of Eqs. (163) and (164). It is readily shown that

$$\upsilon_{11} = [c. - \gamma_1(n^*\ell)s.] , \tag{197}$$

$$\upsilon_{12} = \mu_R^* \{[s. + \gamma_1(n^*\ell)c.] + \gamma_2(n^*\ell)[c. - \gamma_1(n^*\ell)s.]\} , \tag{198}$$

$$\upsilon_{21} = -(\mu_R^*)^{-1}(s.) , \tag{199}$$

and

$$\upsilon_{22} = [c. - \gamma_2(n^*\ell)s.] , \tag{200}$$

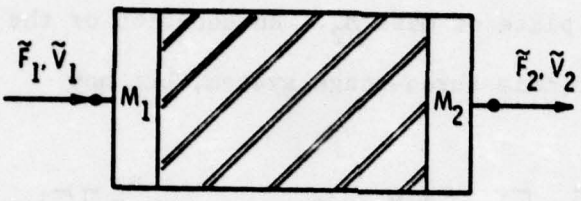

Fig. 86

where $\gamma_1 = M_1/M_R$ and $\gamma_2 = M_2/M_R$. These four-pole parameters relate equally well to a rodlike mount having significant lateral dimensions when n^* is replaced by the complex wavenumber N^* specified by Eqs. (27) - (32).

Of considerable interest is the simplicity of the four-pole parameter υ_{21}, the reciprocal of which describes a blocked quasi-transfer impedance that is independent of the values of M_1 and M_2; thus

$$\frac{1}{\upsilon_{21}} = \frac{\tilde{F}_2}{\tilde{V}_1}\bigg|_{\tilde{V}_2 = 0} = \frac{-\mu_R^*}{\sin n^* \ell} = -\frac{j\omega M_R}{n^* \ell \sin n^* \ell} \quad . \tag{201}$$

Further, at frequencies well below the initial wave-effect frequency ω_1 in the mount, $\sin n^* \ell \to n^* \ell$ and

$$\frac{1}{\upsilon_{21}} = \frac{\omega(\rho A \ell)}{j\ell^2}\left(\frac{E^*}{\omega^2 \rho}\right) = \frac{(AE^*/\ell)}{j\omega} \quad , \tag{202}$$

which is the impedance of a simple spring of complex stiffness $K^* = (AE^*/\ell)$. If this stiffness is symbolized by $K^* = K(1 + j\delta_K)$ then

$$\frac{1}{\upsilon_{21}} = \frac{K}{\omega}(\delta_K - j) \tag{203}$$

and measurements of the imaginary part and of the ratio of the imaginary to real part (tan phase angle) of $1/\upsilon_{12}$ will yield K/ω and the reciprocal of the damping factor δ_K, respectively. The larger the value of δ_K, the greater the accuracy to which the phase angle and, hence, δ_K can be measured. This measurement approach was proposed and utilized in Refs. 27 and 34, where the permissible upper bound of measurement was said to be $0.25\ \omega_1$.

10.2 Resilient Mounting on Nonrigid Substructures

Examined now is the vibration response of a nonrigid substructure of arbitrary impedance Z_T that lies beneath the antivibration mounting considered in the foregoing. The mount and substructure are characterized by the four-pole parameters υ_{ij} [Eqs. (197) - (200)] and α_{ij}, respectively. Initially, the item supported by the mount is assumed to remain masslike at all frequencies. The entire assembly is shown diagrammatically in Fig. 87(a). The same item of mass M is shown rigidly mounted in the reference assembly of Fig. 87(b), where it generates an untenably large vibration of the substructure.

The same exciting force is considered to act upon or to be generated within M in both Figs. 87(a) and (b). This force gives rise to a transmitted force $\tilde{F}_{12}$ at the point of juncture of the mount and the substructure in Fig. 87(a), and to a force $\tilde{F}_{12R}$ at the same location on the substructure in Fig. 87(b). The companion velocities are $\tilde{V}_{12}$ and $\tilde{V}_{12R}$, respectively. Beneath the substructure, the output forces and velocities are $\tilde{F}_2$, $\tilde{V}_2$, and $\tilde{F}_{2R}$, $\tilde{V}_{2R}$.

In prior discussions of the vibration of nonrigid substructures, attention is devoted either to the mount transmissibility $T = |\tilde{F}_2/\tilde{F}_1|$, or to the mount response ratio $R = |\tilde{V}_{12}/\tilde{V}_{12R}|$ -- or its reciprocal, mount effectiveness $E = R^{-1}$. Consequently, it is appropriate to evaluate the quantities T and R in general terms using the four-pole parameter techniques described in the foregoing.

The forces and velocities experienced by the mounted item and substructure in Fig. 87(a) are readily understood to be related by the equation

$$\begin{bmatrix} \tilde{F}_1 \\ \tilde{V}_1 \end{bmatrix} = \begin{bmatrix} 1 & j\omega M \\ 0 & 1 \end{bmatrix} \begin{bmatrix} \upsilon_{11} & \upsilon_{12} \\ \upsilon_{21} & \upsilon_{22} \end{bmatrix} \begin{bmatrix} \tilde{F}_{12} \\ \tilde{V}_{12} \end{bmatrix} , \tag{204}$$

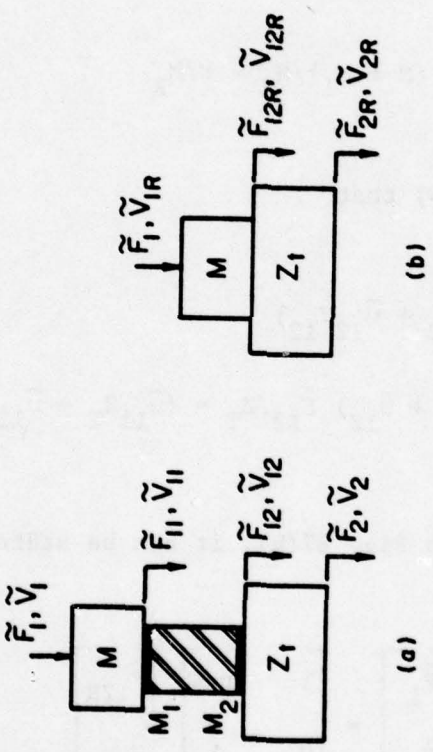
$\tilde{F}_1, \tilde{V}_1$
M
M_1
M_2
$\tilde{F}_{11}, \tilde{V}_{11}$
$\tilde{F}_{12}, \tilde{V}_{12}$
Z_1
$\tilde{F}_2, \tilde{V}_2$
(a)
$\tilde{F}_1, \tilde{V}_{1R}$
M
Z_1
$\tilde{F}_{12R}, \tilde{V}_{12R}$
$\tilde{F}_{2R}, \tilde{V}_{2R}$
(b)

Fig. 87

where the matrix product can be written as the third matrix

$$\begin{bmatrix} \bar{\upsilon}_{11} & \bar{\upsilon}_{12} \\ \upsilon_{21} & \upsilon_{22} \end{bmatrix}$$

in which $\bar{\upsilon}_{11}$, $\bar{\upsilon}_{12}$, υ_{21}, and υ_{22} are again defined by Eqs. (197) - (200), the only change being that the mass ratio γ_1 in Eqs. (197) and (198) for $\bar{\upsilon}_{11}$ and $\bar{\upsilon}_{12}$ is redefined as

$$\gamma_1 = (M + M_1)/M_R \approx M/M_R \quad . \tag{205}$$

It is evident from Eq. (204) that

$$\begin{aligned} \tilde{F}_1 &= (\bar{\upsilon}_{11}\tilde{F}_{12} + \bar{\upsilon}_{12}\tilde{V}_{12}) \\ &= (\bar{\upsilon}_{11}Z_T + \bar{\upsilon}_{12})\ \tilde{F}_{12}/Z_T = (\bar{\upsilon}_{11}Z_T + \bar{\upsilon}_{12})\tilde{V}_{12} \quad . \end{aligned} \tag{206}$$

Likewise, from reference to Fig. 87(b), it can be stated that

$$\begin{bmatrix} \tilde{F}_1 \\ \tilde{V}_{1R} \end{bmatrix} = \begin{bmatrix} 1 & j\omega M \\ 0 & 1 \end{bmatrix} \begin{bmatrix} \tilde{F}_{12R} \\ \tilde{V}_{12R} \end{bmatrix} \tag{207}$$

and, consequently, that

$$\tilde{F}_1 = (\tilde{F}_{12R} + j\omega M\tilde{V}_{12R}) = (Z_T + j\omega M)\ \tilde{V}_{12R} \quad . \tag{208}$$

From Eqs. (206) and (208) it is possible to write down the transmissibility and response ratio of the mounting system directly; thus

$$T = \left|\frac{\tilde{F}_{12}}{\tilde{F}_1}\right| = \left|\frac{Z_T}{(\bar{v}_{11}Z_T + \bar{v}_{12})}\right| \tag{209}$$

and

$$R = \left|\frac{\tilde{V}_{12}}{\tilde{V}_{12R}}\right| = \left|\left(\frac{Z_T + j\omega M}{\bar{v}_{11}Z_T + \bar{v}_{12}}\right)\right| \quad . \tag{210}$$

Response ratio, the magnitude of the substructure velocity observed when M is resiliently mounted to the velocity observed when M is attached rigidly to the foundation, provides a measure of the vibration reduction that the mounting affords -- the smaller the value of R, the greater the reduction of substructure velocity and the more beneficial the mounting. Note that, because

$$Z_T = \tilde{F}_{12}/\tilde{V}_{12} = \tilde{F}_{12R}/\tilde{V}_{12R} \quad , \tag{211}$$

the response ratio could have been defined equally well as the ratio $|\tilde{F}_{12}/\tilde{F}_{12R}|$ of the forces exerted on the substructure in the resiliently and rigidly mounted cases. Note also that R is not as small at T unless $Z_T >> j\omega M$; that is to say, if $j\omega M$ is comparable with, or greater than, Z_T the mount will be <u>less</u> effective than predicted by its transmissibility curve. Physically, this reflects the fact that the beneficial action of the antivibration mount in Fig. 87(a) will be countered, to some extent, by the greater freedom of the foundation to respond to a given applied force than was possible in Fig. 87(b). Thus, the foundation in Fig. 87(a) is no longer relieved of part of the applied force by the inertia of the mass M -- an acute disadvantage if M is large, as it may well be. In this circumstance, it has been suggested[1] that the response of the substructure be restrained by an auxiliary

mass m having a significant fraction of the mass M of the mounted item. The relevant expressions for transmissibility and response ratio follow immediately from Eqs. (209) and (210) if the mass ratio $\gamma_2 = M_2/M_R$ that appears in the four-pole parameter $\overline{U}_{12}$ of these equations is redefined as

$$\gamma_2 = (M_2 + m)/M_R \approx m/M_R \quad . \tag{212}$$

One further result follows from consideration of the matrix equation for the substructure,

$$\begin{bmatrix} \tilde{F}_{12} \\ \tilde{V}_{12} \end{bmatrix} = \begin{bmatrix} \alpha_{11} & \alpha_{12} \\ \alpha_{21} & \alpha_{22} \end{bmatrix} \begin{bmatrix} \tilde{F}_2 \\ \tilde{V}_2 \end{bmatrix} \quad , \tag{213}$$

and its constituent equations

$$\tilde{F}_{12} = \alpha_{11}\tilde{F}_2 + \alpha_{12}\tilde{V}_2 \tag{214}$$

and

$$\tilde{V}_{12} = \alpha_{21}\tilde{F}_2 + \alpha_{22}\tilde{V}_2 \quad . \tag{215}$$

Thus, the output velocity can be eliminated from these equations to yield

$$\tilde{F}_2 = \tilde{V}_{12}\,(\alpha_{22}Z_T - \alpha_{12}) \quad ; \tag{216}$$

likewise,

$$\tilde{F}_{2R} = \tilde{V}_{12R}\,(\alpha_{22}Z_T - \alpha_{12}) \quad . \tag{217}$$

Consequently, an additional definition can be stated for response ratio, which now has the triple significance

$$R = \left|\frac{\tilde{V}_{12}}{\tilde{V}_{12R}}\right| = \left|\frac{\tilde{F}_2}{\tilde{F}_{2R}}\right| = \left|\frac{\tilde{F}_{12}}{\tilde{F}_{12R}}\right| \quad . \tag{218}$$

The new definition of R describes the ratio $|\tilde{F}_2/\tilde{F}_{2R}|$ of the forces that are transmitted to the termination of the substructure in the resiliently and rigidly mounted cases. Further, a companion force transmissibility across the entire system can logically be defined and determined from Eqs. (206) and (216) as

$$T_{overall} = \left|\frac{\tilde{F}_2}{\tilde{F}_1}\right| = \left|\left(\frac{\alpha_{22}Z_T - \alpha_{12}}{\bar{\upsilon}_{11}Z_T + \bar{\upsilon}_{12}}\right)\right| \quad . \tag{219}$$

This significant quantity differs from both R and T as previously specified. Note that the quantities $\bar{\upsilon}_{11}$ and $\bar{\upsilon}_{12}$ are related to the (transmissibility)$^{-1}$ and transfer impedance of the mount [Eqs. (170) and (171)].

The results of one independent calculation of $T_{overall}$ for a rectangular platelike substructure with an aspect ratio of 0.5 are plotted in Fig. 88 as the dashed-line curve. The mounted item is driven by a vibratory force $\tilde{F}_1$ and is supported by four antivibration mounts that are located symmetrically about the plate center, each at coordinates of one-third the length and breadth of the plate from the nearest plate corner. The mounting points have the same driving-point impedance and experience the same velocity. The output force $\tilde{F}_2$ comprises four discrete forces at the plate corners plus distributed forces along the simply supported plate boundaries. Transmissibility $T_{overall} = |\tilde{F}_2/\tilde{F}_1|$ has been calculated in terms of the frequency ratio $\Omega = \omega/\omega_o$, where ω_o is the natural frequency of the mounting system calculated as though the platelike substructure were ideally rigid. The mounted item is four times more massive than the substructure, and the fundamental plate resonance is assigned the frequency $4\,\omega_o$. The mounts and the substructure have the damping factors 0.05 and 0.01, respectively. The

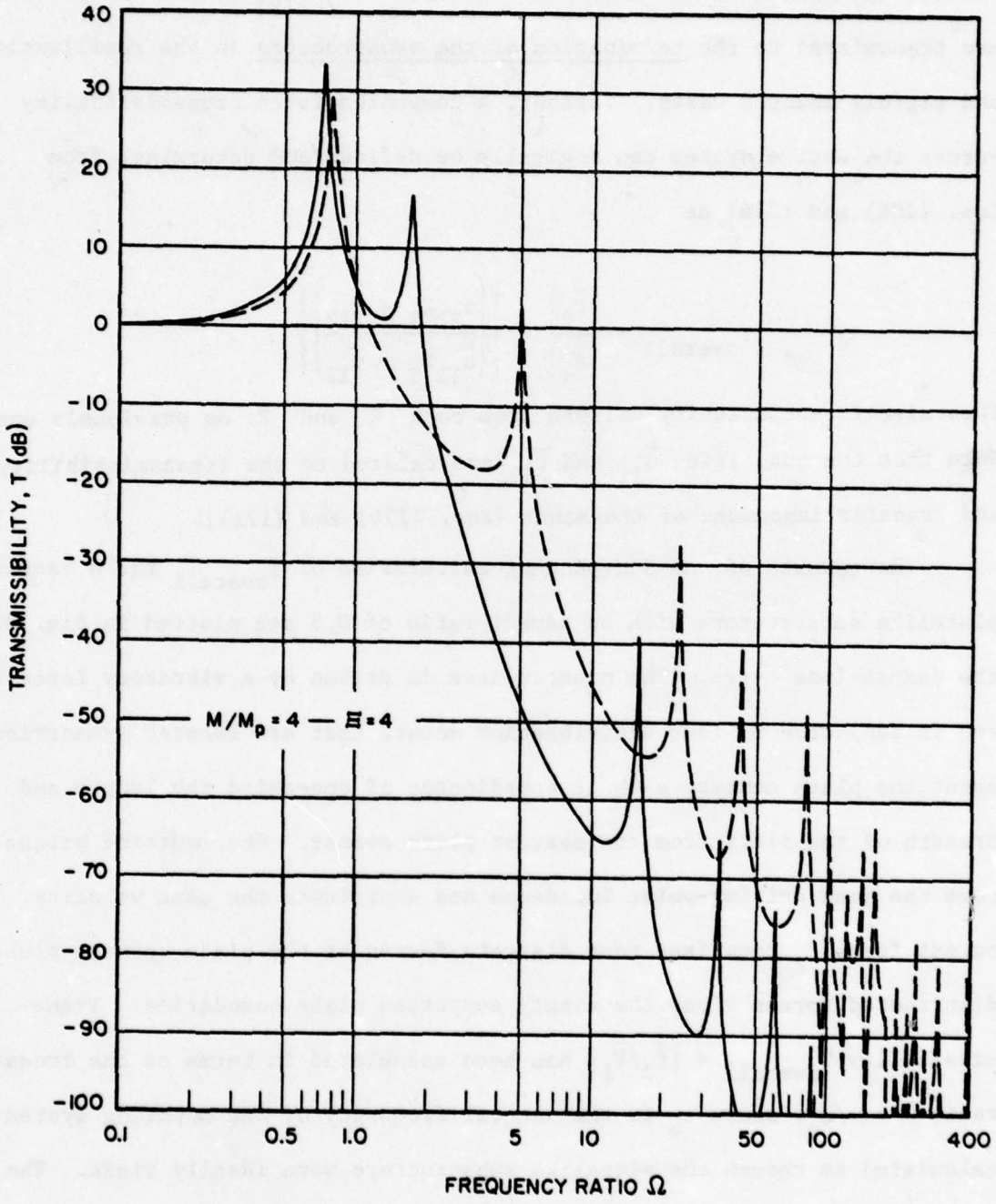
40
30
20
10
0
-10
-20
-30
-40
-50
-60
-70
-80
-90
-100
TRANSMISSIBILITY, T (dB)
M/Mp = 4 — Ξ = 4
0.1
0.5
1.0
5
10
50
100
400
FREQUENCY RATIO Ω

Fig. 88

transmissibility curve at high frequencies is characterized by many plate resonances; moreover, the number of plate resonances that are excited can detrimentally increase if the mounts are located at other, less favorable, positions.[36]

The overall transmissibility across an identical mounting system to which lumped masses have been added to each mount location is shown by the solid-line curve. The total added mass m is equal to that of the mounted item (m = M). Use of such heavy mass loading is necessary if the level of the transmissibility curve is to be reduced significantly. For added mass equal to 0.25M, the resultant transmissibility curve would lie approximately halfway between the solid-line and dashed-line curves at frequencies above the fundamental plate resonance (Ω = 8). Such small added mass as 0.05M would be ineffectual in reducing transmissibility much below the level of the dashed-line curve except at very high frequencies where the impedance of the loading mass m would eventually predominate the plate impedance.

10.3 Nonrigidity of Mounted Item

To conclude this Section, it is appropriate to demonstrate how readily the effects of nonrigidity in the mounted item can be accounted for in the preceding four-pole equations. Thus, if the mounted item is characterized by the four-pole parameters φ_{ij}, then the forces and velocities experienced by the mounted item and the substructure in Fig. 87(a) will be related, not by Eq. (204), but as follows:

$$\begin{bmatrix} \tilde{F}_1 \\ \tilde{V}_1 \end{bmatrix} = \begin{bmatrix} \upsilon'_{11} & \upsilon'_{12} \\ \upsilon'_{21} & \upsilon'_{22} \end{bmatrix} \begin{bmatrix} \tilde{F}_{12} \\ \tilde{V}_{12} \end{bmatrix} , \tag{220}$$

where

$$\upsilon'_{11} = (\varphi_{11}\upsilon_{11} + \varphi_{12}\upsilon_{21}) \quad , \tag{221}$$

$$\upsilon'_{12} = (\varphi_{11}\upsilon_{12} + \varphi_{12}\upsilon_{22}) \quad , \tag{222}$$

$$\upsilon'_{21} = (\varphi_{21}\upsilon_{11} + \varphi_{22}\upsilon_{21}) \quad , \tag{223}$$

and

$$\upsilon'_{22} = (\varphi_{21}\upsilon_{12} + \varphi_{22}\upsilon_{22}) \quad . \tag{224}$$

In these equations, υ_{11}, υ_{12}, υ_{21}, and υ_{22} are defined precisely as before by Eqs. (197) - (200) in which the initial definition of $\gamma_1 = M_1/M_R$ pertains. Because Eqs. (204) and (220) are closely similar, the expressions that were derived previously for transmissibility can be restated, by inspection, as follows:

$$T = \left|\frac{\tilde{F}_{12}}{\tilde{F}_1}\right| = \left|\frac{Z_T}{(\upsilon'_{11}Z_T + \upsilon'_{12})}\right| \tag{225}$$

and

$$T_{\text{overall}} = \left|\frac{\tilde{F}_2}{\tilde{F}_1}\right| = \left|\left(\frac{\alpha_{22}Z_T - \alpha_{12}}{\upsilon'_{11}Z_T + \upsilon'_{12}}\right)\right| \quad . \tag{226}$$

Response ratio can also be restated simply by noting from Eq. (220) that

$$\tilde{F}_1 = (\upsilon'_{11}Z_T + \upsilon'_{12})\,\tilde{V}_{12} \quad , \tag{227}$$

and by noting from the relation between the forces and velocities experienced by the mounted item and substructure in Fig. 87(b) that

$$\tilde{F}_1 = (\varphi_{11}\tilde{F}_{12R} + \varphi_{12}\tilde{V}_{12R})$$

$$= (\varphi_{11}Z_T + \varphi_{12})\,\tilde{V}_{12R} \quad ; \tag{228}$$

in consequence,

$$R = \left|\frac{\tilde{V}_{12}}{\tilde{V}_{12R}}\right| = \left|\left(\frac{\varphi_{11}Z_T + \varphi_{12}}{\upsilon_{11}Z_T + \upsilon_{12}}\right)\right| \quad . \tag{229}$$

11. RELATIVE PERFORMANCE OF MOUNTING SYSTEMS

The relative performance of mounting systems or, rather, their relative transmissibility has been defined as the difference in dB between a reference transmissibility curve and the transmissibility curve of the mounting system under consideration. The reference transmissibility curve is that of the simple mounting system having a mount or mounts with frequency-independent properties; namely,

$$T = \frac{(1 + \delta_K^2)^{\frac{1}{2}}}{[(1 - \Omega^2)^2 + \delta_K^2]^{\frac{1}{2}}} \quad , \tag{230}$$

where, as usual, the frequency ratio $\Omega = \omega/\omega_o$ in which ω_o is the natural frequency of the mounting system and ω is the impressed frequency. In each case, ω_o has been adjusted to coincide with the natural frequency of the mounting system under consideration. In both mounting systems, it has been assumed that the mount damping factors $\delta_K = 0.05$, whereas the damping factor of the foundation of the mounting system under consideration has been equated to unity. If T_1 is the transmissibility of this mounting system, then

$$\text{Relative Transmissibility} = (20 \log_{10} T - 20 \log_{10} T_1) \quad . \tag{231}$$

An improvement in transmissibility above that of the simple mounting system is therefore reflected by positive values of Relative Transmissibility in dB.

11.1 Beamlike Foundation[35]

The relative transmissibility of a mounted item supported by eight mounts along the length of a clamped-clamped beam of length L is shown in Fig. 89. The mounts are uniformly spaced at distances of 0.125L, 0.375L, 0.625L, and 0.875L from each beam termination. The mounted item is ten times more massive than the beam and the fundamental resonance of the beam occurs at the frequency 10 ω_o. By contrast, the relative transmissibility of a mounted item with four mounts spaced at distances of 0.25L and 0.75L from each termination appears in Fig. 90. Now, beneath each of the four mounts is placed a concentrated mass; the total mass is two and one-half times that of the beam mass. The mounted item again has ten times the beam mass and the fundamental natural frequency of the beam equals 10 ω_o. The performance of the same mounting system but with viscously damped dynamic absorbers attached to the beam at each of the four mount locations is shown in Fig. 91 (the mounts remain located at distances of 0.25L and 0.75L from each beam termination). The absorbers have one-fourth of the beam mass and are tuned to a frequency of 0.88 ω_o; their damping ratios equal 0.226.

Finally, the performance of the compound mounting system is plotted in Fig. 92 as the three solid-line curves for which the mass ratio $\beta = 0.1$, 0.2, and 1.0 (the intermediate mass one-tenth, one fifth, and equally massive as the mounted item). Also plotted is the performance of the simple mounting system for which $\beta = 0$. In each case, the mounts are located at distances of 0.25L and 0.75L from each beam termination. As before, the mass of the

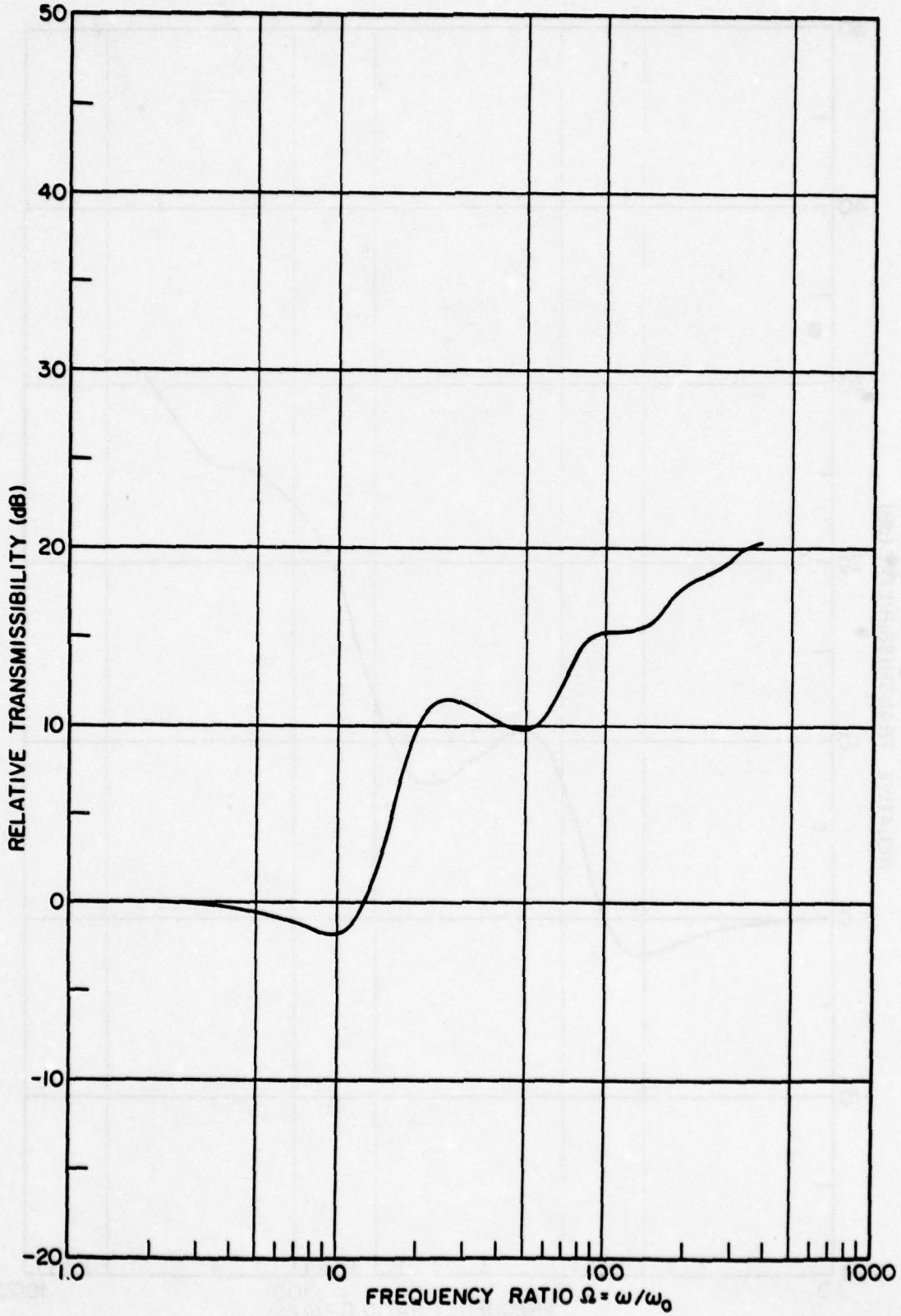
50
40
30
20
10
0
-10
-20
RELATIVE TRANSMISSIBILITY (dB)
1.0
10
100
1000
FREQUENCY RATIO Ω = ω/ω0

Fig. 89

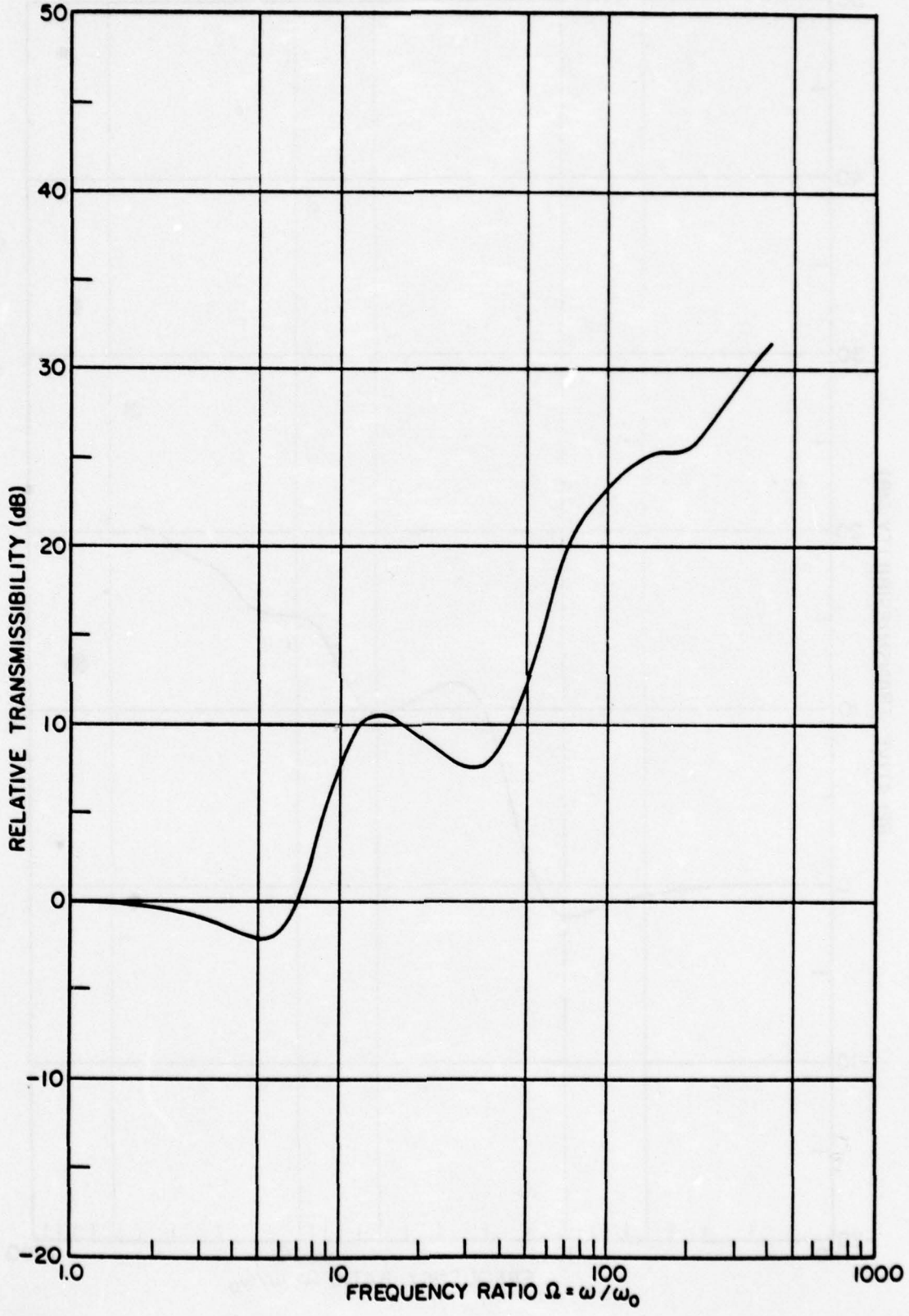
50
40
30
20
10
0
-10
-20
RELATIVE TRANSMISSIBILITY (dB)
1.0
10
100
1000
FREQUENCY RATIO Ω = ω/ω0

Fig. 90

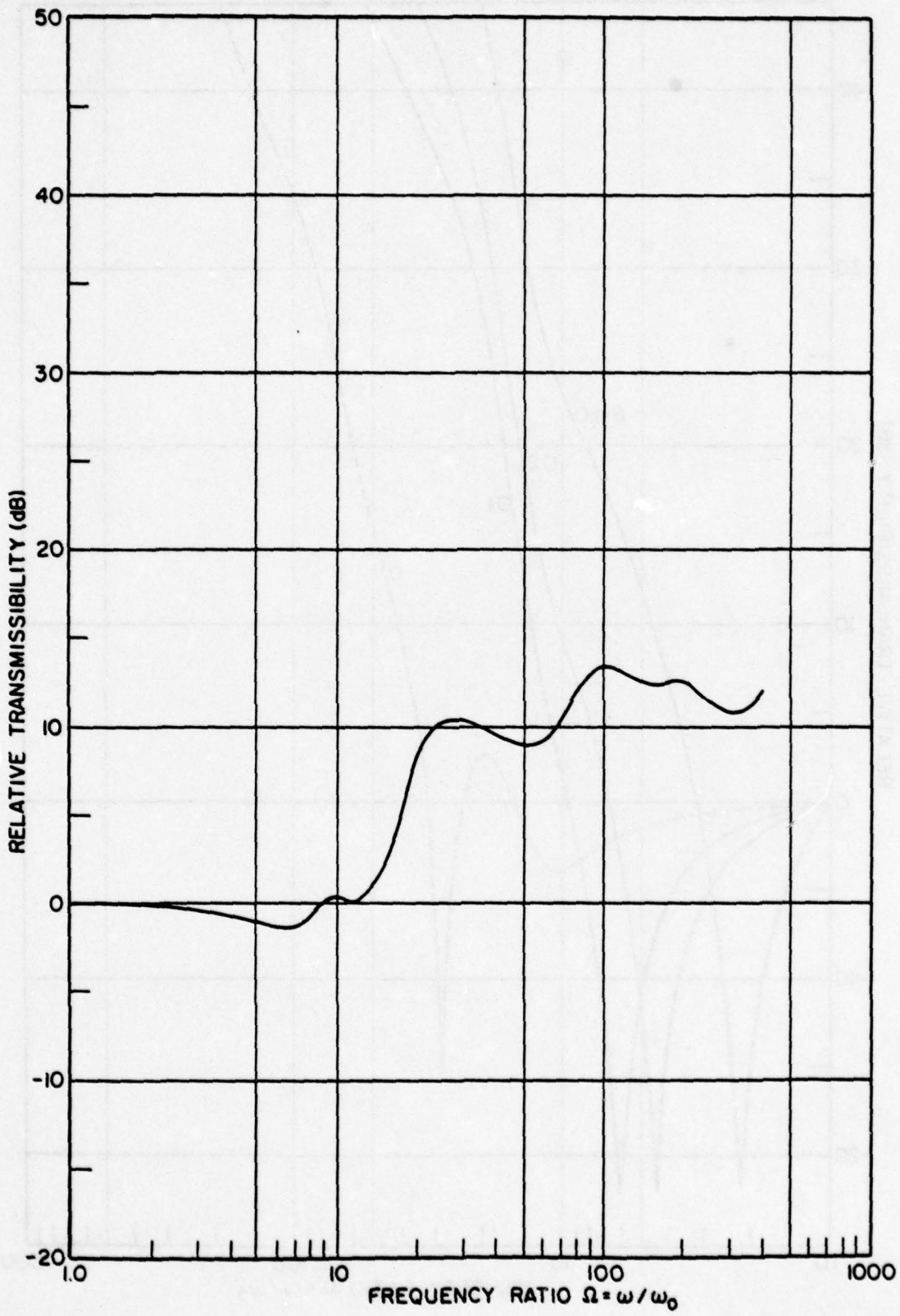
50
40
30
20
10
0
-10
-20
RELATIVE TRANSMISSIBILITY (dB)
1.0
10
100
1000
FREQUENCY RATIO Ω = ω/ω0

Fig. 91

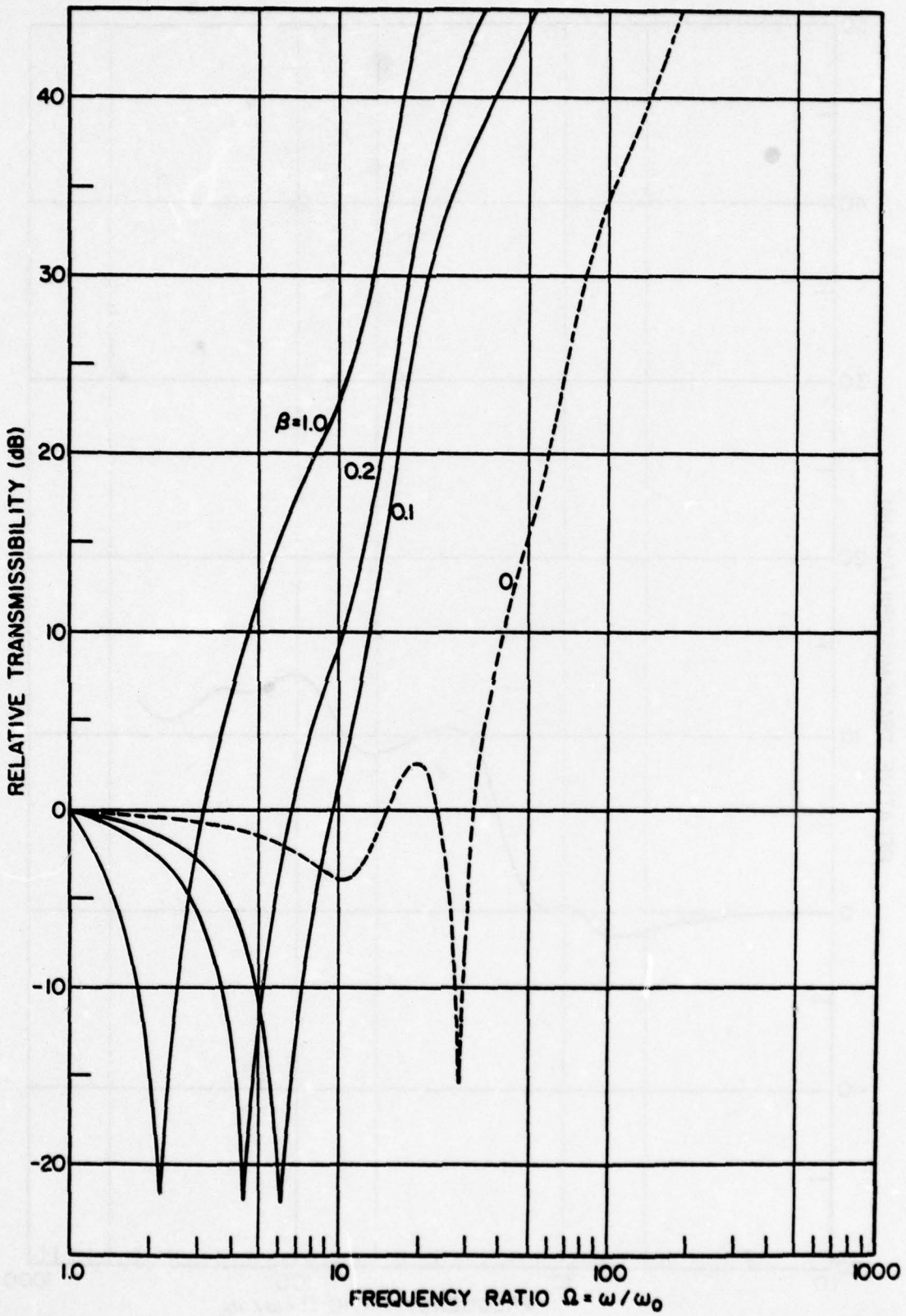
RELATIVE TRANSMISSIBILITY (dB)
40
30
20
10
0
-10
-20
β=1.0
0.2
0.1
0
1.0
10
100
1000
FREQUENCY RATIO Ω = ω / ω0

Fig. 92

mounted item is 10 times that of the beam and the fundamental frequency of the beam is 10 ω_o, where ω_o is now the reference frequency of the compound system [Eq. (58)]. The performance of the compound system clearly exceeds that of the simple system and that of the mounting systems considered previously in Figs. 89 - 91.

11.2 Platelike Foundations[17,36]

The relative transmissibility of the simple mounting system supported by a square platelike foundation is shown in Fig. 93 as the solid-line curve. The mounted item is supported by a total of eight mounts that are symmetrically located about the plate center. The mounts are located at distances of 0.2a and 0.4a from the plate corners in one direction, and at distances of a/3 and 2a/3 from the plate corners in the other direction, where a is the length of the plate sides. The mounted item is four times more massive than the simply supported plate beneath it, and the fundamental natural frequency of the plate equals 4 ω_o, where ω_o is now the natural frequency of the mounting system calculated as though the platelike foundation were ideally rigid. The dashed-line curve shows the performance of the same mounting system but with the mounted item supported by only four mounts, again located symmetrically about the plate center at distances of a/4 from each plate corner in both directions.

The relative transmissibility of a simple mounting system that is supported by a rectangular plate with an aspect of 0.5 is shown in Fig. 94. The plate is simply supported and beneath each of the four mounts -- which are located at distances of a/3 from the plate corners in one direction, and at distances of a/6 from the plate corners in the other direction (a is the length of the longer plate sides) -- are placed concentrated masses that are one or four times more massive than the plate (γ = 1 or 4). For comparison, the performance of the mounting system on the bare (unloaded) plate

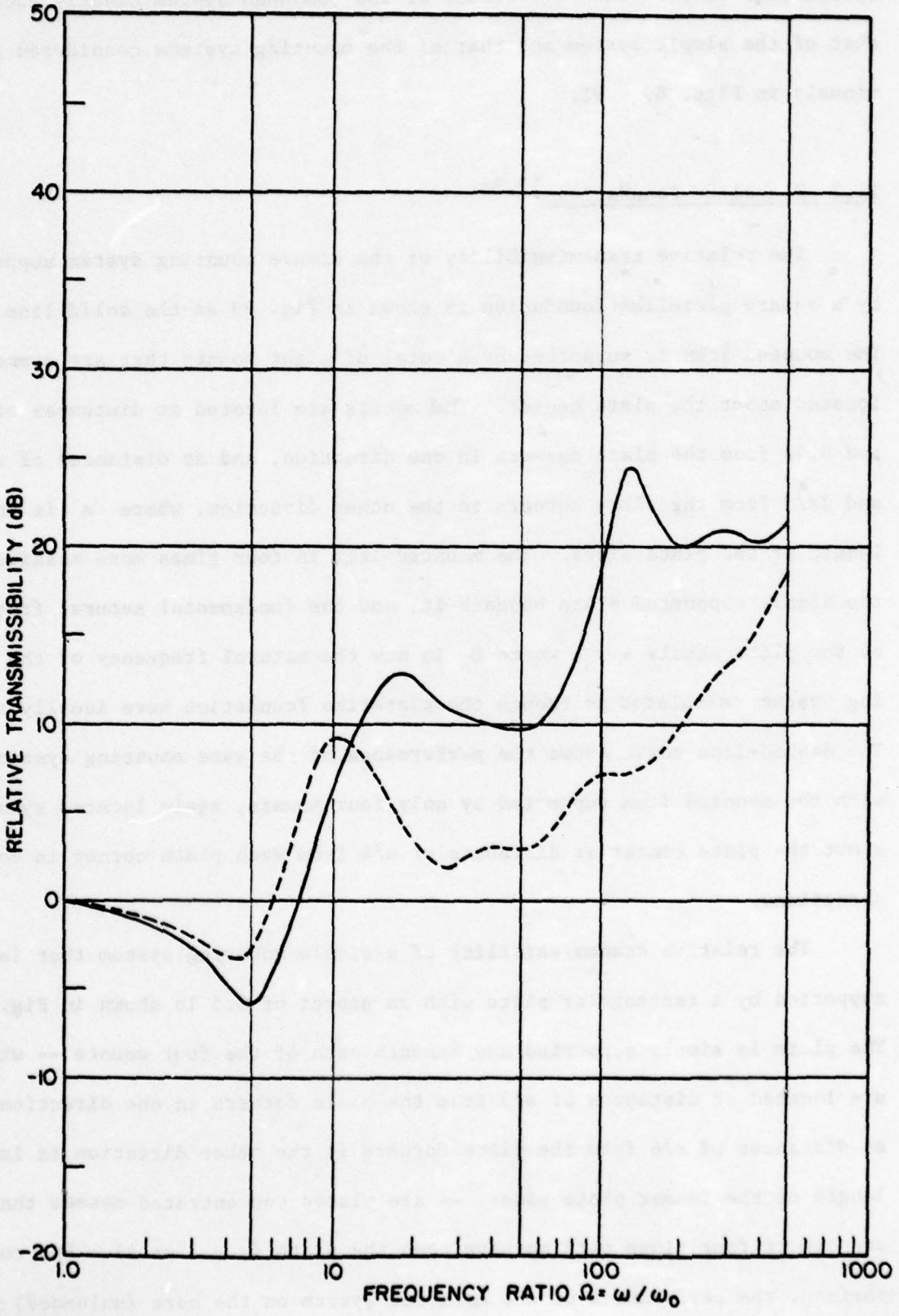
50
40
30
20
10
0
-10
-20
RELATIVE TRANSMISSIBILITY (dB)
1.0
10
100
1000
FREQUENCY RATIO Ω = ω / ω0

Fig. 93

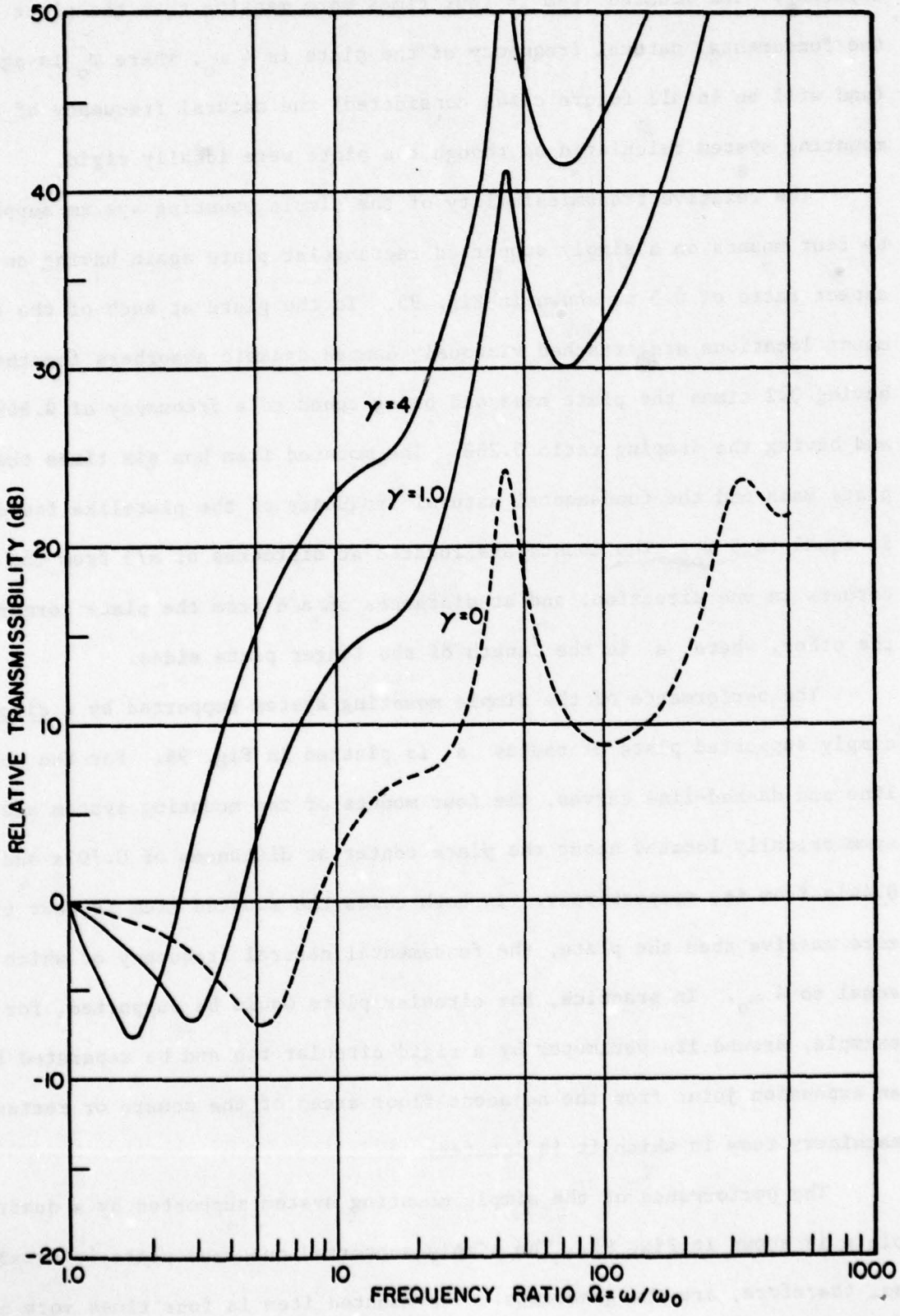
50
40
30
20
10
0
-10
-20
RELATIVE TRANSMISSIBILITY (dB)
γ=4
γ=1.0
γ=0
1.0
10
100
1000
FREQUENCY RATIO Ω=ω/ω₀

Fig. 94

($\gamma = 0$) is also shown. The advantage of heavy mass loading is clearly apparent. The mounted item is four times more massive than the plate and the fundamental natural frequency of the plate is 4 ω_o, where ω_o is again (and will be in all future cases considered) the natural frequency of the mounting system calculated as though the plate were ideally rigid.

The relative transmissibility of the simple mounting system supported by four mounts on a simply supported rectangular plate again having an aspect ratio of 0.5 is shown in Fig. 95. To the plate at each of the four mount locations are attached viscously damped dynamic absorbers together having 0.2 times the plate mass and being tuned to a frequency of 0.869 ω_o, and having the damping ratio 0.268. The mounted item has six times the plate mass and the fundamental natural frequency of the platelike foundation is equal to 5 ω_o. The mounts are located at distances of a/3 from the plate corners in one direction, and at distances of a/6 from the plate corners in the other, where a is the length of the longer plate sides.

The performance of the simple mounting system supported by a circular simply supported plate of radius a is plotted in Fig. 96. For the solid-line and dashed-line curves, the four mounts of the mounting system are symmetrically located about the plate center at distances of 0.707a and 0.441a from it, respectively. In both cases the mounted item is four times more massive than the plate, the fundamental natural frequency of which is equal to 4 ω_o. In practice, the circular plate would be supported, for example, around its perimeter by a rigid circular rib and be separated by an expansion joint from the adjacent floor areas of the square or rectangular machinery room in which it is located.

The performance of the simple mounting system supported by a quadrant plate is shown in Fig. 97. The simply supported quadrant plate is square and so, therefore, are the quadrants. The mounted item is four times more massive

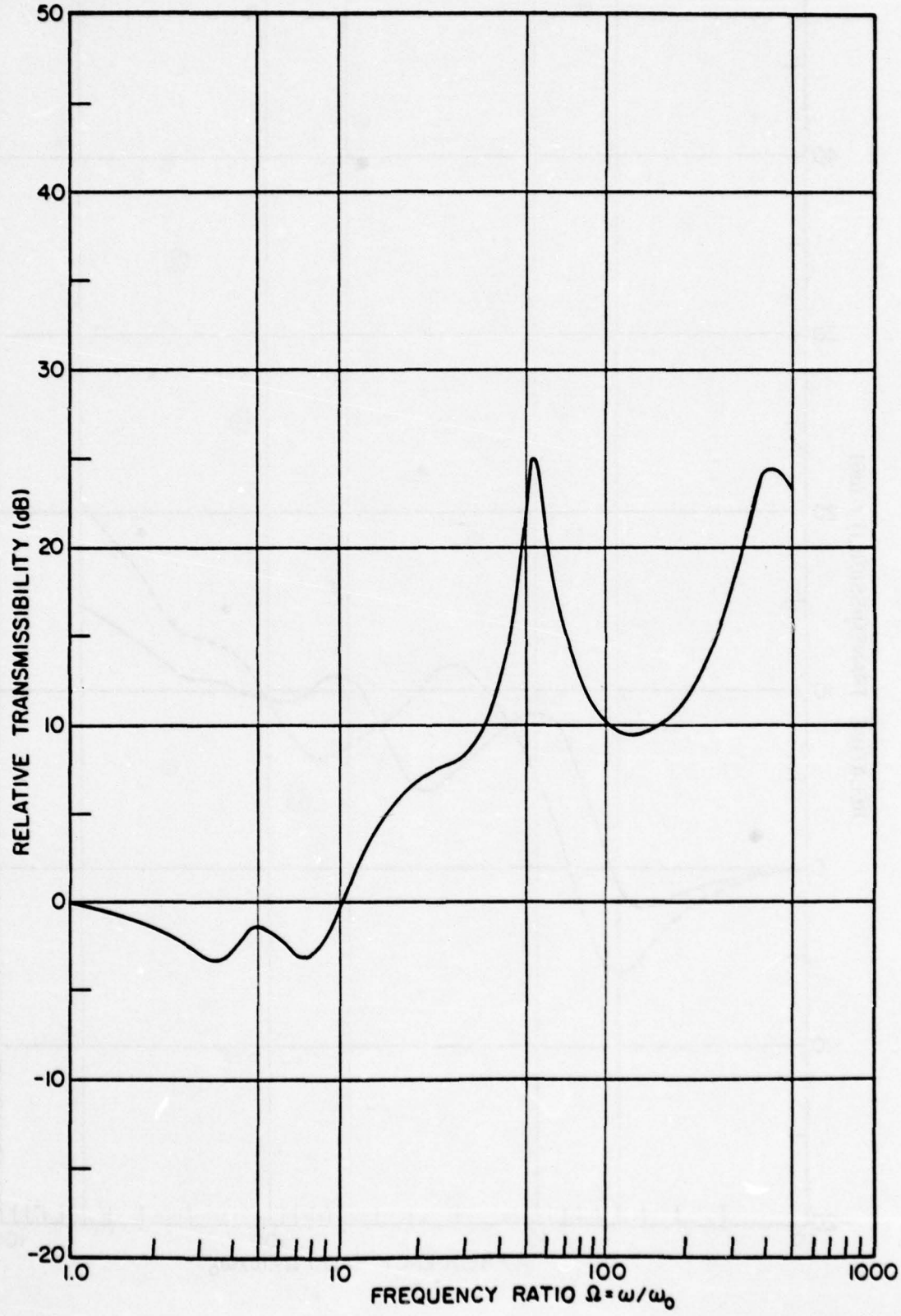
50
40
30
20
10
0
-10
-20
RELATIVE TRANSMISSIBILITY (dB)
1.0
10
100
1000
FREQUENCY RATIO Ω = ω/ω0

Fig. 95

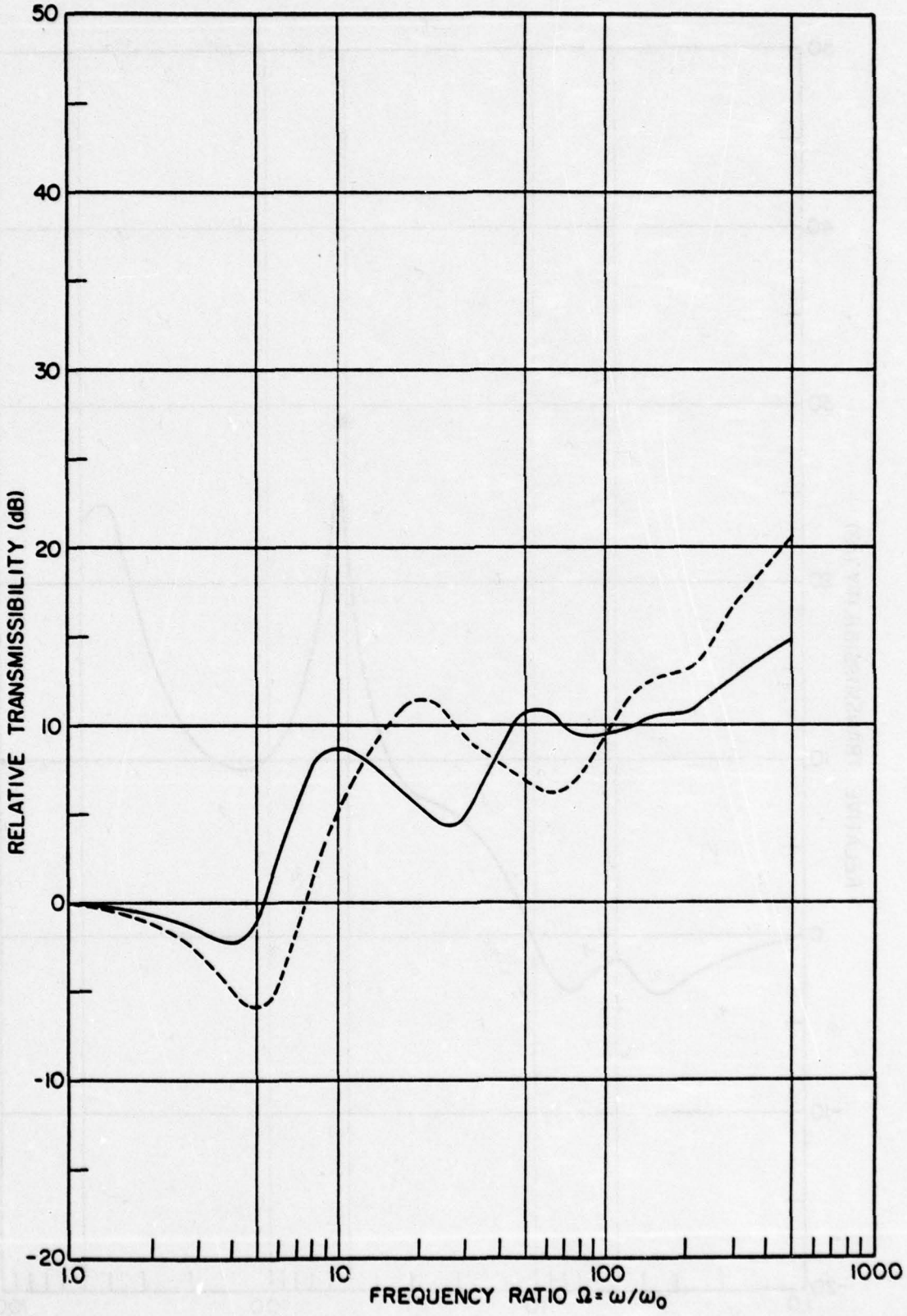
50
40
30
20
10
0
-10
-20
RELATIVE TRANSMISSIBILITY (dB)
1.0
10
100
1000
FREQUENCY RATIO Ω = ω/ω0

Fig. 96

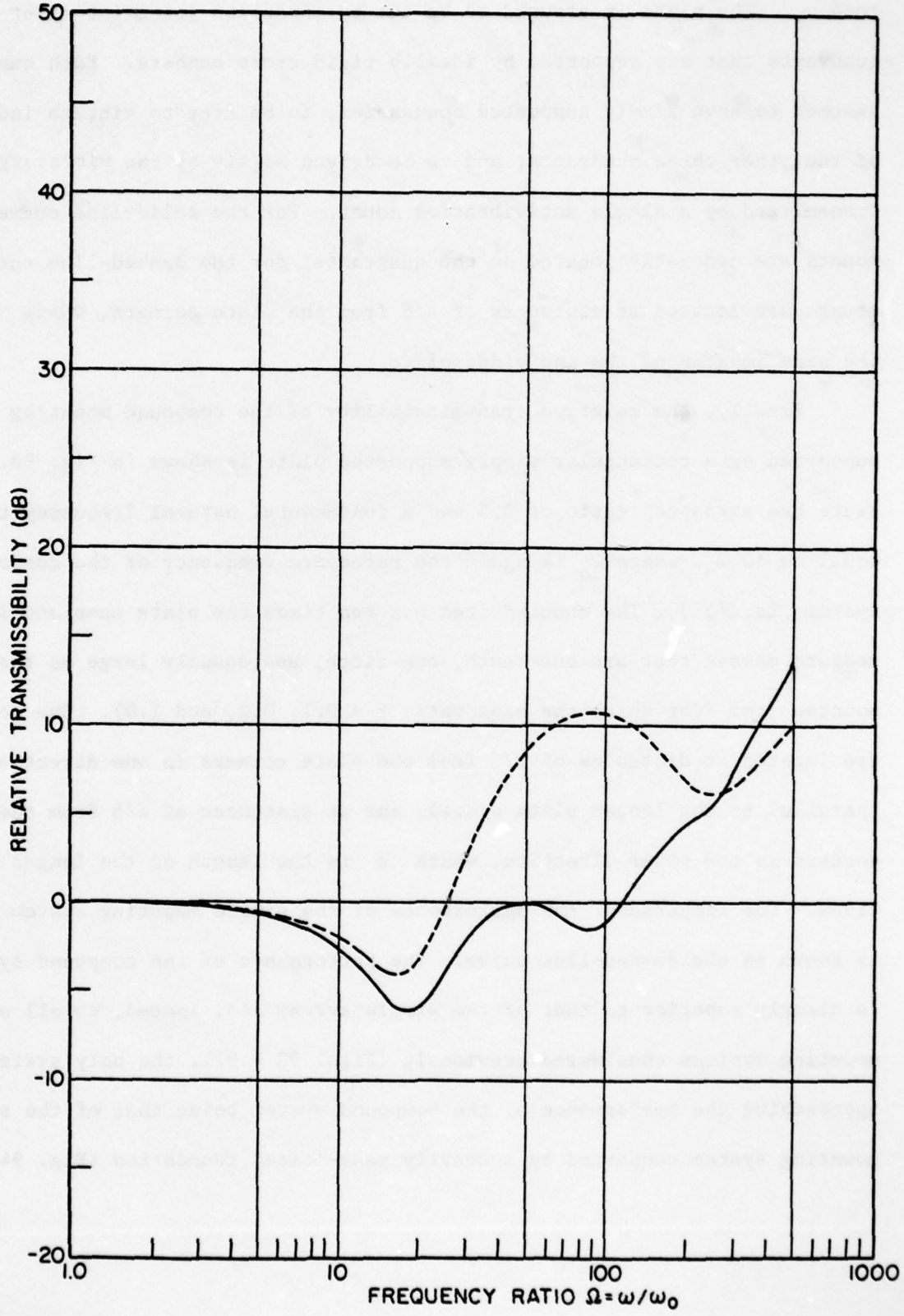
50
40
30
20
10
0
-10
-20
RELATIVE TRANSMISSIBILITY (dB)
1.0
10
100
1000
FREQUENCY RATIO Ω = ω/ω0

Fig. 97

than the undivided plate, the fundamental natural frequency of which is equal to 4 ω_o. The plate is assumed to be cut by expansion joints into four identical quadrants that are supported by ideally rigid cross members. Each quadrant is assumed to have simply supported boundaries, to be free to vibrate independently of the other three quadrants, and to be driven solely by the vibratory force transmitted by a single antivibration mount. For the solid-line curve, the mounts are centrally located on the quadrants; for the dashed-line curve, the mounts are located at distances of a/6 from the plate corners, where a is the side lengths of the undivided plate.

Finally, the relative transmissibility of the compound mounting system supported by a rectangular simply supported plate is shown in Fig. 98. The plate has an aspect ratio of 0.5 and a fundamental natural frequency that is equal to 10 ω_o, where ω_o is again the reference frequency of the compound system [Eq. (58)]. The mounted item has ten times the plate mass and intermediate masses that are one-tenth, one-fifth, and equally large as the mounted item (for which the mass ratio β = 0.1, 0.2, and 1.0). The mounts are located at distances of a/3 from the plate corners in one direction (parallel to the longer plate sides), and at distances of a/6 from the plate corners in the other direction, where a is the length of the longer plate sides. For comparison, the performance of the simple mounting system (β = 0) is shown as the dashed-line curve. The performance of the compound system is clearly superior to that of the simple system and, indeed, to all of the mounting systems considered previously (Figs. 93 - 97), the only system approaching the performance of the compound system being that of the simple mounting system supported by a heavily mass-loaded foundation (Fig. 94).

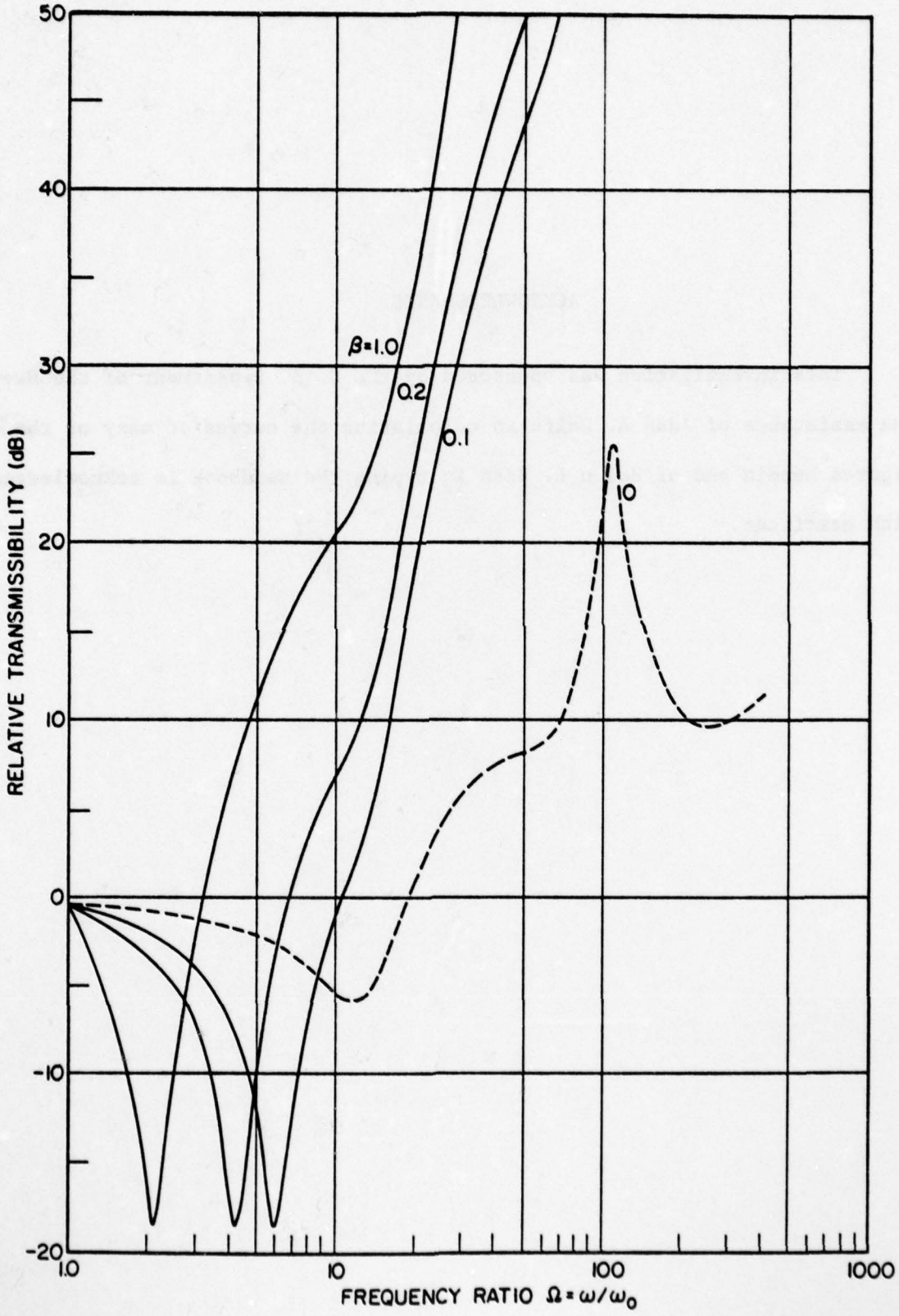
50
40
30
20
10
0
-10
-20
1.0
10
100
1000
RELATIVE TRANSMISSIBILITY (dB)
FREQUENCY RATIO Ω = ω/ω0
β=1.0
0.2
0.1
10

Fig. 98

ACKNOWLEDGMENTS

This investigation was sponsored by the U. S. Department of the Navy. The assistance of Adah A. Wolfe in calculating the curves of many of the figures herein and of Helen L. Bish in typing the handbook is acknowledged with gratitude.

REFERENCES

1. J. C. Snowdon, Vibration and Shock in Damped Mechanical Systems (John Wiley and Sons, Inc., New York, 1968).

2. W. E. Burton, Ed., Engineering with Rubber (McGraw-Hill Book Company, New York, 1949).

3. P. B. Lindley, Engineering Design with Natural Rubber (Natural Rubber Producers Research Association, London, 1970), 3rd. Ed.

4. Anon., Handbook of Molded and Extruded Rubber (The Goodyear Tire and Rubber Co., Akron, 1959), 2nd. Ed..

5. W. P. Fletcher and A. N. Gent, "Nonlinearity in the Dynamic Properties of Vulcanized Rubber Compounds," Rubber Chem. Technol. 27, 209-222 (1954).

6. A. O. Sykes, "Vibration Isolation when Machine and Foundation Are Resilient and Wave Effects Occur in the Mounts," David W. Taylor Model Basin Rept. No. 1404 (1960).

7. A. O. Sykes, "The Evaluation of Mounts Isolating Nonrigid Machines from Nonrigid Foundations," David W. Taylor Model Basin Rept. No. 1094 (1957).

8. A. O. Sykes, "The Effects of Machine and Foundation Resilience and of Wave Propagation on the Isolation Provided by Vibration Mounts," David W. Taylor Model Basin Rept. No. 1296 (1959).

9. E. E. Ungar and C. W. Dietrich, "High-Frequency Vibration Isolation," J. Sound Vib. 4, 224-241 (1966).

10. A. Sorensen, Jr., "A Discussion of the Vibration Characteristics of a Simple Mechanical Connection," J. Engr. Ind., Trans. ASME, Ser. B, 82, 415-422 (1960).

REFERENCES -- CONTINUED

11. E. E. Ungar, "Wave Effects in Viscoelastic Leaf and Compression Spring Mounts," J. Engr. Ind., Trans ASME, Ser. B, 85, 243-246 (1963).

12. A. Major, Vibration Analysis and Design of Foundations for Machines and Turbines (Collet's Holdings Ltd., London, 1962).

13. J. C. Snowdon, "Isolation and Absorption of Machinery Vibration," Acustica 28, 307-317 (1973).

14. J. C. Snowdon, "Dynamic Vibration Absorbers that have Increased Effectiveness," Journal of Engineering for Industry, Trans ASME, Series B, 96, 940-945 (1974).

15. J. C. Snowdon, "Mechanical Four-Pole Parameters and their Application," Journal of Sound and Vibration, 15, No. 3, 307-323 (1971).

16. J. C. Snowdon and M. A. Nobile, "Beamlike Dynamic Vibration Absorbers," Applied Research Laboratory, The Pennsylvania State University, Rept. to the Naval Sea Systems Command, Technical Memorandum TM 77-46, Feb. 17, 1977.

17. J. C. Snowdon, "Vibration of Simply Supported Square Plates to which Lumped Masses and Dynamic Vibration Absorbers are Attached," J. Acoust. Soc. Am. 57, 646-654 (1975).

18. J. C. Snowdon, "Compound Mounting Systems that Incorporate Dynamic Vibration Absorbers," Journal of Engineering for Industry, Trans. ASME, Series B, 97, 1204-1211 (1975).

19. M. A. Nobile and J. C. Snowdon, "Viscously Damped Absorbers of Conventional and Novel Design," J. Acoust. Soc. Am. 61, 1198-1208 (1977).

20. J. C. Snowdon, "Platelike Dynamic Vibration Absorbers," Journal of Engineering for Industry, Trans. ASME, Series B, 97, 88-93 (1975).

REFERENCES -- CONTINUED

21. R. M. Gorman, "Design and Advantages of a Two-Stage Mounting System for Major Machines in Ship's Engine Room," Shock. Vib. Bull. 35, Pt. 5, 227-234 (1966).

22. W. I. Young and R. J. Hanners, "Compound-Two-Stage Resilient Isolation Mounting for Use in Attenuating Mechanical Vibrations," U. S. Patent 3,764,100 (October 9, 1973).

23. R. T. McGoldrick, David W. Taylor Model Basin Rept. 1420 (1960).

24. L. Katz, David W. Taylor Model Basin Rept. 1480 (1961).

25. M. Harrison, A. O. Sykes, and M. Martin, "Wave Effects in Isolation Mounts," J. Acoust. Soc. Am. 24, 62-71 (1952).

26. E. H. Hull, "Influence of Damping in the Elastic Mounting of Vibrating Machines," J. Appl. Mech., Trans. ASME, Pt. II, 53, 155-165 (1931).

27. F. Schloss, "Recent Advances in Mechanical Impedance Instrumentation and Applications," David W. Taylor Model Basin Rept. 1960 (1965).

28. J. C. Snowdon, "How External Loads Alter the Natural Frequencies of Beams and Plates," Machine Design, 44, No. 7, 126-129 (1972).

29. W. P. Mason, Physical Acoustics and the Properties of Solids, (D. Van Nostrand Co., Inc., New York, 1958).

30. J. C. Snowdon, "Forced Vibration of Internally Damped Circular Plates with Supported and Free Boundaries," J. Acoust. Soc. Am. 47, 882-891 (1970).

31. J. C. Snowdon, "Forced Vibration of Internally Damped Circular and Annular Plates with Clamped Boundaries," J. Acoust. Soc. Am. 50, 846-858 (1971).

REFERENCES -- CONTINUED

32. J. C. Snowdon, "Forced Vibration of Internally Damped Rectangular and Square Plates with Simply Supported Boundaries," J. Acoust. Soc. Am. 56, 1177-1184 (1974).

33. J. C. Snowdon, Mechanical Four-Pole Parameters: Transmission Matrices, The Pennsylvania State University, Applied Research Laboratory, Rept. to the Naval Sea Systems Command, TM 76-122 (April, 1976).

34. F. Schloss, "New Methods for Determining the Loss Factors of Materials and Systems," David W. Taylor Model Basin Rept. 1702 (1963).

35. J. C. Snowdon, "Isolation of Machinery Vibration from Nonrigid Substructures Using Multiple Antivibration Mountings," contribution to Isolation of Mechanical Vibration Impact, and Noise, edited by J. C. Snowdon and E. E. Ungar (American Society of Mechanical Engineers, New York, September, 1973). Chapter 5, pp. 102-127.

36. J. C. Snowdon, "Resilient Mounting of Machinery on Platelike and Modified Platelike Substructures," J. Acoust. Soc. Am. 61, 986-994 (1977).

FIGURE LEGENDS

Fig. 1 Simple deformations of a rubberlike material.

Fig. 2 Dependence of the apparent modulus of elasticity E_a on the shape factor S for natural rubbers of various hardnesses (Ref. 3).

Fig. 3 Stress-strain curves of 40 durometer rubber in compression with various shape factors (Ref. 4).

Fig. 4 Equivalence between the damping factor δ employed in this handbook and other commonly employed measures of damping.

Fig. 5 Dependence of (a) the dynamic shear modulus $G_{\omega,\theta}$, and (b) the shear damping factor $\delta_{G\omega,\theta}$ of a rubberlike material on angular frequency ω and temperature θ (Ref. 1).

Fig. 6 Frequency dependence of (a) the dynamic shear modulus and (b) the shear damping factor possessed by unfilled natural rubber (Ref. 1).

Fig. 7 Frequency dependence of (a) the dynamic shear modulus and (b) the shear damping factor possessed by natural rubber filled with 50 parts by weight of HAF carbon black per 100 parts rubber (Ref. 1).

Fig. 8 Frequency dependence of (a) the dynamic shear modulus and (b) the shear damping factor possessed by an unfilled SBR rubber (75/25 butadiene styrene) (Ref. 1).

Fig. 9 Frequency dependence of (a) the dynamic shear modulus and (b) the shear damping factor possessed by unfilled Thiokol RD rubber (Ref. 1).

Fig. 10 Frequency dependence of (a) the dynamic shear modulus and (b) the shear damping factor possessed by unfilled plasticized polyvinyl acetate (Ref. 1).

FIGURE LEGENDS -- CONTINUED

Fig. 11 Frequency dependence of (a) the dynamic shear modulus and (b) the shear damping factor possessed by butyl rubber filled with 40 parts by weight of MPC carbon black per 100 parts rubber (Ref. 1).

Fig. 12 Dependence on vibration amplitude (% shear) of the dynamic shear modulus of natural rubber filled by various parts by volume of MPC carbon black per 100 volumes of rubber (Ref. 5).

Fig. 13 Dependence on vibration amplitude (% shear) of the shear modulus damping factor of natural rubber filled with various parts by volume of MPC carbon black per 100 volumes of rubber (Ref. 5).

Fig. 14 Simple mounting system with an antivibration mount of rubberlike material.

Fig. 15 Transmissibility of antivibration mounts of natural rubber, natural rubber filled with carbon black, and Thiokol RD rubber at 20°C; natural mounting frequency = 5 Hz.

Fig. 16 Natural frequency of a simple mounting system versus the static deflection of its antivibration mount.

Fig. 17 Frequency dependence of (a) the dynamic shear modulus and (b) the shear damping factor possessed by a parallel combination of natural and Thiokol RD rubbers (Ref. 1).

Fig. 18 Transmissibility of a simple mounting of natural rubber filled with 40 parts by weight of EPC channel black at 19°C. The dashed-line curve has been calculated from Eq. (13) assuming that G_ω and δ_{G_ω} are frequency independent quantities (Ref. 1).

Fig. 19 Transmissibility of simple mountings that incorporate (a) a helical spring (solid-line curve), (b) a natural-rubber cylinder (chain-line curve), and (c) a commercial shear mount (dashed-line curve). (Ref. 6).

FIGURE LEGENDS -- CONTINUED

Fig. 20 Transmissibility of a simple mounting with wave effects calculated from the "long-rod" theory. Damping factor $\delta_E = 0.1$, mass ratio $\gamma = 50$, 100, and 250; natural mounting frequency = 5 Hz (Ref. 1).

Fig. 21 Transmissibility calculated from the Love theory of rod vibration for simple mountings of unfilled natural rubber, natural rubber filled with 50 parts by weight of HAF carbon black, and Thiokol RD rubber. Cylindrical mounts have a length-to-diameter ratio of 5; mass ratio $\gamma = 200$; natural mounting frequency = 5 Hz (Ref. 1).

Fig. 22 Simple mounting system with an ideally rigid mounted item supported via nonrigid (multiresonant) feet.

Fig. 23 Simple mounting system with essentially the situation pictured in Fig. 22 (Ref. 12).

Fig. 24 Transmissibility of the simple mounting system of Fig. 22 with shear-beam resonances in feet of the mounted item. Mass ratio $\gamma_F = 40$; stiffness ratio $\Gamma = K_F/K = 5$, 25, and 100; damping factors $\delta_K = 0.05$ and $\delta_F = 0.01$ (Ref. 13).

Fig. 25 Vibrating item to which is attached a dynamic vibration absorber with damping of the viscous type.

Fig. 26 Dynamic vibration absorbers attached (a) to the end, (b) to the mid-point, and (c) to both the end and the midpoint of a cantilever beam driven at its free end by a sinusoidally varying force.

Fig. 27 Values of the optimum tuning ratio for the dynamic absorber of Fig. 26(a) when tuned to the first or second beam resonance (Ref. 1).

Fig. 28 Values of the optimum damping ratio for the dynamic absorber of Fig. 26(a) when tuned to the first or second beam resonance (Ref. 1).

FIGURE LEGENDS -- CONTINUED

Fig. 29 Values of the optimum tuning ratio for the dynamic absorber of Fig. 26(b) when tuned to the first or second beam resonance (Ref. 1).

Fig. 30 Values of the optimum damping ratio for the dynamic absorber of Fig. 26(b) when tuned to the first or second beam resonance (Ref. 1).

Fig. 31 Maximum values of transmissibility at the first and second resonances of the beam of Fig. 26(a) (Ref. 1).

Fig. 32 Maximum values of transmissibility at the first and second resonances of the beam of Fig. 26(b) (Ref. 1).

Fig. 33 Transmissibility of the dynamic absorber with damping of the viscous type. Optimum absorber tuning and damping for values of the mass ratio μ = 10/11, 5/6, and 1/2 (M_2/M_1 = 0.1, 0.2 and 1.0) (Ref. 1).

Fig. 34 Transmissibility across the beam of Fig. 26(a); mass ratio γ_a = 0.25; tuning ratio (ω_a/ω_m) = 0.551; damping ratio = 0.460 (Ref. 1).

Fig. 35 Transmissibility across a centrally driven circular plate that is clamped around its boundary and which carries a dynamic absorber attached to its midpoint. Mass ratio γ_a = 0.1 and 0.25 for the solid-line and chain-line curves, respectively, and γ_a = 0 for the dashed-line curve (Ref. 15).

Fig. 36 Transmissibility across a simply supported square plate with a central driving force and a central dynamic absorber. For the solid-line curve, γ_a = 0.05; for the chain-line curve γ_a = 0.25; for the dashed-line curve γ_a = 0. Plate damping factors $\delta_E = \delta_G$ = 0.01 (Ref. 17).

Fig. 37 Single cantilever absorber attached to an end-driven stanchion.

Fig. 38 Transmissibility across the stanchion of Fig. 37 when the mass ratio γ_1 = 0.2 (Ref. 16).

FIGURE LEGENDS -- CONTINUED

Fig. 39 Transmissibility across the primary system of Fig. 25 to which a dynamic absorber with damping of the solid type is attached ($\delta_G = 0.01$); the primary system has damping of the viscous type for which $\delta_R = 0.5$; the tuning ratio n is successively equal to 2/3, 1.0, and 3/2 (Ref. 1).

Fig. 40 Transmissibility across the primary system of Fig. 25 to which is attached a dynamic absorber with negligible damping ($\delta_R = 0.01$) that is tuned off resonance with a tuning ratio successively equal to 0.2, 0.5, 2.0, and 5.0; mass ratio $\mu = 5/6$ ($M_2 = M_1/5$).

Fig. 41 Transmissibility across a simply supported rectangular plate with an aspect ratio of 3 that is centrally driven and loaded by a dynamic absorber having one-tenth of the plate mass; the absorber is tuned to 0.2 of the fundamental resonant frequency of the plate; the quantity u is the length of the longer plate sides.

Fig. 42 Transmissibility across a clamped circular plate that is centrally driven and loaded by a dynamic absorber having one-tenth of the plate mass and that is tuned to 0.2 of the fundamental natural frequency of the plate.

Fig. 43 Transmissibility across a simply supported square plate that is centrally driven and loaded by a dynamic absorber having one-tenth of the plate mass and that is tuned to 3.0 times the fundamental natural frequency of the plate; the quantity u is the common length of the plate sides.

Fig. 44 Simple mass-spring systems with a platelike dynamic absorber.

Fig. 45 Section through (a) a platelike dynamic absorber held centrally, and (b) an annular platelike absorber held around its inner perimeter.

FIGURE LEGENDS -- CONTINUED

Fig. 46 Values of the optimum damping factor and of the square of the optimum tuning ratio for the platelike absorber utilized as in Fig. 44 (Ref. 20).

Fig. 47 Transmissibility across the mass-spring systems of Fig. 44 with the platelike absorbers tuned and damped as specified in Fig. 46. Absorber mass ratios μ = 50/51, 10/11, and 2/3 (M_2/M_1 = 1/50, 1/10, and 1/2).

Fig. 48 Compound mounting system with an ideally rigid machine mass M_1 and an intermediate mass M_2 that is supported (a) directly and (b) via non-rigid (multiresonant) flanges or feet (Ref. 13).

Fig. 49 Transmissibility of the compound mounting system employing natural-rubber mounts. Mass ratio $\beta = M_2/M_1$ = 0, 0.1, 0.2, and 1.0 (Ref. 1).

Fig. 50 Compound mounting of 17,000 lb and 80,000 lb diesel generators on one extensive intermediate mass (Ref. 21).

Fig. 51 Small-scale compound mounting with an intermediate mass M_2 comprising two cylindrical masses 10 and a spacer yoke 12 (resilient elements comprise 16) (Ref. 22).

Fig. 52 Transmissibility across the compound system of Fig. 48(a) (solid-line curve) and Fig. 48(b) (chain-line curve). Mass ratios $\beta = M_2/M_1$ = 0.2 and $\gamma_F = M_2/2M_F$ = 40; stiffness ratio Γ = 5; damping factors δ_K = 0.05 and δ_F = 0.01. Transmissibility of the simple mounting system (β = 0) shown by the dashed-line curve; damping factors δ_K = 0.05 (Ref. 13).

Fig. 53 Compound mounting system with a machine mass M_1 and an intermediate mass M_2 plus a dynamic vibration absorber of mass M_a (Ref. 18).

Fig. 54 Transmissibility across the compound mounting system of Fig. 53. Mass ratios β = 0.1, 0.2, and 1.0, and μ = 5/6 ($M_a = M_2/5$). Damping

FIGURE LEGENDS -- CONTINUED

factor $\delta_K = 0.05$. Absorber damping ratio $\delta_R = 0.25$, and tuning parameter $\varepsilon = 0.76$. For the chain-line curve, $\mu = 25/26$ ($M_a = M_2/25$), $\beta = 1.0$, $\delta_R = 0.12$, and $\varepsilon = 0.90$ (Ref. 18).

Fig. 55 Transmissibility across a compound mounting system supported by a simply supported rectangular plate with an aspect ratio of 0.5. Primary mass is four times more massive than the plate; fundamental natural frequency of plate is four times the reference frequency of the compound system. Mounts are located symmetrically about the plate center at distances of 1/3 of the lengths of the plate sides from each plate corner. The mass ratio $\beta = M_2/M_1 = 1.0$, 0.2, 0.1, and 0 (simple mounting system); mount damping factors $\delta_K = 0.05$; plate damping factors $\delta_E = \delta_G = 0.01$.

Fig. 56 (a) apparatus and (b) electronic equipment used in a direct measurement of mount transmissibility (Ref. 25).

Fig. 57 Apparatus for the indirect measurement of mount transmissibility by a four-pole technique (Ref. 27).

Fig. 58 Values of the dimensionless parameter N_R for the first three natural frequencies of a cantilever beam that is mass loaded at its free end (Ref. 28).

Fig. 59 Values of the dimensionless parameter N_R for the first three natural frequencies of a simply supported beam that is centrally mass loaded (Ref. 28).

Fig. 60 Values of the dimensionless parameter N_R for the first three natural frequencies of a clamped-clamped beam that is centrally mass loaded (Ref. 28).

AD-A071 485 PENNSYLVANIA STATE UNIV UNIVERSITY PARK APPLIED RESE--ETC F/G 20/11
HANDBOOK OF VIBRATION AND NOISE CONTROL.(U)
APR 79 J C SNOWDON N00024-79-C-6043
UNCLASSIFIED ARL/PSU/TM-79-75 NL

3 OF 3
AD
A071485

END
DATE
FILMED
8-79
DDC

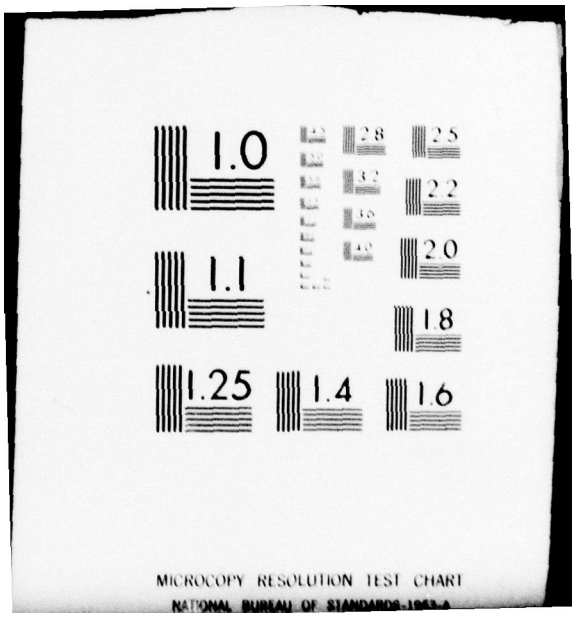
1.0
1.1
1.25
1.4
1.6
2.8
2.5
2.2
2.0
1.8
MICROCOPY RESOLUTION TEST CHART
NATIONAL BUREAU OF STANDARDS-1963-A

FIGURE LEGENDS -- CONTINUED

Fig. 61 Values of the dimensionless parameter N_R for the first three natural frequencies of a simply supported circular plate that is centrally mass loaded (Ref. 28).

Fig. 62 Values of the dimensionless parameter N_R for the first three natural frequencies of a clamped circular plate that is centrally mass loaded (Ref. 28).

Fig. 63 Values of the dimensionless parameter N_R for the first four natural frequencies of a clamped annular plate of radius a; the central concentric circular aperture has the radius μa.

Fig. 64 Values of the dimensionless parameter N_R for the first three natural frequencies of a clamped annular plate with its central aperture filled by a mass of radius 0.1a, where a is the plate radius.

Fig. 65 Values of the dimensionless parameter N_R for the first three natural frequencies of a clamped annular plate with its central aperture filled by a mass of radius 0.2a, where a is the plate radius.

Fig. 66 Values of the dimensionless parameter N_R for the first three natural frequencies of a clamped annular plate with its central aperture filled by a mass of radius 0.3a, where a is the plate radius.

Fig. 67 Values of the dimensionless parameter N_R for the first three natural frequencies of a clamped annular plate with its central aperture filled by a mass of radius 0.4a, where a is the plate radius.

Fig. 68 Values of the dimensionless parameter N_R for the first three natural frequencies of a clamped circular plate loaded by a concentric annular rib of radius 0.2a, where a is the plate radius.

FIGURE LEGENDS -- CONTINUED

Fig. 69 Values of the dimensionless parameter N_R for the first three natural frequencies of a clamped circular plate loaded by a concentric annular rib of radius 0.4a, where a is the plate radius.

Fig. 70 Values of the dimensionless parameter N_R for the first three natural frequencies of a clamped circular plate loaded by a concentric annular rib of radius 0.6a, where a is the plate radius.

Fig. 71 Values of the dimensionless parameter N_R for the first three natural frequencies of a clamped circular plate loaded by a concentric annular rib of radius 0.8a, where a is the plate radius.

Fig. 72 Values of the dimensionless parameter N_R for the first natural frequency of a simply supported circular plate of radius a driven and mass loaded at an arbitrary point distant 0.2a, 0.4a, 0.6a, and 0.8a from the plate center.

Fig. 73 Values of the dimensionless parameter N_R for the second natural frequency of a simply supported circular plate of radius a driven and mass loaded at an arbitrary point distant 0.2a, 0.4a, 0.6a, and 0.8a from the plate center.

Fig. 74 Values of the dimensionless parameter N_R for the third natural frequency of a simply supported circular plate of radius a driven and mass loaded at an arbitrary point distant 0.2a, 0.4a, 0.6a, and 0.8a from the plate center.

Fig. 75 Values of the dimensionless parameter N_R for the first three natural frequencies of a cantilever beam of length ℓ loaded at a distance $\mu\ell$ from its free end by a concentrated mass having a finite moment of inertia for which the parameter σ = 0, 0.05, 0.1, 0.25, and 0.5.

FIGURE LEGENDS -- CONTINUED

Fig. 76 Values of the dimensionless parameter N_R for the first three natural frequencies of a cantilever beam of length ℓ loaded at a distance $\mu\ell$ from its free end by a concentrated mass having a finite moment of inertia for which the parameter σ = 0, 0.05, 0.1, 0.25, and 0.5.

Fig. 77 Values of the dimensionless parameter N_R for the first natural frequency of a simply supported square plate of side length a driven and mass loaded at arbitrary points having the coordinates (a/2, a/8), (a/2, a/4), (a/2, 3a/8) as measured from one plate corner.

Fig. 78 Values of the dimensionless parameter N_R for the first natural frequency of a simply supported square plate of side length a driven and mass loaded at arbitrary points having the coordinates (a/5, a/5), (a/4, a/4), (a/3, a/3), (a/2, a/2) as measured from one plate corner.

Fig. 79 Values of the dimensionless parameter N_R for the second natural frequency of a simply supported square plate of side length a driven and mass loaded at arbitrary points having the coordinates (a/2, a/8), (a/2, a/4), (a/2, 3a/8) as measured from one plate corner.

Fig. 80 Values of the dimensionless parameter N_R for the second natural frequency of a simply supported square plate of side length a driven and mass loaded at arbitrary points having the coordinates (a/5, a/5), (a/4, a/4), (a/3, a/3), (a/2, a/2) as measured from one plate corner.

Fig. 81 Values of the dimensionless parameter N_R for the third natural frequency of a simply supported square plate of side length a driven and mass loaded at arbitrary points having the coordinates (a/2, a/8), (a/2, a/4), (a/2, 3a/8) as measured from one plate corner.

Fig. 82 Values of the dimensionless parameter N_R for the third natural frequency of a simply supported square plate of side length a driven

FIGURE LEGENDS -- CONTINUED

and mass loaded at arbitrary points having the coordinates (a/5, a/5), (a/4, a/4), (a/3, a/3), (a/2, a/2) as measured from one plate corner.

Fig. 83 (a) General four-terminal mechanical system, and (b) system reversed so that its input and output terminal pairs are interchanged.

Fig. 84 (a) Lumped mass obeying Newton's second law, and (b) a massless spring obeying Hooke's law.

Fig. 85 Series connection of n four-terminal systems.

Fig. 86 Antivibration mount with end plates of masses M_1 and M_2 to which the boundaries of a uniform rodlike sample of rubberlike material are attached.

Fig. 87 (a) Antivibration mount of Fig. 86 isolating the vibration of a mounted item of mass M from a nonrigid substructure of arbitrary impedance Z_T, and (b) the rigid attachment of M to the substructure at the same location as in (a).

Fig. 88 $T_{overall}$ for an item of mass M that is resiliently mounted near each corner of a rectangular platelike substructure with simply supported boundaries and with an aspect ratio of 0.5; M is four times more massive than the plate. The antivibration mounts are symmetrically and favorably located about the plate center, and are terminated on the plate by lumped masses of total mass m = M. The damping factors of the mounts and the platelike substructure are 0.05 and 0.01, respectively. The dashed-line curve shows $T_{overall}$ for the same mounting system without the loading masses (m = 0) (Ref. 36).

Fig. 89 Relative transmissibility of a simple mounting system in which the mounted item is supported by eight mounts along the length of a

FIGURE LEGENDS -- CONTINUED

clamped-clamped beam of length L with the mounts located at distances of 0.125L, 0.375L, 0.625L, and 0.875L from each bean termination. The mounted item has ten times the beam mass and the fundamental natural frequency of the beam occurs at ten times the natural frequency (10 ω_o) of the mounting system; mount and beam damping factors $\delta_K = 0.05$ and $\delta_E = 1.0$.

Fig. 90 Relative transmissibility of a simple mounting system in which the mounted item is supported by four mounts along the length of a clamped-clamped beam of length L with the mounts located at distances of 0.25L and 0.75L from each beam termination. Beneath each mount is a lumped mass loading the beam; the total added mass is 2.5 times the beam mass. The mounted item has ten times the beam mass, and the fundamental natural frequency of the beam is equal to 10 ω_o; the mount and beam damping factors $\delta_K = 0.05$ and $\delta_E = 1.0$.

Fig. 91 Relative transmissibility of a simple mounting system in which the mounted item is supported by four mounts along the length of a clamped-clamped beam of length L with the mounts located at distances of 0.25L and 0.75L from each beam termination. Beneath the beam at each mount location, dynamic vibration absorbers are positioned; together the absorbers have 0.25 times the beam mass whereas the mounted item is ten times more massive than the beam; the fundamental natural frequency of the beam is 10 ω_o. The mount and beam damping factors $\delta_K = 0.05$ and $\delta_E = 1.0$.

Fig. 92 Relative transmissibility of the compound mounting system in which the intermediate mass is supported by four mounts along the length of a clamped-clamped beam of length L; the mounts are located at distances of 0.25L and 0.75L from each beam termination. The mounted item has

FIGURE LEGENDS -- CONTINUED

ten times the beam mass; the fundamental natural frequency of the beam is equal to ten times the reference frequency of the compound system. Mass ratio β = 1.0, 0.2, 0.1, and 0 (simple mounting system). Mount and beam damping factors δ_K = 0.05 and δ_E = 1.0.

Fig. 93 Relative transmissibility of a simple mounting system supported by eight or by four mounts on a simply supported square plate of side length a. The mounted item is four times more massive than the plate and the fundamental natural frequency of the plate is four times greater (4 ω_o) than the natural frequency of the mounting system. For the solid-line curve, eight mounts are located at distances of 0.2a, a/3 and 0.4a, a/3 from each plate corner; for the dashed-line curve four mounts are located at distances of 0.25a from each plate corner. Mount and plate damping factors δ_K = 0.05 and $\delta_E = \delta_G$ = 1.0.

Fig. 94 Relative transmissibility of a simple mounting system supported by four mounts on a simply supported rectangular plate with an aspect ratio of two. Mounted item is four times more massive than the plate; fundamental natural frequency of the plate is equal to 4 ω_o. Mounts are located at distances of a/3 and a/6 from each plate corner, where a is the length of the longer plate sides. Beneath each mount is located a lumped mass that is a factor of γ times greater than the plate mass. Mount and plate damping factors δ_K = 0.05 and $\delta_E = \delta_G$ = 1.0.

Fig. 95 Relative transmissibility of a simple mounting system supported by four mounts on a simply supported rectangular plate with an aspect ratio of two. Mounted item is six times more massive than the plate; fundamental natural frequency of the plate is equal to 5 ω_o. Mounts

FIGURE LEGENDS -- CONTINUED

are located at distances of a/3 and a/6 from each plate corner, where a is the length of the longer plate sides. Beneath the plate at the mount locations are positioned four dynamic vibration absorbers, the total mass of which is one-fifth of the plate mass. Mount and plate damping factors $\delta_K = 0.05$ and $\delta_E = \delta_G = 1.0$.

Fig. 96 Simple mounting system supported by four mounts on a simply supported circular plate of radius a. The mounts are symmetrically located about the plate center at distances of 0.707a and 0.441a from the plate center (solid-line and dashed-line curves, respectively). The mounted item is four times more massive than the plate and the fundamental natural frequency of the plate is equal to $4\ \omega_o$. Mount and plate damping factors $\delta_K = 0.05$ and $\delta_E = \delta_G = 1.0$.

Fig. 97 Relative transmissibility of a simple mounting system supported by four mounts on a simply supported square plate that has been divided by rigid cross members into four identical quadrants that are free to vibrate independently of one another; each quadrant supports an antivibration mount. The mounted item is four times more massive than the undivided plate; the fundamental natural frequency of the undivided plate is equal to $4\ \omega_o$. The mounts are located at distances of a/2 from the plate corners (solid-line curve) or at distances of a/3 from the plate corners (dashed-line curve), where a is the length of the undivided plate sides. Mount and plate damping factors $\delta_K = 0.05$ and $\delta_E = \delta_G = 1.0$.

Fig. 98 Relative transmissibility of the compound mounting system, the intermediate mass of which is supported by four mounts on a simply supported rectangular plate with an aspect ratio of two. The primary mass of the compound system is ten times more massive than the plate; the

FIGURE LEGENDS -- CONTINUED

fundamental natural frequency of the plate is ten times greater than the reference frequency of the compound system. Mass ratio β = 1.0, 0.2, 0.1, and 0 (simple mounting system). Mount and plate damping factors δ_K = 0.05 and $\delta_E = \delta_G$ = 1.0.

DISTRIBUTION LIST FOR UNCLASSIFIED TM 79-75

Commander
Naval Sea Systems Command
Department of the Navy
Washington, DC 20362
Attn: SEA 924N
(Copy No. 1)

Commander
Naval Sea Systems Command
Department of the Navy
Washington, DC 20362
Attn: PMS-393
(Copy No. 2)

Commander
Naval Sea Systems Command
Department of the Navy
Washington, DC 20362
Attn: PMS-395
(Copy No. 3)

Commander
Naval Sea Systems Command
Department of the Navy
Washington, DC 20362
Attn: PMS-396
(Copy No. 4)

Commander
Naval Sea Systems Command
Department of the Navy
Washington, DC 20362
Attn: Mr. Stephen M. Blazek
SEA 05H
(Copy Nos. 5, 6, 7, 8)

Commander
Naval Sea Systems Command
Department of the Navy
Washington, DC 20362
Attn: Mr. Stephen G. Wieczorek
SEA 05H
(Copy Nos. 9 and 10)

Commander
Naval Sea Systems Command
Department of the Navy
Washington, DC 20362
Attn: Mr. C. C. Taylor
SEA 05H
(Copy Nos. 11 and 12)

Commander
Naval Ship Engineering Center
Center Building
Prince George's Center
Hyattsville, MD 20782
Attn: NAVSEC 6103E
(Copy Nos. 13 and 14)

Commander
Naval Ship Engineering Center
Center Building
Prince George's Center
Hyattsville, MD 20782
Attn: NAVSEC 6105C
(Copy Nos. 15 and 16)

Commander
Naval Ship Engineering Center
Center Building
Prince George's Center
Hyattsville, MD 20782
Attn: Mr. Kenneth G. Hartman
NAVSEC 6105N
(Copy Nos. 17, 18, 19, 20, 21, 22)

Commander
Naval Ship Engineering Center
Center Building
Prince George's Center
Hyattsville, MD 20782
Attn: NAVSEC 6111B
(Copy Nos. 23 and 24)

Commander
Naval Ship Engineering Center
Center Building
Prince George's Center
Hyattsville, MD 20782
Attn: NAVSEC 6111D
(Copy Nos. 25 and 26)

Commander
Naval Ship Engineering Center
Center Building
Prince George's Center
Hyattsville, MD 20782
Attn: NAVSEC 6113C
(Copy Nos. 27 and 28)

Commander
Naval Ship Engineering Center
Center Building
Prince George's Center
Hyattsville, MD 20782
Attn: NAVSEC 6113D
(Copy Nos. 29 and 30)

Commander
Naval Ship Engineering Center
Center Building
Prince George's Center
Hyattsville, MD 20782
Attn: NAVSEC 6120
(Copy Nos. 31 and 32)

Commander
Naval Ship Engineering Center
Center Building
Prince George's Center
Hyattsville, MD 20782
Attn: NAVSEC 6129
(Copy Nos. 33 and 34)

Naval Ship Research and Development Center
Annapolis Division
Annapolis, MD 21402
Attn: Mr. J. Smith
(Copy No. 35)

Naval Ship Research and Development Center
Annapolis Division
Annapolis, MD 21402
Attn: Mr. L. J. Argiro
(Copy Nos. 36, 37, 38, 39, 40, 41)

Naval Ship Research and Development Center
Bethesda, MD 20084
Attn: Dr. M. Sevik
Code 19
(Copy Nos. 42 and 43)

Naval Ship Research and Development Center
Bethesda, MD 20084
Attn: Dr. W. W. Murray
Code 17
(Copy Nos. 44 and 45)

Naval Ship Research and Development Center
Bethesda, MD 20084
Attn: Dr. M. Strasberg
Code 1901
(Copy No. 46)

Naval Ship Research and Development Center
Bethesda, MD 20084
Attn: Dr. G. Maidanik
Code 1902
(Copy No. 47)

Naval Ship Research and Development Center
Bethesda, MD 20084
Attn: Dr. G. Chertock
Code 1903
(Copy No. 48)

Naval Ship Research and Development Center
Bethesda, MD 20084
Attn: Dr. D. Feit
Code 196
(Copy Nos. 49, 50, 51, 52, 53, 54)

Naval Ship Research and Development Center
Bethesda, MD 20084
Attn: Dr. J. T. Shen
Code 1942
(Copy No. 55)

Director
Defense Documentation Center
Cameron Station
Alexandria, VA 22314
(Copy Nos. 56, 57, 58, 59, 60, 61, 62, 63, 64, 65, 66, 67)

Director
Naval Research Laboratory
Washington, DC 20390
Attn: Code 8440
(Copy Nos. 68 and 69)

Ocean Structures Branch
U. S. Naval Research Laboratory
Washington, DC 20390
Attn: Mr. G. J. O'Hara
(Copy No. 70)

Office of Naval Research
Department of the Navy
Arlington, VA 22217
Attn: Dr. G. Boyer
Code 222
(Copy Nos. 71, 72, 73)

Office of Naval Research
Department of the Navy
Arlington, VA 22217
Attn: Dr. A. O. Sykes
Code 222
(Copy Nos. 74, 75, 76)

Office of Naval Research
Department of the Navy
Arlington, VA 22217
Attn: Mr. Keith M. Ellingsworth
Code 473
(Copy No. 77)

Office of Naval Research
Department of the Navy
Arlington, VA 22217
Attn: Dr. N. Perrone
Code 474
(Copy No. 78)

Commander
Mare Island Naval Shipyard
Vallejo, CA 94592
(Design Division)
(Copy No. 79)

Commander
Portsmouth Naval Shipyard
Portsmouth, NH 03801
(Copy No. 80)

Supervisor of Shipbuilding,
Conversion and Repair
General Dynamics Corporation
Electric Boat Division
Groton, CT 06340
Attn: Mr. John Wilder
Dept. 440
(Copy Nos. 81 and 82)

Supervisor of Shipbuilding,
Conversion and Repair
Ingalls Shipbuilding Corporation
Pascagoula, MS 39567
(Copy No. 83)

Supervisor of Shipbuilding,
Conversion and Repair
Newport News Shipbuilding and Drydock Company
Newport News, VA 23607
(Copy No. 84)

Naval Ship Research and
Development Center
Underwater Explosion Research
Division
Code 780
Portsmouth, VA 23709
(Copy No. 85)

Naval Underwater Systems Center
New London Laboratory
New London, CT 06320
Attn: Mr. G. F. Carey
(Copy No. 86)

Naval Underwater Systems Center
New London Laboratory
New London, CT 06320
Attn: Dr. R. S. Woollett
(Copy No. 87)

Naval Undersea Warfare Center
San Diego, CA 92152
Attn: Mr. G. Coleman
(Copy No. 88)

Dr. J. Barger
Bolt Beranek and Newman, Inc.
50 Moulton Street
Cambridge, MA 02138
(Copy No. 89)

Dr. D. I. G. Jones
Air Force Materials Laboratory
Wright-Patterson Air Force Base
Ohio 45433
(Copy No. 90)

Dr. M. C. Junger, President
Cambridge Acoustical Associates, Inc.
1033 Massachusetts Avenue
Cambridge, MA 02138
(Copy No. 91)

Acquisitions Supervisor
Technical Information Service
American Institute of Aeronautics
and Astronautics, Inc.
750 Third Avenue
New York, NY 10017
(Copy No. 92)

Dr. R. S. Ayre
Department of Civil Engineering
University of Colorado
Boulder, CO 80302
(Copy No. 93)

Dr. D. Frederick
Chairman, Engineering Science and Mechanics Department
Virginia Polytechnic Institute and State University
Blacksburg, VA 24061
(Copy No. 94)

Dr. D. E. Hudson
Department of Mechanics
California Institute of Technology
Pasadena, CA 91109
(Copy No. 95)

Dr. G. Herrmann, Chairman
Department of Applied Mechanics
Stanford University
Stanford, CA 94305
(Copy No. 96)

Dr. A. Kalnins
Department of Mechanical Engineering and Mechanics
Leheigh University
Bethlehem, PA 18015
(Copy No. 97)

Dr. D. D. Kana
Southwest Research Institute
8500 Culebra Road
San Antonio, TX 78206
(Copy No. 98)

Dr. Y. -H. Pao, Chairman
Department of Theoretical and Applied Mechanics
Cornell University
Ithaca
New York, NY 14850
(Copy No. 99)

Dr. J. R. Rice
School of Engineering
Brown University
Providence, RI 02912
(Copy No. 100)

Dr. P. S. Symonds
School of Engineering
Brown University
Providence, RI 02912
(Copy No. 101)

Dr. W. J. Worley
Department of Theoretical and Applied Mechanics
University of Illinois
Urbana, IL 61801
(Copy No. 102)

Dr. Dana Young
Southwest Research Institute
8500 Culebra Road
San Antonio, TX 78206
(Copy No. 103)

Commander
Naval Sea Systems Command
Department of the Navy
Washington, DC 20362
Attn: SEA-09G32-Library
(Copy Nos. 104 and 105)

Dr. R. M. Gorman
Bolt Beranek and Newman, Inc.
Union Station
New London, CT 06340

Commander
Naval Sea Systems Command
Department of the Navy
Washington, DC 20362
Attn: Ms. Wanda L. Schultz
Code 62 MD